Kb, Rb AND Tl DISTRIBUTIONS BETWEEN COEXISTING NATURAL AND SYNTHETIC ROCK-FORMING MINERALS

BY

PATRICK CHUEN-FAI FUNG

A Thesis

Submitted to the School of Graduate Studies

in Partial Fulfilment of the Requirements

for the Degree

Doctor of Philosophy

McMaster University

September, 1978

© PATRICK CHUEN-FAI FUNG 1978

K, Rb AND Tl DISTRIBUTIONS

DOCTOR OF PHILOSOPHY (1978)
(Geology)

McMASTER UNIVERSITY
Hamilton, Ontario

TITLE: K, Rb AND Tl DISTRIBUTIONS BETWEEN COEXISTING NATURAL AND SYNTHETIC ROCK-FORMING MINERALS

AUTHOR: PATRICK CHUEN-FAI FUNG, B.Sc. (Lakehead)

SUPERVISOR: PROFESSOR DENIS M. SHAW

NUMBER OF PAGES: i-xviii, 1-263

ABSTRACT

Distributions of K, Rb and Tl in alkali feldspar measured for different systems of alkali feldspar-vapour, alkali feldspar-phlogopite-vapour and alkali feldspar-phlogopite-amphibole-plagioclase-rhyolite-vapour at P_{H_2O} = 1.5 Kbar depend strongly on the composition but also vary with the structure and previous thermal history of the alkali feldspar. Such variations can be reduced by initial heating of the capsule at high temperature (900°C) to fuse the feldspar so that it re-crystallizes into a homogeneous high sanidine. The following results, measured for one or more of the above-mentioned systems appear to be consistent with results obtained for natural materials and also with previously reported experimental results:

	D(Rb)	D(Tl)	K_D(Rb/Tl)	K_D(K/Rb)	K_D(K/Tl)
sanidine-vapour 800°C	2.8	0.42	7.6	1.7	11
phlogopite-sanidine 700°C	2.3	1.3	1.9	0.31	0.56
amphibole-plagioclase 700°C	1.5	1.5	1.0	1.1	1.1

For the alkali feldspar-vapour and alkali feldspar-rhyolite pairs, D(Rb) and D(Tl) increase while K_D(Rb/Tl), K_D(K/Rb) and K_D(K/Tl) decrease from high to low temperature.

For natural minerals, the following series of decreasing element concentrations and ratios together with the corresponding D and K_D values for adjacent pairs of minerals are observed:

Rb: biotite—alkali feldspar—amphibole—plagioclase

D(Rb) 2.3 9.0 2.0

Tl: biotite—alkali feldspar—amphibole—plagioclase

D(Tl): 3.5 3.3 3.0

Rb/Tl: alkali feldspar—biotite—plagioclase—amphibole

K_D(Rb/Tl): 1.7 1.1 1.9

K/Rb: alkali feldspar—plagioclase—amphibole—biotite

K_D(K/Rb): 1.1 1.2 3.7

K/Tl: alkali feldspar—plagioclase—amphibole—biotite

K_D(K/Tl): 2.7 2.4 2.5

Observed Tl concentrations for natural sulfides and oxides are generally lower than those for potassic silicates but higher than those for non-potassic silicates.

In a normal fractionation sequence of rocks the later crystallates will be enriched in Rb and Tl, due to the early crystallization of mafic minerals and calcic plagioclase, and if alkali feldspar crystallizes at high temperatures, will have lower K/Rb and K/Tl ratios. Formation of rocks of lower ratios will be favoured by low temperature crystallization of K-minerals, particularly micas, and incorporation of vapour. On the other hand, Rb/Tl ratios are more constant in silicate minerals but can be fractionated by sulfides and oxides, leading to lower Rb/Tl ratios.

ACKNOWLEDGEMENTS

I am very grateful to my supervisor, Dr. D.M. Shaw, for his supervision and guidance throughout this study, for suggesting part of the project, the study of natural minerals, and also for providing some of the samples. I am also indebted to the other members of my supervisory committee, Drs. H.P. Schwarcz and J.D. Embury for their supervision.

I wish to express my appreciation to the following persons for their valuable assistance:

Drs. B.J. Burley and A.E. Beswick for teaching me many aspects of hydrothermal experiments, and also to AEB for supplying the sanidine and phlogopite gels,

Mr. J.R. Muysson and M. Fratta for teaching me many analytical techniques,

Drs. C.A.R. De Albuquerque, H. Beatis, E. Cameron, N. Church, T.N. Irvine, C.F. Gower and F.J. Longstaffe for providing some of the samples and also CFG for doing some of the analyses and many valuable discussions,

Mrs. J. Allen and Mrs. C. Wilson for typing the final manuscript,

Connie for her patience and support.

Finally, I want to acknowledge the financial support of the National Research Council of Canada and the Geology Department, McMaster University.

TABLE OF CONTENTS

		Page
CHAPTER 1	INTRODUCTION	1
	1-1. Purpose of the Study	1
	1-2. Geochemistry of K, Rb and Tl	5
	1-3. Definitions	8
	1-4. Methods for partition coefficient measurement	11
	1-5. Problems involved	13
	1-6. Previous work	13
CHAPTER 2	EXPERIMENTAL STUDY ON THE SYSTEM ALKALI FELDSPAR AND VAPOUR	18
	2-1. Experimental Procedure and data processing	18
	2-1-1. Introduction	18
	2-1-2. Element losses	22
	2-1-3. Analysis error estimates	25
	2-1-4. Other errors	27
	2-1-5. Unsuccessful runs	27
	2-2. Data and data evaluation, Sl-vapour runs	28
	2-2-1. Test of equilibrium	28
	2-2-1a. Time required to reach equilibrium	32
	2-2-1b. Temperature reversal runs	34
	2-2-1c. Concentration reversal runs	36
	2-2-2. Discussion of results	40
	2-2-3. Temperature effect	43
	2-3. Other feldspar-vapour runs	49
	2-3-1. Ml-vapour runs	49
	2-3-2. Fusion runs	51
	2-4. Discussion of all feldspar-vapour runs	54
	2-4-1. Comparison with previous experimental data	54
	2-4-1a. K_D(K/Rb)	54
	2-4-1b. K_D(Rb/Tl) and K_D(K/Tl)	56
	2-4-1c. Na-K distributions	59

Page

2-4-2. Factors affecting trace element distribution 63
2-4-2a. Structural change 63
2-4-2b. Composition 66
2-4-2c. Kinetics 69
2-4-2d. Starting materials 72
2-5. Conclusion 73

CHAPTER 3 K, Rb AND Tl DISTRIBUTIONS BETWEEN RHYOLITE-VAPOUR AND ALKALI FELDSPAR-RHYOLITE 77

3-1. Introduction 77
3-2. Experimental technique 78
3-3. Results and discussion 79
3-3-1. Rhyolite-vapour runs 79
3-3-2. Feldspar-rhyolite results 81
3-3-2a. Results calculated from two pairs of SSV runs 81
3-3-2b. Results measured directly by MSV techniques 84
3-4. Applications 86
3-4-1. Fractionation trends 86
3-4-2. Comparison with natural feldspar-rock pairs and geothermometry 89
3-4-2a. Ignimbrites and granodiorite from Tuscany 91
3-4-2b. Granite and granodiorite from Portugal 95
3-4-2c. D(Rb) and K_D(K/Rb) for other suites 99
3-4-2d. Miscellaneous rocks from the Canadian Shield 102
3-5. Conclusion 107

CHAPTER 4. K, Rb AND Tl DISTRIBUTIONS BETWEEN PHLOGOPITE AND SANIDINE 109

4-1. Introduction 109
4-1-1. Choice of technique 109
4-1-2. Previous work with MSV technique 110
4-1-3. The system alkali feldspar-phlogopite 111
4-2. Experimental procedure 112
4-2-1. Experiment with synthetic materials 112
4-2-2. Other experiment with natural materials 113

Page

4-3. Experimental results 113
4-3-1. Final products 113
4-3-2. Results 115
4-4. Discussion of results 117
4-4-1. Evaluation of equilibrium 117
4-4-2. Comparison with previous experimental data 124
4-4-3. Comparison with data for natural biotite-feldspar 126
4-5. Conclusion 130

CHAPTER 5. K, Rb AND Tl DISTRIBUTION IN MULTI-PHASE SYSTEM FROM HYDROTHERMAL EXPERIMENTS AND ROCKS 132

5-1. Introduction and experimental procedure 132
5-2. Experimental results and discussions 133
5-2-1. Final products 133
5-2-2. Results 134
5-2-3. Discussions 136
5-2-4. Comparison with published results 140
5-3. K, Rb and Tl distributions between natural alkali feldspar, biotite, amphibole and plagioclase 142
5-3-1. Data 142
5-3-2. Comparison with experimental data 152
5-3-3. K, Rb and Tl fractionation trends 155
5-3-4. Rb and Tl enrichment in potassic-minerals 160
5-4. Other natural minerals 162
5-4-1. Muscovite 167
5-4-2. Pyroxene 167
5-4-3. Olivine 171
5-5. Tl in non-silicate minerals 171
5-5-1. Pyrrhotite 172
5-5-2. Pyrite 173
5-5-3. Magnetite 173
5-5-4. Summary 173
5-6. Conclusion 174

		Page
CHAPTER 6	APPLICATION OF DATA: K, Rb AND Tl TRENDS IN MAJOR ROCK UNITS	177
	6-1. Introductory statement	177
	6-2. K-Rb trends	177
	6-2-1. Introduction	177
	6-2-2. Discussion of the main trend	179
	6-2-3. K/Rb fractionation trends: hypothetical models	183
	6-3. Crustal fractionation of Tl	195
	6-3-1. Introduction	195
	6-3-2. In continental plutonic rocks	198
	6-3-3. In basalts	198
	6-4. Conclusion	203
CHAPTER 7	CONCLUSION	205
APPENDIX 1	EXPERIMENTAL TECHNIQUES	211
	A-1-1. Preparation of Capsules	211
	A-1-1-1. SSV runs	211
	A-1-1-2. MSV runs	213
	A-1-2. Experimental procedure	213
	A-1-3. Treatment of run products	214
APPENDIX 2	X-RAY DIFFRACTION TECHNIQUE	216
APPENDIX 3	PREPARATION OF NATURAL SAMPLES	221
APPENDIX 4	ANALYTICAL TECHNIQUE	222
APPENDIX 5	EVALUATION OF ANALYTICAL UNCERTAINTIES	225
APPENDIX 6	ANALYTICAL RESULTS ON NATURAL SAMPLES	230
REFERENCES		245

APPENDICES

LIST OF TABLES

		Page
A-1	Dimension of capsules and pressure vessels (in inches)	212
A-2	XRD data for alkali feldspar identifications, using the three peak method of Wright (1968)	218
A-3	K, Rb and Tl abundances of some reference samples from this study	226
A-4	Summary of K, Rb and Tl for some reference rocks	227
A-5	Description of samples used in this study	231
A-6.	K, Rb and Tl analyses of rocks and minerals from this study	234

LIST OF TABLES

TABLE		Page
1-1.	Principal physical and crystallochemical properties of K, Rb, Tl and related elements	6
2-1.	Data on starting minerals used in feldspar-vapour SSV experiments	19
2-2.	Experimental conditions of alkali feldspar-vapour SSV runs	21
2-3.	Material balance calculation, using run 30-DH (500°C) as an example	24
2-4.	Estimation of the effect of analytical error, using run 30-DH as an example	26
2-5.	Data for feldspar (Sl)-vapour, SSV, regular runs	29
2-6.	Data for time-test runs	33
2-7.	Data for temperature-reversal test runs	35
2-8.	Data for concentration-reversal test runs, using spiked feldspar and solution CC	37
2-9.	Summary of data for feldspar (Sl)-vapour experiments	41
2-10.	Data for regular runs with Ml and fusion runs with Sl, S2 and Ml	50
2-11.	K_D(K/Rb) for alkali feldspar-vapour from several workers	55
2-12.	K, Rb and Tl distribution between synthetic sanidine-vapour (from Sretenskaya, 1967)	58
2-13.	K-Na distribution data	60
2-14.	Comparison of starting and final materials	65
2-15.	Partition coefficients of Rb, Cs, Ba and Sr for the pair alkali feldspar/plagioclase at 600°C and 1 Kbar (Iiyama, 1968)	65

		Page
2-16.	Diffusion coefficients of Na, K and Rb in microcline and orthoclase	70
3-1.	Data for rhyolite-vapour runs	80
3-2.	Summary of results for the pair feldspar-rhyolite	85
3-3.	Summary of data on the ignimbrites and granodiorites from Tuscany, Italy (Dupuy et al., 1973)	92
3-4.	Summary of data on the granite and granodiorites from N. Portugal (Albuquerque, 1971 and 1975)	96
3-5.	Summary of Rb and K/Rb data for the pair alkali feldspar-rock from the Palmer region and Corsica	100
3-6.	Summary of alkali feldspar-rock data for rocks from the Canadian Shield	103
4-1.	Data for starting materials used in phlogopite-feldspar experiments	114
4-2.	Data for phlogopite-alkali feldspar MSV runs	116
4-3.	Summary of published K_D(K/Rb) data for the pairs of feldspar-vapour and phlogopite-vapour	125
4-4.	Summary of data for coexisting natural biotite-alkali feldspar	127
5-1.	Concentration data for MSV regular runs with five solids and vapour EX	135
5-2.	Matrices of D and K_D values ($\bar{x}$ + 1s) for pairs of experimental phases	137
5-3.	Series of relative element concentration or ratios for the experimental phases	138
5-4.	Listing of samples from this study and selected literature reports	143
5-5.	Matrix of D(Rb) values for coexisting natural phases	144
5-6.	Matrix of D(Tl) values for coexisting natural phases	146
5-7.	Matrix of K_D(Rb/Tl) values for coexisting natural phases	147
5-8.	Matrix of K_D(K/Rb) values for coexisting natural phases	148
5-9.	Matrix of K_D(K/Tl) values for coexisting natural phases	150

		Page
5-10.	Summary matrices of D and K_D values ($\bar{x}$ + 1s) for pairs of natural phases	151
5-11.	Series of relative element concentration or ratios for natural phases	152
5-12.	Matrices of reduced D and K_D values ($\bar{x} \pm 1s$) for natural phases not included in Tables 5-5 to 5-9.	163
6-1.	Contributions of K and Rb from the constituent minerals in 1g of each of three rocks	182
6-2.	Data for crystallization model calculations	184
6-3.	K and Rb concentrations and K/Rb ratios of the residual liquid for the crystallization of the mineral assemblages shown in Table 6-2	188

LIST OF FIGURES

		Page
2-1.	Tl distribution between feldspar (Sl)-vapour as an example of concentration-reversal experiments	38
2-2.	Rb distribution between feldspar (Sl)-vapour as an example of concentration-reversal experiments	39
2-3.	Rb distribution between feldspar (Sl)-vapour	44
2-4.	Tl distribution between feldspar (Sl)-vapour	45
2-5.	Correlation of Rb/Tl between feldspar (Sl)-vapour	46
2-6.	Correlation of K/Tl between feldspar (Sl)-vapour	47
2-7.	Correlation of K/Rb between feldspar (Sl)-vapour	48
2-8.	D(Rb) and D(Tl) for different pairs of feldspar-vapour at different temperatures	52
2-9.	K_D(Rb/Tl), K_D(K/Rb) and K_D(K/Tl) for different pairs of feldspar-vapour at different temperatures	53
2-10.	K-Na distributions between alkali feldspar-vapour and alkali feldspar-melt for data from literature	61
2-11.	Na-K distribution between alkali feldspar-vapour	62
2-12.	Plots of $2\theta_{\bar{2}04}$ vs. $2\theta_{060}$ for alkali feldspars using $CuK\alpha_1$ radiation	64
2-13.	Variation of K_D(Cs/Na+K) with composition of the feldspar	68
2-14.	Variation of alkali feldspar-vapour D and K_D values with the composition of the feldspar and temperature	76
3-1.	Plot of D and K_D vs. $1/T(^oK)$ for the pair Sl-melt	82
3-2.	Plot of D and K_D vs. $1/T(^oK)$ for the pair Ml-melt	83
3-3.	Relationship between Rb and Tl in common crustal rocks and pegmatitic feldspars	88

		Page
3-4.	Histogram of D and K_D for the pair feldspar-rock for the rocks from Tuscany, Italy	94
3-5.	Histogram of D and K_D values for the pair feldspar-rock for the rocks from N. Portugal	97
3-6.	Histogram of D(Rb) and K_D(K/Rb) for the pair feldspar-rock for the rocks from Corsica and the Palmer region, S. Australia	101
3-7.	Histogram of D and K_D values for the pair feldspar-rock for the rocks from the Jackfish Lake complex, N.W. Ontario	104
3-8.	Histogram of D and K_D for the pair feldspar-rock for the rocks from the English River Belt, N.W. Ontario	106
4-1.	Rb distribution between phlogopite-feldspar	118
4-2.	Correlation of K/Rb between phlogopite-feldspar	119
4-3.	Tl distribution between phlogopite-feldspar	120
4-4.	Correlation of K/Tl between phlogopite-feldspar	121
4-5.	Correlation of Rb/Tl between phlogopite-feldspar	122
5-1.	Rb-Tl relationships in natural minerals and their host rocks	157
5-2.	K-Rb relationships in natural minerals and their host rocks	158
5-3.	K-Tl relationships in natural minerals and their host rocks	159
5-4.	K-Rb relationships in sediments and some minerals not included in Figs. 5-1 to 5-3.	168
5-5.	Rb-Tl relationships in sediments and some minerals	169
5-6.	K-Tl relationships in sediments and some minerals	170
6-1.	Summary of possible and probable K-Rb fractionation trends in igneous and associated rocks	178
6-2.	K and Rb correlations in rocks and their constituent minerals	185

		Page
6-3.	Composition of the residual liquids after crystallization of some of the hypothetical solids as shown in Table 6-3	189
6-4.	K and Rb concentrations of initial liquid W and after fractional crystallization of 10% alkali feldspar or albite	191
6-5.	Plot of Rb vs. K in mica and some coexisting feldspars	193
6-6.	Summary of K-Tl relationships in some major crustal rock units	196
6-7.	Summary of Rb-Tl relationships in some major rock units	197
6-8.	K/Rb and K/Cs vs. K content of submarine tholeiites	201
A-4-1.	Device for introducing the external buffer into the aspiration chamber of the AAS unit	224

CHAPTER I

INTRODUCTION

1-1. Purpose of the Study

K and Rb (and the K/Rb ratio) are among the most extensively used elements in petrologic interpretations, generally as indicators of fractionation, equilibrium, genetic relationships and alteration and in the construction of many petrologic models.

Thus Taylor et al. (1960) distinguished three generations of alkali feldspars in a pegmatite on the basis of their K/Rb ratios. Similarly, Butler et al. (1962) were able to separate the Younger Granites of northern Nigeria into different groups, which would otherwise be impossible due to their similarities in mineralogy and major element chemistry. Whitney (1969) used K/Rb ratios as an indictor of metamorphic grade for the gneisses from the Adirondacks. More recently, Albuquerque (1975), based on the abundances and K/Rb ratios (among others) concluded that the two modes of occurrence of alkali feldspars, both as the matrix and megacryst, crystallized in equilibrium with each other and with other minerals in the porphy-

ritic granitic rocks from northern Portugal. Bernotat et al. (1976) used K/Rb ratios in alkali feldspar and biotite to distinguish three groups of granitic rocks from Sinai, and also as a criterion for the detection of hydrothermal alteration.

Due to its low abundance and consequent analytical problems, Tl is not as widely used, although, as pointed out by Taylor (1965), K/Tl should be more sensitive and in many aspects more useful than K/Rb. This was demonstrated by Taylor et al. (1960); Zlobin (1958); Kogarko (1969) and others. The affinity of Tl to the sulfophiles has led to its use as an exploration tool for sulphide and gold deposits as suggested by Smith et al. (1974), and Ewart and and Keays (1977) (see also summary by Ivanov et al., 1960). It is also one of the most important volatile elements that played an important role in the condensation model for the origin of the meteorites (Larimer and Anders, 1967, and also Grossman and Larimer, 1974).

Since the development of basic theories and equations of anatexis due mainly to Gast (1968) and Shaw (1970), partition coefficients have become very popular tools in constructing petrogenetic models, as e.g., the genesis of basalts and composition of the mantle (e.g., Gast, 1968; Griffin and Murthy, 1969, and Philpotts and

Schnetzler, 1970) and crustal rocks (e.g., Shaw, 1972; Arth and Hanson, 1972, 1975; Arth, 1976, and Condie, 1976). Rb is one of the most extensively used elements in many of these models. Due to the lack of partition coefficient data, Tl has not been similarly exploited, with the exception of the work by Dupuy et al. (1973) who used Rb and Tl partition coefficients to model the crystallization history of the ignimbrites and related rocks from Tuscany, Italy.

Another application of K-Rb partition is in geothermometry. Thus Beswick (1973) calibrated a thermometer based on $K_D(K/Rb)$ for the pair biotite/alkali feldspar (see also Albuquerque, 1975, and Bernotat et al., 1976), and Volfinger (1976), for the pair muscovite/alkali feldspar.

The purpose of this study is threefold:

a. to contribute to the data for Tl partition coefficients in relation to K and Rb among the common rock-forming minerals;

b. to study some of the factors affecting partition coefficients;

c. to exploit some of the above-mentioned applications, such as geothermometry and petrologic indicators.

Both experimental (hydrothermal) and natural (rock) systems were studied, involving mainly phases of silicic igneous rocks, but also including some basalts, metamorphic and sedimentary rocks.

A greater portion of the study has been devoted to the experimental approach, of varying degrees of complexity. The simplest of such studies, employing conventional hydrothermal techniques (e.g., see Beswick, 1973, and Zielinsky and Frey, 1974), involved the pairs alkali feldspar-vapour and rhyolite glass-vapour. By using various kinds of feldspars and experimental conditions, the effect of several variables has been studied with the pair feldspar-vapour. By combining with the data for the rhyolite-vapour pair, the distributions of K, Rb and Tl between the pair feldspar-rhyolite has been calculated and extrapolated to similar natural systems.

Using an exploratory technique, two or more solid phases have been equilibrated directly with a common vapour acting as the transporting agent. Such a technique has been applied to the systems alkali feldspar-phlogopite-vapour and a simplified 'granitic' system of

alkali feldspar-phlogopite-plagioclase-amphibole-rhyolite glass-vapour. Studies on these systems essentially established the feasibility of such technique, although the results for the more complex granitic system need further confirmation.

The second part of this study dealt with natural phases separated from various types of rocks, using conventional mineral separation techniques. The minerals examined included all those used in the experimental studies as well as pyroxene, olivine, pyrrhotite, pyrite and magnetite.

Finally, an attempt has been made to correlate the trends as observed for the major crustal rocks to the mineral data.

1-2. Geochemistry of K, Rb and Tl

The geochemistry of an element is governed mainly by its physical and crystallochemical properties. Some of these properties for K, Rb, Tl and other related elements are summarized in Table 1-1.

In many aspects, K, Rb and Tl are very similar to each other and have long been recognized as a coherent triad, discussed in many papers dealing with trace element distributions (e.g., Ahrens, 1952; Ringwood, 1955, and Nockolds, 1965). In many natural materials, Rb and Tl substitute for the major element K, so much so that Rb, although a relatively abundant element, never forms a separate mineral, and Tl only forms minerals of the sulfosalt clan. These

Properties	K	Rb	Cs	Zn	Hg	Tl	Pb
Atomic number	19	37	55	30	80	81	82
Atomic weight	39.10	85.48	132.91	65.38	200.61	204.39	207.21
Density	0.86	1.53	1.9	7.20	14.19	11.85	11.34
Atomic volume	45.4	55.8	71.0	9.08	14.14	p7.25	18.27
Ionic radius (Å)	1.68	1.81	1.96	0.83(II)#	1.22(II)	1.84(I)	1.02(IV)
						1.08(III)	1.37(II)
Melting point (°K)	336	311	299	692	234	575	600
Boiling point (°K)	1035	688	670	1183	630	1730	2020
Electronegativity** (Kcal/g-atom)	100	97	89	208	215	140(I)	170(II)
						30(III)	42.5(IV)
Ionization potential (eV)+	4.32	4.16	3.88	27.2	29.1	6.08(I), 2.86(III)	14.91(II)
Ionic potential	0.75	0.67	0.61	2.41	1.79	0.67(I)	1.51(II)
Valence	I	I	I	II	I	I(III)	II(IV)

*Whittaker and Muntus (1970), **Ringwood (1955), # Roman numerals indicate the valence of the element, +Ahrens (1952).

Table 1-1. Principal physical and crystallochemical properties of K, Rb, Tl and related elements.

elements all belong to the large ion lithophile (LIL) group of incompatible elements, being strongly enriched in the crust of the earth (Albuquerque et al., 1972) and their abundances increase from ultrabasic to acidic rocks. In many petrologic processes, K, Rb and Tl concentrations increase as a group with fractionation.

The alkalis, K and Rb are particularly similar to each other and have been studied by numerous workers. The 10% difference in their ionic radii is responsible for their fractionation under more severe conditions. The constancy of the K/Rb ratio has been a subject of long and heated debate and has been thoroughly reviewed by Shaw (1968). The geochemistry of K and Rb has been summarized by Heier and Adams (1964) and Taylor (1965).

Tl has relatively higher electronegativity and ionization potential and forms a slightly more covalent bond with oxygen. Hence the coherence of Tl and K is rather restricted. However, the ionic radii of Tl and Rb are almost identical and the coherence of Rb and Tl has been well documented (e.g., Ahrens, 1945, 1948 and Shaw, 1952). As was pointed out by Taylor (1965) the K/Tl ratio should provide a more sensitive indicator of fractionation than K/Rb and Rb/Tl.

Tl also is highly enriched in the Cs mineral pollucite, as might be expected, apparently replacing Cs in this mineral.

The occurrence of Tl^{3+} has been suggested by several workers to explain its occurrence in cafemic rocks and minerals (e.g., Shaw, 1957), but is generally considered unlikely except under extreme oxidizing environments (e.g., see Ivanov et al., 1960).

Tl also resembles the sulfophile elements, particularly Pb and Hg (Table 1-1) and thus also exhibit sulfophile properties, as was observed by Shaw (1952), Voskresenskaya (1961 and 1969); Meituv (1962) and recently by Ewards and Keays (1977). However, Meituv (1962) showed that in the ore deposits of the Klichkinskii region, Tl was concentrated in the silicate gangue minerals in preference to the coexisting sulfides. Recently, Greenland and Campbell (1977) demonstrated that in the Great Lake tholeiitic dolerite intrusion of Tasmania, Tl abundances increased smoothly with fractionation, and were not affected by the precipitation of sulfides, which occurred in two zones of the intrusion.

Thus, the geochemistry of Tl is dominated by its occurrence as monovalent ion and lithophile character. The behaviour of K/Rb, K/Tl and Rb/Tl ratios in the major rock units are particularly important to this study and will be discussed in detail in Chapter 6.

1-3. Definitions

Fundamental to the understanding of the behaviour of a trace element during geologic processes is knowledge of its partition coeffi-

cient between the various phases coexisting in equilibrium. Theoretical aspects of partition coefficients were treated in detail by McIntyre (1963) and many aspects of it were discussed by Berlin and Henderson (1968), Philpotts and Schnetzler (1970), Shaw (1977) and others.

A partition coefficient (D) can be defined as follows: if two phases a and b coexist in equilibrium at some temperature and pressure and contain a dissolved component i, by the Nernst law for ideal solutions, the ratio

$$X_i^a / X_i^b = D_i'(a/b), \text{ a constant} \qquad (1)$$

where X_i^a = mole fraction of i in phase a and X_i^b = mole fraction of i in phase b.

Another useful function, K_D, can be defined by the law of mass action. Thus for an exchange reaction of two uni-valent elements i and j, regarded as end-members, between two phases a and b, such as: $a_i + b_j = a_j + b_i$, and if the exchange is ideal,

$$X_j^a . X_i^b / X_i^a . X_j^b = K, \text{ the equilibrium constant} \qquad (2)$$

Note that $$K = (X_j^a/X_j^b)/(X_i^a/X_i^b)$$

$$= D_j'(a/b)/D_i'(a/b), \quad (3)$$

and that $$K = (X_j^a/X_i^a)/(X_j^b/X_i^b). \quad (4)$$

Although mole fractions of compounds were used in these definitions, in practice, weight concentrations of elements C_i and C_j, as % or part per million (ppm), are commonly used instead. Hence, equation (1) can be written as, e.g.

$$D(Tl) = C_{Tl}^a/C_{Tl}^b \text{ or simply } (Tl)^a/(Tl)^b, \quad (5)$$

and similarly, equation (4) can be written simply as

$$K_D(Rb/Tl) = (Rb/Tl)^a/(Rb/Tl)^b, \quad (6)$$

using the symbols for the elements as their weight concentrations. Equations (5) and (6) are used throughout this study and are expressed as D(Tl) and K_D(Rb/Tl) values for the pair a/b.

Expressions (1) through (6) hold only if ideal behaviour is obeyed and then are true irrespective of the presence of the other components or phases and of the concentrations of the components, provided they are sufficiently low.

Departure from ideal behaviour and consequently non-consistent D and K_D values will occur when the concentration of a component is higher than a certain level, generally called the limit of ideality (e.g., see Iiyama and Volfinger, 1976).

D and K_D values will also vary with temperature, pressure and composition of the system. Generally, dependence on composition for K_D for pairs of similar elements is less than for their respective D values (e.g., see Banno and Matsui, 1973). The dependence of partition coefficient on temperature and pressure of equilibration has been extensively used for geothermometry and geobarometry calibrations (e.g., see Beswick, 1973, and Hakli and Wright, 1967).

1-4. Methods for partition coefficient measurement

Partition coefficient data can be obtained from two separate sources, both of which are being extensively applied at the present time:

a. analysis of coexisting minerals in rocks;

b. experimental studies, normally by equilibrating two or more phases, containing the elements of interest, under desired temperature and pressure.

The two methods are usually complimentary to each other and provide a good way of cross-checking the data obtained (e.g., see Shimizu, 1974, and Hart and Brooks, 1974). Experimental studies provide data for simplified systems and under closely controlled conditions.

In addition, such a method permits the study of the effect of many variables and gives a simple means for geothermometer and geobarometer calibrations. However, the extrapolation of such data to the immensely complex systems, the rocks, is sometimes very difficult, if not impossible (e.g., see Albuquerque, 1975; Volfinger, 1976).

Traditionally, mineral analysis, and hence partition coefficient measurement required mineral separation (see Appendix 4). This also limited the early experimental studies to simple systems such as solid-vapour or solid-salt which permit ready separation of the equilibrated phases. Due mainly to the difficulties involved in the quantitative recovery of the vapour phase, only relative concentrations and hence K_D values were published.

Recently, with the advent of the electron microprobe (e.g., Drake and Weill, 1975) and auto-radiographic techniques (e.g., Mysen and Seitz, 1974), in-situ analysis of some elements can be performed on polished sections. However, both methods are only applicable to certain elements and the low sensitivity of the electron microprobe limits its application to mainly major elements, at least for natural specimens.

In addition, several techniques are available for directly equilibrating several solids and a vapour phase, which permit ready separation of the equilibrated phases and hence analysis with conventional

techniques (see Fung and Shaw, 1978 and Chapter 4).

1-5. Problems involved

There are many theoretical and practical uncertainties associated with partition coefficient measurements, which can be broadly divided into four categories:

a. the achievement and preservation of equilibrium;

b. mode of occurrence of an element in a mineral;

c. effect of temperature, pressure, crystal structure and composition;

d. experimental error.

These apply to studies of both experimental and natural systems, although the treatment will be slightly different for each. For the sake of brevity, the following discussion deals mainly with studies of natural materials, leaving the experimental studies, as well as most of c. till later, in conjunction with discussions of the experimental results (mostly in Chapter 2).

The fundamental requirement of any partition coefficient measurement is that the phases of interest coexist in equilibrium with each other. It is common practice to assume, either implicitly or explicitly, that the minerals from a sample of interest, such as a hand specimen, coexisted in equilibrium upon their crystallization and that

the equilibrium state was preserved as the magma solidified into a rock. However, such an assumption cannot always be satisfied due to:

a. most common minerals are solid solutions of two or more end-members and hence would crystallize at a range of temperature; sometimes, the different parts of such a crystal fail to reach equilibrium with each other, due to the sluggishness of the reaction, and only the outermost rim was at equilibrium with the melt at any particular time. Common expressions of such a process are crystal zoning and exsolution.

b. a mineral could have crystallized elsewhere in the magma body, and later brought to the site where a rock was eventually formed, as e.g., by gravity settling observed in many large layered complexes.

c. due to the slow rate of diffusion of ions (see Chapter 2), local disequilibrium may develop in a magma around a crystal.

d. the equilibrium state, if established during crystallization and solidification of a magma, may be disturbed by secondary processes such as alteration, metasomatism and metamorphism. Such processes may lead to equilibrium under a new set of conditions, but sometimes they do not, due to difference in susceptibility of different minerals and kinetic effects.

Another important assumption is that a trace element occurs in a structural site of a mineral, substituting for a major element. However, non-structural occurrence of elements is possible, as e.g., by surface absorption, in cracks and cleavage planes, as inclusions or in crystal defects.

Finally, the most common experimental errors are mineral impurities and analytical.

Some of these problems may be overcome by careful textural and petrologic studies and greater care of the operator, and, if possible by cross-checking with results from other sources. In many cases, one can only assume that the samples are suitable, and seek confirmation from collecting a large enough volume of data to choose those which show consistent results, and if possible, by cross-checking with results from other sources, such as experimental studies (e.g., see Shimizu, 1974, c.f. Hart and Brooks, 1974). These and similar problems related to partition coefficient measurements have been thoroughly reviewed by Shaw (1977).

1-6. Previous work

D(Rb) and K_D(K/Rb) values have been reported by numerous authors for different mineral-pairs and from different types of rocks. More recent works include those by Murthy and Griffin, 1970; Philpotts

and Schnetzler, 1970; Dudas et al., 1971; Albuquerque, 1975, and Bernotat et al., 1976, just to mention a few.

On the other hand such data for Tl are very scarce, although several early papers reported considerable amount of data for many individual minerals (mainly K-minerals), e.g., Ahrens, 1945 and 1948; Shaw, 1952 and 1957 (see also summaries by Albuquerque & Shaw, 1972, and Ivanov et al., 1960). The relevant studies include:

Tauson and Buzae (1957), on alkali feldspar, biotite and amphibole;

Demin and Khitarov (1958), on alkali feldspar, plagioclase and biotite;

Kogarko (1957), on biotite, amphibole and plagioclase;

Voskresenskaya (1959), on biotite and feldspars, and

Dupuy et al. (1973), on biotite, alkali feldspar and plagioclase.

Considerable amounts of experimental data have been published for K_D(K/Rb) for pairs of vapour and alkali feldspar, biotite, muscovite, plagioclase or leucite, mainly by Iiyama and co-workers (e.g., see summaries by Iiyama and Volfinger, 1976, and Volfinger, 1976). Other contributors are Chelischev (1967) and Beswick (1973).

Two workers measured D(Rb) between coexisting pairs of

solids:

Iiyama (1968), alkali feldspar and plagioclase,

Shimizu (1974), clinopyroxene and melt.

In contrast, only two publications dealt with experimental measurement of Tl distributions, namely Eugster (1954), and Sretenskaya (1967), both on sanidine-vapour. However, data from the former were not published and those from the latter appear to be unsatisfactory (see section 2-4-1).

All the above-mentioned experimental studies were performed under vapour pressure of 1-2 Kbar H_2O and 500-800°C, with the exception of that of Shimizu, which was performed under dry conditions, 15-30 Kbar and 1100-1200°C. The vapour phase used was a chloride solution, which also carried the element studied.

CHAPTER 2

EXPERIMENTAL STUDY ON THE SYSTEM ALKALI FELDSPAR AND VAPOUR

2-1. Experimental procedure and data processing

2-1-1. Introduction

This chapter deals with the distribution of K, Rb and Tl between coexisting alkali-feldspar and vapour under hydrothermal conditions. All experiments were conducted under a total vapour pressure of 1.5 Kbars. Experimental temperature varied between 500° to 800° in order to study the effects of temperature.

Standard hydrothermal technique was employed in this study (e.g. see Beswick, 1973) and is described in the Appendix (A-1).

A natural sanidine S1, microcline M1 and a synthetic sanidine S2, made from a gel of the composition of pure orthoclase (Or_{100}) were used as the starting minerals (Table 2-1). The vapour was an aqueous solution containing different concentrations of KCl, RbCl and TlCl or $TlNO_3$.

Table 2-1. Data on starting materials used in alkali feldspar-vapour SSV[+] experiments

Minerals	Composition(%) (Mole %) Or	Ab	An	Concentrations K(%)	Rb(%)	Tl(ppm)	Descriptions[#]	Source and Donor
Sanidine (S1)	35	63	2	4.66	0.014	0.59	M: fresh, homogeneous X: high sanidine; exsolved	Sanidine trachyte; Ischia; Shaw, D.M.
Microcline (M1)	80	13	1	11.2	2.0	130	X: max. microcline; homogeneous	Pegmatite, Bernic L.; Nickel (1961)
Orthoclase (S2)	100	0	0	14.0	0	0	gel	Beswick (1973)
Solutions								
CC				4.65	0.07	12.0	Aqueous solutions made from reagent grade KCl, RbCl and TlCl or $TlNO_3$	
DD				2.33	0.14	59.0		
EE				4.65	0.14	118.0		
FF				2.00	0.11	500.0		
EX*				2.00	0.10	500.0		

M: microscope description; X: XRD studies

* Also contained 0.1% each of Li, Na, Ca, Sr, Mg and Ba.

+ single solid-vapour

Generally two slightly different heating procedures were employed in the experiments (see also A-1-3). In most cases, the capsules were heated directly to the desired temperature and maintained for approximately 30 days (regular runs, table 2-2). In some runs, the capsules were first maintained at 900°C for 1-2 days and were then lowered to the desired temperature for an additional 30 days (fusion runs, batch 14, Table 2-2). The initial 900° heating was intended to fuse and homogenize the feldspars.

Some experiments were designed specifically for testing whether equilibrium had been attained during the experiment. The conditions of these test runs are described separately (section 2-2-1).

The purpose of using several feldspars as well as regular and fusion runs is to study the effect of variables such as structure, composition and thermal history of the minerals, on the distributions.

In some runs, mostly with Sl, there were small amounts of very fine dust-like particles that clung to the filter paper and wall of container. These particles are probably amorphous. No other unexpected phases were observed.

For each run, most of the solid (except the small portion used for X-ray and microscope studies in some runs and small amounts lost during sample treatment) and all the liquid were separately analysed for K, Rb and Tl, using the techniques of AAS described in Appendix-4.

Table 2-2. Experimental conditions of alkali feldspar-vapour SSV runs

Batch No.	Starting Materials		Type of runs	Temperature
	Feldspars	Vapours		
1-8	S1	CC-FF	Regular	500, 600 & 700°C
9	M1	DD	Regular	500 & 700°C
14	S1, M1, S2	EX	Fusion	700 and 800°C

Li, Na, Ca, Sr, Mg and Ba were also analysed in batch 14, and also in the MSV runs, batches 13 and 15. Only results for K, Rb and Tl will be discussed in detail in this thesis, and Na will be discussed only in relationship to K, in section 2-5-3.

2-1-2. Element losses

By material balance calculations, the sum of the masses of K, Rb and Tl in each capsule was calculated for the starting materials and the final products. There is usually a marked loss (up to 40%, generally 10-30%) and sometimes a small gain (<10%) in the final products. A small gain or loss can be attributed to experimental error (see discussion in 2-1-3), since each capsule is a closed system.

In the case of excessive loss (>10%), the most possible cause is loss of liquid during opening of the capsule and subsequent filtering and transferring. Some liquids (and solids) might also have been trapped in the dead space of the capsule. A loss of solid will not affect the results since a weighed amount was analysed. Loss of liquid would result in proportional loss of all elements. However, the loss of different elements in a run is rarely the same, Tl usually being proportionately the most, and K the least affected. This preferential loss raises the possibility of adsorption onto the wall of the Au capsule. Hence, Tl, being the most similar to Au in physicochemical properties and at the lowest level of concentration, is most likely to be affected. At one point during

the study, a large number of used capsules (already opened and cleaned) were boiled intensively in water, which was then analysed for Tl. A considerable amount of Tl was detected (0.36 μg per capsule or 6% of total). Subsequently, all capsules (and contents) were boiled in water which was then added to the extracted vapour sample to be analysed. However, loss of elements still persisted and hence correction had to be made in the following manner.

It was assumed that element-loss did not affect the position of the equilibrium achieved during the heating so that a loss would only reduce the mass of the element of interest in the final vapour. Hence a correction can be applied to this concentration, using the element mass in the final solid and the sum of mass in the starting materials (corrected mass in final vapour = sum of mass in starting materials - mass in final solid). Data from run 30-DH provides a typical example (Table 2-3). Material balance calculations show a loss of 14% Tl, 13% Rb and a gain of 5.0% K in the final products. After correction to the final vapour, its concentrations change from 18 to 26 ppm for Tl and 282 to 485 ppm for Rb, while K remains at 0.45%. Runs that show losses in any element have been thus corrected and no correction has been applied to the elements that show a small gain (table 2-5), which is attributed to analytical error.

	Starting Materials			Final Products		
	Tl	Rb	K	Tl	Rb	K
Concentrations	(From table 2-1)			(From table 2-5)		
Sl	0.59(ppm)	140(ppm)	4.66(%)	24(ppm)	802(ppm)	6.32(%)
DD	59.	1400	2.33	18	283	0.45
Masses (μg)**						
Sl	0.04	9.	2880.	1.48	49.6	3906.
DD	2.60	62.	1028.	0.79	12.5	198.
Sum	2.64	71.	3908.	2.27	62.1	4104.
Loss(μg)				0.37	8.9	-196.
Loss(%)				14.0	12.5	-5.0
Corrected masses in vap. DD#				1.16	21.4	198.*
Corrected concentration in DD				26.39(ppm)	489. (ppm)	0.45(%)

\# Corrected mass in vap. = initial sum of masses - mass in final Sl.

* No correction, due to gain in final mass.

** Wt. of Sl = 0.0618, wt. of DD = 0.0441 gm

Table 2-3. Material balance calculation, using run 30-DH (500°) as an example.

2-1-3. Analysis error estimates

The analytical errors for all three elements K, Rb and Tl were estimated to be about ±5% by comparison with analyses of reference samples. Table 2-4 shows the possible effect of this error on the results of D and K_D values. Since material balance calculations are based on the concentration in the final feldspar, only the error in the feldspar needs to be considered. Three cases were dealt with in these estimates, namely by adding and subtracting 5% from the analytical results for the feldspar. The masses and hence concentrations of the elements in the vapour were then calculated by material balance as described in section 2-1-2. Finally, a combination of these two extreme cases was also considered, using the high concentrations for the vapour and the low ones for the feldspar.

In the case of K, an addition of 5% to the feldspar reduced the masses in the vapour to less than zero and hence the original analytical data were used to calculate the K_D values in which K was involved.

These calculations demonstrate that a ±5% analytical error has very little effect on the final D and K_D values [maximum 19% in D(Rb)], certainly not enough to account for the spreads observed in table 2-5, which ranges up to C=64%.

	K	Rb	Tl	D(Rb)	D(Tl)	K_D(Rb/Tl)	K_D(K/Rb)	K_D(K/Tl)
ORIGINAL DATA*								
Initial masses (Sl+DD) (μg)	3908	71	2.64					
Final mass in feldspar (μg)	3906	49.6	1.48					
Final conc. in feldspar	6.32%	802 ppm	24 ppm					
Results				1.64	0.91	1.80	8.6	15.5
COMPUTED DATA								
Case 1.								
Conc. in final Sl	6.00%	762 ppm	22.8 ppm					
Mass in final Sl (μg)	3708	47.1	1.41					
Mass in final DD (μg)	200	23.9	1.23					
Conc. in final DD	0.45%	542 ppm	27.9 ppm					
Results				1.41	0.81	1.74	9.5	16.4
Case 2.								
Conc. in final Sl	6.64%	842 ppm	25.2 ppm					
Mass in final Sl	4103	52.0	1.56					
Mass in final DD	--	19.0	1.08					
Conc. in final DD	0.45%#	431 ppm	24.5 ppm					
Results				1.95	1.03	1.89	7.6	14.4
Case 3.								
Conc. in final Sl	6.00%	762 ppm	22.8 ppm					
Conc. in final DD	0.45%	431 ppm	24.5 ppm					
Results				1.77	0.93	1.90	7.5	14.3

* Initial sums of masses from table 2-3; concentration, D and K_D values from table 2-5.

Original analytical data is used here since mass of K in vapour is reduced to less than zero.

Table 2-4. Estimation of the effect of analytical error, using run 30-DH as an example. Case 1, based on 5% overestimate of analytical results; Case 2, based on 5% underestimate; Case 3, a combination of 1 and 2, using Sl data from 1 and vapour data from 2.

2-1-4. Other experimental errors

There are two other sources of experimental errors that are more or less random:

Firstly, there was sometimes a small but variable amount of very fine gold dust in the sample of feldspar to be analysed, which came from the capsule while being cut open. This will make the determined concentrations lower than the true ones. The second possibility came from the loss of weight of the filled capsule during welding. This loss was assumed to be due to loss of solution (both water and the dissolved salts) by vaporization and the weight of the initial liquid was adjusted accordingly. However, it is also possible that the loss in weight is due to loss of Au by volatilization, or to evaporation of pure water with little or no dissolved salts. These latter possibilities would affect the initial masses of the elements which is critical in the mass balance calculations.

2-1-5. Unsuccessful runs

A number of runs were discarded forthright for various reasons. The most obvious reasons were rupturing and leakage of the capsules during the experiment. Evidence of these was provided by loss in weight in the final capsule, or revealed by X-ray and microscope studies. In some runs the K concentration in the final feldspar was very low, thus suggesting leaching or alteration (e.g. see Morey and Chan,

1955 and Morey and Hesselgesser, 1951). In these runs, the results were usually anomalous and were hence discarded.

Finally, a number of solutions having low concentrations of Rb (<200 ppm) and Tl (<10 ppm) were used in the early stage of this study, in order to provide a larger range of results. However, the resulting low concentrations in the final products were very uncertain. These runs were discarded.

This process of elimination reduced the number of successful runs from 48 to 17 for 500°C, 38 to 20 for 600°C and 23 to 15 for 700°C (Table 2-5). The relatively large number of discarded runs for 500°C arises from a number of unsuccessful test-runs which will be discussed later, and a large number of runs with low concentrations.

2-2. Data and data evaluation

The major part of this study was devoted to the pair feldspar and vapour SSV runs. Table 2-5 shows the concentrations of K, Rb and Tl for all the successful runs, including those from the test-runs as discussed in the following. For each run, D and K_D values for Sl/vapour are also reported.

2-2-1. Tests for equilibrium

In order to test whether equilibrium had been attained during the experiments, three sets of test runs were conducted at 500°C and

Table 2-5. Data for feldspar (Sl)-vapour, SSV, regular runs

		Feldspar (Sl)			Vapour #			D		K_D		
No.	Sol.	K(%)	Rb(ppm)	Tl(ppm)	K(%)	Rb(ppm)	Tl(ppm)	Rb	Tl	Rb/Tl	K/Rb	K/Tl
500°C, routine runs												
30-DH	DD	6.32	802	24.1	0.45*	489	26.4	1.6	0.91x	1.8x	8.6x	16
31-DL	DD	5.38	338	7.6	0.43*	194	16.3	1.8	0.47	3.7	7.1	27x
32-EH	EE	8.44	962	42.2	0.89	581	76.5	1.7	0.55	3.0	5.7	17
33-EL	EE	5.53	309	11.7	0.92*	360	47.1	0.86x	0.25x	3.5	7.0	24x
500°C, test runs												
6-1	CC	7.19	1160	31.4	2.53	641	74.5	1.8x	0.42	4.3x	1.6+	6.7+
6-2	CC	6.86	1240	24.3	2.54	662	106.	1.9x	0.23+	6.1+	1.4+	12 x
6-5	EE	9.09	1140	61.7	2.04	823	82.7	1.4	0.75+	1.9+	3.2+	6.0+
6-10	DD	7.11	1171	44.2	1.26	962	40.4	1.2	1.1+	1.1+	4.6x	5.2+
T-1	EE	7.44	111	49.4	0.95	120	53.9	0.93+	0.92+	1.0+	8.5x	8.6x
T-1-2	EE	7.28	696	29.6	0.89	531	72.4	1.3	0.41	3.2	6.2	20.
T-2-2	EE	6.93	668	27.4	0.87	527	73.4	1.3	0.37	3.4	6.3	21.
T-3-1	EE	6.86	697	30.8	1.23	558	86.4	1.3	0.36	3.5	4.5x	16.
T-3-2	EE	6.73	630	28.6	1.17	604	72.2	1.0x	0.40	2.6	5.5	15.

Table 2-5 (Cont'd)

		Feldspar (Sl)			Vapour #			D		K_D		
No.	Sol.	K(%)	Rb(ppm)	Tl(ppm)	K(%)	Rb(ppm)	Tl(ppm)	Rb	Tl	Rb/Tl	K/Rb	K/Tl
600°D, routine runs												
3-1	DD	5.64	599	13.6	0.24*	449	31.8	1.3	0.43	3.1	18. x	56x
3-3	EE	5.95	460	19.1	0.82*	485	64.1	0.95	0.30	3.2	7.7	24
3-4	EE	10.7	1300	59.2	1.65	836	89.5	1.6	0.66x	2.3x	4.2	9.8
3-9	EE	9.91	1090	43.9	1.59	858	93.4	1.3	0.47	2.7	4.9	13
R-16	DD	6.03	1050	20.0	1.07	577	41.5	1.8	0.48	3.8	3.1	12
R-17	EE	5.44	351	13.4	0.54*	340	51.3	1.0	0.26	3.9	9.7x	38x
R-18	EE	8.02	843	20.4	1.01*	654	97.3	1.3	0.21x	6.2x	6.2	38x
6-4	DD	8.53	1620	28.3	0.63	763	47.2	2.1	0.60	3.5	6.4	23
8-4	CC	5.58	268	1.8	1.03	255	6.8	1.1	0.26	4.0	5.2	21
8-5	CC	7.70	629	3.46	2.04	290	9.41	2.2x	0.37	5.9x	1.7x	10
8-6	CC	10.7	934	4.1	2.00	358	10.33	2.6x	0.40	6.6x	2.0	14
8-7	DD	6.35	451	11.9	1.54*	559	27.8	0.81x	0.43	1.9x	5.1	9.7
8-8	DD	6.05	1070	24.2	1.23	683	40.7	1.6	0.59	2.6	3.2	8.3
8-9	DD	9.22	2223	41.8	0.76	694	45.2	3.2x	0.93x	3.5	3.8	13
8-10	EE	7.02	737	31.1	1.65	657	79.6	1.1	0.39	2.9	3.8	11
8-11	EE	7.45	852	39.5	1.51	612	74.8	1.4	0.53	2.6	3.6	9.4
8-12	EE	10.4	1330	18.6	2.68	996	112.	1.3	0.17x	8.1x	2.9	23
600°C, test runs												
6-7	CC	10.1	1080	39.7	0.99*	660	99.6	1.6	0.40	4.1	6.2	26
6-11	EE	9.57	1110	30.8	1.57	805	99.7	1.4	0.31	4.5	4.4	20
6-12	FF	6.93	1280	47.8	0.66	1008	134.	1.3	0.36	3.6	7.1	25

Table 2-5 (Cont'd)

No.	Sol.	Feldspar (Sl) K(%)	Feldspar (Sl) Rb(ppm)	Feldspar (Sl) Tl(ppm)	Vapour # K(%)	Vapour # Rb(ppm)	Vapour # Tl(ppm)	D Rb	D Tl	K_D Rb/Tl	K_D K/Rb	K_D K/Tl
700°C, routine runs												
1-CH	DD	5.72	433	5.96	0.60*	571	44.0	0.76	0.14	5.6	13.x	70.x
2-CL	CC	6.06	203	1.11	1.21*	429	9.69	0.47	0.11	4.1	11.	44.
3-CH	CC	6.68	317	1.24	1.32	404	10.8	0.79	0.12	6.8	6.5	44.
6-EH	EE	6.57	388	10.4	1.25*	781	93.9	0.50	0.11	4.5	11.	48.
7-DL	DD	5.23	235	3.05	0.68	515	36.2	0.46	0.08	5.4	17.x	92.x
8-EH	EE	5.70	292	8.46	1.08	596	76.6	0.49	0.11	4.4	11.	48.
9-EL	EE	5.15	287	6.95	1.07	344	66.0	0.83	0.11	7.9	5.8	46.
10-EL	EE	5.62	255	5.71	1.24*	735	82.1	0.35x	0.07	5.0	13.x	65.
R-7A	DD	4.68	250	3.06	2.09	422	35.8	0.59	0.09	6.9	3.8	26.
R-10	EE	4.91	251	5.02	2.78	654	86.7	0.38x	0.06x	6.6	4.6	31.
6-14	EE	9.04	880	8.40	1.50	880	113.	1.0	0.07	14. x	6.0	81.x
8-16	EE	6.96	717	25.6	1.77	694	87.4	1.0	0.29x	3.5	3.8	13.x
8-17	EE	7.09	738	26.3	1.39	616	84.3	1.2x	0.31x	3.8	4.3	16.x
8-18	EE	10.4	1130	29.2	2.60	1050	108.	1.1x	0.27	4.0	3.7	15.x
T-4-1	EE	5.65	844	20.5	3.58	659	110.	1.3x	0.19	6.9	1.2x	8.5x

\# All results for the vapour have been corrected by material balance checks, except those marked by (*).

\+ This value from unsuccessful test run was eliminated when calculating data for table 2-9a.

x This value lies outside the $\bar{x} \pm 1s$ interval shown in table 2-9a, and hence was eliminated when calculating data for table 2-9b.

600°C. The results are reported in tables 2-6 to 2-8 and compared to the results from the routine runs in Table 2-5. These routine results are used as reference since they represent runs of duration of about 30 days, twice as long as the estimated time required to reach equilibrium (see 2-2-1a). Due to a shortage of data at 500°C and to the similarity between these and those at 600°C (see table 2-5 and later discussions), the results at 500°C and 600°C were combined to compute the pooled mean ($\bar{x}$) and standard deviation (s) for testing (Tables 2-6 to 2-8).

In order to interpret the results from a test run, a significance level of $\bar{x} \pm 1s$ was chosen from the pooled results. Any value falling outside this range was judged to indicate that equilibrium had not been reached and is marked by an (x) in tables 2-6 to 2-8.

2-2-1a. Time required to attain equilibrium. For this purpose, the duration of the runs varied in progression of 1, 3, 5, 7, 14 and 28 days as indicated in Table 2-6.

Most of the runs of shorter than 14 days gave variable results outside the $\bar{x} \pm 1s$ range. For the others of longer duration, values of D and K_D remained more or less constant. Hence the results became consistent after 14 days and it was reasonably sure that equilibrium had been reached.

Table 2-6. Data for time-test runs*

Capsule	Days	D(Rb)	D(Tl)	K_D(Rb/Tl)	K_D(K/Rb)	K_D(K/Tl)
T-3	1	0.35(x)	0.48	0.73(x)	1.8(x)	13.0
T-4	3	0.97	0.71(x)	0.99(x)	9.7(x)	9.4
T-2	5	0.72(x)	0.73(x)	1.0(x)	8.5	9.6
T-1	7	0.93(x)	0.92(x)	1.0(x)	8.5	8.6
T-1-2	7	1.3	0.41	3.2	6.2	20.
T-2-2	14	1.3	0.37	3.4	6.3	21.
T-3-1	28	1.3	0.36	3.5	4.4	16.
T-3-2	28	1.0	0.40	2.6	5.5	15.
Initial		0.10	0.005	3.2	10.	200.
$\bar{x}$ (table 2-5)#		1.55	0.46	3.74	5.71	20.
s (table 2-5)#		0.59	0.20	1.63	3.50	12.

* All runs were at 500°C and using solution EE

\# Computed from table 2-5, after pooling the results from 500°C and 600°C, but excluding all those from test-runs.

(x) A result that lies outside the range of $\bar{x} \pm 1s$.

2-2-1b. Temperature reversal runs. The purpose of this set of tests was to determine whether equilibrium at one temperature can be reached after preliminary reaction at a higher temperature.

A set of capsules was maintained at 700°C for seven days, and then, without quenching, reduced to 500°C or 600°C for a further period of 14 or 30 days as specified in Table 2-7.

For runs at 600°C, most of the results compare favourably with the general results for the routine runs, except for D(Tl) and K_D(K/Tl) in run T-4-2, the only run of final 14 days duration.

At 500°C, all results of D(Rb) and K_D(K/Rb) fell within the range of $\bar{x} \pm 1s$ of the routine results. Results for D(Tl) and hence K_D(Rb/Tl) and K_D(K/Tl) were mixed, generally indicating a lack of consistency with the routine results. From another point of view, although D(Rb) and K_D(K/Rb) show successful reversals in all the runs, all the other results indicate unsuccessful equilibration.

Hence it appears that if equilibrium is to be approached from a higher temperature, a higher final temperature and longer duration, such as 600°C and 30 days, are required for complete equilibration.

This observation can be explained in terms of the rate and mechanism of reaction. At the beginning of the run, the system was greatly out of equilibrium, and the faster reactions such as dissolution and recrystallization would occur. Also, since the concentration contrast

Table 2-7. Data for temperature-reversal test runs.

No.	Sol.	Temperature*	Duration*	D(Rb)	D(Tl)	K_D(Rb/Tl)	K_D(K/Rb)	K_D(K/Tl)
6-5	EE	500	30	1.4	0.75(x)	1.9(x)	3.2	6.0(x)
6-10	DD	500	30	1.2	1.1 (x)	1.1(x)	4.6	5.2(x)
T-4-3	EE	500	14	1.8	0.21(x)	8.2(x)	2.4	20.
6-11	EE	600	30	1.4	0.31	4.5	4.4	20.
6-12	FF	600	30	1.3	0.36	3.6	7.0	25.
T-4-2	EE	600	14	1.1	0.17(x)	6.8(x)	3.2	22.
$\bar{x}$ #				1.55	0.46	3.75	5.71	20.
s #				0.59	0.20	1.63	3.5	12.

* All runs were initially heated to 700°C for 7 days.

\# See table 2-6

between the feldspar and the solution was also large, diffusion would occur at a faster rate. When the temperature was reduced to 500°C or 600°C, at the end of one week, the faster reactions would have completed or greatly slowed down and re-equilibration would be dominated by the slower diffusion mechanism with a lower concentration gradient (see also section 2-4-3c). Hence, complete equilibration would only be realized at a higher temperature and longer duration.

The different behaviour of Rb relative to Tl is probably due to the greater similarity of Rb to the major element K in the feldspar, and higher rate of diffusion (section 2-4-3c)

2-2-1c. Concentration reversal runs. In the routine runs, concentrations of Rb and Tl in the vapour were much higher than in the feldspar Sl. Thus equilibrium was approached by Sl taking in Tl and Rb from the coexisting vapour (Fig. 2-1 and Fig. 2-2). In order to determine whether the direction of exchange could be reversed, i.e. for the vapour to take in the trace elements from the feldspar, a set of test-runs was made using the same feldspar, but previously spiked with a solution of high Tl (and Rb) concentrations. These spiked feldspars (SP-1 and SP-2) were then re-equilibrated with solution CC for 30 days at temperatures of 500°C and 600°C (Table 2-8).

Table 2-8. Data for concentration-reversal test runs, using spiked feldspar and solution CC.

No.	Feldspar*	Temperature	D(Rb)	D(Tl)	K_D(Rb/Tl)	K_D(K/Rb)	K_D(K/Tl)
6-1	SP-1	500°C	1.8	0.42	4.3	1.6(x)	6.7(x)
6-2	SP-2	500°C	1.9	0.23(x)	8.1(x)	1.4(x)	12.
6-7	SP-1	600°C	1.6	0.40	4.1	6.2	26.
Initial*			1.45	14.4	0.10	0.72	0.072
$\bar{x}$ #			1.55	0.46	3.75	5.71	20.
s #			0.59	0.20	1.63	3.50	12.

* Feldspar composition: SP-1 K=4.88%, Rb=1020 ppm, Tl=171 ppm;
SP-2 K=5.60%, Rb=1160 ppm, Tl=204 ppm;

\# See table 2-6.

(x) A result that lies outside the range of $\bar{x} \pm 1s$.

Fig. 2-1. Tl distribution between feldspar (Sl)-vapour as an example of concentration-reversal experiments. Circles final composition; triangles starting composition; open symbols routine runs; closed symbols reversal runs; arrows direction of exchange. Concentration in ppm (log-log scale). Data obtained at 500°C and 600°C, see Table 2-5.

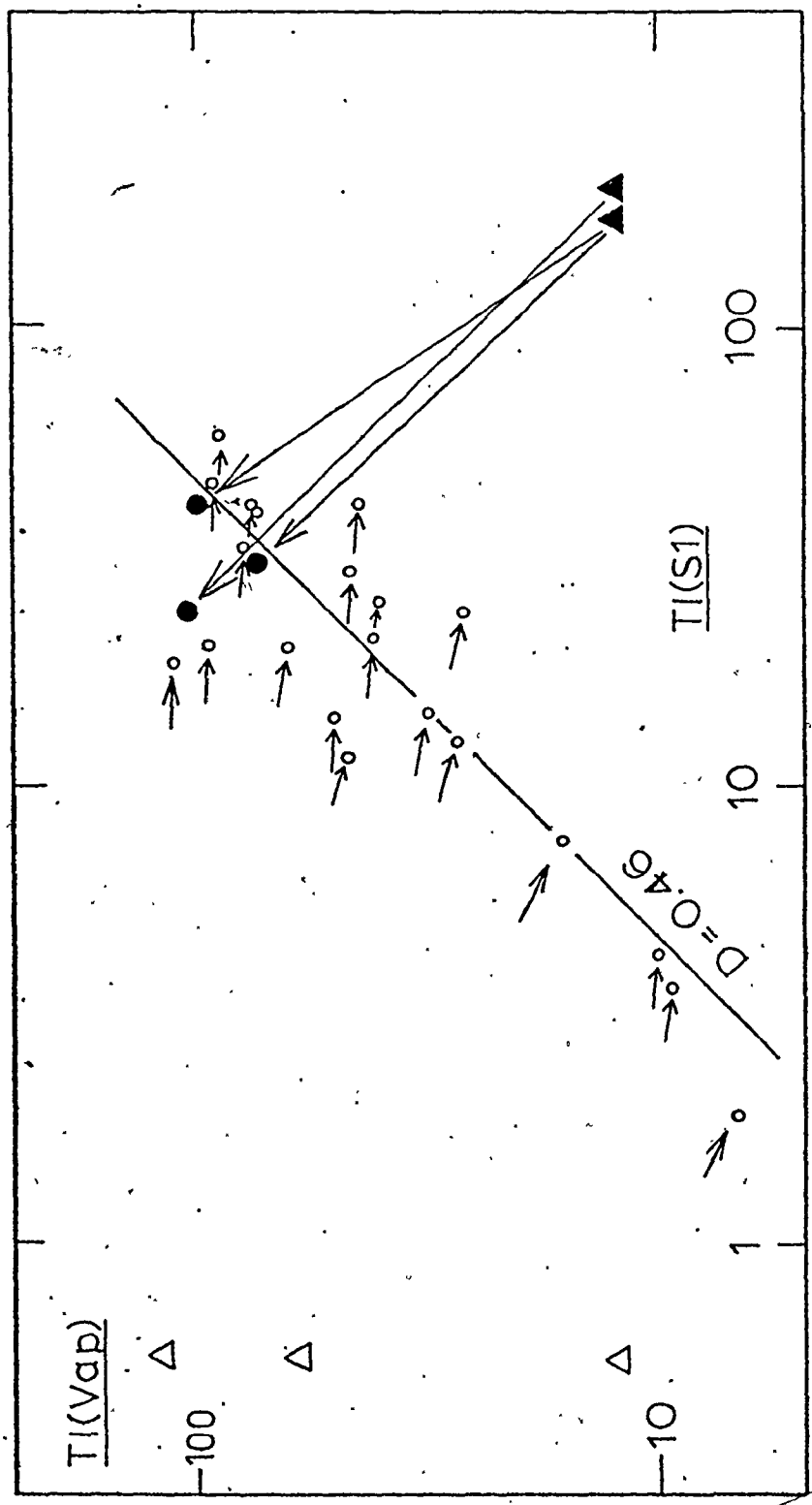
TI(S1)
100
10
1
D=0.46
TI(Vap)
100
10

Fig. 2-2. Rb distribution between feldspar (sl)-vapour as an example of concentration-reversal experiments. Symbols same as in fig. 2-1.

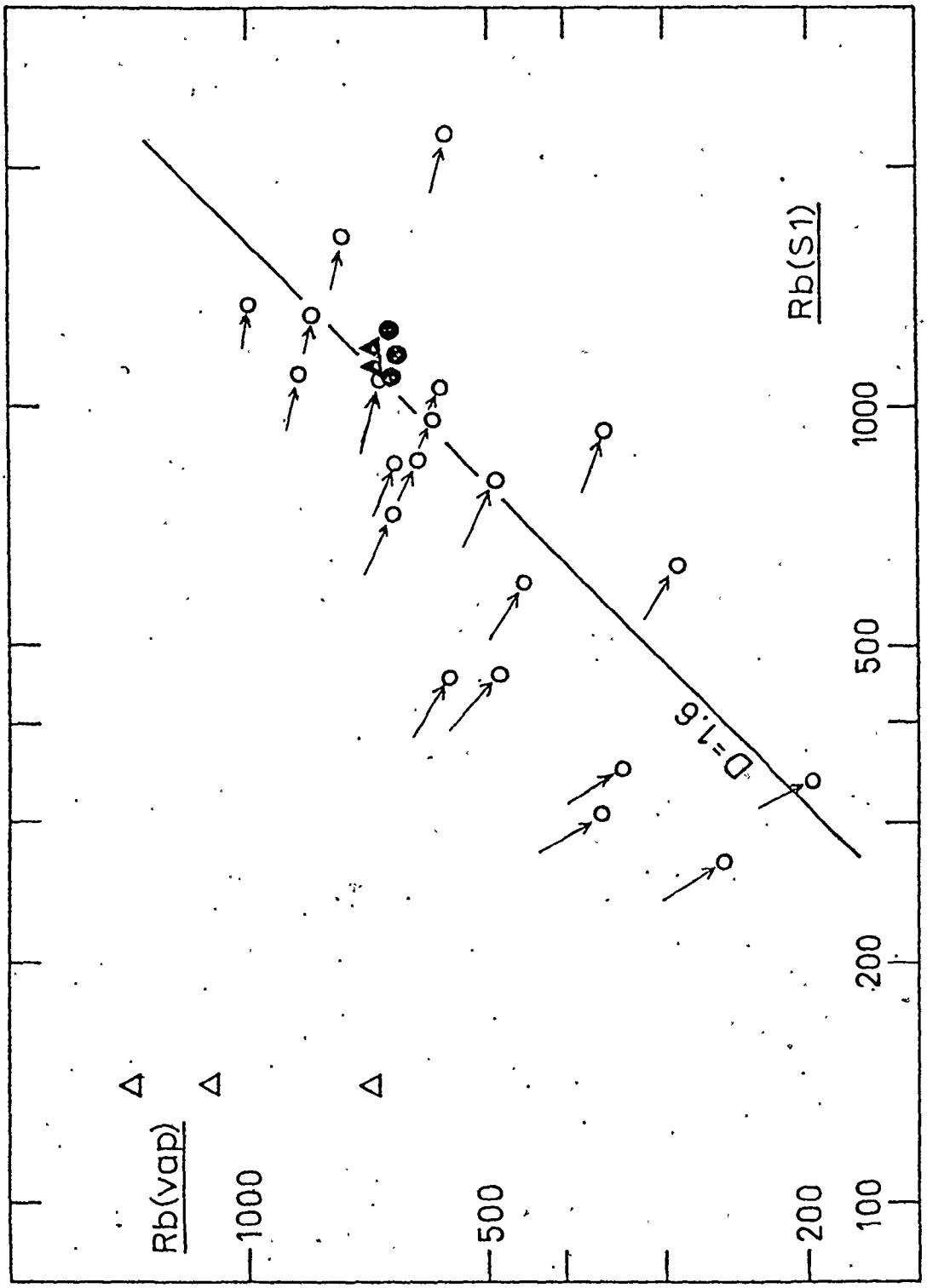
Rb(S1)
1000
500
200
100
D=1.6
Rb(vap)
1000
500
200

All the results for D(Rb), D(Tl) and K_D(Rb/Tl) fell within the range of $\bar{x} \pm 1s$ from the pooled results except for D(Tl) and K_D(Rb/Tl) in run 6-2. This anomalous behaviour is due to a relatively low D(Tl), which probably arose from experimental error.

Two of the results for K_D(K/Rb) and one for K_D(K/Tl), however, were too low, which may again be due to the fact that K is a major element in Sl and does not obey Henry's law.

Apart from the anomalies noted above, it can be concluded that the results are reversible with respect to concentration for Rb and Tl (and Rb/Tl).

2-2-2. Discussion of results

From Table 2-5, the mean, standard deviation and coefficient of variation ($C = 100\ s/\bar{x}$) were computed for each temperature, using all the data available, including those from the successful test-runs (Table 2-9a).

The results generally show large spread, with C ranging from 22% to 65%. As discussed previously, part of the spread might be due to random errors such as contamination by gold dust and loss of vapour during welding of the capsules.

Table 2-9. Summary of data for feldspar (S1)-vapour experiments

	500°C				600°C				700°C			
	$\bar{x}$	s	C(%)	n	$\bar{x}$	s	C(%)	n	$\bar{x}$	s	C(%)	n
a.												
D(Rb)	1.43	0.33	23	12	1.54	0.59	38	20	0.75	0.31	42	12
D(Tl)	0.46	0.19+	41	9	0.43	0.18	42	20	0.14	0.08	59	12
K_D(Rb/Tl)	3.22	0.71	22	9	3.95	1.59	40	20	5.9	2.5	42	12
K_D(K/Rb)	6.40	1.43	22	10	5.45	3.54	65	20	7.6	4.49	59	12
K_D(K/Tl)	17.6	5.5	31	10	20.2	12.4	61	20	43.	25.5	59	12
b.												
D(Rb)	1.45	0.22	15	8	1.4	0.30	21	16	0.69	0.22	32	10
D(Tl)	0.43	0.066	15	7	0.41	0.10	24	16	0.10	0.03	33	12
K_D(Rb/Tl)	3.3	0.37	26	7	3.4	0.60	18	14	5.4	1.4	26	14
K_D(K/Rb)	6.3	0.65	10	6	4.7	1.6	34	17	6.1	3.0	45	11
K_D(K/Tl)	18	2.4	13	6	16	6.4	38	17	44	12	27	8

a. All data from table 2-5, except those from unsuccessful test-runs (marked +).

b. Same as a. after further discarding those results that fall outside the range of $\bar{x} \pm 1s$ from a. (marked x) (see footnote in table 2-5).

In order to counteract such random errors and to facilitate later discussions, it was desirable to identify and eliminate some of the anomalous values from table 2-5. Using the same treatment as in section 2-2-1, all those values that fall outside the range of $\bar{x} \pm 1s$ were discarded. From the remaining values, new $\bar{x}$, s and C were computed (Table 2-9b). These new $\bar{x}$ values are generally not too different from the old ones, but the spread is naturally reduced. Hence the results for D(Rb), D(Tl) and K_D(Rb/Tl) show variations ranging from 11% to 33%, which are not too uncommon in such experiments. Moreover, higher variation is usually associated with Tl [both D(Tl) and K_D(Rb/Tl)], which may be due to the additional possibility of the oxidation of Tl to the +3 state since the experiments were not buffered. Also, Tl was probably affected the most by adsorption by the gold capsule, due to its low bulk concentration and similarity in chemical properties to gold. Higher variations are also observed for the 700°C results relative to those of lower temperatures. This will be discussed in the next section.

Nevertheless, the Rb and Tl results were reversible with respect to temperature and concentration at least for the runs at 500°C and 600°C; also they show rather strong linear trends and are hence amenable to interpretations.

2-2-3. Temperature effect

Fig. 2-3 shows the distribution of Rb between the feldspar Sl and the coexisting vapour for all the values in table 2-5, except those marked + and x. For each temperature, the average D(Rb) value is also shown.

D(Rb) is very similar for both the 500°C and 600°C runs, but decreases rather markedly from 600°C to 700°C. D(Tl) behaves very similarly to D(Rb) (Fig. 2-4), except the gap between 700°C and the lower temperatures is slightly wider.

The behaviour of K_D(Rb/Tl) (Fig. 2-5) and K_D(K/Tl) (Fig. 2-6) are similar except that the trends with temperatures are reversed.

The trend for K_D(K/Rb) (Fig. 2-7) is not clear. Although the mean at 700°C is, like K_D(K/Tl), greater than that at 600°C (6.5 and 4.7 respectively) it is very similar to that at 500°C (6.3). There is much scatter in the data points rendering any temperature effect very doubtful.

According to the work of Tuttle and Bowen (1950), alkali feldspars of intermediate composition would form a homogeneous phase at 700°C and above, but would unmix at lower temperatures. Hence Sl must have undergone mixing at 700°C, but failed to form a single phase due to the sluggishness of the reaction (see sections 2-4-1c and 2-4-2a). At 600°C and 500°C, unmixing did not take place. Such difference may explain the gap between the results at 700°C and those at lower tempera-

Fig. 2-3. Rb distribution between feldspar (Sl)-vapour. Concentrations in ppm. The 600°C points have been displaced by a factor of 10X to prevent overlap.

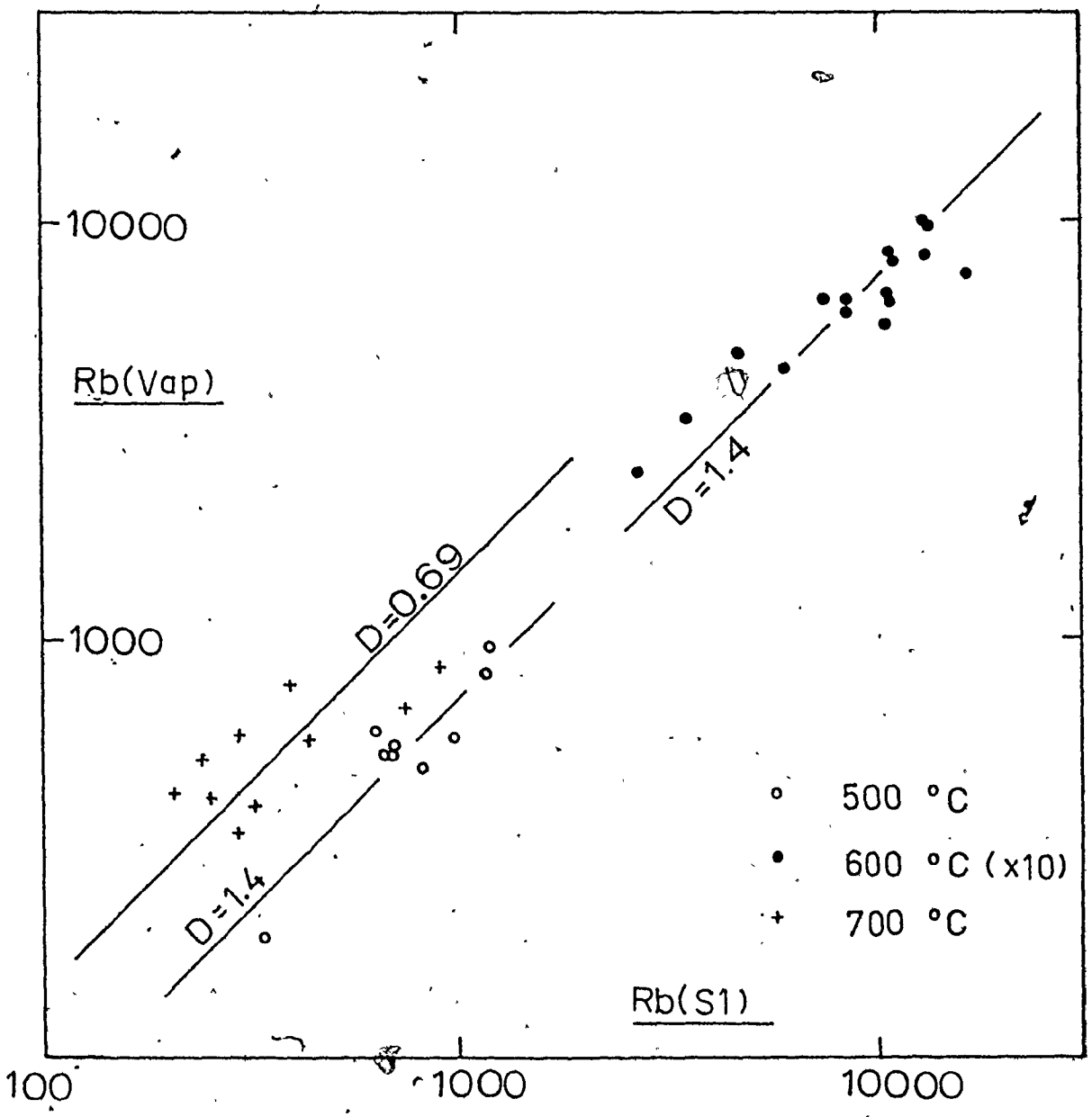
10000
1000
100
1000
10000
Rb(Vap)
Rb(S1)
D=0.69
D=1.4
D=1.4
500 °C
600 °C (x10)
700 °C

Fig. 2-4. Tl distribution between feldspar (Sl)-vapour.

Concentration in ppm. Symbols same as in Fig. 2-3.

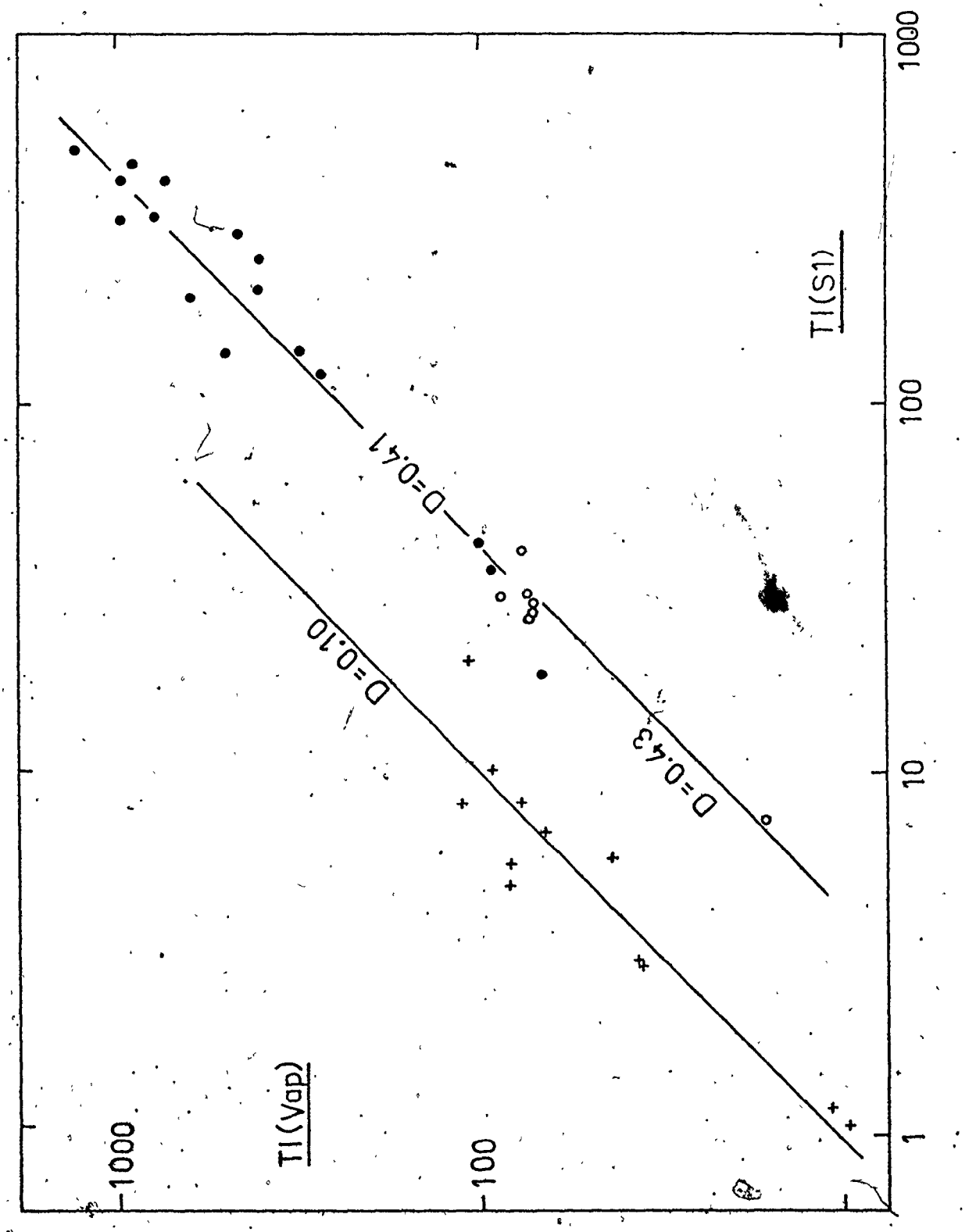
TI(S1)
TI(Vap)
1000
100
10
1
1000
100
D=0.41
D=0.43
D=0.10

Fig. 2-5. Correlation of Rb/Tl between feldspar (Sl)-vapour. Symbols same as in Fig. 2-3.

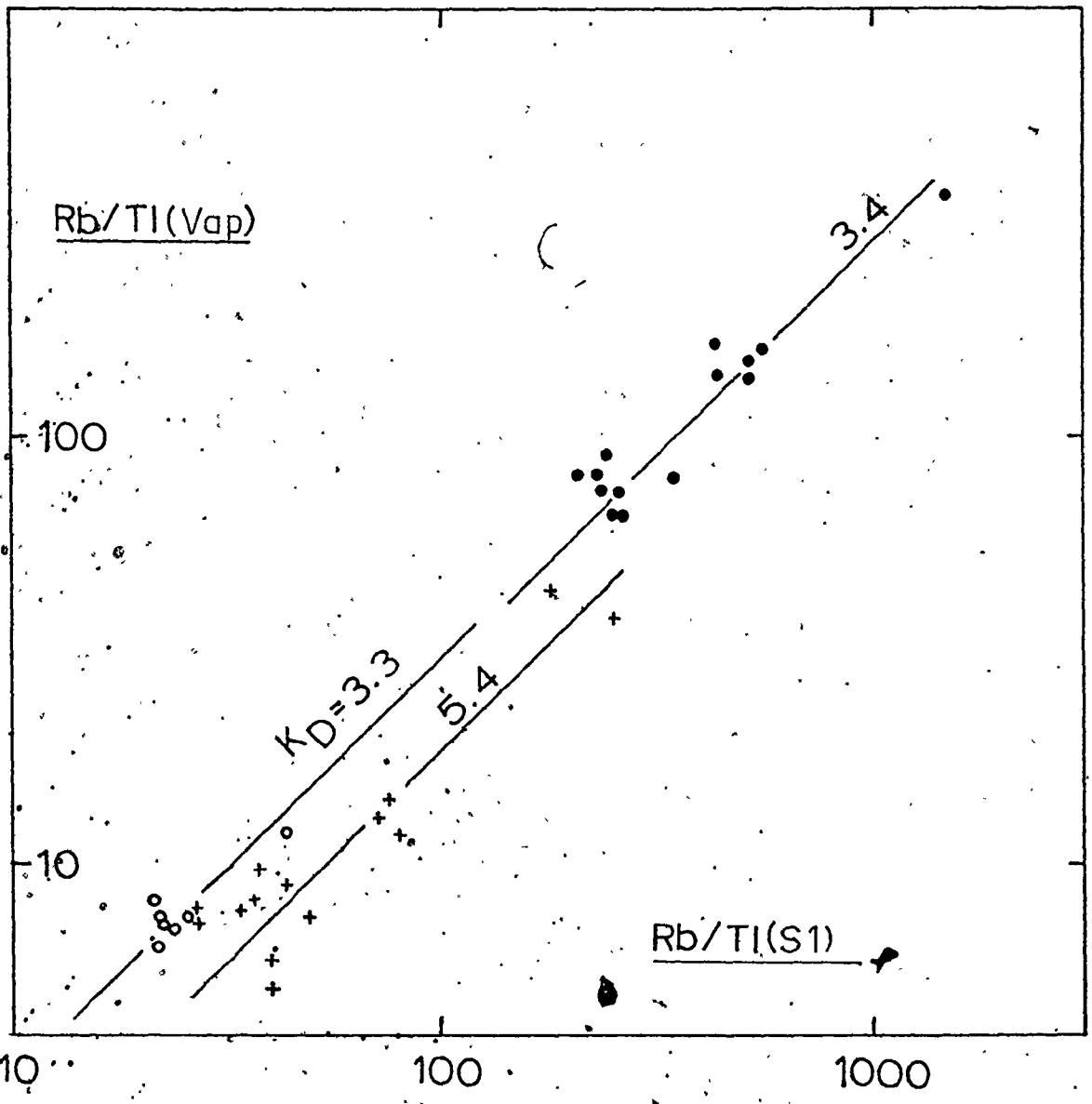
Rb/Tl(Vap)
100
10
10
100
1000
Rb/Tl(S1)
K_D=3.3
5.4
3.4

Fig. 2-6. Correlation of K/Tl between feldspar (Sl)-vapour. Symbols same as in Fig. 2-3.

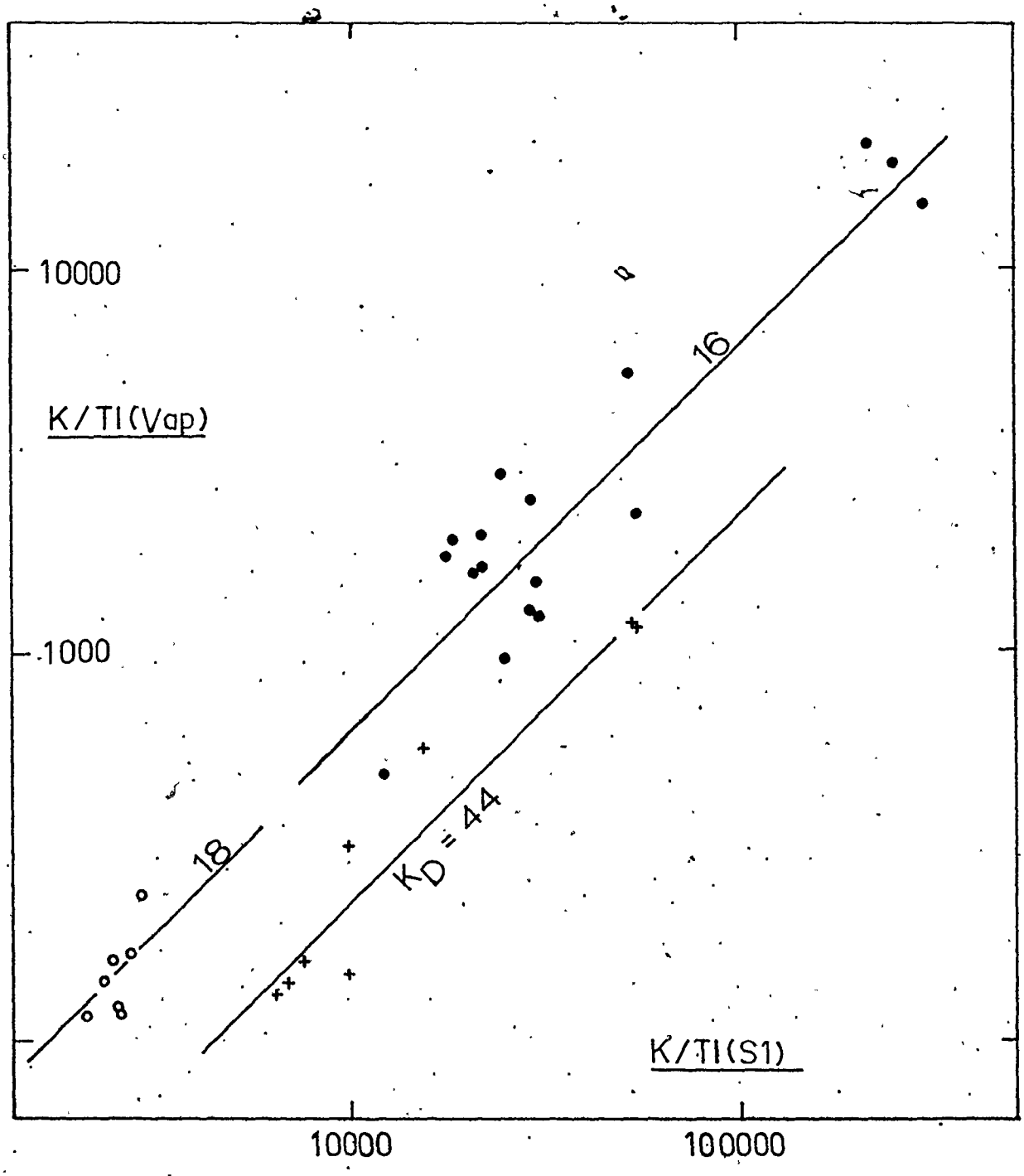
10000
1000
K/TI(Vap)
16
18
8
$K_D = 44$
K/TI(S1)
10000
100000

Fig. 2-7. Correlation of K/Rb between feldspar (Sl)-vapour.

Symbols same as in Fig. 2-3.

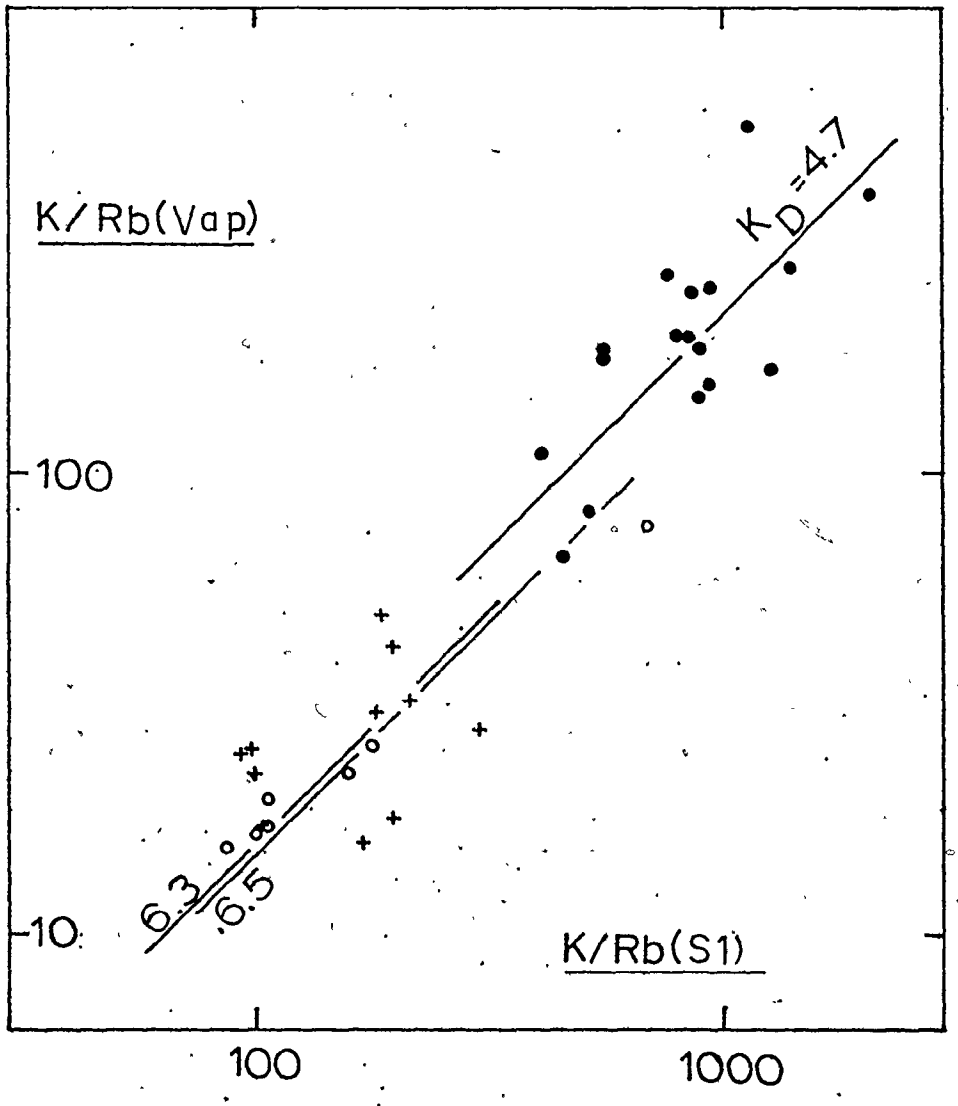
K/Rb(Vap)
100
10
100
1000
K/Rb(S1)
K_D=4.7
6.3
6.5

tures, as well as the former being generally more variable (section 2-4-2a). The general similarities of the results at 500°C and 600°C reflect the coherence of the elements K, Rb and Tl.

2.3. Other feldspar-vapour SSV+ runs

In this section, results for runs with microcline Ml and vapour and all the fusion runs will be discussed. The experimental details of these runs have been described in section 2-1-1. The data are reported in Table 2-10. Analyses of the vapour in most of these runs have been corrected by material balance as described in section 2-1-2, where necessary.

Fig. 2-8 shows graphically the value of D(Rb) and D(Tl) for all the feldspar-vapour runs. Results for Sl are shown only as the $\bar{x} \pm 1s$ ranges from the final data reported in Table 2-9b, while the rest are shown individually. Fig. 2-9 is similar to Fig. 2-8 for all the K_D values.

2-3-1. Ml regular runs

All the results for Ml-vapour regular runs show the same trends with temperature as for Sl. Hence both D(Rb) and D(Tl) decrease while all the K_D values increase from 500°C to 700°C (although the trend for K_D(K/Rb) in Sl is not as clear).

+ single solid-vapour

Table 2-10. Data for regular runs with Ml and fusion runs with Sl, S2 and Ml

		Feldspar			Vapour #			D		K_D		
No.	Sol.	K(%)	Rb(%)	Tl(ppm)	K(%)	Rb(%)	Tl(ppm)	Rb	Tl	Rb/Tl	K/Rb	K/Tl
500°C, Ml-vapour, regular runs.												
9-1	DD	12.70	2.06	137	1.35	0.10	55.0	21	2.5	8.3	0.45	3.6
9-3	DD	12.72	1.69	145	1.14	0.085	46.0	23	3.2	7.3	0.48	3.5
9-5	DD	12.34	2.09	138	1.60	0.082	54.0	25	2.6	10.	0.31	3.0
700°C, Ml-vapour, regular runs.												
9-4	DD	12.60	2.02	102	0.93	0.120	88.0	17	1.2	15	0.81	12
9-6	DD	13.18	2.07	104	0.73	0.087	81.0	24	1.3	19	0.75	14
700°C, Sl-vapour, fusion runs.												
14-1	EX	5.94	0.077	180	0.90	0.047	346	1.6	0.52	3.1	4.0	13
14-2	EX	6.08	0.075	180	0.90	0.055	372	1.4	0.48	2.9	4.9	14
700°C, Ml-vapour, fusion runs.												
14-3	EX	11.23	1.42	314	1.98	0.488	361	2.9	0.87	3.3	1.9	6.6
14-4	EX	10.94	1.41	320	2.20	0.502	356	2.8	0.90	3.1	1.8	5.6
800°C, Sl-vapour, fusion runs.												
14-5	EX	5.65	0.094	197	1.23	0.039	347	2.4	0.57	4.2	1.9	8.1
14-6	EX	5.57	0.093	235	1.32	0.042	325	2.2	0.72	3.1	1.9	5.9
800°C, S2-vapour, fusion runs.												
14-9	EX	13.75	0.073	156	2.79*	0.026*	416	2.8	0.38	7.5	1.8	13
14-10	EX	13.91	0.064	180	3.05*	0.022*	391	2.9	0.46	7.7	1.6	9.9
800°C, Ml-vapour, fusion runs.												
14-7	EX	11.19	1.42	260	2.00	0.505	398	2.8	0.65	4.3	2.0	8.6
14-8	EX	11.32	1.46	208	1.92	0.441	446	3.3	0.47	7.0	1.8	13

All the data for the vapour have been corrected by material balance, except those marked by (*).

However, the magnitude of all the results differs considerably. Results for Ml are higher in D(Rb), D(Tl) and K_D(Rb/Tl) but are lower in K_D(K/Rb) and K_D(K/Tl). The greatest difference, up to over an order of magnitude, is in D(Rb) while the least is in K_D(Rb/Tl), which differs only by a factor of about 3.

2-3-2. Fusion runs

In the fusion runs, both the natural sanidine Sl and microcline Ml were used at 700°C and 800°C, while the gel S2 was used only at 800°C.

At 700°C, most of the results for Ml in these fusion runs differ markedly from those in the regular runs, namely most of the D and K_D values are relatively lower [except for K_D(K/Rb)]. D(Rb) in particular, is lower by 5-9 times while D(Tl) is lower only by less than two times. Turning to Sl at 700°C, all the results for the fusion runs are similar to those for the regular runs at 600°C but different from those at the same temperature. The differences in most of the results between Sl and Ml observed in the regular runs are generally reduced in the fusion runs, especially for D(Rb). For D(Tl), such difference is only slightly reduced and for K_D(K/Tl) it is actually enhanced.

At 800°C, most of the results for all the different initial feldspars, including those for S2, are very similar to each other. The trends with temperature for the results of Ml in the fusion runs are

Fig. 2-8. D(Rb) and D(Tl) ($\log_{10}$) for different pairs of feldspar-vapour at different temperatures. Solid symbols regular runs; open symbols fusion runs; circles S1; triangles M1; squares S2; error bars ± 1s (S1 regular runs only).

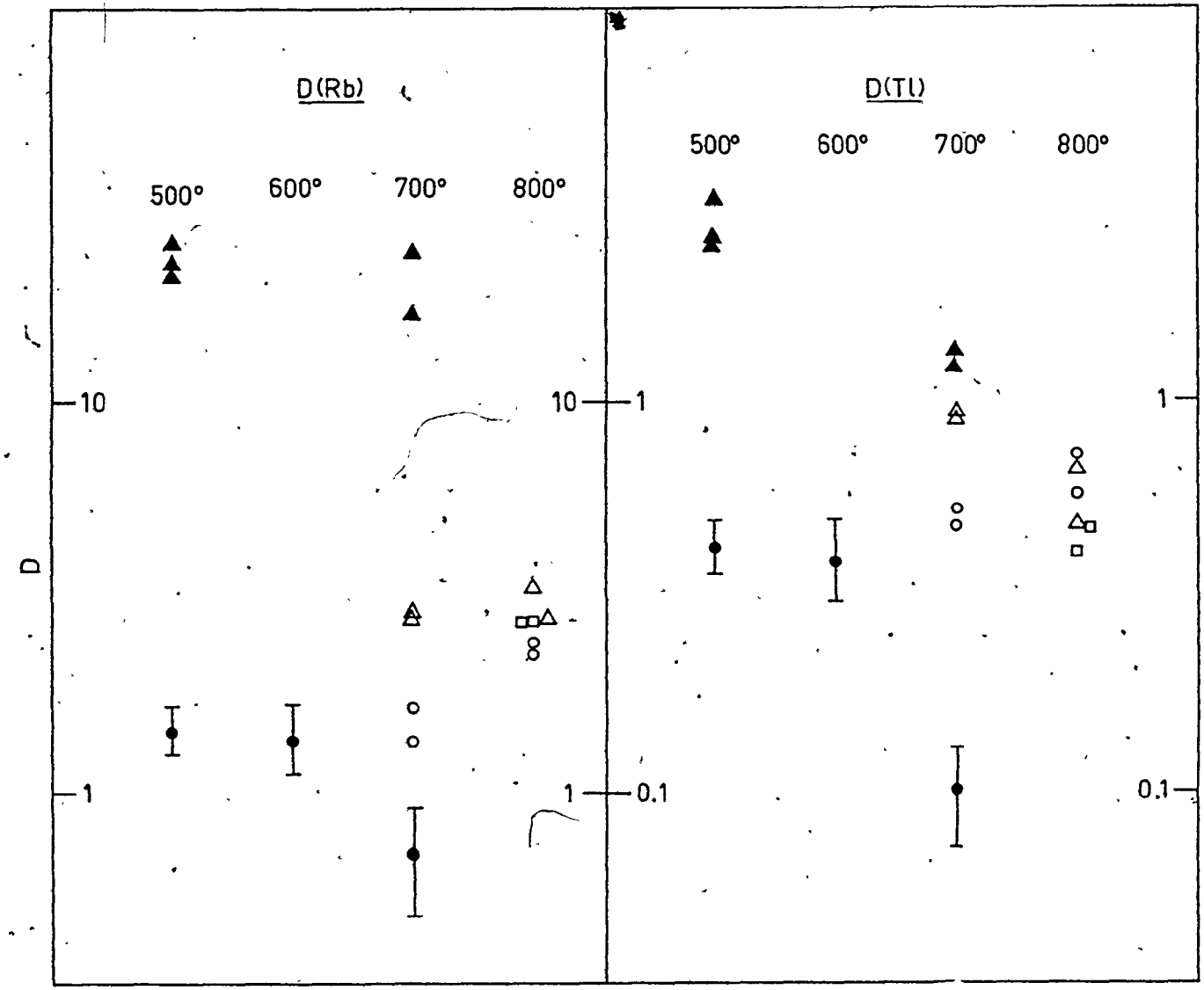
D(Rb)
500°
600°
700°
800°
10
1
D
10
1
D(Tl)
500°
600°
700°
800°
1
0.1
D
0.1

Fig. 2-9. K_D(Rb/Tl), K_D(K/Rb) and K_D(K/Tl) ($\log_{10}$) for different pairs of feldspar-vapour at different temperatures. Symbols same as Fig. 2-8; arrows range reported in literature for K_D(K/Rb).

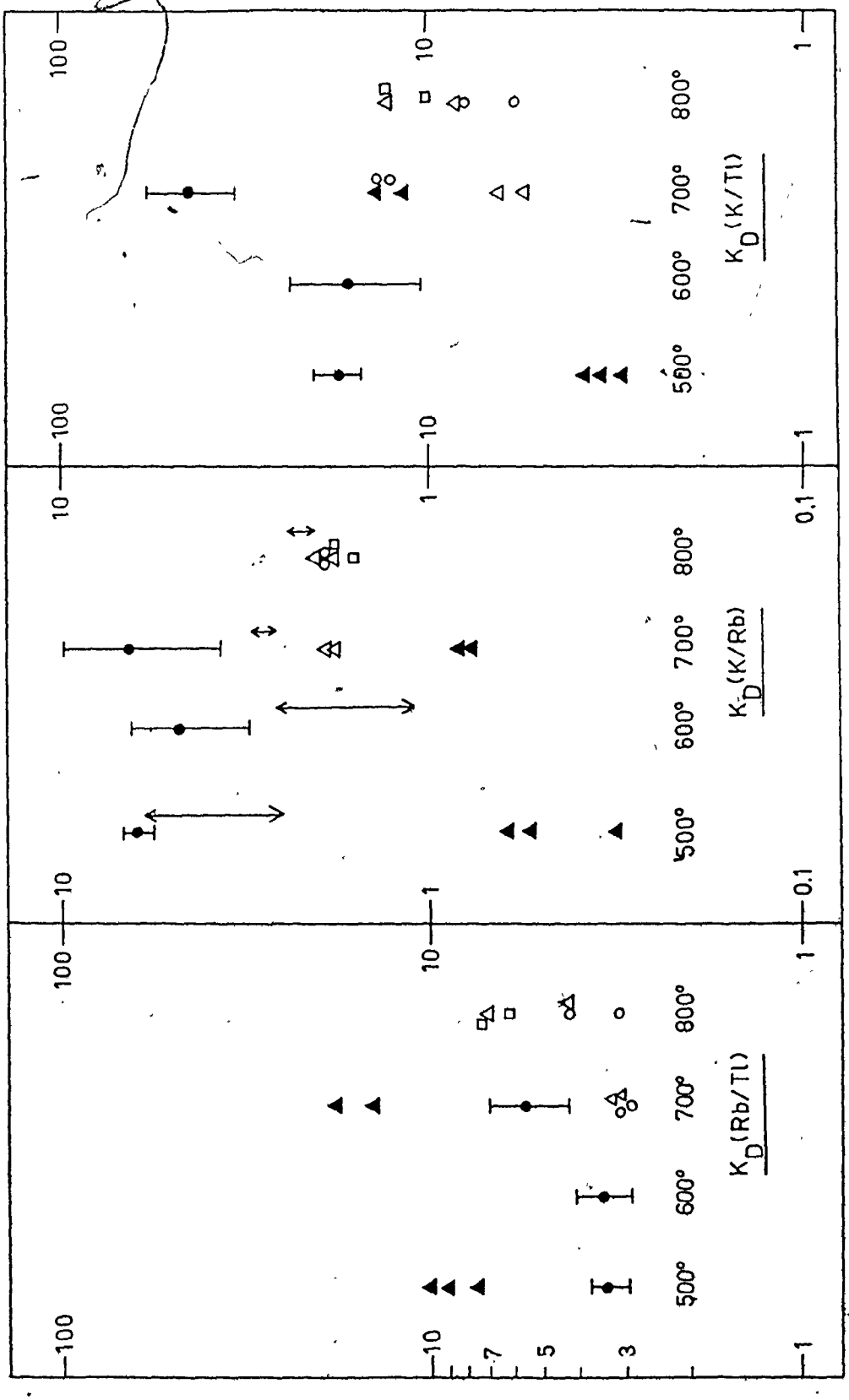
100
10
1
500°
600°
700°
800°
K_D(K/Tl)
100
10
1
0.1
500°
600°
700°
800°
K_D(K/Rb)
100
10
7
5
3
1
500°
600°
700°
800°
K_D(Rb/Tl)

similar to those in the regular runs. However, with the exception of K_D(Rb / Tl), all the trends for Sl in the fusion runs are different from those in the regular runs.

In summary, the results for the regular runs differ markedly between the two initial feldspars Sl and Ml. Such differences are generally reduced in the fusion runs at 700°C and all become very similar at 800°C.

2-4. Discussion of all feldspar-vapour results

The previous discussions have summarized the experimental results, and showed considerable and unexpected variations in the various partition ratios. The reasons for these variations will be further analysed in the following.

2-4-1. Comparison with previous experimental data

2-4-1a. K_D(K/Rb). Several workers reported K_D(K/Rb) data for the pair alkali feldspar-vapour for various temperatures and pressures ranging from 0.5 to 2 Kbar (Table 2-11). Most workers used synthetic K-feldspar in the experiments except for Foland (1973) and Hofmann and Giletti (1970) who used natural K-rich orthoclase. As pointed out by Bernotat et al. (1976), agreement among most of the data is rather good at higher temperatures, but poor at lower temperatures.

Table 2-11. K_D (K/Rb) for alkali feldspar-vapour from several workers.

References	Temperature (°C)									
	400	500	510	600	610	650	670	700	745	800
Chelishchev (1967)	5.0	2.5		1.1						
Sretenskaya (1967)	6.2		2.5		1.2		0.74	0.54		
Lagache (1968)				2.4						
Hofmann and Gilette (1970)*				2.6			2.1			
Beswick (1973)		5.9						3.0		2.2
Foland (1973)*								2.6	2.3	2.1
Lagache and Sabatier (1973)						2.1				
Volfinger (1976)	3.8	2.5		2.4						2.4
This study:										
Sl, fusion								4.5		1.9
Ml, fusion								1.9		1.9
S2, fusion										1.7
Sl, regular		6.3		4.7				6.5		
Ml, regular		0.41						0.78		

* natural orthoclase was used as initial feldspar, all others used synthetic minerals.

In comparison, most of the results for the fusion runs from this study are slightly lower (Fig. 2-9), but are within experimental error from those reported by other workers, except for Sl at 700°C, which is higher by about 50%. As for the regular runs, results for Sl are again relatively higher, but are rather compatible with the others. Results for Ml, however, are relatively much too low (by up to ten times). Moreover, all previous workers reported either a decrease or constant K_D(K/Rb) with higher temperature, similar to all sets of data from this study except for Ml regular runs, which show a marked increase.

Thus it appears that most of the K_D(K/Rb) results from this study are generally compatible with but somewhat different from those reported in the literature. The most satisfactory results are those for the fusion runs with the K-rich feldspars Ml and S2, followed by those for the fusion and regular runs with Sl. The results for the Ml regular runs show the most discrepancy, due probably to a combination of factors, as will be discussed in section 2-4-2.

2-4-1b. K_D(K/Tl) and K_D(Rb/Tl). Very little experimental work has been done on Tl distribution between feldspar and vapour and the data available are either incomplete or unsatisfactory.

Thus Hopson and Eugster (1954) reported that K_D(K/Tl) decreased slightly from 500°C to 800°C, without reporting the actual data.

D(Rb) and D(Tl) calculated from the data reported by Sretenskaya (1967) show very little consistency, due probably to loss of the final vapour and gold capsule adsorption of Tl. Hence, only the K_D values will be discussed, since they should not be affected by loss of the final vapour. This is reflected in the generally better consistency in the results, especially those at higher temperatures (Table 2-12). Thus K_D(K/Tl) shows a decrease from 400°C to 700°C, similar to the trends observed by Hopson and Eugster (1954) and to those for the Sl fusion runs in this study. However, there is very little similarity in the values to any set of data from this study, possibly with the exception at 500°C, which agree with those for the Ml regular runs at 500°C (c.f. Table 2-9 and 2-10).

Similarly, her data for K_D(Rb/Tl), which show no variation with temperature are about 3-20 times lower than those from this study, which generally show an increase with higher temperature (c.f. Fig. 2-9).

The general conclusion to be drawn from the above comparisons, including those for K_D(K/Rb) to a lesser extent, is that the distribution of K, Rb and Tl between feldspar and vapour is still not well known.

Table 2-12. K, Rb and Tl distributions between synthetic and sanidine-vapour (from Sretenskaya, 1967)

T(°C)	K_D(Rb/Tl)#	Mean	K_D(K/Tl)	Mean
400	1.4, 0.50	0.94	4.4, 6.5	5.5
510	1.5, 2.9*, 0.67	1.1	3.4*, 1.8, 1.8	1.8
610	0.87, 1.2*, 0.86	0.86	0.92, 1.4, 1.0	1.1
670	0.87, 0.95	0.91	0.77, 0.59	0.68
700	0.90, 0.98	0.94	0.45, 0.58	0.52

K_D(Rb/Tl) data was computed from the published data, K_D(K/Tl) was given in the article except for 400°C.

* This value is considered anomalous and is not included when computing the mean.

2-4-1c. Na-K distributions. Orville (1963) studied the distribution of Na-K in the system feldspar-vapour under 2 Kbar P_{H_2O} and 500°C-700°C, as summarized in fig. 2-10a. Fig. 2-10b, also taken from Orville, shows similar data from Tuttle and Bowen (1958) on the same system and from Yoder et al. (1957) on the system feldspar-melt at 700°C. In both these diagrams, mole fraction of K/K+Na in the vapour (or melt) was plotted against that in the coexisting feldspar. As pointed out by Orville (1963), there was very little difference between the two systems feldspar-vapour and feldspar-melt with respect to the Na-K distributions. He also attributed the slight difference between his data and those of Tuttle and Bowen (1958) to the difference in starting materials used (gel and glass; see also section 2-4-2).

Na has been analysed in the final products of batch 14 and 13 (MSV runs, Chapter 5) and the data summarized in Table 2-13. No correction had been applied to these data, since this is not feasible for the MSV runs and would involve too much uncertainty. Correction is not necessary due to a) only relative values of Na and K are used and b) such data will only be affected by loss of vapour (assuming no adsorption by the gold capsule) which will result in proportional loss of both elements. These data came from three kinds of different initial feldspars and three different experimental techniques which would explain the minor spread

Fig. 2-10. K-Na distributions (from Orville, 1963)

a. Between alkali feldspar and vapour. Horizontal dashed lines represent extent of feldspar immiscibility. Data from Orville (1963).

b. Between feldspar and melt. Solid line 5Kbar, data from Yoder et al. (1957); dashed lines variable pressure, data from Tuttle and Bowen (1958).

a.

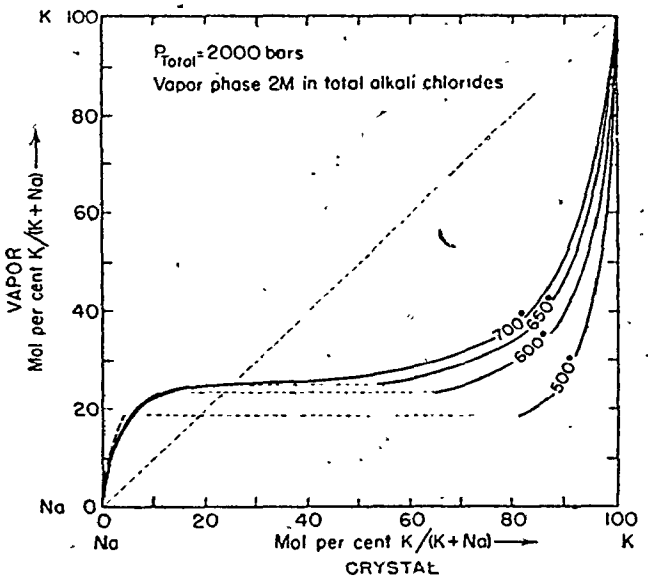
K 100
80
60
40
20
Na 0
P_{Total} = 2000 bars
Vapor phase 2M in total alkali chlorides
VAPOR
Mol per cent K/(K+Na)
700°
650°
600°
500°
0
20
40
60
80
100
Na
Mol per cent K/(K+Na)
K
CRYSTAL

b.

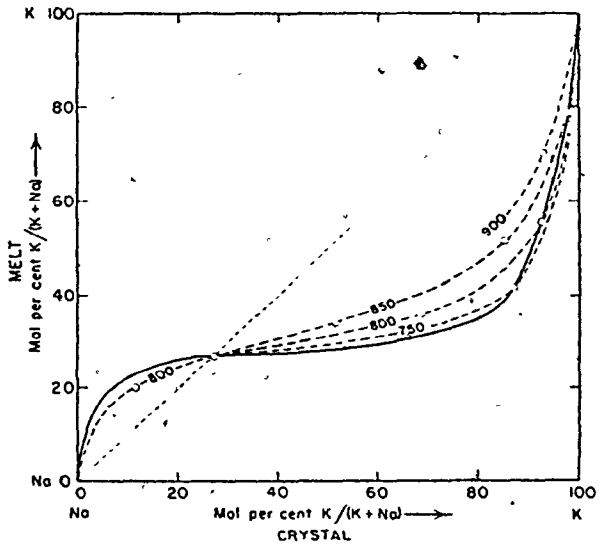
K 100
80
60
40
20
Na 0
MELT
Mol per cent K/(K+Na)
900
850
800
750
0
20
40
60
80
100
Na
Mol per cent K/(K+Na)
K
CRYSTAL

No.	Initial Fs	FELDSPAR K(%)	FELDSPAR Na(%)	FELDSPAR X(Fs)	VAPOUR K(%)	VAPOUR Na(%)	VAPOUR X(Vap)
600°C, MSV regular runs							
13-4	Sl	7.09	3.40	0.55	0.39	1.08	0.18
13-5	Sl	6.63	3.78	0.51	0.53	1.10	0.22
13-6	Ml	10.49	1.87	0.77	0.34	0.76	0.21
14-13A	Ml	9.64	1.78	0.76	0.25	0.75	0.16
14-13B	Sl	6.84	3.46	0.54	0.25	0.75	0.16
14-15	Ml	9.49	1.17	0.83	0.40	0.52	0.31
14-16	Ml	11.24	1.23	0.85	0.44	0.52	0.33
700°C, MSV regular runs							
13-2	Ml	10.54	1.94	0.76	0.72	0.92	0.32
13-3	Ml	10.58	1.43	0.81	0.55	0.59	0.36
13-1	Ml	11.05	1.22	0.85	0.88	0.85	0.38
700°C, SSV fusion runs							
14-1	Sl	5.94	2.42	0.59	0.48	0.67	0.29
14-2	Sl	6.08	2.41	0.60	0.47	0.73	0.27
14-3	Ml	11.23	0.66	0.91	0.63	0.41	0.47
14-4	Ml	10.94	0.69	0.91	0.60	0.41	0.46
800°C, MSV fusion runs							
14-5	Sl	5.65	4.63	0.42	0.39	0.79	0.23
14-6	Sl	5.57	4.52	0.42	0.47	0.80	0.23
14-7	Ml	11.19	0.73	0.90	0.74	0.30	0.59
14-8	Ml	11.32	0.80	0.89	0.76	0.30	0.60
14-9	S2	13.75	0.16	0.98	2.79	0.058	0.97
14-10	S2	13.91	0.18	0.98	3.05	0.072	0.96

Table 2-13. K-Na distribution data. X(Fs), X(Vap) mole fraction of K/K+Na in feldspar and vapour respectively.

Fig. 2-11. Na K distributions between alkali feldspar-vapour (after Orville, 1963).

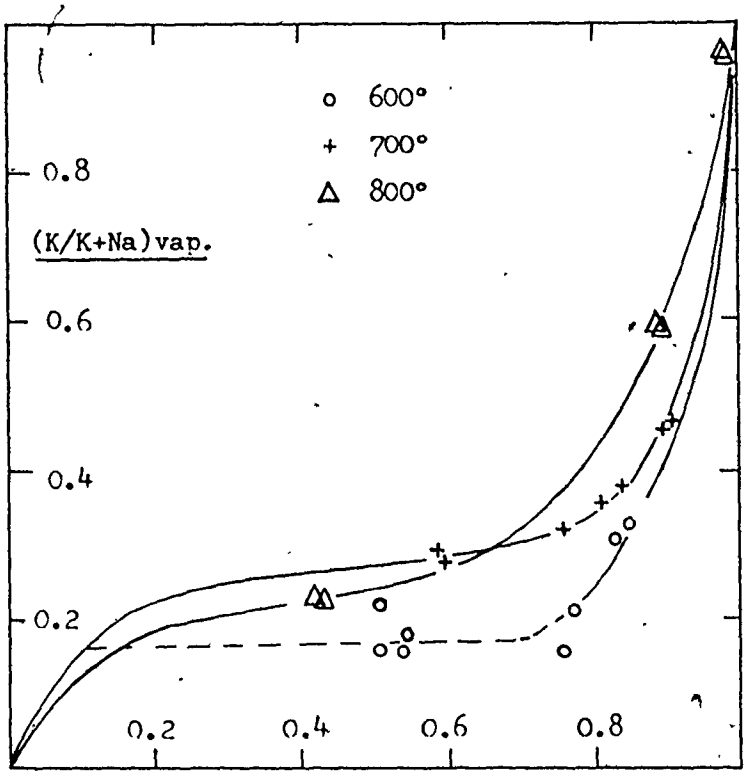
o 600°
+ 700°
△ 800°
0.8
(K/K+Na)vap.
0.6
0.4
0.2
0.2
0.4
0.6
0.8
(K/K+Na)feldspar

of the data points (Fig. 2-11, after Orville, 1963) and discrepancies in the position of some of the lines as compared to Fig. 2-10. The resemblance in the general outline of these diagrams is reasonable.

2-4-2. Factors affecting trace element distributions

There are several differences between the three starting minerals Sl, Ml and S2 and between the fusion and regular runs that might cause the differences in their Rb and Tl distribution patterns as discussed previously. These differences are listed in Table 2-14 and will be discussed in the following sections in conjunction with the possible factors that affect trace element distributions in minerals.

2-4-2a. Structural changes. X-ray diffraction studies (described in Appendix 2) show that both Sl and Ml retained their initial structural states in the regular runs. However, there was a tendency for Sl towards lower and Ml towards higher states (Fig. 2-12a, Table 2-14).

In the fusion runs, Ml (and Sl) became high sanidine at both 700°C and 800°C. The gel S2 also crystallized into a high sanidine.

Sl remained exsolved into two feldspars in all the regular runs and many of the diffraction peaks were rather poorly defined. In the 800°C fusion runs, Sl became a homogeneous sanidine. The two fusion runs at 700°C gave rather poor diffraction patterns, due partly to the fact that the crystals were rather coarse and no grinding was per-

Fig. 2-12. Plot of $2\theta_{\bar{2}04}$ vs. $2\theta_{060}$ for alkali feldspars using CuKα_1 radiation (after Wright, 1968). a. SSV runs, b. MSV runs. + S1 regular runs, ▲ S1 fusion runs, ■ S2 fusion runs, O M1 regular runs, ● M1 fusion runs. 2θ data from Table A-2.

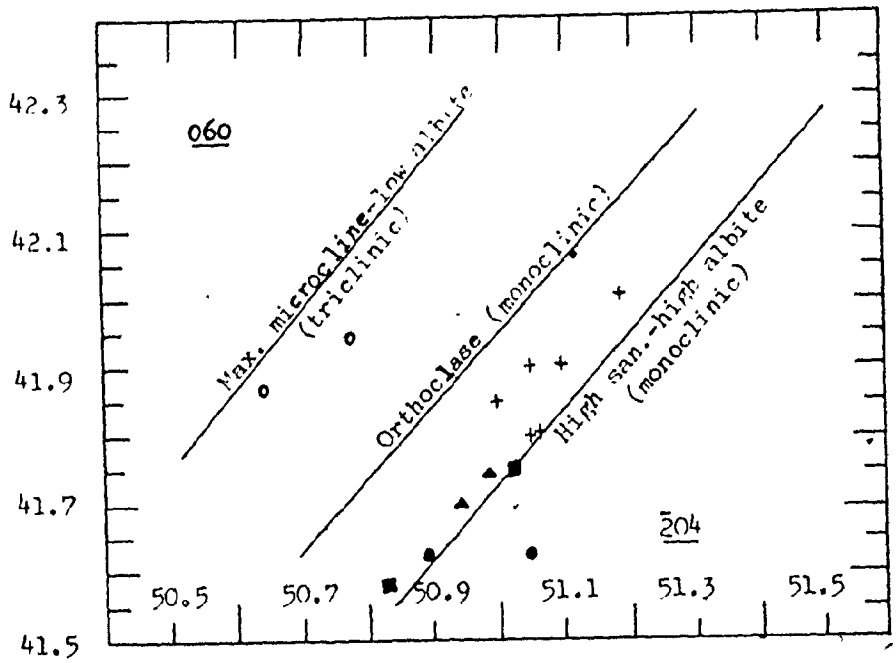
060
Max. microcline-low albite (triclinic)
Orthoclase (monoclinic)
High san.-high albite (monoclinic)
$\bar{2}04$
42.3
42.1
41.9
41.7
41.5
50.5
50.7
50.9
51.1
51.3
51.5

a.

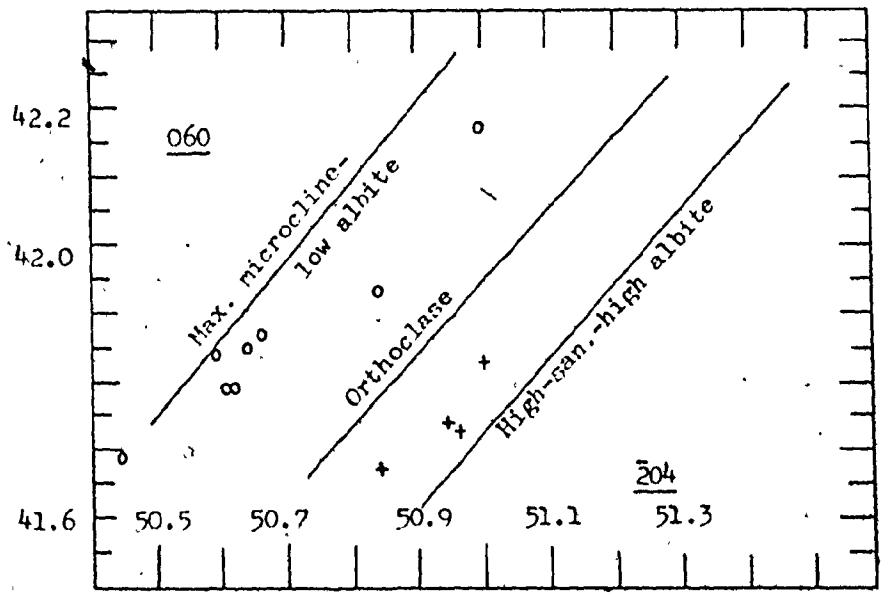
060
Max. microcline-low albite
Orthoclase
High-san.-high albite
$\bar{2}04$
42.2
42.0
41.6
50.5
50.7
50.9
51.1
51.3

b.

Table 2-14. Comparison of starting and final materials.

Minerals	Initial Structure	K(%)	Rb(%)	Final Structure (regular run)	Structure (fusion run)
S1	E; monoclinic	4.66	0.14	E; monoclinic	E(700°);H(800°); monoclinic
M1	H; triclinic	11.3	2.14	H; triclinic	H. monoclinic
S2	gel	14.0	0.00		H. monoclinic

E=exsolved into Ab(Na)-rich and Or(K)-rich phases

H=homogeneous

Table 2-15. Partition coefficients of Rb, Cs, Ba and Sr for the pair Alkali feldspar/plagioclase at 600°C. and 1 Kbar (Iiyama, 1968)

Phases	D(Rb)	D(Cs)	D(Ba)	D(Sr)
$Or_{75}Ab_{25}/An_{30}Ab_{25}$	9.6	4.2	0.78	0.80
$Or_{85}Ab_{15}/An_{50}Ab_{50}$	25.	3.0	0.80	0.85
Or_{100}/An_{100}	40.	4.7	0.52	0.85

formed (on any final material) to prevent loss of material.

These observations also apply to the feldspars for the MSV runs, as shown in fig. 2-12b (see also discussion in Chapter 4).

The effect of ordering-disordering and mixing-unmixing on trace element distributions is not well known. According to Rhodes (1969), ordering in natural feldspars did not affect their trace element concentrations. Longstaffe (1978) however, found an increase in Rb and Tl concentrations in feldspar of higher triclinicity.

Under the experimental conditions of this study, the stable structure of feldspar in all the runs would be sanidine, due to Al-Si disordering. This was not achieved in the Ml regular runs but was achieved in the fusion runs. Such difference in structure, together with the different behaviour of Rb (as will be discussed in the next section), might have caused the differences in the results for Ml between the regular and fusion runs.

2-4-2b. Composition. The effect of composition in the host mineral on trace element distribution has been discussed by many workers both on theoretical and empirical grounds (e.g. McIntyre, 1963 and Lagache and Sabatier, 1971).

Iiyama (1968) measured experimentally the partition coefficients (D) of Rb, Cs, Sr and Ba between coexisting pairs of alkali feldspar and plagioclase in the presence of a vapour phase (MSV tech-

nique). He found that the effect of composition of the feldspars varied from element to element, being relatively the strongest for D(Rb) (Table 2-15). Lagache (1971) demonstrated that the K_D(Cs/K+Na) for the pair sanidine-vapour varied with the composition of the sanidine, being relatively higher for sanidine of intermediate (K, Na) composition (Fig. 2-13).

Of the three different initial feldspars used in this study, the main differences in their compositions are the low concentration of K (and high Na) in Sl and the relatively high concentration of Rb in Ml (Table 2-14). These differences probably account for the difference in Tl distribution between Sl and Ml for both the regular and fusion runs and also the small difference in Rb distribution for the fusion runs, in a manner similar to the observations of Iiyama (1968) and Lagache (1971).

The relatively much larger difference in Rb distribution for Ml between the fusion and regular runs may be due to the possibility that Rb in Ml behaved as a major element in the regular runs and hence will not tolerate extensive exchange with the vapour phase without a breakdown of the microcline structure (see section 2-4-2a). In the fusion runs, this breakdown was achieved and hence the behaviour of Rb approached that of a trace element. This possibility is supported by a) the similarity of most of the results for Ml fusion runs to those for Sl in both the regular and fusion runs, b) D(Tl) does not show as much

Fig. 2-13. Variation of K_D(Cs/Na+K) for alkali feldspar/vapour with composition of the feldspar (Lagache, 1971).

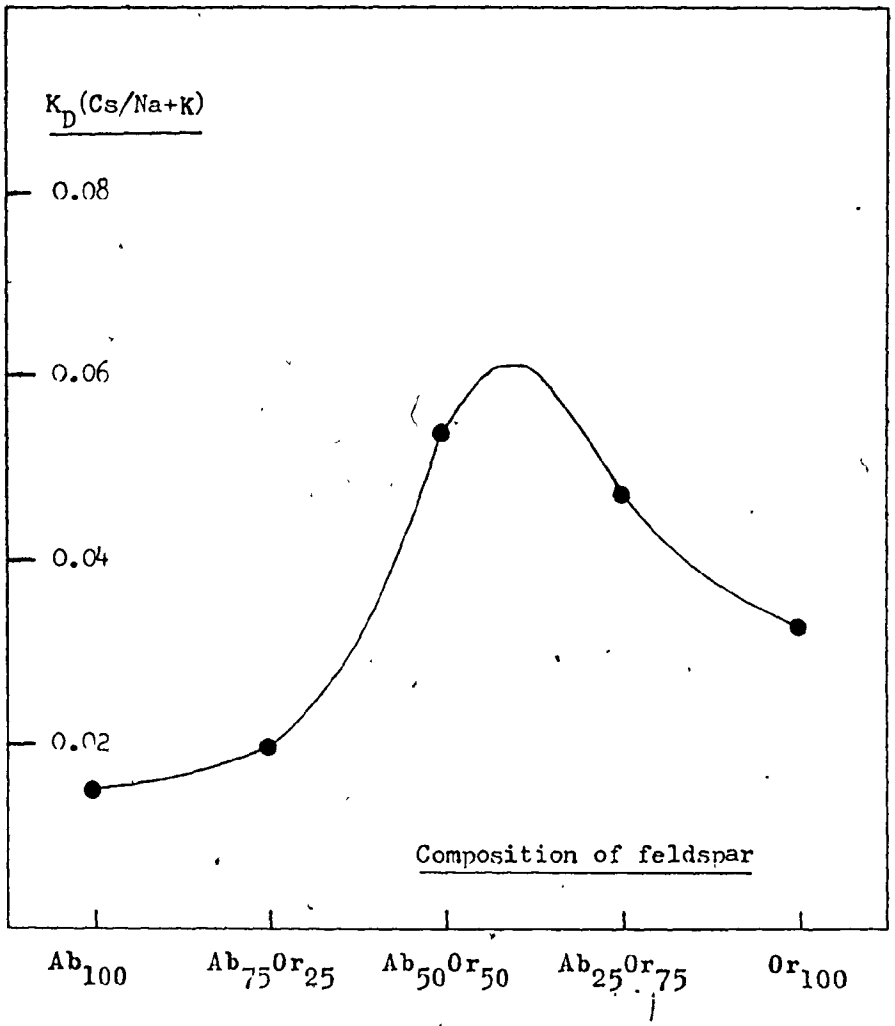
K_D(Cs/Na+K)
0.08
0.06
0.04
0.02
Composition of feldspar
Ab_{100}
$Ab_{75}Or_{25}$
$Ab_{50}Or_{50}$
$Ab_{25}Or_{75}$
Or_{100}

difference between the fusion and regular runs, but rather forms a smooth trend, decreasing from 500°C to 800°C, as it should if Tl behaved ideally, c) Rb concentration in Ml for the fusion runs is very similar to that in the initial Ml (c.a. 2%) but is somewhat lower in the fusion runs (c.a. 1.4%, see table 2-10).

2-4-2c. Kinetics. The possibility of disequilibrium in the results of this study must be considered, in the light of the spread in some of the data and the differences between the results for the different feldspars, and between the regular and fusion runs. It will, however, be recalled (2-2-1) that the test runs suggested that equilibrium was approached in the sanidine (Sl)-vapour runs.

As pointed out previously (2-2-1b), after the initial fast reactions at high temperature, subsequent cation exchange would probably be controlled by the slower mechanism of diffusion through the lattice of the crystals.

Diffusion coefficients of K, Na and Rb have been reported by several workers (Table 2-16). There are considerable differences in the results. In the temperature range of interest, diffusion coefficients for Na, K and Rb are in the ranges of 10^{-10} to 10^{-12}, 10^{-12} to 10^{-16} and 10^{-14} to 10^{-15} respectively. According to Foland (1974), diffusion coefficient of ions of the same charge varies with their size, decreasing with larger ions. Hence Tl^{1+} will have diffusion

Table 2-16. Diffusion coefficients of Na, K and Rb in microcline (#) and orthoclase (all others)

Element	Temperature (°C)	Diffusion coefficient (cm^2/sec)	References
Na	850	5×10^{-11}	Sippel (1963)
Na	850	2×10^{-10}	Sippel (1963)#
Na	800	9×10^{-11}	Foland (1974)
Na	700	6×10^{-12}	Foland (1974)
Na	600	3×10^{-13}	Foland (1974)
Na	600	1×10^{-10}	Lin and Yund (1972)
Na	500	1×10^{-11}	Lin and Yund (1972)
K	800	1×10^{-13}	Foland (1974)
K	800	8×10^{-13}	Lin and Yund (1972)
K	700	4×10^{-15}	Foland (1974)
K	700	2×10^{-14}	Lin and Yund (1972)
K	600	1×10^{-16}	Foland (1974)
K	600	4×10^{-16}	Lin and Yund (1972)
Rb	800	3×10^{-14}	Foland (1974)
Rb	700	3×10^{-15}	Foland (1974)
Rb	600	1×10^{-15}	Foland (1974)

coefficient smaller than but similar to Rb^{1+}. Taking approximate median values of 10^{-11}, 10^{-13} and 10^{-14} cm^2/sec for Na, K and Rb (and Tl) respectively and since $d = x^2/t$ or $t = x^2/d$ where t is the average time taken for an ion to diffuse through a distance of x, the time taken to diffuse through a distance of 10 μm (10^{-3} cm) will be:

$(10^{-3})^2/10^{-11} = 10^5$ sec or 1.16 days for Na, and similarly 116 days for K and 1160 days for Rb and Tl. Although the uncertainty in these calculations is large, the relative values are probably useful for the present purpose.

Zielinsky and Frey (1974) studied Gd distribution between synthetic diopside and aqueous vapour at 800°C and 1 Kbar P_{H_2O}. They found that the diopside crystals were zoned with respect to Gd concentrations. They proposed a diffusion model to explain their observations on which the following is based.

If the true equilibrium values of D(Rb) and D(Tl) for the feldspar-vapour pair are intermediate between those for Sl and Ml in the regular runs, somewhat similar to those for the fusion runs, in order to achieve equilibrium, Ml had to lose and Sl had to gain Rb and Tl from the vapour phase. Exchange proceeded by the mechanisms outlined in section 2-2-1b to the end of the experiment. Hence the results observed represent various stages of exchange, probably mainly by diffusion, preserved by quenching. The degree of completion of the

exchange would be more advanced for the fusion runs relative to the regular runs, and also with each type of run, for the ones at higher temperatures. For Na, due to its much faster rate of diffusion, equilibrium was reached in all the runs.

This model can explain the behaviour of D(Rb) and D(Tl) for Ml, which decrease from the regular to the fusion runs and from lower to higher temperature, and probably for the Sl fusion runs which increase with higher temperature. However, it contrasts with their behaviour in the Sl regular runs which remained more or less constant at 500°C and 600°C and decreased rather markedly at 700°C. The similarities in the results for all the fusion runs to these Sl regular runs as well as the outcome of the test runs (section 2-2-1) further suggest that equilibrium had been approximated in these runs.

2-4-2d. Starting materials. The possible effect of different starting materials and their previous thermal history on trace element distributions has been quoted by several workers to explain differences in results. For example, Orville (1963) used glass in his study of Na-K distribution between alkali feldspar and vapour and found slight difference in his results from those of Tuttle and Bowen (1954) who used gels (2-4-1c). Beswick (1973) meausred K_D(Rb/K) for the pair sanidine-vapour using previously synthesized sanidine as starting material. His results were generally higher than those from Lagache (1968) who used gel as starting material. Zielinsky

and Frey (1974) demonstrated conclusively that D(Gd) for the pair diopside-vapour varied, depending on whether previously synthesized diopside or oxide mixes of diopside were used in the experiment. They attributed such discrepancies to a disequilibrium effect due to the slow rate of diffusion of Gd in diopside.

In this study, the most difference in the results is observed between Sl and Ml for the regular runs, which can be due to the differences between the two initial feldspars. In the fusion runs, such differences were presumably obliterated by the early fusion as the results for the two feldspars become very similar to each other and to those for S2.

2-5. Conclusion

Rb and Tl distributions between feldspar and vapour vary somewhat with the different initial feldspars and heating procedures employed in this study. Such variations can be attributed to a number of factors, such as composition, structure and thermal history of the feldspars and the kinetics of the exchange reaction. These factors often interact with each other and hence cannot easily be assessed separately.

For the sanidine Sl, the most important factor is its high Na concentration, which may be responsible for the lower D(Rb) and D(Tl) and higher K_D(K/Rb) and K_D(K/Tl) values relative to those for

M1 and S2. Another consequence of the high Na contents of S1 is that it is subject to mixing-unmixing reactions at 700°C and above. Due probably to the sluggishness of such reactions, complete mixing was not materialized in the regular runs, but may be responsible for the change of the Rb-Tl distribution patterns at 700°C as compared to those at lower temperatures.

For the microcline M1, the most important factors are its high Rb content and structure. Thus Rb may have behaved as a major element in the regular runs in which the stable structure (sanidine) was not attained, resulting in very high D(Rb), K_D(Rb/Tl) and low K_D(K/Rb) values relative to the other runs and also relative to other results reported in the literature.

The most satisfactory results appear to be those for the fusion runs because they are most consistent both among all the three feldspars (including the sanidine gel S2) used in this study and also in comparison with literature reports [for K_D(K/Rb)]. This is possibly a consequence of the initial heating and melting at 900°C and subsequent recrystallization into homogeneous feldspars at lower temperatures. Average results at 800°C fusion runs for S2, which is the most K-rich are: D(Rb) = 2.8; D(Tl) = 0.42; K_D(Rb/Tl) = 7.6; K_D(K/Rb) = 1.7 and K_D(K/Tl) = 11. As mentioned previously, presence of excess Na in the

feldspar such as in S1, lowers D(Rb) and D(Tl) and raises K_D(K/Rb) and K_D(K/Tl), while the presence of excess Rb, such as in M1, raises D(Rb) and K_D(Rb/Tl) and lowers K_D(K/Rb). This effect of the compositions of the alkali feldspar is shown in Fig. 2-14.

Due to the lack of data, temperature effects can be assessed only for the regular runs with S1 and M1. Thus a rise in temperature lowers D(Rb) and D(Tl) and raises K_D(Rb/Tl) and K_D(K/Tl) with little change in K_D(K/Rb).

With the possible exception of the regular runs for S1 at 700°C and for M1 at 500°C and 700°C, equilibrium appears to have been achieved in the other runs of 14 days or longer, as suggested by: a) the results of the test-runs and b) the general similarities in the results for the different initial feldspars and in comparison to those reported in the literature.

Fig. 2-14. Variation of alkali feldspar-vapour D and K_D values with the composition of the feldspar and temperature. Temperature trends for the pure K-feldspar (broken lines) are inferred.

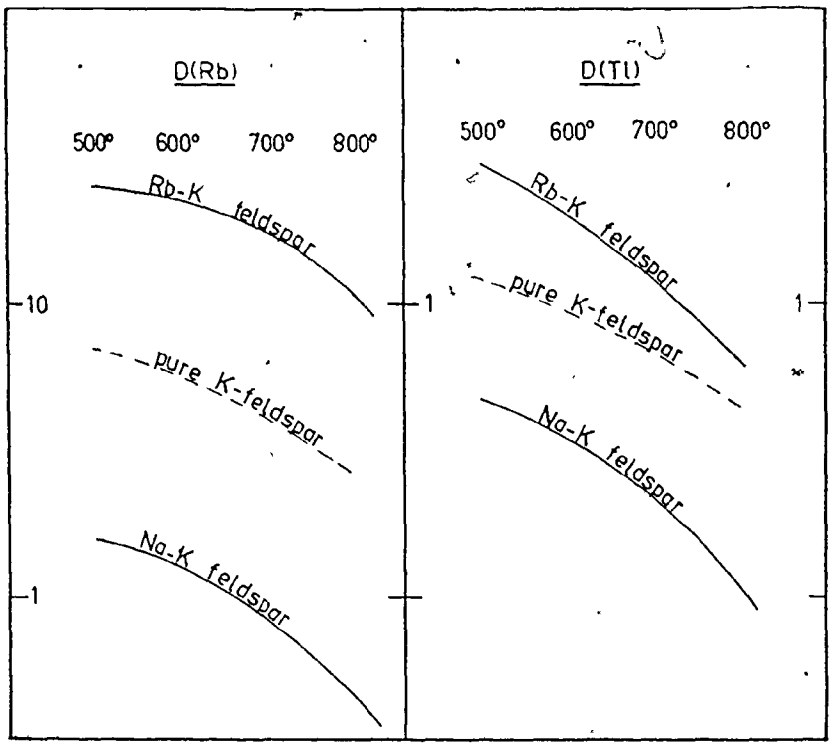
D(Rb)
500° 600° 700° 800°
Rb-K feldspar
pure K-feldspar
Na-K feldspar
10
1
D(Tl)
500° 600° 700° 800°
Rb-K feldspar
pure K-feldspar
Na-K feldspar
1

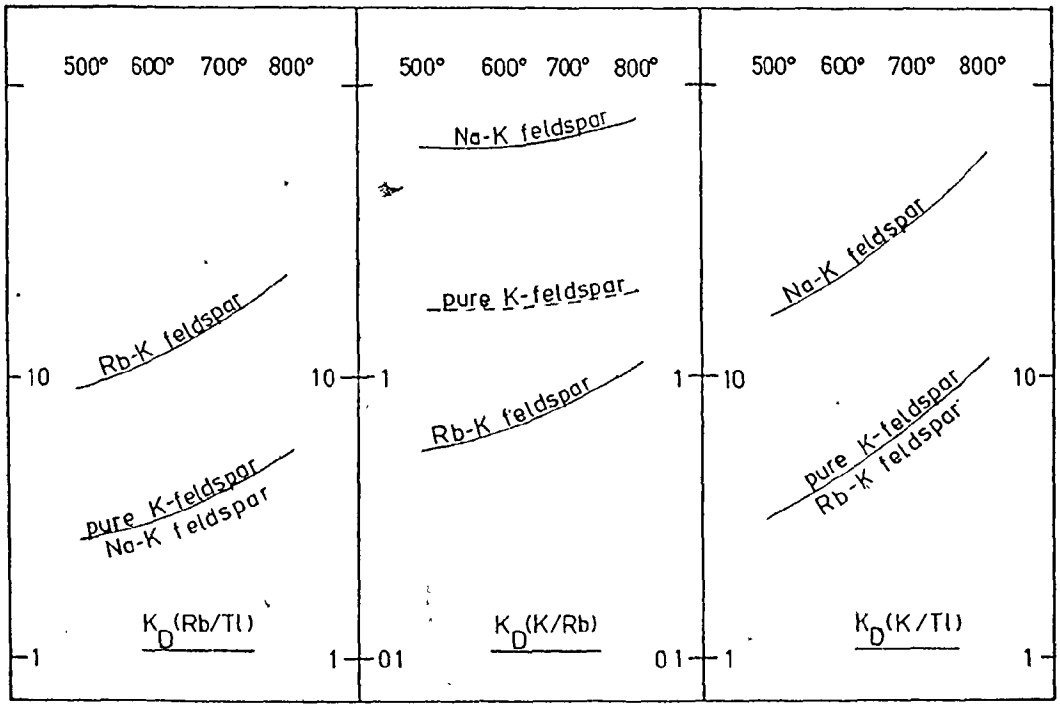
500° 600° 700° 800°
Rb-K feldspar
pure K-feldspar
Na-K feldspar
10
1
K_D(Rb/Tl)
500° 600° 700° 800°
Na-K feldspar
pure K-feldspar
Rb-K feldspar
1
01
K_D(K/Rb)
500° 600° 700° 800°
Na-K feldspar
pure K-feldspar
Rb-K feldspar
10
1
K_D(K/Tl)

CHAPTER 3

K, Rb AND Tl DISTRIBUTIONS BETWEEN RHYOLITE-VAPOUR AND ALKALI FELDSPAR-RHYOLITE

3-1. Introduction

Experimental studies of trace element distribution between coexisting mineral-vapour pairs contribute to our understanding of the behaviour of trace elements in simple hydrothermal systems such as the kinetics and mechanisms of exchange reactions (e. g. Zielinsky and Frey, 1974); factors governing trace element distributions (e. g. Iiyama, 1972, 1978, Iiyama and Volfinger, 1976) and in some natural systems involving a vapour, as an interpretational tool (e. g. Shaw, 1978). However, in most geologic materials, the vapour phase is not available for analysis (even if it existed), except in a few special cases such as chemical precipitates and fluid inclusions in some minerals. Most studies in natural materials involve coexisting solid phases which are assumed to represent the products of reactions at higher temperatures, where the state of equilibrium was preserved during solidification.

Conventional experimental measurements of partition coefficients between solid pairs involve separate measurements for coexisting solid-vapour pairs. From these data, partition coefficients for solid pairs are calculated with the assumption that if a vapour is separately in equilibrium with solids A and B, A and B could have been in equilibrium with each other (Zeroth law).

Since the development of theoretical models (Gast, 1968 and Shaw, 1970, for example), partition coefficients for mineral-melt pairs have been used extensively in constructing models of melting and crystallization. Hence study on Rb and Tl distributions between a rhyolite melt and vapour was undertaken in order to obtain partition data for the pair feldspar-melt.

In addition, results obtained from direct equilibration of feldspar and melt will also be included in this chapter (see chapter 5).

3-2. Experimental technique

The rock used in this study was a rhyolite from the Bull Arms, Newfoundland and was donated by Dr. S. Papezik (Benchmark standard sample B-3, distributed by the Volcanology Subcommittee, National Research Council of Canada). The powder sample was fused in an oven at 1300°C and ground to pass through a 200 mesh sieve before being used. The final powder was completely amorphous and contained 4.72% K, 136 ppm Rb and 1.15 ppm Tl.

Two runs were conducted at each of 500°C, 600°C and 700°C with solution EE (Table 2-1) as the vapour phase. The experimental technique was that of the regular SSV runs (see section 2-1-1) and the duration of the runs was also thirty days.

Experimental technique for the direct equilibration of feldspar-melt (MSV+ runs) is described in Chapter 4.

3-3. Results and discussions

3-3-1. Rhyolite-vapour runs

The product of runs was a dark glass with some (up to 10%) crystals of mainly sanidine, and probably some quartz. Data on element concentrations, D and K_D values are reported in table 3-1. D(K) is excluded, as with the feldspar-vapour pairs, in Chapter 2.

For each temperature, the D and K_D values are similar to each other. The small discrepancies observed in some data can be attributed mainly to experimental error, and partly to the different degree of crystallinity of the melt. Hence the mean values for each temperature pairs will be used in the following discussions.

There is a small increase in D(Rb) and D(Tl) and a small decrease in all the K_D values from low to high temperatures. These trends are generally opposite to those observed for all the feldspar-vapour pairs with the possible exception of the fusion Sl-vapour pair.

+ multiple solid-vapour

	Rhyolite			Vapour			D			K_D	
No.	K(%)	Rb(ppm)	Tl(ppm)	K(%)	Rb(ppm)	Tl(ppm)	Rb	Tl	Rb/Tl	K/Rb	K/Tl
500°C											
5-1	7.28	663	25.5	1.68	748	89.2	0.89	0.29	3.1	4.9	15.2
5-2	7.22	634	25.0	2.33	910	95.7	0.70	0.26	3.1	4.4	11.9
						$\bar{x}$	0.80	0.28	2.9	4.7	13.6
600°C											
5-4	6.55	618	32.2	1.98	620	69.2	1.00	0.47	2.1	3.3	7.2
5-5	6.83	715	34.4	2.90	884	89.3	0.81	0.39	2.1	2.9	6.1
						$\bar{x}$	0.91	0.43	2.1	3.1	6.7
700°C											
5-7	6.51	714	36.6	2.41	606	70.7	1.18	0.52	2.3	2.3	5.2
5-8	6.82	627	41.6	3.04	828	85.5	1.00	0.49	2.1	2.2	4.9
						$\bar{x}$	1.1	0.51	2.2	2.3	4.9

$\bar{x}$ average

Table 3-1. Data for rhyolite glass-vapour runs

Except for K_D(Rb/Tl), all these temperature trends are smooth and weak. As for K_D(Rb/Tl), there is no difference between the 600°C and 700°C results ($\bar{x}$ = 2.2 and 2.1), though it is also higher at 500°C ($\bar{x}$ = 2.9).

Beswick (1973) reported a K_D(K/Rb) value of 1.1 for the pair of granitic melt-vapour at 800°C which agrees reasonably well with that from this study when extrapolated to 800°C [K_D(K/Rb) = 4.7, 3.1 and 2.2 for 500°C, 600°C and 700°C respectively]. No other data are available for comparison.

3-3-2. Results for the pair feldspar-rhyolite

3-3-2a. Results calculated from two pairs of SSV runs. D and K_D values for the feldspar-rhyolite pair (Table 3-2a and b) were obtained indirectly by dividing the D and K_D values for the feldspar-vapour pair by those for the melt-vapour pair. Since there are several sets of feldspar-vapour data available (with different initial feldspars Sl or Ml, and heating procedures, regular or fusion runs), the results will be discussed separately.

For this purpose, the data obtained by using the feldspar-vapour data for the regular runs, particularly Sl-vapour are most adequate. The temperature trends for both Sl-melt (Fig. 3-1) and Ml-melt (Fig. 3-2) more or less follow those for the respective

Fig. 3-1. Plot of log(D) and log(K_D) vs. 1/T(^{o}K) for the pair Sl-rhyolite.

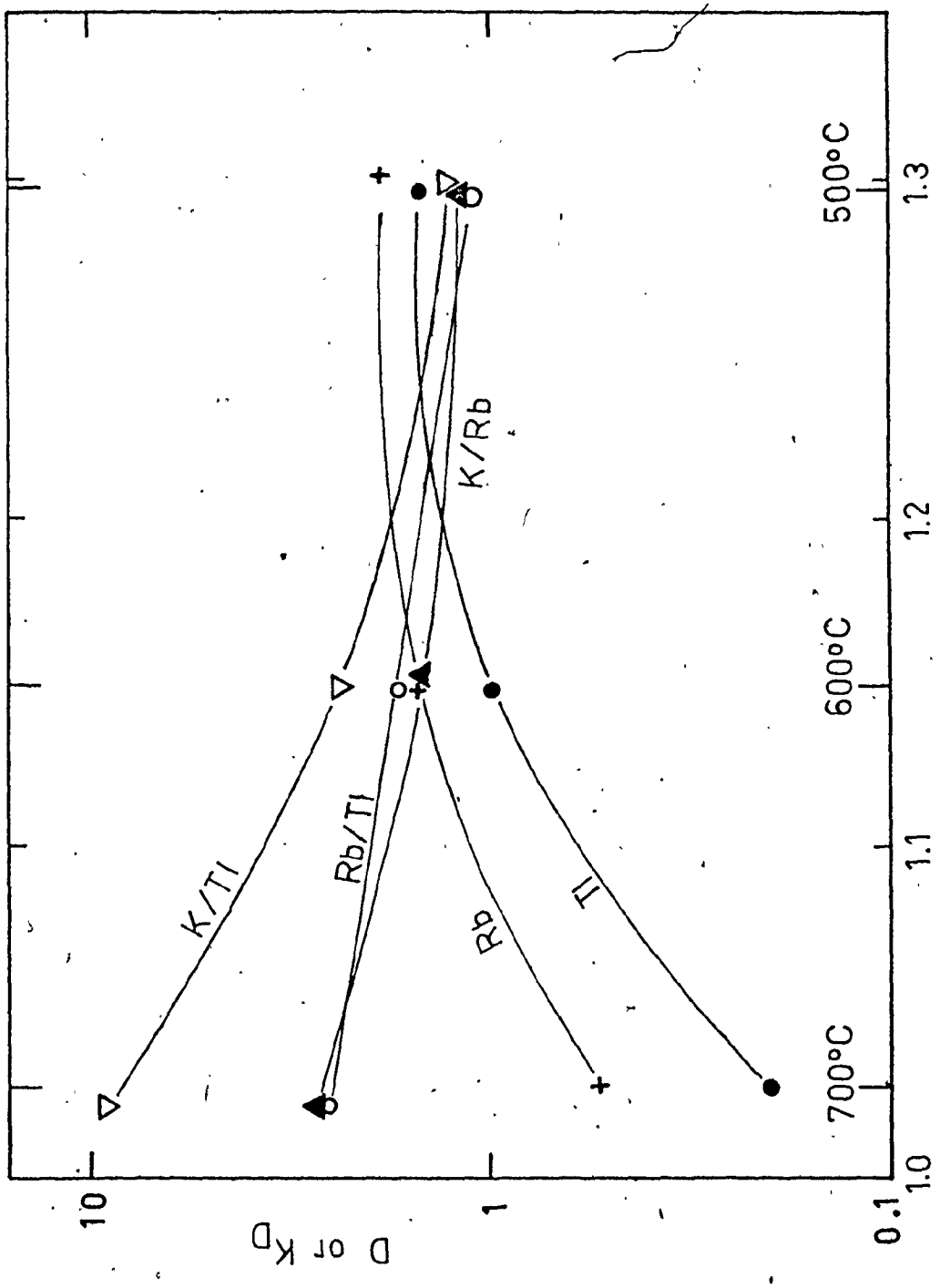
D or K_D
10
1
0.1
1.0
1.1
1.2
1.3
700°C
600°C
500°C
1000X 1/T(°K)
K/Tl
Rb/Tl
Rb
Tl
K/Rb

Fig. 3-2. Plot of log(D) and log(K_D) vs. $1/T(^{o}K)$ for the pair Ml-melt.

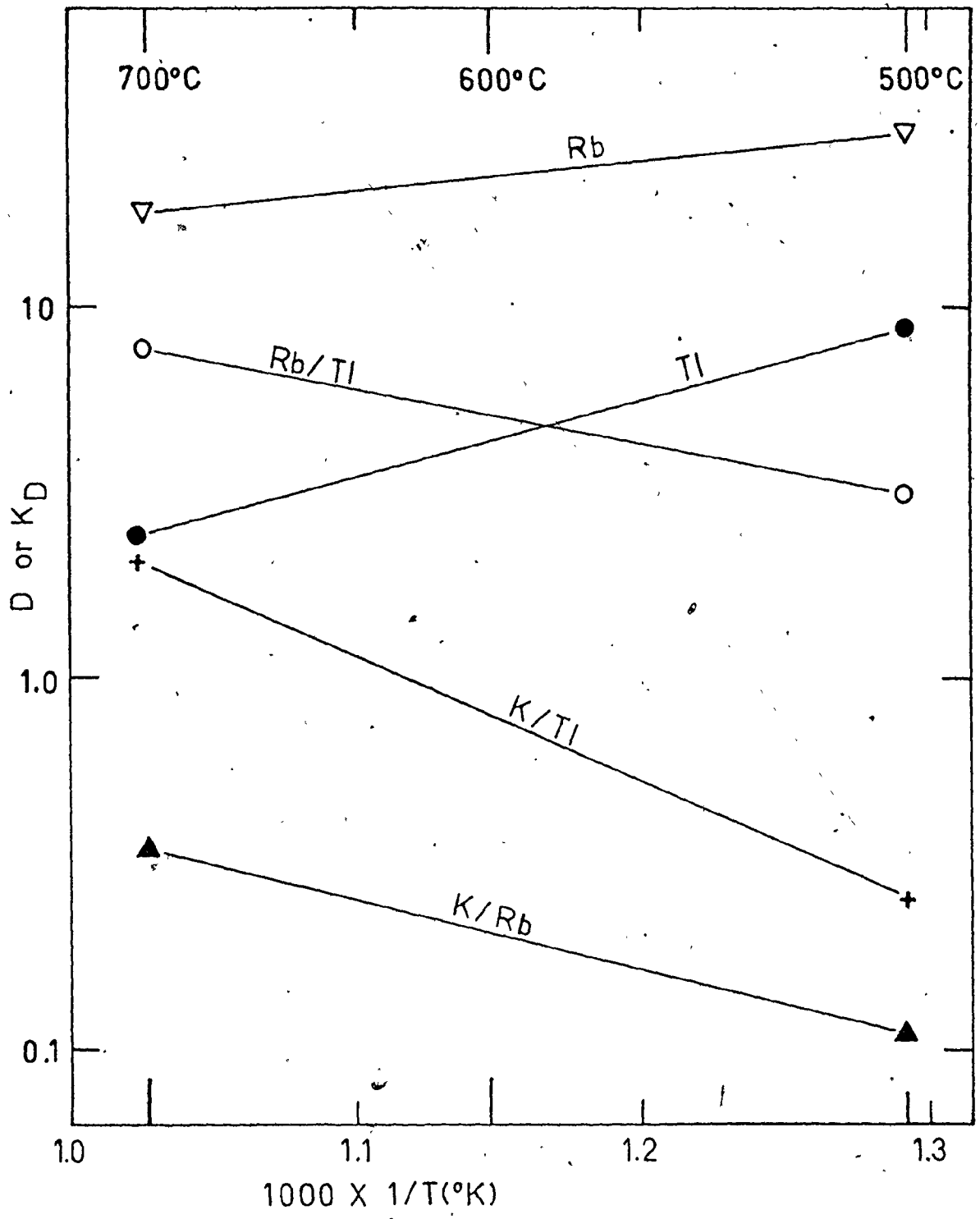
700°C
600°C
500°C
Rb
Rb/Tl
Tl
K/Tl
K/Rb
10
1.0
0.1
D or K_D
1.0
1.1
1.2
1.3
1000 X 1/T(°K)

feldspar-vapour pairs (see Figs. 2-8 and 2-9). That is; D(Rb) and D(Tl) decrease while all the K_D values increase with higher temperatures. Like the Sl-vapour pair, there is also very little difference between most results at 500°C and 600°C for the pair Sl-melt. Since the same set of data for the pair melt-vapour is used for calculating both sets (and other sets) of feldspar-melt results, the difference in the results between Sl-melt and Ml-melt pairs are the same as between the Sl-vapour and Ml-vapour pairs (see Figs. 2-9 and 2-10), namely up to as much as twenty times. Similarly, the fusion feldspar-melt pairs at 700°C (Table 3-2c) which are very similar to each other, are also similar to those for the regular Sl-melt pair at 600°C (not shown in Figs. 3-1 and 3-2; see Figs. 2-8 and 2-9).

3-3-2b. Results measured directly by MSV techniques. Most Sl-melt results obtained by direct equilibration, using MSV, regular techniques (see Chapters 4 and 5) at 600°C are surprisingly similar to those calculated from two separate SSV regular runs (Table 3-2c, Fig. 3-1), as are also the K_D values for the two sets of Ml-melt data (Table 3-2c, Fig. 3-1). D(Rb) and D(Tl) for the latter two sets however, show considerable discrepancies, being relatively lower (by 2 to 3 times) for the MSV results. Such behaviour would be expected from Ml, as demonstrated in the Ml-vapour runs (see Chapter 2) due to its high Rb concentration. The

Table 3-2. Summary of results for the pair feldspar-rhyolite

Phases	T(°C)	D(Rb)	D(Tl)	K_D(Rb/Tl)	K_D(K/Rb)	K_D(K/Tl)
a. Regular SSV runs*						
Sl-rhyolite	500	1.8	1.5	1.1	1.3	1.3
	600	1.5	0.95	1.6	1.5	2.4
	700	0.63	0.20	2.5	2.8	9.0
Ml-rhyolite	500	29	8.9	3.1	0.11	0.26
	700	18	2.4	7.5	0.35	2.0
b. Fusion SSV runs**						
Sl-rhyolite	700	1.4	0.98	1.4	1.9	2.8
Ml-rhyolite	700	2.6	1.7	1.3	0.80	1.2
c. Regular MSV runs #						
Sl-rhyolite	600	0.64	0.56	0.85	2.8	3.2
Ml-rhyolite	700	8.2	0.93	9.2	0.30	2.5

* Calculated from Sl-vapour (Table 2-9b) or Ml-vapour (Table 2-10) and rhyolite–vapour (Table 3-1) pairs.

** Same as for *, with feldspar-vapour data from Table 2-10.

\# Direct measurement for coexisting feldspar-melt pair (Table 5-1).

general similarities between the results obtained from two such different techniques further substantiate the previous claim that equilibrium was achieved in the experiments with the Sl-vapour and melt-vapour pairs (see also discussions in Chapters 4 and 5 for the MSV experiments).

3-4. Applications

3-4-1. Fractionation trends

Both D(Rb) and D(Tl) for alkali feldspar-rhyolite and feldspar-vapour increase while K_D(Rb/Tl) and K_D(K/Tl) decrease from high to low temperature. Hence, if alkali feldspar alone fractionates from a melt with or without a vapour phase, and if the composition of the melt remains more or less constant, the Rb and Tl concentrations in the alkali feldspar will increase, while its ratios of Rb/Tl and K/Tl will fall in the later differentiates.

Many of these predicted trends have been documented in the literature. Hence the early works of Ahrens (1952), Shaw (1957), Heier and Taylor (1959), Taylor and Heier (1960) and Borovik-Romanova and Sosedko (1960) all reported increase in Rb and Tl concentrations and decrease in Rb/Tl ratios in the feldspars of the later differentiates. Similar increase in Rb concentrations and decrease in K/Rb ratios have been reported by numerous workers (e.g. see summary by Heier and Adams, 1964).

Ivanov et al. (1960), after examining a large number of Tl analyses, concluded that Tl concentrations increase in the sequence of sanidine-orthoclase-microcline-amazonite, namely from high to low temperature forms. Solodov (1959) noted that Rb concentrations in the microclines from zoned pegmatites increased from edge to centre, corresponding to early and late pegmatitic processes.

Taylor (1965) noted a general increase of Rb and Tl concentrations in the sequence of basalt-syenite-granodiorite-granite-pegmatite microcline and a decrease in the Rb/Tl ratio in the pegmatite microcline (Fig. 3-3). In the felsic rocks (except basalt), these trends probably reflect those of the alkali feldspar, which is the main carrier of both Rb and Tl (e.g. see Shaw, 1957) except in some biotite-rich rocks. Similarly, Albuquerque and Shaw (1972) noted a general increase of Tl concentration in feldspars from the following sequence of rocks: granulite-alkalic rocks-granodiorite-gneiss-granite-pegmatite.

Increase in Rb and Tl concentrations in feldspars could result from increases in the melt from which the feldspars crystallized out. Hence we need to consider the pair feldspar-melt instead. This will be discussed in the next section. Also, the presence of other phases, particularly the micas needs also to be considered. This is discussed in the next chapter.

Fig. 3-3. Relationship between Rb and Tl in common crustal rocks and pegmatitic feldspars (from Taylor, 1965).

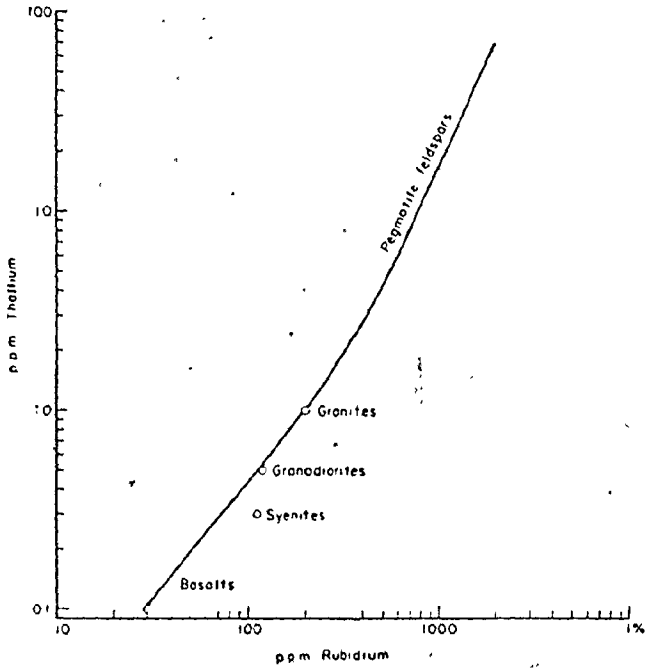
100
10
1.0
0.1
p.p.m Thallium
Pegmatite feldspars
Granites
Granodiorites
Syenites
Basalts
10
100
1000
1%
p.p.m Rubidium

Finally, both D(Rb) and D(Tl) are less than unity in the Sl-melt pair at 700°C but increase to 1.8 and 1.5 respectively at 500°C. Hence both elements will be enriched in the melt at high temperature but will be enriched in the feldspar at lower temperature. This is consistent with the observations of Dupuy et al. (1973) who reported that in ignimbrites (high temperature rocks) both Rb and Tl concentrations are higher in the matrix than in the feldspars and vice versa for granodiorites (see also discussions in section 3-4-2a). As will be discussed later, the results from the pair Ml-melt are considered to be anomalous (see also previous discussions, Chapter 2).

3-4-2. Comparison with natural feldspar-rock pairs and geothermometry.

The experimental pair of alkali feldspar-rhyolite melt is analogous to the natural pair of alkali feldspar-matrix in porphyritic volcanic rocks. In these natural meterials, the equilibrium state of reaction at high temperature is assumed to be preserved as the rock solidified upon extrusion, with the crystals forming the phenocrysts and the melt the matrix.

In plutonic rocks, the original melt crystallized and part of it (e.g. the vapour phase with some volatile components) might have been lost at some stage of the evolution. For such rocks, it is assumed that

prior to solidification, the sample collected for study had acted as a closed system, with the feldspar crystals in equilibrium with the whole rock as the melt (see Berlin and Henderson, 1968 and Korringa and Noble, 1971).

However, even if these assumptions are valid, trace element distribution between crystal and melt, whether in natural or experimental systems, will vary with the composition of the host rock and the nature of the feldspar. In natural systems, further complications may arise from subsolidus and secondary reactions such as alteration and metamorphism.

In spite of such limitations, geothermometers based on the feldspar-rhyolite D and K_D values can be tested. Only the SSV regular Sl-rhyolite pair (Fig. 3-1) will be used for this purpose since these results are the most complete and satisfactory. Moreover, among the three feldspars used in this study, composition of Sl is closest to natural feldspars. It will be recalled (section 3-3-2b), however, that similar results were obtained with the MSV runs at 700°C for Sl.

Data for the regular SSV Ml-melt pair are not used, because of the possibility of non-ideal behaviour. Since most data for all the 700°C SSV fusion runs are similar to those adopted at 600°C (3-3-2a), temperatures measured would be 100°C lower if these fusion run data were used instead. However, the temperature trends are the same for

all the experimental pairs, with the possible exception of the fusion SSV Sl-melt pair, as was demonstrated previously (2-3).

Ideally, the temperature recorded by a trace element geothermometer would be that at which the exchange reactions had stopped as the rock solidified by cooling. However, in the case of the more mobile elements such as K, Rb and Tl, exchange might continue to take place after solidification of the rock, well into the subsolidus regime. Secondary reactions, as noted earlier, might also mobilize these elements and hence reset the thermometer. In plutonic rocks, further complications arise from the unmixing and ordering of the feldspars (see section 2-4-2). Hence the following discussions can only be semi-quantitative, and are concerned with published data suitable for such testing.

3-4-2a. Ignimbrites and granodiorites from Tuscany. Dupuy et al. (1973) studied the distribution of Rb and Tl between coexisting feldspar, biotite, matrix and rock from a suite of ignimbrites and granodiorites from Tuscany, Italy. Data for the alkali feldspar-melt pair are summarized in table 3-3 and shown as histograms (Fig. 3-4) together with the adopted geothermometers (upper part of the diagram).

Table 3-3. Summary of data on the ignimbrites and granodiorites from Tuscany, Italy (Dupuy et al. 1973)

No.	Phases	D(Rb)	D(Tl)	K_D(Rb/Tl)	K_D(K/Rb)	K_D(K/Tl)
Ignimbrites						
C1	Fs/r	1.2			2.0	
	Fs/m	0.8			2.7	
C5	Fs/r	1.1	1.0	1.1	2.1	2.3
C24	Fs/r	1.0			2.3	
	Fs/m	0.86			2.4	
C12	Fs/r		1.3			1.7
	Fs/m	0.76	0.88	0.87	2.3	2.0
C14	Fs/r	0.99	1.3	0.73	2.3	1.7
	Fs/m	0.67	0.76	0.89	2.5	2.2
C6	Fs/r	1.2			1.9	
	Fs/m	0.83			2.3	
C7	Fs/r	1.2			1.0	
	Fs/m	1.0			1.0	
V4	Fs/r	0.91	1.1	0.80		
	Fs/m	0.74	0.77	0.96		
V11	Fs/r	0.95			2.7	
	Fs/m	0.78			3.0	
V12	Fs/r	0.97			2.6	
	Fs/m	0.72			3.1	
R3	Fs/r	0.99	1.1	0.88	2.2	2.0
	Fs/m	0.76	0.81	0.94	2.7	2.5
R5	Fs/r	1.0			2.4	
	Fs/m	0.79			3.0	

Tabl3 3-3 (cont'd.)

No.	Phases	D(Rb)	D(Tl)	K_D(Rb/Tl)	K_D(K/Rb)	K_D(K/Tl)
Ignimbrites						
A1	Fs/r	1.0	1.3	0.79	2.1	1.7
	Fs/m	0.73	0.82	0.89	2.9	2.6
A10	Fs/r	0.97	1.2	0.83	2.1	1.8
	Fs/m	0.77	0.75	1.0	2.6	2.7
A25	Fs/r	1.1	1.1	0.96	2.0	2.0
A33	Fs/r	1.1	1.2	0.91	2.0	1.8
	Fs/m	1.0	0.68	1.3	2.0	2.6
Granodiorites						
E8	Fs/r	1.8	1.6	1.1	1.8	2.0
E10	Fs/r	1.6	1.3	1.2	1.9	2.3
E11	Fs/r	1.6	1.6	1.0	1.9	1.9
E17	Fs/r	2.0	1.9	1.1	1.5	1.6
E20	Fs/r	1.7	1.4	1.2	2.0	2.3

Fs alkali feldspar, r rock, m matrix

Fig. 3-4. Histogram of D and K_D for the pair feldspar-rock for the rocks from Tuscany, Italy (Dupuy et al., 1973). Temperatures are from Sl-melt.

↑ granodiorites, ⊤ ignimbrites (feldspar/rock), ⊤ ignimbrites (feldspar/matrix).

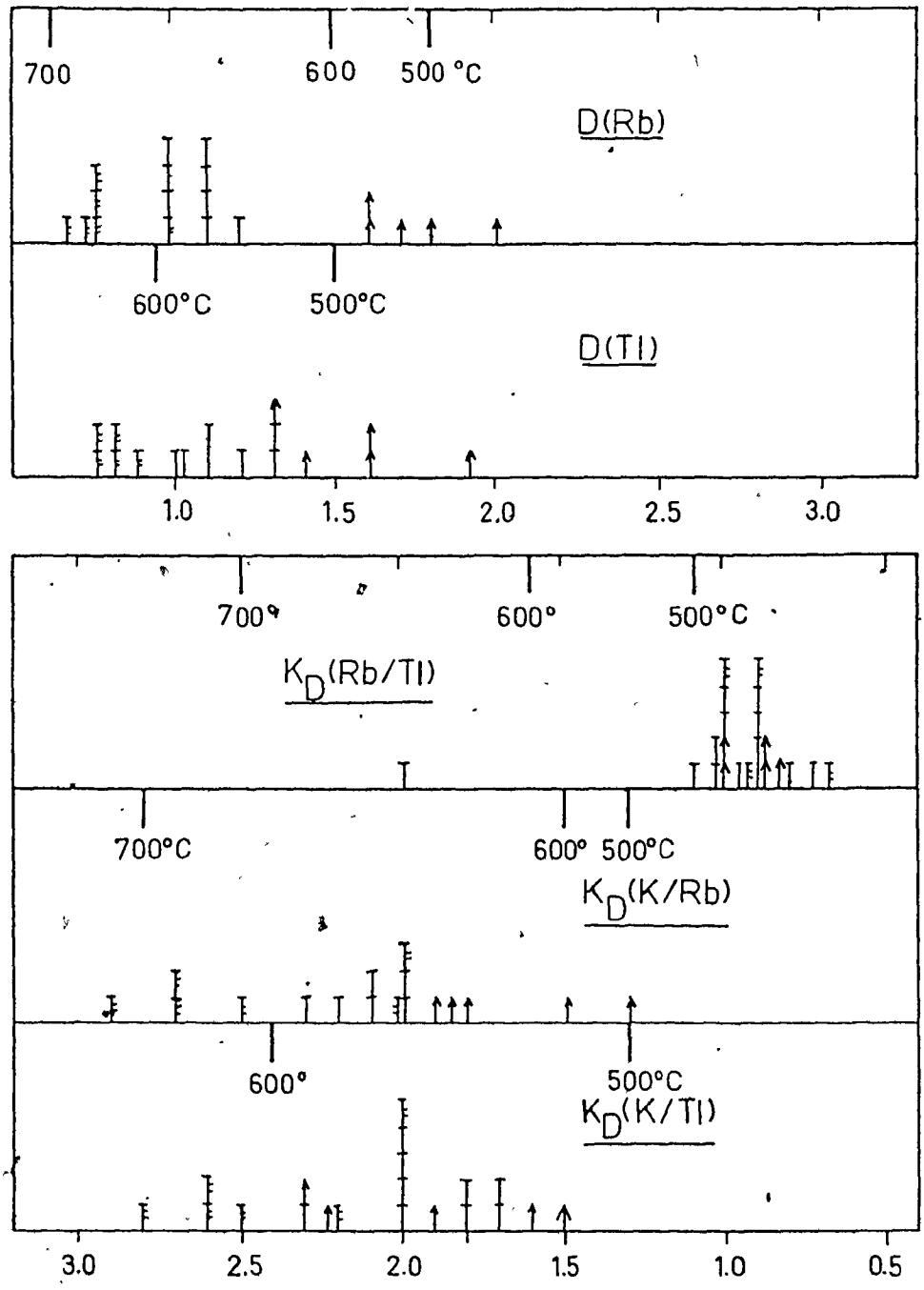
700
600
500 °C
D(Rb)
600°C
500°C
D(TI)
1.0
1.5
2.0
2.5
3.0
700°
600°
500°C
K_D(Rb/TI)
700°C
600° 500°C
K_D(K/Rb)
600°
500°C
K_D(K/TI)
3.0
2.5
2.0
1.5
1.0
0.5

As expected from petrologic considerations, temperatures for the ignimbrites are generally higher than those of the granodiorites for each of the thermometers except K_D(Rb/Tl), which shows no clear separation of the two groups of rocks. Temperatures for the feldspar-matrix pair are generally higher than those for the feldspar-rock pair, as one would expect if the matrix represent that part of the melt frozen at a higher temperature. The actual temperatures obtained from all the thermometers range from 500°C to 700°C, which are quite reasonable, especially if only the matrix data are considered.

3-4-2b. Granites and granodiorites from Portugal.

Most of the data from the granites and granodiorites from Northern Portugal (Albuquerque, 1973 and 1975) show considerable scatter (Table 3-4 and Fig. 3-5). Only D(Rb) values show a clear separation of the two groups of rocks with the expected relative temperature of granodiorite>granite. In all the other thermometers, however, the two groups overlap considerably with many of the granites at a higher temperature relative to the granodiorites.

Such inconsistency was also noted by Albuquerque (1975) (see also Bernotat et al. 1976) for these as well as other plutonic rocks reported in the literature, using the geothermometer of Beswick (1973) with the K_D(Rb/K) data for the biotite-feldspar pair. Albuquerque attributed this mainly to the effect of composition and subliquidus reactions.

Table 3-4. Summary of data on the granite and granodiorites from N. Portugal (Albuquerque, 1973 and 1975)

No.	Phases	D(Rb)	D(Tl)	K_D(Rb/Tl)	K_D(K/Rb)	K_D(K/Tl)
Granodiorites						
A46	Fs/r	1.5	3.0	0.49	2.6	1.2
A79	Fs/r	1.1	3.5	0.32	3.1	1.0
A156	Fs/r	1.4	2.2	0.63	1.0	1.2
A202	Fs/r	1.2	1.9	0.62	2.8	1.8
A328	Fs/r	1.4	1.6	0.89	2.4	2.1
A17*	Fs/r	2.0	2.1	0.97	1.5	1.5
A81**	Fs/r	2.2	-	-	1.3	-
Granites						
A190	gF/r	1.9	4.7	1.4	2.5	1.0
	mF/r	1.9	1.9	0.97	3.0	3.6
A280	gF/r	2.1	2.9	0.73	2.2	1.6
	mF/r	1.7	1.6	1.1	2.3	2.5
A293	gF/r	1.7	1.6	1.1	1.6	1.8
	mF/r	1.5	1.3	1.2	1.8	2.2
A509	gF/r	2.0	2.0	1.0	1.5	1.5
	mF/r	1.7	1.9	1.1	1.8	1.5
A546	Fs/r	1.7	4.3	0.4	1.4	0.56
Vein granites						
A190A	Fs/r	3.0	1.8	1.7	0.76	1.3
A72	Fs/r	2.7	3.0	0.91	-	-

-/not available. Fs/alkali feldspar. gF/feldspar in the ground mass. mF/feldspar as megacryst. r/rock. * composite sample. ** contaminated composite sample.

Fig. 3-5. Histogram of D and K_D values for the pair feldspar-rock for the rocks from N. Portugal (Albuquerque, 1973, 1975). Temperatures are from Sl-melt.

granite, tie-lines join groundmass (G) and megacryst (M) feldspars from the same rock. vein granite, granodiorite.

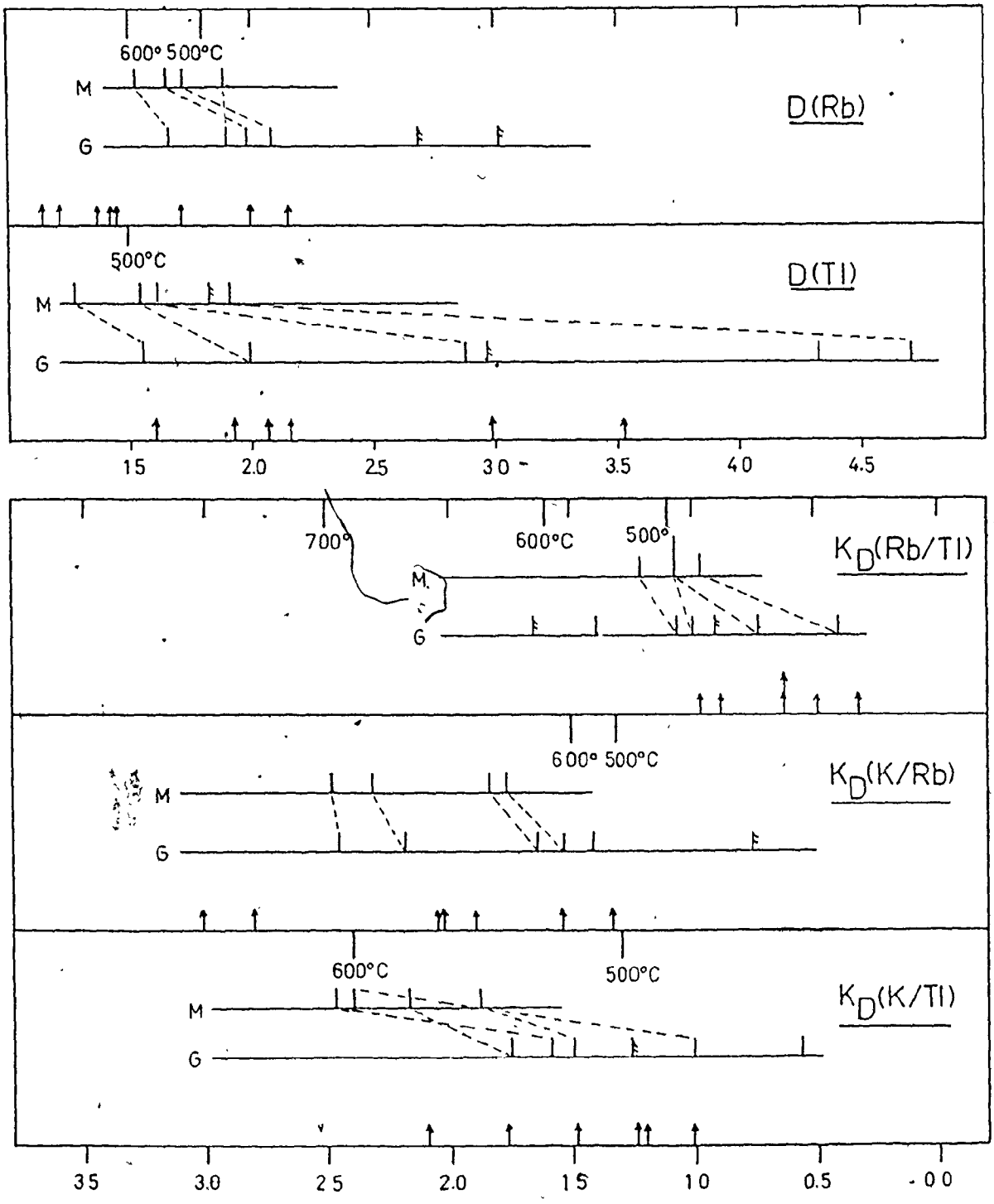
600° 500°C
M
G
D(Rb)
500°C
M
G
D(TI)
1.5
2.0
2.5
3.0
3.5
4.0
4.5
700°
600°C
500°
M
G
K_D(Rb/TI)
600° 500°C
M
G
K_D(K/Rb)
600°C
500°C
M
G
K_D(K/TI)
3.5
3.0
2.5
2.0
1.5
1.0
0.5
0.0

Albuquerque (1973) also noted two modes of occurrence of the alkali feldspar in the granites, those in the matrix and those forming megacrysts and with very little difference between their trace element concentrations. There is also very little difference between the two modes of feldspars (shown separately in Fig. 3-5) for most of the data here, except for D(Tl), which is higher and for K_D(K/Tl), which is lower in the megacryst relative to the matrix feldspars. Also, temperatures for the megacryst feldspars are always higher, albeit only slightly in most cases, than the coexisting matrix feldspars. Lower temperatures for one of the vein granites (A-72) are indicated by all the thermometers as expected but only by D(Rb), K_D(K/Rb) and K_D(K/Tl) for the other (A-190A).

Sample A-17 came from a composite pluton of granite and granodiorite, and A-81 is similar to A-17, except it is contaminated (Albuquerque, personal communication, 1976). Low temperatures are indicated for both by both D(Rb) and K_D(K/Rb) but in the case of A-17, it is not clear from the other thermometers. Unfortunately, A-81 was not available for Tl analysis.

The measured temperatures from most of these thermometers are low, about 500°C or less, for D(Rb) and K_D(Rb/Tl), but are mostly above 500°C for K_D(K/Rb) and K_D(K/Tl). Subsolidus reaction and low-temperature alteration are possible explanations for such behaviour.

3-4-2c. D(Rb) and K_D(K/Rb) for other suites. The following deals with several suites of rocks for which only K and Rb data were published. Temperatures for the granodiorites from Corsica (Table 3-5b, from Carron & Lagache, 1969) are all lower than 500°C in the D(Rb) thermometer, but are mostly between 600 and 700°C in the K_D(K/Rb) thermometer (Fig. 3-6a).

Similar conclusions can be drawn for the rocks from the Palmer region (White, 1966), as shown in Table 3-5a and Fig. 3-6b. These rocks consist of migmatite, gneiss and granite. Temperatures from both thermometers show a decrease in the same order, which is expected if the migmatite was formed by partial melting and the gneiss by metamorphism of the granite.

Philpotts and Schnetzler (1970) reported K and Rb analysis for a porphyritic rhyodacite which yield D(Rb) of 0.66 and K_D(K/Rb) of 2.27. The temperatures are slightly less than 700°C for both thermometers.

According to the summary of Beswick (1973), K_D(K/Rb) in porphyritic volcanic rocks ranges from 1.40 to 3.3, corresponding to temperatures of slightly below 600°C to well above 700°C. His data for some Corsican granodiorites (from Carron and Lagache, 1968) range from 1.4 to 1.7, corresponding to temperatures of about 600°C, with the thermometer in this study.

Table 3-5. Summary of Rb and K/Rb data for the pair alkali feldspar-rock from the Palmer region (a) and Corsica (b)

No.	Rock	D(Rb)	K_D(K/Rb)	No.	Rock	D(Rb)	K_D(K/Rb)
Migmatites from the Palmer Region (White, 1966).				Granodiorites from Corsica (Carron and Lagache, 1969).			
192	mg	1.9	2.0	1	gd	2.9	1.7
193	mg	1.6	2.1	2	gd	2.3	1.7
191	mg	1.5	2.5	3	gd	2.3	2.0
220	gn	2.2	2.0	4	gd	2.2	2.3
188	gn	2.1	2.5	5	gd	2.3	1.6
186	gn	2.6	1.6	6	gd	3.3	1.4
221	gn	3.4	1.2	7	gd	2.6	1.4
189	gn	2.9	1.7	8	gd	2.4	1.7
215	gr	3.2	1.2	9	gd	2.8	1.5
212	gr	3.1	1.2	10	gd	2.7	1.5
210	gr	3.2	1.0				
211	gr	3.0	1.1				
206	gr	2.8	1.2				
216	gr	3.0	1.4				

vo volcanic, mg migmatite, gn gneiss, gr granite, gd granodiorite.

Fig. 3-6. Histogram of D(Rb) and K_D(K/Rb) for the pair feldspar-rock for the rocks from a. Corsica (Carron and Lagache, 1969) and b. the Palmer region, S. Australia (White, 1966). Temperatures are from Sl-melt.
| granodiorite, T gneiss, ⊦ migmitite.

a.

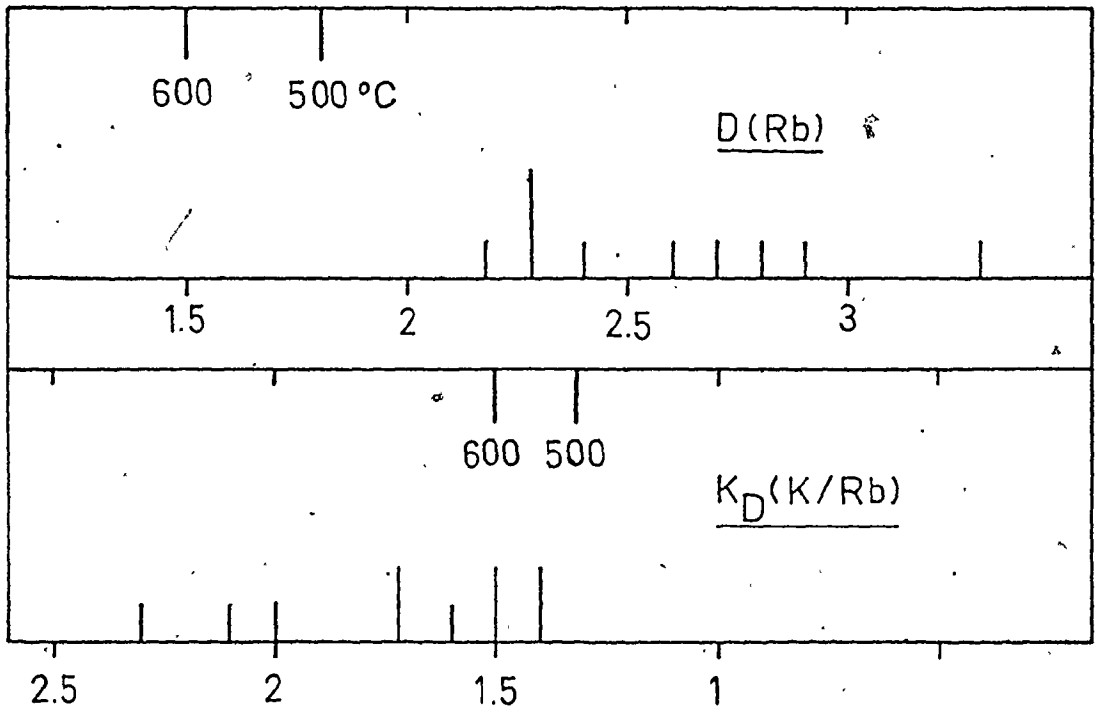
600
500 °C
D(Rb)
1.5
2
2.5
3
600 500
K_D(K/Rb)
2.5
2
1.5
1

b.

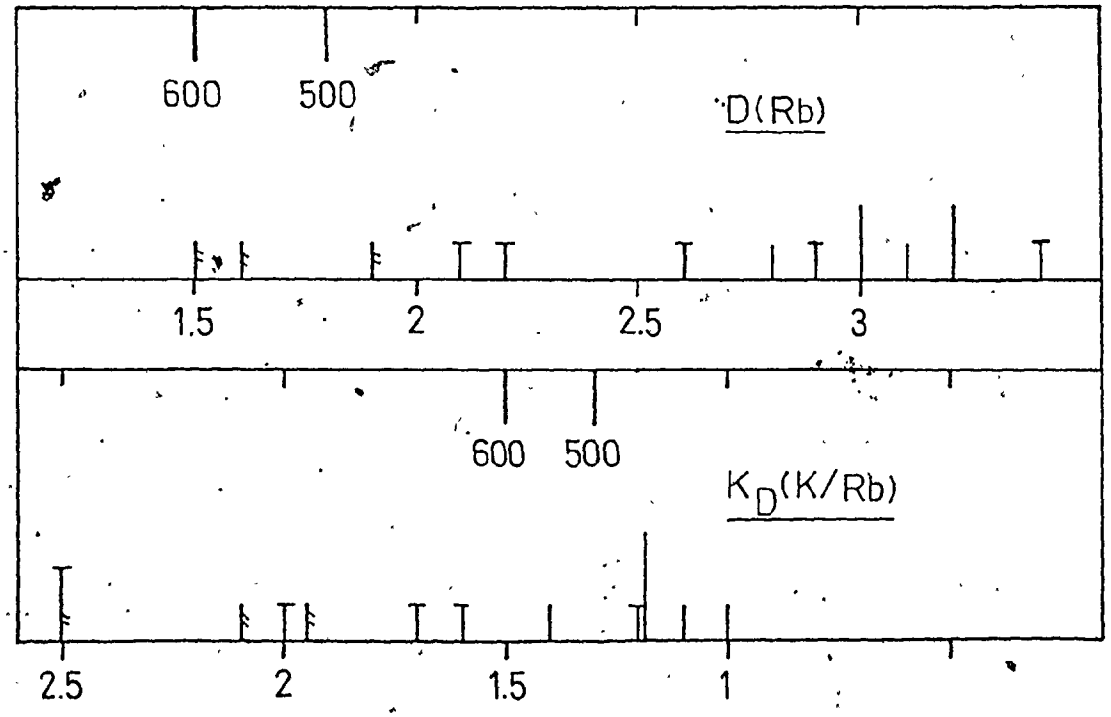
600
500
D(Rb)
1.5
2
2.5
3
600 500
K_D(K/Rb)
2.5
2
1.5
1

3-4-2d. Miscellaneous rocks from the Canadian Shield. Data from the Archean rocks from the Jackfish Lake area, Northern Ontario (Longstaffe, 1977) yield the following general temperature trend (Table 3-6a, Fig. 3-7):

diorite > granodiorite > gneiss > syenite,

which is, with the exception of the single sample of syenite, in agreement with petrologic evidence. Temperatures from D(Rb) and D(Tl) are very low, but those from all the K_D values range from 500° to 600°C, which are quite reasonable and are consistent with temperature estimates from oxygen isotope data (Longstaffe, 1977).

According to Longstaffe (1977), the syenite is a thin layer overlying the granodiorite body, and is formed by metasomatic process at about 500°C. This would account for the relatively low temperature of the syenite from all the geothermometers.

Sample F150 shows relatively low D(Rb), D(Tl), high K_D(Rb/Tl) and very high K_D(K/Rb) and K_D(K/Tl) values, corresponding to relatively high temperatures in all cases. Oxygen isotope and other evidence also show that this rock has undergone high temperature alteration with many of the minerals, including the feldspar, out of equilibrium with each other.

Table 3-6. Summary of alkali feldspar/rock data on rocks from the Canadian Shield#

No.	Rock	D(Rb)	D(Tl)	K_D(Rb/Tl)	K_D(K/Rb)	K_D(K/Tl)
a.	Jackfish Lake complex (Longstaffe, 1977).					
F98	gn	4.5	3.7	1.2	1.3	1.6
F151	gn	4.2	3.0	1.4	2.2	3.0
F110	gn	3.0	2.4	1.2	1.2	1.4
F73	gn	4.1	2.8	1.5	1.5	2.2
F150	gn	2.6	2.3	1.1	6.5	7.4
F37	gd	2.9	2.5	1.2	1.5	1.8
F118	gd	3.5	2.7	1.3	1.3	1.7
D1	gd	3.6	2.4	1.5	1.5	2.2
F26	gd	3.2	2.6	1.2	1.3	1.6
F3	gd	3.7	2.1	1.8	1.2	2.2
F46	sy	4.3	3.0	1.4	0.90	1.3
F135	md	2.4	1.0	2.4	2.3	5.4
b.	English River belt (Gower, in prep.)					
G145	gr	2.7	2.1	1.3	1.0	1.3
G886	gr	2.9	2.7	1.1	1.2	1.3
G110A	gr	2.8	2.5	1.1	1.0	1.2
G135	gd	4.0	3.3	1.2	1.5	1.8
G596A	tn	2.6	1.8	1.4	3.0	4.3
G350B	pg	3.1	3.0	1.0	0.84	0.88
c.	Miscellaneous (this study)					
	am	1.2	0.51	2.4	3.0	7.1
	am	6.7	0.95	7.1	1.4	10.
	pg	6.7	9.0	0.75	2.2	1.6
	gr	3.3	1.1	3.0	0.88	2.6
	no	4.8	1.8	2.7	1.3	3.5

gn gneiss, gd granodiorite, sy syenite, md monzodiorite, gr granite, tn tonalite, pg pegmatite, am amphibolite, no norite.
from Table A-6.

Fig. 3-7. Histogram of D and K_D values for the pair feldspar-rock for the rocks from the Jackfish Lake complex, N.W. Ontario (Longstaffe, 1977).

D monzodiorite, S syenite, ↑ gneiss, ↑ granodiorite.

Temperatures are from Sl-melt.

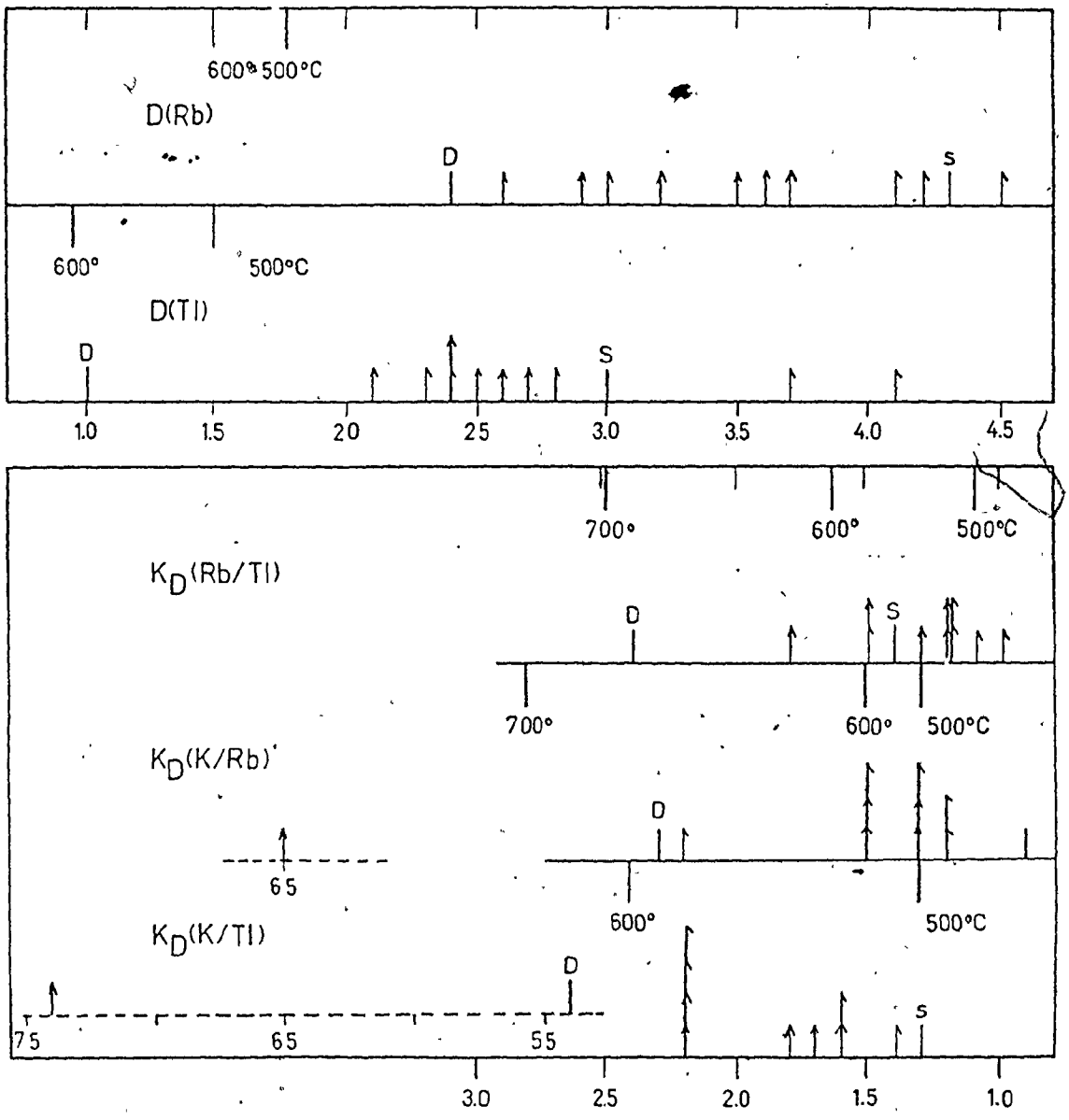
600° 500°C
D(Rb)
D
S
600°
500°C
D(Tl)
D
S
1.0
1.5
2.0
2.5
3.0
3.5
4.0
4.5
700°
600°
500°C
K_D(Rb/Tl)
D
S
700°
600°
500°C
K_D(K/Rb)
D
65
600°
500°C
K_D(K/Tl)
D
S
75
65
55
3.0
2.5
2.0
1.5
1.0

The Archaean rocks from the English River Belt, near Fort Francis (Gower, 1978) also yield very low temperature from the D(Rb) and D(Tl) data (Table 3-6b and Fig. 3-8). Temperatures from all the K_D values, as in the last case, cluster around 500°C, in agreement with petrologic arguments (Gower, 1978). Also, the general temperature trend as expected is

tonalite > granodiorite > granite > pegmatite

from all the thermometers except for one granodiorite (G135) and only in the D(Rb) and D(Tl) scales.

Similarly, data from several other rocks from different parts of the Canadian Shield (Table 3-5c) show low temperatures from the D values and relatively higher temperatures from the K_D values.

Besides being plutonic rocks and hence subject to the validity of the assumptions discussed previously, these old rocks are likely to have undergone alteration. As demonstrated by Hart (1969) for basalts, the alkalis (probably also Tl, because of their similarities) are very susceptible to seawater alteration. The data from this study show that, if alteration (whether by seawater or otherwise) was responsible for the low temperatures recorded by the D values, the K_D values are less affected.

Fig. 3-8. Histogram of D and K_D for the pair feldspar-rock for the rocks from the English River Belt, N.W. Ontario (Gower, 1978). Temperatures are from Sl-melt.

tonalite, granodiorite, granite, pegmatite.

the tonalite plots at 4.3 and is not included.

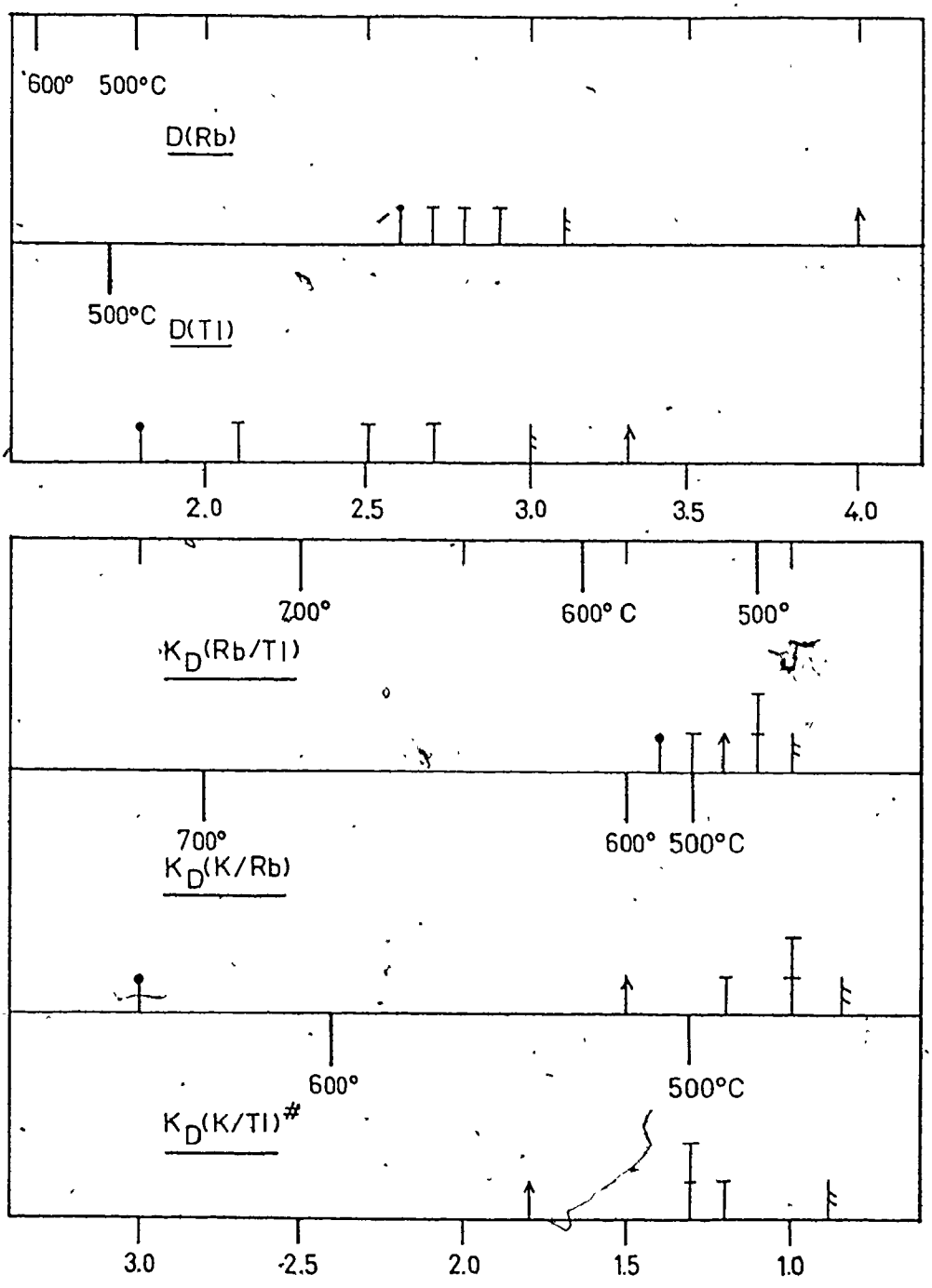
600° 500°C
D(Rb)
500°C D(Tl)
2.0
2.5
3.0
3.5
4.0
200°
600° C
500°
K_D(Rb/Tl)
700°
600° 500°C
K_D(K/Rb)
600°
500°C
K_D(K/Tl)#
3.0
2.5
2.0
1.5
1.0

3-5. Conclusions

Experimental results for the rhyolite-vapour pair show that both Rb and Tl partition with a slight preference for the vapour phase, except for Rb at 700°C, which shows equal partition. The effect of temperature on the Rb and Tl distribution is rather weak. Hence the temperature trend of the partition coefficients for the feldspar-melt pair, as calculated from the two solid-vapour pairs, are generally similar to those for the feldspar-vapour pair. Thus D(Rb) and D(Tl) decrease, while K_D(Rb/Tl), K_D(K/Rb) and K_D(K/Tl) increase from low to high temperatures for both the calculated Sl-melt and Ml-melt results. These trends are generally consistent with observations for many natural materials. Similar data at 700°C were also obtained by the MSV technique involving the direct equilibration of feldspar and melt (see Chapter 5).

An attempt was made to use the data for the sanidine Sl-melt pair semiquantitatively as geothermometers. The temperatures thus obtained for most volcanic rocks appear to be rather reasonable. For plutonic rocks, particularly those that are demonstrably altered, the D-thermometers usually give low temperatures. Subsolidus exchange and low-temperature secondary reactions, such as alteration or contamination, leading to disequilibration or re-equilibration at a low temperature, are possible explanations. In some of these cases, higher temperatures are recorded by some of the K_D-thermometers. Such differences be-

tween the D and K_D values may be useful in detecting secondary reactions.

Finally, the most serious problems faced by these and other similar geothermometers are:

a. the effect of the composition and nature of the feldspar;

b. lack of accurate means for assessing the composition of the original melt;

c. complications due to subsolidus, secondary reactions and other kinetic factors.

CHAPTER 4

RB AND TL DISTRIBUTION BETWEEN PHLOGOPITE AND SANIDINE

4-1. Introduction

4-1-1. Choice of technique

Due to the difficulties involved in separating small amounts of solids, conventional experimental studies on trace element distributions deal only with simple systems of solid-vapour pairs, as discussed previously.

Two methods have been developed for the direct measurement of solid-solid partition coefficients, namely, in situ analysis and simultaneous equilibration of multiple solids through a common vapour (MSV). In the in situ method, the phases studied are usually crystallized directly from a single charge and are spot-analysed (e.g. Mysen and Seitz, 1974; Drake and Weill, 1975).

In the MSV method, the solids are placed separately inside the same sample container and communicate through the vapour phase, so that all the equilibrated phases can be separated readily. Analysis can be performed with any technique suitable for small quantities of

material and low concentrations. This method allows simultaneous studies of any number of elements and two or more solids in one experiment. It can also be employed in other studies such as isotope fractionation and X-ray diffraction properties.

4-1-2. Previous work with MSV method

Iiyama (1968) used two gold pans, hanging in a reservoir of aqueous solution to measure partition coefficients of Sr, Ba, Cs and Rb between coexisting alkali feldspar and plagioclase (see section 2-4-2).

Kajiwara et al. (1969) used a quartz tube, divided into two compartments with quartz-wool, to study sulphur isotope fractionation between coexisting sulphide minerals.

However, the apparatus used in both these studies was very cumbersome and was limited to low temperature and pressure conditions.

Beswick (1973) inserted the mineral into an inner capsule and the vapour into an outer capsule in his study of K-Rb distributions between the pairs of phlogopite-vapour and sanidine-vapour. The inner capsule was crimped but not welded at both ends to allow the vapour to pass through.

By a similar technique, Blattner and Bird (1974) used two inner capsules to study the oxygen isotope fractionation between coexist-

ing alkali feldspar and quartz. The advantage of this double capsule method over those described previously is that the capsules can be treated in the conventional way in hydrothermal experiments, thus permitting studies over a wide range of temperature and pressure. Also, by varying the size of the inner and outer capusules, one can equilibrate more than two solids in the same run (see Chapter 5).

This technique was adopted in this study for the direct equilibration of coexisting feldspar and phlogopite at 700° C and 1.5 Kbar.

4-1-3. The system alkali feldspar-phlogopite

The mineral pair biotite-alkali feldspar provide hosts for a number of trace elements, especially the alkalis, alkaline earths, rare earths and Tl. The Fe-free experimental analogues sanidine-vapour and phlogopite-vapour have been studied by many workers with respect to trace element partitioning (e.g. Chelishchev, 1967; Roux et al., 1971; Beswick, 1973; and Volfinger, 1976).

Beswick (1973) demonstrated that the function K_D(Rb/K) for the pair phlogopite-sanidine, as extrapolated from the separate systems of sanidine-vapour and phlogopite-vapour, can be used as a geothermometer for volcanic rocks.

However, Albuquerque (1975) and Bernotat et al. (1976) showed that when applied to plutonic rocks, the temperatures obtained were usually contrary to petrologic evidence. Volfinger (1976) also

measured K_D(Rb/K) for the pairs phlogopite-vapour and sanidine-vapour and found little temperature dependence when extrapolated to the pair phlogopite-sanidine. Bernotat et al. (1976) argued that the uncertainty in the experimental data and the lack of agreement between published data renders such a geothermometer very unreliable.

One of the problems involved in such extrapolation of mineral-pair data from two pairs of mineral-vapour is the possible effect of the difference in composition on the solution chemistry. It is often uncertain whether the sanidine and phlogopite, e.g., are really at equilibrium with each other. By using the MSV technique, the two systems can be studied in a single experiment and hence no extrapolation is required. Moreover, many of the uncertainties involved in dealing with a vapour phase, as discussed previously (Chapter 2), can be avoided.

4-2. Experimental Procedure

4-2-1. Experiment with synthetic materials

Three synthetic gels were used as the starting material in the main part of this study (Table 4-1a), namely, a sanidine gel S2 which has been described previously (Table 2-1); phlogopite gels P1 and P2 containing 1.0 and 3.6 wt.% Rb respectively. The vapour was one of the aqueous solutions A to E containing 0.1 to 0.3% each of Li, Na, Rb, Tl, Ca, Sr, Mg and approximately 5% K such that the total cation

concentration was 2 molar, as chlorides and nitrates. In these experiments, either P1 or P2 was equilibrated with S2 (groups I and II respectively) with one of the solutions A to E (Table 4-1b) as the transporting agent. Procedure for sample preparation was as described for the MSV technique (A-1-1-2). The capsules were first heated to 900°C for one week, before being reduced to 700°C for an additional 30 days (fusion runs).

4-2-2. Other experiments with natural materials

In addition to the above two groups of runs, other MSV runs had also been conducted equilibrating the natural feldspars S1 or M1, which were also used in the feldspar-vapour SSV experiments (Chapter 2 and table 2-1), with a natural phlogopite P3 (Table 4-1a) (Groups III and IV respectively). In these two groups of runs, three other phases (albite, tremolite and rhyolite melt) were also present in the same capsule, but only the results for the feldspar-phlogopite pair will be discussed in this chapter (see Chapters 3 and 5). For these two groups of runs, the technique for regular runs was employed.

4-3. Experimental Results

4-3-1. Final products

As in the SSV runs (section 2-3-3) the sanidine gel S2 crystallized into a high sanidine (Fig. 2-12b, after Wright, 1968).

Table 4-1. Data for starting materials used in phlogopite-feldspar experiments. *

Material	K(%)	Rb(%)	Tl(ppm)	Description and source
a. MINERAL				
phlogopite P1	5.50	1.00	0	gels; Beswick (1973)
phlogopite P2	4.78	3.60	0	
sanidine S2	14.0	0	0	
phlogopite P3	5.86	0.038	3.1	phlogopite from Gib Lake; Shaw et al. (1965)
b. SOLUTIONS #				
A	5.04	0.30	0.30	aqueous solutions prepared from reagent grade KCl, RbCl and KNO_3
B	5.26	0.25	0.25	
C	5.50	0.20	0.20	
D	5.73	0.15	0.15	
E	5.95	0.10	0.10	

* Data for other starting feldspars, Sl and Ml were reported in Table 2-1.

\# Also contained 0.30% (A)-0.10% (E) Li and Na, and 0.10% (A)-0.30% (E) Ca, Sr, Mg and Ba.

The phlogopite gels P1 and P2 crystallized into phlogopites with Rb concentrations of 0.40-0.55 wt.% and 1.3-2.0 wt.% respectively. However, of the approximately 30 mg each of the gels used in each run, only about 10 mg of mineral was formed.

As was the case in the SSV runs, there was essentially no change in the structure of the natural feldspars: M1 remained a microcline and S1 an exsolved sanidine. There was also no change in the natural phlogopite P3.

4-3-2. Results

Data on the concentration of K, Rb and Tl and the phlogopite/sanidine D and K_D values for the four types of runs are shown in table 4-2, and also graphically in Figs. 1 to 5, as phlogopite (ordinate) against feldspar.

Pairs of Rb concentrations show three distinct but tight clusters according to the concentration of Rb in the minerals (Fig. 4-1). Hence, for those runs with high Rb concentration in the phlogopite (group II), D(Rb) is the highest ($\bar{x}$ = 6.1) and for those with high Rb in the feldspar (group III), D(Rb) is the lowest ($\bar{x}$ = 0.12). For those runs in which Rb is relatively low in both phlogopite and feldspars (groups I and IV), D(Rb) is intermediate between the two extremes, averaging to 2.3, with very little difference between them. Behaviour of K_D(K/Rb) is very similar, (Fig. 4-2) averaging 0.11 for group II; 6.5 for group III

		PHLOGOPITE			FELDSPAR			D		K_D		
No.	Sol.	K(%)	Rb(%)	Tl(ppm)	K(%)	Rb(%)	Tl(ppm)	Rb	Tl	Rb/Tl	K/Rb	K/Tl
I.	P1-S2											
15-1	A	9.12	0.49	410	13.2	0.21	610	2.3	0.68	3.4	0.30	1.0
15-2	A	8.90	0.40	360	13.2	0.20	260	2.0	1.4	1.4	0.34	0.48
15-3	A	10.8	0.52	290	12.3	0.19	130	2.7	2.2	1.2	0.32	0.41
15-4	B	9.66	0.45	560	12.4	0.22	330	2.0	1.7	1.2	0.38	0.45
15-5	B	10.0	0.52	290	14.3	0.21	140	2.5	2.0	1.3	0.28	0.35
15-6	B	9.93	0.55	350	14.1	0.22	140	2.5	2.6	0.96	0.28	0.28
15-7	C	9.29	0.44	280	13.8	0.24	250	1.8	1.1	1.6	0.37	0.61
15-8	C	9.18	0.44	160	12.8	0.25	180	1.8	0.85	2.1	0.41	0.84
15-9	E	8.99	0.45	170	11.8	0.14	120	3.3	1.4	2.4	0.23	0.54
II.	P2-S2											
15-10	C	7.99	1.79	110	12.2	0.28	82	6.4	1.3	4.8	0.10	0.49
15-11	C	8.40	1.37	100	12.3	0.26	120	5.3	0.86	6.2	0.13	0.80
15-12	D	8.36	1.95	540	12.9	0.33	600	5.9	0.90	6.6	0.11	0.72
15-13	D	8.14	1.90	650	12.4	0.31	630	6.1	1.0	6.1	0.11	0.63
15-14	E	8.41	1.52	100	11.6	0.24	110	6.3	0.90	7.0	0.11	0.80
15-15	E	8.25	1.62	88	12.4	0.25	97	6.5	0.91	7.1	0.10	0.74
III.	P3-M1											
13-1	EE	7.88	0.22	150	11.1	1.58	170	0.14	0.88	0.16	5.1	0.81
13-2	EE	7.82	0.16	110	10.5	1.45	140	0.11	0.79	0.14	6.8	0.94
13-3	EE	7.67	0.16	220	10.6	1.68	160	0.095	1.4	0.071	7.2	0.52
13-6	EE	8.06	0.19	270	10.5	1.72	170	0.11	1.6	0.069	7.0	0.48
IV.	P3-S1											
13-4	EE	7.88	0.13	200	7.09	0.073	130	1.8	1.5	1.2	0.62	0.74
13-5	EE	8.44	0.17	150	6.63	0.065	120	2.6	1.3	2.0	0.49	0.98

Table 42. Data for phlogopite-alkali feldspar MSV runs.

and 0.32 for group I. For the two runs in group IV, K_D(K/Rb) are slightly lower than, but relatively very similar to those of group I (0.49 and 0.62).

Turning to Tl as shown in Fig. 4-3, the data show more scatter. There is nevertheless a strong linear trend for all the pairs of data, with no tendency for the four groups of runs to behave differently. Average D(Tl) for all the data is 1.3. The behaviour of K/Tl is similar (Fig. 4-4), with K_D(K/Tl) averaging to 0.65.

The behaviour of Rb/Tl more or less follows that of Rb, and is also separable into three distinct clusters (Fig. 4-5). K_D(Rb/Tl) averages 6.5 for group II; 0.11 for group III; 1.7 for group I and 1.6 for group IV.

Hence it appears that only the behaviour of Rb, K/Rb and Rb/Tl is different from group to group, while Tl and K/Tl behave similarly for all the runs.

4-4. Discussion of results

4-4-1. Evaluation of Equilibrium

The differences observed in some of the results for the different groups of runs suggest either a lack of equilibration during the experiment or a variation in relation to the differences in the minerals. These differences include composition and nature of the starting (and final) materials and experimental technique, as discussed previously.

Fig. 4-1. Rb distribution between phlogopite-feldspar.

Concentration in wt. %, 0 P1-S2 (I), ● P2-S2 (II),

▲ P3-M1 (III), Δ P3-S1.

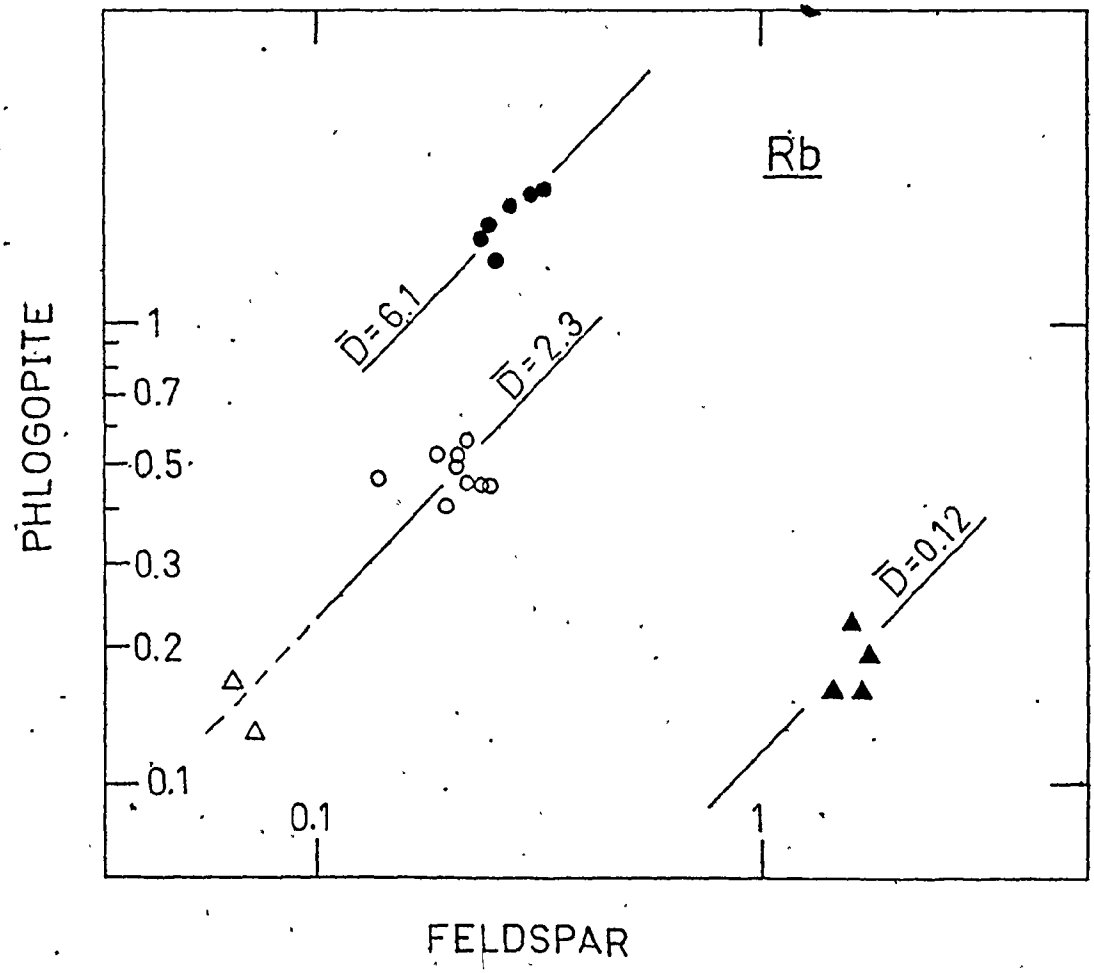
Rb
D=6.1
D=2.3
D=0.12
PHLOGOPITE
FELDSPAR
1
0.7
0.5
0.3
0.2
0.1
0.1
1

Fig. 4-2. Correlation of K/Rb between phlogopite-feldspar. Symbols same as in Fig. 4-1. # average for P1-S2.

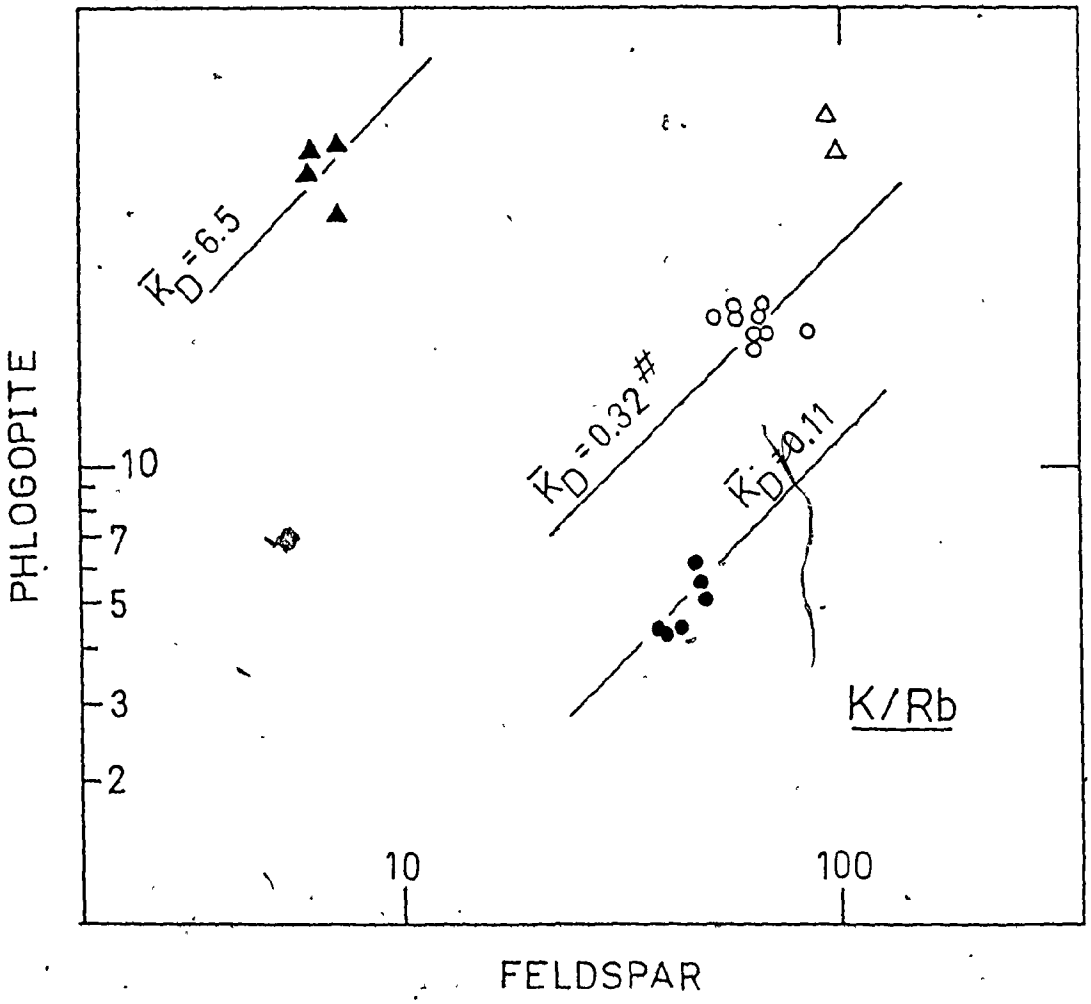
PHLOGOPITE
FELDSPAR
10
7
5
3
2
10
100
$\bar{K}_D$=6.5
$\bar{K}_D$=0.32
$\bar{K}_D$=0.11
K/Rb

Fig. 4-3. Tl distribution between phlogopite-feldspar.

Concentration in %, symbols same as in Fig. 4-1.

average for P1-S2.

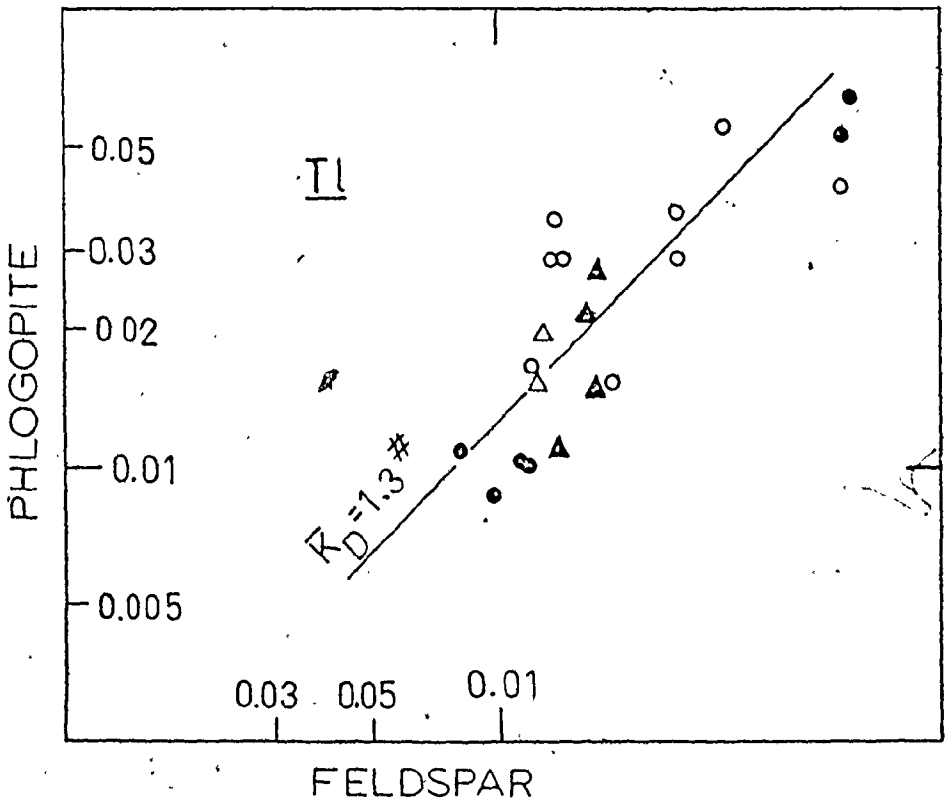
Tl
0.05
0.03
0 02
0.01
0.005
PHLOGOPITE
K_D=1.3*
0.03
0.05
0.01
FELDSPAR

Fig. 4-4. Correlation of K/Tl between phlogopite-feldspar. Symbols asme as in Fig. 4-1. #average for P1-S2.

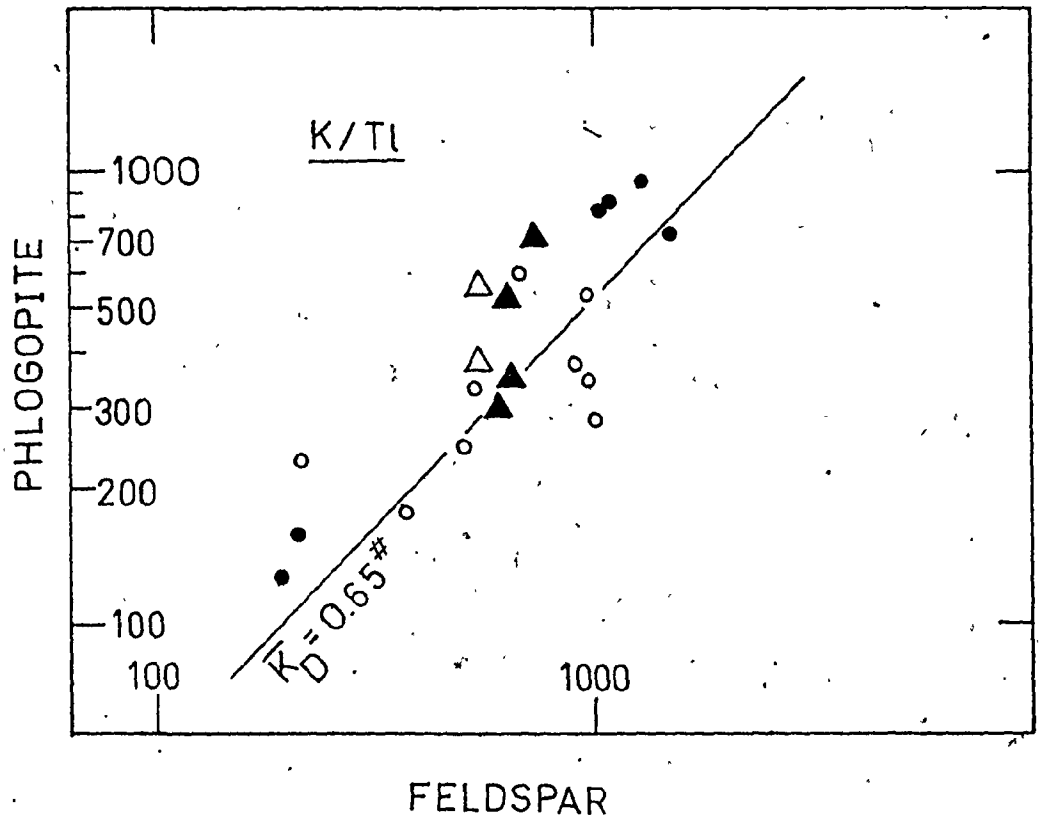
K/Tl
1000
700
500
300
200
100
100
1000
PHLOGOPITE
FELDSPAR
K_D=0.65#

Fig. 4-5. Correlation of Rb/Tl between phlogopite-feldspar. Symbols same as in Fig. 4-1.

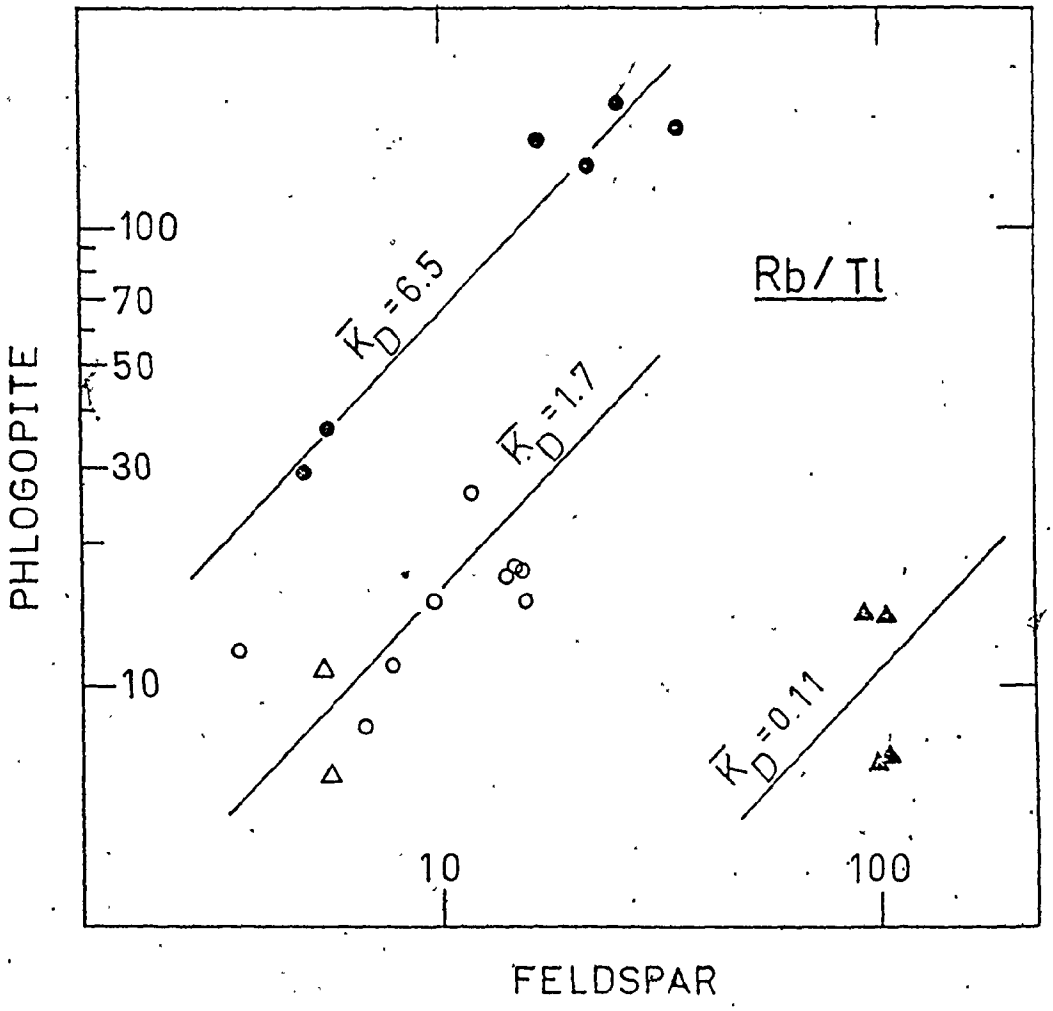
Rb/Tl
$\bar{K}_D$=6.5
$\bar{K}_D$=1.7
$\bar{K}_D$=0.11
100
70
50
30
10
PHLOGOPITE
10
100
FELDSPAR

That equilibrium was achieved in these experiments is suggested by the following arguments.

1. Both D(Tl) and K_D(K/Tl) are very similar in all the runs, including those for groups II and III. This is interpreted as a reflection on the similarity in the bulk Tl concentration in all the charges and that equilibrium in Tl distribution was achieved in all the runs.

2. Similarly, D(Na) and K_D(K/Na) are very similar for groups I and II which have very similar Na bulk composition (see Fung and Shaw, 1978).

3. Even for D(Rb), K_D(K/Rb) and K_D(Rb/Tl), which show deviation from constancy as a whole, results are very similar for both groups I and IV which are both low in bulk Rb concentration.

Thus constancy in D and K_D values are observed in those runs of similar bulk concentrations.

Beswick (1973) and Volfinger (1976) studied the distribution of K/Rb ratios between the pairs sanidine-vapour and phlogopite-vapour. Beswick concluded that K_D(K/Rb) deviated from constancy when K/Rb ratio in the phlogopite was less than about 5. The K/Rb ratio for P2 in this study ranges from 6.1 to 4.2, which is very close to this limit, but is much higher in the other phlogopites (18-61). In addition, the average K_D(K/Rb) values obtained by both Beswick and Volfinger are very similar to those for groups I and IV, but are markedly different from those for either group II or III (see section 4-3-4).

Beswick (1973) also concluded that K_D(K/Rb) for the pair sanidine-vapour deviated from constancy when K/Rb ratio in the sanidine was lower than 10 at 700°C. K/Rb ratio in Ml ranges from 6.1 to 7.2, all lower than this limit, but are much higher in the other feldspars (39-102). Hence, the devious behaviour of Rb observed for group III can be attributed to the deviation of Rb from ideality in Ml. This is probably due to a combination of structural and compositional effects, as discussed previously (section 2-4-1).

Moreover, Beswick did most of his 700°C runs in less than 30 days and Volfinger did his at 800°C in three days, suggesting that equilibrium can be reached within a relatively short time, as also was demonstrated in the time-variable test runs with Sl (Section 2-2-1).

Hence the devious behaviour of the pair P2-S2 is most likely to be due to the deviation of Rb from ideal behaviour in the phlogopite and that of the pair P3-Ml is due to a combination of structural and compositional effect in Ml, as pointed out previously (section 2-4-3-2).

4-4-2. Comparison with previous experimental data

Several workers have studied K/Rb distributions between the pairs sanidine-vapour (see also section 2-4-1) and phlogopite-vapour (Table 4-3). K_D(K/Rb) range from 0.58 to 0.90 and 1.8 to 3.0 respectively for the pairs phlogopite-vapour and sanidine-vapour at 700°C. Hence K_D(K/Rb), when calculated for the pair phlogopite-sanidine

REFERENCES	TEMPERATURE (°C)								
	400	450	500	550	600	650	700	745	800
a. Feldspar/vapour									
Lagache (1968)					2.38	2.1	(1.8)		
Chelishchev (1967)			2.5		1.1				
Foland (1973)							2.6	2.3	2.1
Beswick (1973)			5.9				3.0		2.2
Hofmann and Giletti (1970)					2.6	2.1.			
Volfinger (1976)	3.8		2.5		2.4		(2.4)		2.4
b. Phlogopite/vapour									
Chelishchev (1967)	3.3	2.0							
Hofmann and Gilette (1970)				0.81		0.82	0.83		
Beswick (1973)			1.6				0.90		0.78
Volfinger (1976)			0.82		0.65		(0.58)		0.53

Table 4-3. Summary of published K_D(K/Rb) data for the pairs feldspar-vapour and phlogopite-vapour. ( ) extrapolated.

ranges from 0.19 to 0.50, which agree very well with that for the pair P1-S2 ($\bar{K}_D$=0.32) and probably also within experimental uncertainty for the pair P3-S1 ($\bar{K}_D$=0.56). Data for the pair P2-S2 are too low (K_D=0.11), whi[illegible]hose for the pair P3-M1 are too high (K_D=6.5).

The calculated data, which involve two separate SSV experiments, would be affected by experimental and other uncertainties due to the differences in the nature and thermal history of the minerals (see section 2-4-2). Hence it will be more appropriate to discuss data reported by the same worker for both mineral-vapour pairs, namely those from Beswick (1973) and Volfinger (1976). Thus K_D(K/Rb) for Volfinger's data, when interpolated to 700°C, are 0.58 and 2.4 respectively for phlogopite-vapour and sanidine-vapour, and hence will be 0.24 when calculated for the pair phlogopite-sanidine, which is only slightly lower than that for P1-S2 ($\bar{K}_D$=0.32). Similarly, Beswick's results of 0.98 and 3.0 for the same two mineral-vapour pairs yield K_D=0.33 for the phlogopite-sanidine pair, which agrees very well with that of P1-S2.

4-4-3. Comparison with data from natural biotite-feldspar

Many workers reported K and Rb analyses for coexisting biotite and alkali feldspar, thus permitting the calculation of the biotite/feldspar D and K_D values (Table 4-4). The following is a general comparison of these data with those for the experimental phlogopite-feldspar pairs from this study. Only data for the pair P1-S2 will be used for this

D(Rb)	D(Tl)	K_D(Rb/Tl)	K_D(K/Rb)	K_D(K/Tl)	Rock Type and Locality	Reference
0.85-3.4			0.22-0.55		gr: Sinai	Bernotat et al., 1976
1.9 -2.7			0.24-0.34		gr,gd: N. Portugal	Albuquerque, 1973 and 1975
0.80-3.9			0.25-0.38		gr,ms: New England	Lange et al., 1966
2.4 -3.1			0.21-0.27		gr,gn,mg: Palmer	White, 1966
1.2 -2.5			0.22-0.51		gr,gd: Corsica	Carron and Lagache, 1969,1971
1.8 -2.9			0.27-0.34		gr,gd,to: S. California	Sen et al. 1959
1.4			0.48		rd: Mt. Proceda	Philpotts and Schnetzler,1970
			0.24-0.28		gn: N.W. Adirondacks	Whitney, 1969
1.4 -2.9			0.23-0.56		mg: Front Range	Hart, 1964
1.6 -4.8			0.15-0.27		gr: Lone Grove	Zartman, 1964
1.3 -2.1			0.34-0.39		ig: Tuscany	Barbieri et al., 1968
1.6 -2.0			0.22-0.55		gd,ig: Tuscany	Dupuy and Allegre, 1972
	1.9-3.2	0.50-0.91			gd,ig: Tuscany	Dupuy et al., 1973
	1.6-3.0				sy: Mt. Sandyk	Zlobin, 1958
2.5 -2.7	2.5-3.0	0.83-1.1			gr: Tyrny-Auz	Voskresenskaya, 1959
0.90-3.0	2.3-7.5	0.20-1.0	0.13-0.36	0.08-0.34	gn,gd,di: Jack Fish L.	Longstaffe, 1977
1.6 -3.6	2.1-4.4	0.52-0.82	0.20-0.28	0.11-0.21	gr,gd,gn,to: English R.	Gower, 1978
2.3	1.3	1.9	0.31	0.56		This study*

Table 4-4. Summary of data for coexisting natural biotite-alkali feldspar. gr granite, gn gneiss, gd granodiorite, mg migmatite, ms metasediment, rd rhyodacite, ig ignimbrite, sy syenite, to tonalite, di diorite.
* averages for the pair P1-S2.

purpose since they are most likely to have behaved ideally (section 4-3-1). It will be recalled, however, that D(Rb) and K_D(K/Rb) deviate from consistency in only those runs with high Rb concentration in either the phlogopite (P2) or the feldspar (M1). As expected, these data (Table 4-4, last line) are all outside the range of the data for the natural materials (c.f. Table 4-2).

Thus the experimentally determined D(Rb) value lies within the spread of most of the data for the natural materials except for three suites of rocks (those from Tuscany, Corsica and Mt. Proceda) which are relatively lower ($D < 2.2$). Similarly, there is also good agreement in K_D(K/Rb) values between the experimental and natural mica/feldspar data, except for three suites (those from the Lone Grove and the Palmer region and the English River) which are relatively lower (< 0.28) and one suite (ignimbrite from Tuscany) which is higher (> 0.34).

Turning to Tl, D(Tl) for all the natural biotite-feldspar pairs is generally higher relative to the experimental pair. Consequently, K_D(Rb/Tl) and K_D(K/Tl) are both lower for the natural materials.

Natural biotite contains Fe as a major element and a variable amount of Al substituting for Mg. According to Volfinger (1975), K_D(K/Rb) for the pair phlogopite-vapour was lower by a factor of 3 if Al substituted for Mg, and higher by a factor of 1.4 if Fe substituted for Mg. The reason for such a difference is probably a change in the structure

of the mica, as Rb is not known to substitute for either Al or Fe. If the effect of such a structural change is to favour the substitution of Rb, a larger ion, for K, it would also favour the substitution of Tl, resulting in higher D(Tl) and lower K_D(K/Tl), and possibly also lower K_D(Rb/Tl), as the ionic of Tl (1.84 Å) is slightly bigger than that of Rb (1.81 Å). Another possibility for Tl enrichment in natural biotite is the oxidation of Tl^{1+} to Tl^{3+} which, due to its similarity to the sulfophites (section 1-2), may substitute for Fe.

The effect of temperature was not investigated in this study and is difficult to assess from the published data, due to a lack of agreement even among workers reporting data for both phlogopite-vapour and sanidine-vapour pairs. Thus, although Beswick (1973) noted an increase in K_D(K/Rb) for the pair phlogopite-sanidine (calculated) from 0.24 at 500°C to 0.34 at 800°C, Volfinger (1976) reported a decrease from 0.33 to 0.22 for the same temperature range.

The effect of composition and other factors on the behaviour of feldspar have been discussed previously (section 2-4-2).

In summary, data obtained for the pair P1-S2 and P3-S1, which have low bulk Rb concentration, agree rather well with data for natural systems. Minor differences can easily be accounted for by experimental error and composition of natural biotites. Rb results for experiments with P3-M1 and P2-S2 are not satisfactory, due possibly to the high concen-

tration of Rb in M1 and P2 respectively and hence deviation from ideal behaviour, as the Tl results agree with those from the other runs.

4-5. Conclusion

Rb distribution between coexisting phlogopite-feldspar pairs probably deviates from ideal behaviour when Rb concentration is high in either minerals. Only for the pair P1-S2 (and P3-S1) in which Rb concentrations in phlogopite and feldspar range up to 0.52% and 0.25% respectively is the distribution data in agreement with other experimental data and most data for natural biotite-feldspar pair.

Tl distributions, on the other hand, are very similar for all the different pairs of initial minerals with Tl concentration of up to 650 ppm in phlogopite and 630 ppm in feldspar. However, the experimental data for D(Tl) are slightly lower, while K_D(Rb/Tl) and K_D(K/Tl) are slightly higher relative to the natural analogues. This is probably due to the dual behaviour of Tl, substituting for both K and Fe in the natural biotite. In any case, no serious disagreement between the experimental data from this study and those reported in the literature for either experimental or natural materials is observed.

The most satisfactory data on the Rb and Tl distributions at 700°C (averages for the pair P1-S2) are as follows:

$$D(Rb) = 2.3,\ D(Tl) = 1.3,\ K_D(Rb/Tl) = 1.9,$$

$$K_D(K/Rb) = 0.31,\ K_D(K/Tl) = 0.56$$

Hence, relative to the coexisting alkali feldspar, a phlogopite takes up more Rb and Tl and has lower K/Rb and K/Tl ratios. This can be explained by the relatively larger and looser structure of the mica, thus permitting more substitution of K by the larger Rb and Tl ions. Also the Rb/Tl ratio for a phlogopite is higher than the coexisting feldspar. The reason for this is not clear, since the ionic size for both ions are very similar. These predictions are generally born out by the published data for natural biotite-feldspar pair. In the case of Tl relative enrichment in the biotite is probably enhanced by the presence of Fe in the biotite structure hence allowing additional substitution by Tl.

The most important outcome of this study is the feasibility of the MSV technique as applied to the study of multi-element distributions between two or more coexisting solid phases, as pointed out elsewhere (see Fung and Shaw, 1978).

CHAPTER 5

K, Rb AND Tl DISTRIBUTIONS IN MULTI-PHASE SYSTEMS FROM HYDROTHERMAL EXPERIMENTS AND ROCKS

5-1. Introduction and experimental technique

The MSV technique, as described in Chapter 4, was applied to the system phlogopite-alkali feldspar-amphibole-albite-rhyolite melt to study the distribution of K, Rb and Tl at 600° C and 700° C. In essence, this is a simplified, Fe-free granitic system under subsolidus-subliquidus conditions. Some of the results from this study have already been discussed previously (Chapter 2-4) in relation to other mineral-pair distributions. In this chapter, a more general approach will be adopted to discuss the overall distributions among the phases of interest. Due to the complexity of the system and the simplified approach of such experiments, the discussion will be semi-quantitative. A more detailed discussion will be devoted to the natural material in the latter part of this chapter which will be used later (Chapter 6) in relation to fractionation trends observed in rocks.

Procedure for capsule preparation was that of the MSV technique (sections 4-2-1 and 4-2-2), modified for 5 solid phases (A-1-1-2). Three runs were made at each of 600°C and 700°C for duration of about 30 days. Natural materials were used in all the runs, some of which have already been described: sanidine Sl, microcline Ml (Table 2-1), phlogopite P3 (Table 4-1) and the rhyolite glass (Section 3-2). Two new minerals, an amphibole (Am) and albite (Ab), separated from the same rocks as the phlogopite P3 (see also Shaw et al. 1965) were also used. Their compositions, as determined by the present author were:

	K(%)	Rb(ppm)	Tl(ppm)
Ab	0.12	40	0.17
Am	0.57	32	0.15

In each run, either the sanidine Sl or the microcline Ml was used with all the other four phases. The vapour, used as a transporting agent, was solution EX (Table 2-1). The heating procedure was that of regular runs, in which the capsules were heated directly to the desired temperature and maintained for about 30 days.

5-2. Experimental results and discussions

5-2-1. Final products

The structures of the final sanidine Sl, microcline Ml and phlogopite P3 have been described previously (Sections 2-4-2-1 and 4-3-1).

In essence, there was no major change in the structures of these and the other minerals, amphibole Am and albite Ab. The rhyolite, on the other hand, was partially crystallized (10-30%) into predominantly sanidine, with minor amounts of quartz, plagioclase and mica (biotite).

5-2-2. Results

Table 5-1 shows the K, Rb and Tl abundances in all the phases studied. Although two temperatures were used in these runs, the temperature difference will be ignored in the following discussions, due to the paucity of the results and the fact that the effect of temperature in these runs was greatly overshadowed by other uncertainties involved.

For each run, the D and K_D values for each pair of solid phases were calculated as before. For each of these, the average and range of $\bar{x} \pm 1s$ was computed using all the results, except in the case of the alkali feldspars, in which only the results for the two runs with Sl were used for D(Rb), K_D(Rb/Tl) and K_D(K/Rb), since Rb had been shown previously (section 4-3-1, e.g.) to have behaved non-ideally in Ml. It is worthy of note that the results for D(Tl) and K_D(K/Tl) are very similar regardless of whether Sl or Ml was the alkali feldspar (see also Chapter 4), and the results for the other pairs of phases in a run do not appear to be affected by whether the coexisting alkali feldspar was Sl or Ml.

Temperature	No.	Phase	K(%)	Rb(%)	Tl(ppm)
600°C					
	13-4	P3	7.88	0.130	201
		Sl	7.09	0.083	133
		Am	1.03	0.025	68
		Ab	0.62	0.021	55
		Rhy	4.18	0.124	235
	13-5	P3	8.44	0.172	150
		Sl	6.63	0.085	112
		Am	0.98	0.027	61
		Ab	0.77	0.028	48
		Rhy	3.59	0.140	203
	13-1	P3	7.88	0.217	152
		Ml	11.05	1.58	168
		Am	0.97	0.035	40
		Ab	0.91	0.029	30
		Rhy	3.68	0.225	175
700°C					
	13-2	P3	7.82	0.158	114
		Ml	10.54	1.45	144
		Am	1.10	0.035	46
		Ab	0.78	0.029	32
		Rhy	5.06	0.156	113
	13-3	P3	7.67	0.163	218
		Ml	10.58	1.68	160
		Am	1.34	0.056	98
		Ab	0.66	0.027	47
		Rhy	4.90	0.139	200
	13-6	P3	8.06	0.188	268
		Ml	10.49	1.72	170
		Am	1.45	0.062	106
		Ab	0.67	0.026	68
		Rhy	6.16	0.324	261

Table 5-1. Concentration data for MSV regular runs with five solids and vapour EX (not shown).

The $\bar{x} \pm 1s$ range of all the D and K_D values are shown as a matrix in Table 5-2. In each case, the value shown in the j-th row and i-th column is that for the pair of phase i/phase j (Dij). Dji for the pair phase j/phase i (not shown) is simply the inverse of Dij. For example, D(Rb) for the pair phlogopite/sanidine is 1.8 as shown, and that for sanidine/phlogopite would be 1/1.8 or 0.51.

These two-dimension data can be further condensed by arranging the phases into series of decreasing (average) concentration or ratio of elements (Table 5-3). In such an arrangement, only the D or K_D value between each adjacent pair is shown, but that for any other pair can be approximated by the product of all the intervening values. For example, D(Rb) for the pair phlogopite/albite should be 1.0 x 1.8 x 3.3 x 1.5 or 7.9, a fair estimate for the measured value of 6.4 ± 0.79. Such arrangements (hereafter called preference series) greatly simplify partition data for multi-phase systems. The degree of distortion of the information will naturally depend upon the amount of spread and the availability of data.

5-2-3. Discussion

Average Rb and Tl concentrations both decrease in the same order of

rhyolite > phlogopite > alkali feldspar > amphibole > albite.

	phlogopite	K-feldspar	Amphibole	albite
D(Rb)				
alkali feldspar*	1.8 ± 0.32#			
amphibole	4.7 ± 1.5	3.3 ± 0.11		
albite	6.4 ± 0.79	3.5 ± 0.65	1.5 ± 0.59	
rhyolite	0.99± 0.23	0.64± 0.04	0.22± 0.09	0.16±0.046
D(Tl)				
alkali feldspar*	1.4 ± 0.39			
amphibole	2.7 ± 0.57	2.6 ± 0.38		
albite	4.0 ± 0.71	3.5 ± 1.3	1.5 ± 0.31	
rhyolite	0.93± 0.13	0.80± 0.29	0.35± 0.09	0.24± 0.04
K_D(Rb/Tl)				
alkali feldspar*	1.3 ± 0.35			
amphibole	1.7 ± 0.50	1.7 ± 0.01		
albite	1.6 ± 0.25	1.5 ± 0.26	1.0 ± 0.28	
rhyolite	1.1 ± 0.37	1.1 ± 0.06	0.63± 0.13	0.67± 0.02
K_D(K/Rb)				
alkali feldspar*	0.67± 0.06			
amphibole	1.6 ± 0.27	2.1 ± 0.05		
albite	1.8 ± 0.31	2.9 ± 0.04	1.1 ± 0.23	
rhyolite	1.9 ± 0.49	2.8 ± 0.36	1.2 ± 0.34	1.1 ± 0.44
K_D(K/Tl)				
alkali feldspar	0.74± 0.20			
amphibole	2.7 ± 0.51	3.7 ± 0.83		
albite	2.9 ± 0.69	4.1 ± 1.5	1.1 ± 0.24	
rhyolite	2.0 ± 0.75	2.7 ± 0.60	0.76± 0.26	0.75± 0.36

* only results for the sanidine S1 were used

\# D(Rb) = 1.8 for the pair phlogopite/K-feldspar etc.

Table 5-2. Matrices of D and K_D values ($\bar{x}$ ± 1s) for pairs of experimental phases. See text for explanation of the table.

D(Rb)

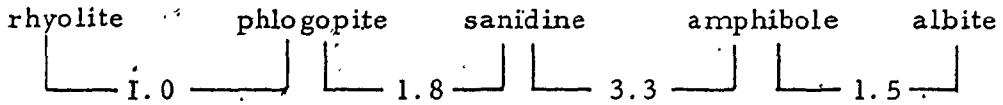

D(Tl)

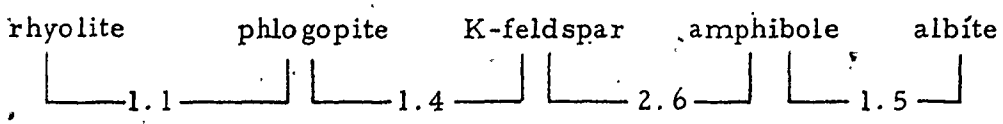

K_D(Rb/Tl)

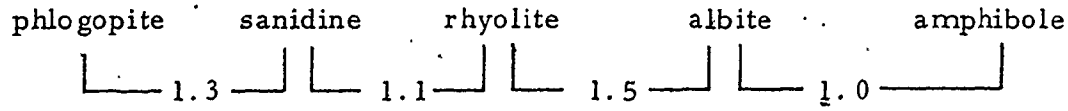

K_D(K/Rb)

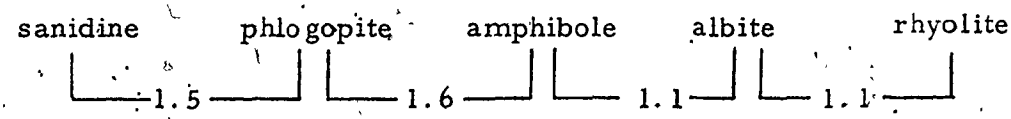

K_D(K/Tl)

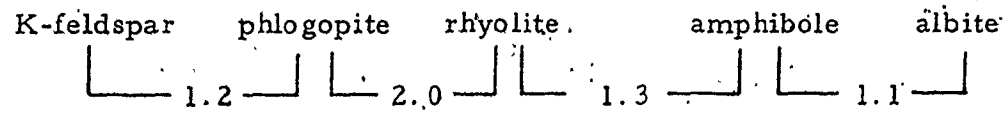

Table 5-3. Series of relative element concentration or ratio for the experimental phases. Average D and K_D values are shown for adjacent pairs.

Hence both Rb and Tl are preferentially concentrated in the melt and the K-phases much more (by a factor of 2.7 to 6.4) than in the coexisting phases in which K is not a major element (amphibole and albite).

This reflects the control of the structure of a phase and the ionic radii of trace elements substituting for a major element. Hence the major cations in albite are Ca and Na (ionic radii = 1.20 and 1.24 respectively) in 8-fold coordination with oxygen and those in amphibole are Ca, Mg and Fe (ionic radii = 1.20, 0.80 and 0.69 respectively) in 6-fold coordination. None of these is suitable for substitution by the larger ions of Rb and Tl (ionic radii = 1.81 and 1.84 respectively). The K-phases (including the rhyolite), on the other hand, all contain K (ionic radius = 1.68) in 12-fold coordination, which can accommodate considerably more substitution by the larger ions. Of the three K-phases, the rhyolite, being mostly molten under the experimental conditions, has the loosest structure and hence can tolerate the most amount of Rb and Tl. Similarly, the K-sites in biotite are loosely bound between sheets of mainly $(Al,Si)O_4$. The structure of alkali feldspar is a three-dimension network of $KAlSiO_3$, and hence is the least tolerant to substitution by the larger cations.

Turning to the K_D values, the relative position of the phases remains more or less unchanged except for the following:

1. Most of the K_D values are closer to 1.0 than the D values, which is as expected, since the ratios of pairs of elements of similar crystallo-chemical properties are usually less fractionated by various minerals relative to the individual elements.

2. Position of the melt is more variable, being the lowest in K/Rb, and intermediate in Rb/Tl and K/Tl.

3. The alkali feldspar is the highest in both K/Rb and K/Tl. Hence the K-phases are also higher in K/Rb, K/Tl and Rb/Tl relative to the non-K phases.

The amphibole appears to be somewhat enriched in both Rb and Tl (by a factor of 1.5) relative to the coexisting albite, and has higher K/Rb and K/Tl ratios. Their Rb/Tl ratios are approximately the same.

The pairs of phlogopite-sanidine and sanidine-melt have been previously discussed (Chapter 3 and 4).

5-2-4. Comparison with published experimental data

Iiyama (1968) measured D(Rb) between coexisting pairs of alkali feldspar/plagioclase by MSV technique similar to that of this study (see also sections 2-4-3b and 4-1-2) as a function of the composition of both phases, at a temperature of 600°C and P_{H_2O} = 1 Kbar. His data (also shown in Table 2-15) together with those from the two Sl/Ab runs are shown in the following:

	D(Rb) (K-feldspar/plagioclase)				
Composition	Or_{100}/An_{100}	Or_{85}/An_{50}	Or_{75}/An_{30}	Or_{51}/An_{85}	Or_{47}/An_{82}
Iiyama (1968)	40	25	9.6		
This study*				3.9	3.0

*Composition of the plagioclase was estimated from the Na concentration.

Hence, the trend of D(Rb) with the composition of the two coexisting feldspars is consistent between the two sets of data.

D(Rb) for the pairs sanidine/melt and phlogopite/melt for the data from Beswick (1973, and personal communication to D. M. Shaw) are compared to those from this study in the following:

D(Rb)	Beswick (1973)	This study#
sanidine/melt	0.3 - 1.8 $\bar{x}$ = 0.64	0.67, 0.61 $\bar{x}$ = 0.64
phlogopite/melt	0.7 - 3.3 $\bar{x}$ = 1.5	0.58 - 1.2 $\bar{x}$ = 0.99

Similarly, the following is a comparison of K_D(K/Rb) for the pairs of sanidine/melt and phlogopite/melt:

K_D(K/Rb) (mean)		500°C	600°C	700°C	800°C
sanidine/melt	Beswick(1973)	5.6		2.9	2.1
	This study#		2.8		
phlogopite/melt	Beswick(1973)	1.5		0.85	0.74
	This study		1.9		

In the case of sanidine/melt, only the result for the two sanidine SI runs were used.

The agreement for sanidine/melt is reasonable in both cases and is probably within experimental error for phlogopite/melt. Other comparisons were discussed in Chapters 3 and 4.

5-3. K, Rb and Tl distribution between natural biotite-orthoclase-amphibole-plagioclase and host rock

5-3-1. Data

A number of rocks and their constituent minerals (Table A-6) have been analysed for their K, Rb and Tl abundances (Table A-7). In this section, only the data for the phases biotite, alkali feldspar, amphibole, plagioclase and their host rocks will be discussed (see Chapter 6). Most of these rocks were plutonic, and mainly silicic (granitic), but some metamorphic (medium to high grade), volcanic and mafic rocks were also included. Similar data from some selected literature reports were also included (Table 5-4).

As before, D and K_D values for each pair of phases were calculated for all the available data. From each suite of rocks (or all those from a single publication or collection), the range of $\bar{x} \pm 1s$ was calculated twice for each D and K_D values; first with all the data and secondly after eliminating those values which fall outside the first $\bar{x} \pm 1s$ range. Such screening was considered necessary in order to reduce

Rock Type	Locality	Donor/Reference
This study#		
a. various plutonics	Jackfish Lake, N. Ont.	Longstaffe (1977)
b. various plutonics	English River Belt, N. Ont.	Gower, in prep. (1978)
c. granites, pegmatites	Preissac-Lacorne area, Que.	Siroonian (1957)
d. pelitic schist	Grenville Province	Kwak (1968)
e. amphibolite	Loon Lake	Chiang (1965)
f. Sudbury irruptives	Strathcona Mine	J.H. Crocket
g. granite, granodiorite	N. Portugal	Albuquerque*(1973, 1974, 1975)
h. basalts and related	various	various
i. meta-pelites	Littleton Formation	Shaw (1954a, b, 1956)
j. sedimentary	various	various
k. miscellaneous	McMaster Univ. collection	various
Literature reports		
l. syenite	Mt. Sandyk massif	Zlobin (1958)
m. ignimbrite, granodiorite	Tuscany	Dupuy et al. (1973) and Barbieri et al. (1968)
o. granodiorite	S.E. Corsica	Carron and Lagache (1968)
p. granite, granodiorite	S. Corsica	---------- (1971)
q. migmatite	Palmer region	White (1966)
r. gneiss	Adirondacks	Whitney (1969)
s. various	various	Hart and Aldricht (1967)
t. various	various	Murthy and Griffin (1970)
u. various plutonic	California Batholith	Sen et al. (1958)
v. granite, tonalite	Malaya Laba massif	Demin and Khitarov (1958)
w. granite	Tyrny-Auz	Voskresenskaya (1959)
x. granite, pegmatite	Karelia region	Lobach-Zhuchenko and Vasilyeva (1970)
y. rhyodacite	Italy	Philpotts and Schnetzler(197(

Table 5-4. Listing of samples from this study and selected literature reports.

analysis results given in Table A-6, description of samples in Table A-5.
* K and Rb data from original author.

Table 5-5. Matrix of D(Rb) values for coexisting natural phases. The number of observations are in parentheses.

	biotite	alkali feldspar	amphibole
alkali feldspar			
	a. 2.2 +0.36 (7)		
	b. 2.5 +0.27 (4)		
	c. 0.55 (1) x		
	v. 2.2 +0.25 (6)		
	w. 2.6 ±0.15 (2)		
	x. 1.9 ±0.08 (3)		
	m. 1.7 +0.05 (12)		
	g. 2.5 ±0.14 (5)		
	o. 2.4 ±0.15 (7)		
	p. 1.9 ±0.24 (21)		
	q. 2.6 ±0.14 (5)		
	r. 10 ±2.6 (7) x		
	e. 1.7 (1)		
	f. 2.5 (1)		
	u. 2.8 ±0.26 (4)		
	y. 1.4 (1)		
	k. 3.3 ±2 (2)		
hornblende			
	a. 23 ±12 (3)	a. 12 ±4.7 (3)	
	c. 64 ±1.0 (2) x	o. 6.9 ±0.9 (6)	
	o. 17 ±1.1 (6)	p. 8.0 ±0.4 (5)	
	p. 17 ±1.1 (6)	u. 53 ±11 (2) x	
	s. 30 ±6.7 (7)		

Table 5-5 (cont'd.) D(Rb)

	biotite	alkali feldspar	amphibole	plagioclase
plagioclase				
	a. 25 ±7.9 (6)	a. 10 ±4.8 (8)	a. 1.7 ±0.54 (3)	
	b. 78 ±38 (8) x	b. 21 ±1.8 (3)	b. 3.5 ±2.3 (2)	
	o. 22 ±3.5 (7)	n. 26 (1)	o. 1.3 ±0.29 (7)	
	p. 23 ±4.7 (19)	q. 1.2 ±0.1 (3) x	p. 1.3 ±0.23 (7)	
	f. 52 ±6.2 (2)	o. 9.7 ±1.3 (7)		
	k. 38 ±27 (3)	p. 12 ±2.5 (23)		
		k. 39 ±3.2 (2)		
rock				
	a. 7.5 ±1.9 (9)	a. 3.5 ±0.48 (8)	a. 0.48±0.28 (5)	a. 0.31±0.11 (10)
	b. 8.7 ±1.5 (7)	b. 2.8 ±0.19 (5)	b. 1.4 ±0.19 (2) x	b. 0.27±0.07 (11)
	c. 5.1 ±0.83 (2)	v. 7.9 (1) x	c. 0.16 (1)	o. 0.24±0.05 (9)
	v. 2.5 ±1.2 (4)	w. 1.1 ±0.39 (4)	o. 0.37±0.43 (7)	f. 0.28±0.09 (3)
	w. 3.3 ±0.11 (2)	x. 1.7 ±0.64 (2)	f. 0.03±0.01 (2) x	k. 0.13±0.05 (2)
	m. 1.9 ±0.33 (16)	m. 1.0 ±0.08 (17)	k. 0.48±0.10 (2)	
	g. 3.6 ±0.16 (3)	g. 1.7 ±0.27 (9)		
	o. 6.0 ±0.4 (6)	o. 2.5 ±0.24 (8)		
	q. 5.8 ±1.1 (3)	q. 2.8 ±0.39 (10)		
	y. 10 ±2.6 (7)	y. 0.5 ±0.18 (10) x		
	e. 1.7 (1)	f. 4.8 (1)		
	f. 2.5 (1)	u. 2.4 (2)		
	u. 2.8 ±0.26 (4)	k. 2.0 ±0.19 (3)		
	1.4 (1)			
	k. 3.3 ±2.0 (2)			
	d. 3.2 ±0.29 (3)	f. 1.8 (1)		
	e. 2.8 ±0.45 (2)	k. 1.0 ±0.1 (2)		
	f. 9.2 ±3.3 (2)			
	k. 9.0 ±0.92 (2)			

Table 5-6. Matrix of D(Tl) for coexisting natural phases.

	biotite	alkali feldspar	amphibole	plagioclase
alkali feldspar				
	a. 4.6 ±1.7 (8)			
	b. 4.8 ±0.47 (5)			
	c. 0.71 (1) x			
	v. 1.1 ±0.20 (4)			
	w. 2.8 ±0.35 (2)			
	l. 2.8 ±0.28 (4)			
	m. 2.5 ±0.45 (7)			
	j. 4.8 (1)			
	f. 4.2 (1)			
hornblende				
	a. 12 ±3.1 (4)	a. 3.1 ±0.90 (5)		
	c. 34 ±1.8 (2)	l. 3.3 ±0.4 (2)		
	l. 9.2 ±2.4 (2)	e. 4.0 (1)		
	e. 25 ±6.7 (6)	k. 2.7 (1)		
	k. 17 ±9.0 (2)			
plagioclase				
	a. 17 ±4.1 (7)	a. 2.6 ±0.60 (6) x	a. 1.3 ±0.65 (6)	
	b. 63 ±32 (9)	b. 10 ±2.6 (5)	b. 7.2 ±3.1 (2) x ?	
	m. 11 ±0.93 (2)	m. 9.6 ±3.1 (3)	k. 6.7 (1) x ?	
	f. 78 ±0.79 (2)	k. 12 ±7.9 (2)		
rock				
	a. 8.5 ±3.0 (9)	a. 2.5 ±0.27 (9)	a. 0.83±0.16 (5)	a. 0.68±0.28 (10)
	b. 13 ±1.8 (8)	b. 2.6 ±0.34 (4)	b. 1.1 ±0.35 (2)	b. 0.18±0.06 (9)
	c. 6.2 ±0.15 (2)	c. 7.9 (1) x	c. 0.29 (1)	m. 0.20±0.03 (3)
	v. 1.5 ±0.23 (5)	v. 1.3 ±0.19 (6)	l. 0.49±0.25 (2)	k. 0.29±0.24 (4)
	w. 3.8 ±0.45 (2)	w. 1.8 ±0.13 (2)	e. 0.15±0.03 (2)	
	l. 3.4 ±1.2 (4)	l. 1.2 ±0.18 (4)	k. 0.35±0.04 (3)	
	m. 2.6 ±0.30 (7)	m. 1.2 ±0.11 (10)		
	g. 2.2 ±0.55 (10)	e. 0.5 (1) x		

Table 5-7. Matrix of K_D(Rb/Tl) for coexisting natural phases.

	biotite	alkali feldspar	amphibole	plagioclase
alkali feldspar				
	a. 0.49±0.34 (9)			
	b. 0.63±0.11 (4)			
	c. 0.78 (1)			
	v. 2.1 ±2.5 (6) x			
	w. 0.96±0.18 (2)			
	m. 0.63±0.10 (7)			
	e. 0.34 (1)			
	f. 0.59 (1)			
	k. 0.38±0.23 (2)			
hornblende				
	a. 2.0 ±0.89 (4)	a. 6.5 ±2.0 (4)		
	b. 1.9 (2)	k. 4.5 (1)		
	e. 1.0 ±0.14 (4)			
plagioclase				
	a. 1.6 ±0.47 (9)	a. 3.3 ±1.1 (7)	a. 1.0 ±0.42 (4)	
	b. 1.1 ±0.29 (8)	b. 1.7 ±0.61 (4)	b. 0.088±0.005(2)	
	j. 1.1 ±0.28 (2)	k. 3.9 ±2.3 (2)	k. 0.51 (1)	
	f. 0.71±0.04 (2)			
	k. 1.2 ±0.05 (3)			
rock	a. 0.89±0.36 (10)	a. 1.4 ±0.36 (11)	a. 0.39±0.22 (6)	a. 0.47±0.12 (10)
	b. 0.93±0.19 (8)	b. 1.1 ±0.08 (5)	b. 1.1 ±0.20 (2)	b. 0.95±0.41 (11)
	c. 0.98±0.06 (2)	c. 0.76 (1)	c. 0.56 (1)	f. 1.8 ±0.75 (3) x
	v. 1.5 ±0.60 (4)	v. 0.78±0.31 (6)	j. 1.7 ±0.9 (2)	k. 1.1 ±0.79 (2)
	w. 0.93±0.44 (2)	w. 0.95±0.30 (2)	k. 1.3 ±0.33 (2)	
	m. 0.66±0.08 (8)	g. 0.81±0.20 (9)		
	d. 2.6 ±2.6 (3) x	e. 2.4 (1) x		
	e. 0.92±0.15 (2)	f. 2.7 (1) x		
	f. 1.4 ±0.26 (2)	k. 1.9 ±1.5 (2)		
	k. 2.2 ±2.3 (2) x			

Table 5-8. Matrix of K_D(K/Rb) for coexisting natural phases.

	biotite	alkali feldspar	amphibole
alkali feldspar			
	a. 0.26±0.07 (9)		
	b. 0.22±0.025(5)		
	c. 2.6 (1) x		
	v. 0.55±0.34 (7)		
	m. 0.39±0.02 (11)		
	o. 0.29±0.03 (8)		
	p. 0.34±0.03 (20)		
	q. 0.25±0.02 (7)		
	r. 0.26±0.01 (9)		
	e. 0.40 (1)		
	f. 0.42 (1)		
	u. 0.31±0.05 (2)		
	k. 0.23±0.10 (2)		
hornblende			
	a. 0.29±0.16 (4)	a. 1.1 ±0.58 (4)	
	c. 0.21±0.05 (2)	p. 1.6 ±0.23 (6)	
	p. 0.46±0.10 (8)	u. 0.68±0.77 (2) x	
	s. 0.17±0.07 (11)		
	e. 0.31±0.07 (5)		
	u. 0.19±0.2 (2)		
plagioclase	a. 0.26±0.08 (9)	a. 1.1 ±1.0 (8)	a. 0.90±0.54 (4)
	b. 0.21±0.04 (6)	b. 0.81±0.077(3)	b. 1.5 ±0.25 (2) x
	p. 0.44±0.076(20)	n. 1.1 (1)	p. 0.79±0.10 (6)
		p. 1.4 ±0.34 (30)	k. 0.84±0.14 (2)
		k. 0.69±0.77 (2) x	

Table 5-8. K_D(K/Rb) (cont'd)

rock	biotite	alkali feldspar	amphibole	plagioclase
a.	0.47±0.11 (21)	1.5 ±0.4 (11)	1.2 ±0.26 (5)	1.8 ±0.42 (11)
b.	0.62±0.27 (6)	1.1 ±0.25 (5)	1.2 ±0.41 (2)	1.5 ±0.36 (9)
c.	0.69±0.18 (2)	2.5 (1) x	3.4 (1) x	
d.	0.61±0.19 (4)			
m.	0.88±0.10 (14)	1.3 ±0.52 (5)		
g.	0.29±0.18 (5)			
o.	0.52±0.08 (10)	1.3 ±0.18 (3)		
q.	0.50±0.07 (4)	2.1 ±0.18 (14)		
d.	0.53±0.17 (2)	1.6 ±0.18 (7)		
r.	0.95 (36)	1.6 ±0.36 (10)		
e.	1.2 ±0.16 (2) x	1.7 ±0.18 (7)		
f.	0.58±0.09 (4)	3.0 (1) x		2.4 ±0.13 (3)
k.	0.25±0.02 (2)	1.3 (1)	0.84±0.14 (2) x	1.3 ±0.05 (2)
		1.2 ±0.39 (2)		

Table 5-9. Matrix of K_D(K/Tl) for coexisting natural phases.

	biotite	alkali feldspar	amphibole	plagioclase
alkali feldspar	a. 0.12±0.09 (9) b. 0.13±0.02 (5) c. 2.0 (1) x m. 0.24±0.07 (5) e. 0.14 (1) f. 0.25 (1) k. 0.075±0.02(2) x			
hornblende	a. 0.56±0.15 (5) c. 0.40±0.065(2) e. 0.25±0.03 (5)	a. 4.9 ±1.3 (4) e. 1.8 (1)		
plagioclase	a. 0.47±0.20 (9) b. 0.26±0.09 (8) f. 0.20±0.02 (2) k. 0.32±0.23 (3)	a. 4.1 ±3.4 (8) b. 1.4 ±0.36 (4) k. 2.7 ±1.8 (2)	a. 0.66±0.41 (7) b. 0.17±0.05 (2)	
rock	a. 0.58±0.45 (13) b. 0.84±0.02 (6) c. 0.68±0.22 (2) v. 1.0 ±0.21 (4) m. 0.53±0.09 (6) d. 0.55±0.12 (2) e. 1.1 ±0.19 (2) f. 0.67±0.02 (3) k. 0.81±0.09 (2)	a. 2.6 ±2.0 (11) b. 1.3 ±0.32 (5) c. 1.9 (1) v. 0.94±0.19 (4) m. 1.8 ±0.12 (9) e. 7.1 (1) x f. 3.5 (1). k. 2.2 ±0.55 (2)	a. 0.56±0.07 (6) x b. 1.3 ±0.23 (2) c. 1.9 (1) f. 5.3 ±2.1 (4) x k. 2.8 ±0.72 (2)	a. 0.88±0.34 (10) b. 1.4 ±0.55 (11) k. 1.2 ±0.84 (2)

	biotite	alkali feldspar	amphibole	plagioclase
D(Rb)				
alkali feldspar	2.3 ±0.49 (15)			
amphibole	22 ±6.2 (4)	9.0 ±2.7 (3)		
plagioclase	32 ±13 (5)	20 ±12 (6)	2.0 ±1.1 (3)	
rock	3.7 ±2.0 (14)	2.9 ±1.9 (12)	0.37±0.15 (4)	0.25±0.07 (5)
D(Tl)				
alkali feldspar	3.5 ±1.4 (8)			
amphibole	19 ±10 (5)	3.3 ±0.54 (4)		
plagioclase	42 ±33 (4)	11 ±1.3 (3)	1.3 ? (1)	
rock	5.5 ±3.7 (12)	1.7 ±0.61 (8)	0.54±0.36 (6)	0.34±0.23 (4)
K_D(Rb/Tl)				
alkali feldspar	0.60±0.20 (8)			
amphibole	1.6 ±0.55 (3)	5.5 ±1.4 (2)		
plagioclase	1.1 ±0.32 (5)	3.0 ±1.1 (3)	0.53±0.46 (3)	
rock	1.0 ±0.28 (8)	1.1 ±0.42 (7)	1.0 ±0.54 (5)	1.1 ±0.55 (4)
K_D(K/Rb)				
alkali feldspar	0.33±0.10 (12)			
amphibole	0.27±0.11 (6)	1.4 ±0.35 (2)		
plagioclase	0.30±0.12 (3)	1.1 ±0.24 (4)	0.84±0.055(3)	
rock	0.62±0.26 (13)	1.5 ±0.29 (10)	1.2 ±0.0 (2)	1.8 ±0.48 (4)
K_D(K/Tl)				
alkali feldspar	0.18±0.06 (5)			
amphibole	0.40±0.16 (3)	3.4 ±2.2 (2)		
plagioclase	0.31±0.12 (4)	2.7 ±1.4 (3)	0.42±0.35 (2)	
rock	0.75±0.20 (9)	2.0 ±0.85 (7)	2.0 ±0.75 (3)	1.2 ±0.26 (3)

Table 5-10. Summary of matrices of D and K_D values ($\bar{x} \pm 1s$) for pairs of natural phases. Data from Table A-6, after rejecting those apparently anomalous ones (marked x). In parentheses is given the number of suites of data (Tables 5-5 to 5-9) whose mean values were used to calculate $\bar{x}$, s.

random errors such as due to sampling and analysis and to reduce the spread observed for each parameter (see also section 2-2-2). From this second set of $\bar{x}$ values (Table 5-5 to 5-9), apparently anomalous data were rejected (marked by an x in the tables) by comparison with the others. The remaining data were weighted equally in computing the final $\bar{x} \pm 1s$ range for each ratio (Table 5-10). Finally, the data were reduced to the preference series (Table 5-11) for comparison with the experimental data (c.f. Table 5-3).

5-3-2. Comparison with experimental data

Such a comparison is subject to enormous uncertainty due to the complexity of the systems involved. As discussed previously (Chapters 2, 3 and 4), some of the important factors which appear to influence trace element distributions include composition (including bulk composition), temperature, structure and thermal history of the species of interest. In natural systems, there is very little knowledge concerning these variables. Moreover, the spread observed in the data for the natural materials, the lack of data for some pairs of phases and the necessary process of simplification used in this study introduce further uncertainty and distortion of the data. Finally, the problems associated with the estimation of melt compositions, particularly of the plutonic rocks, have been discussed previously (Chapter 3).

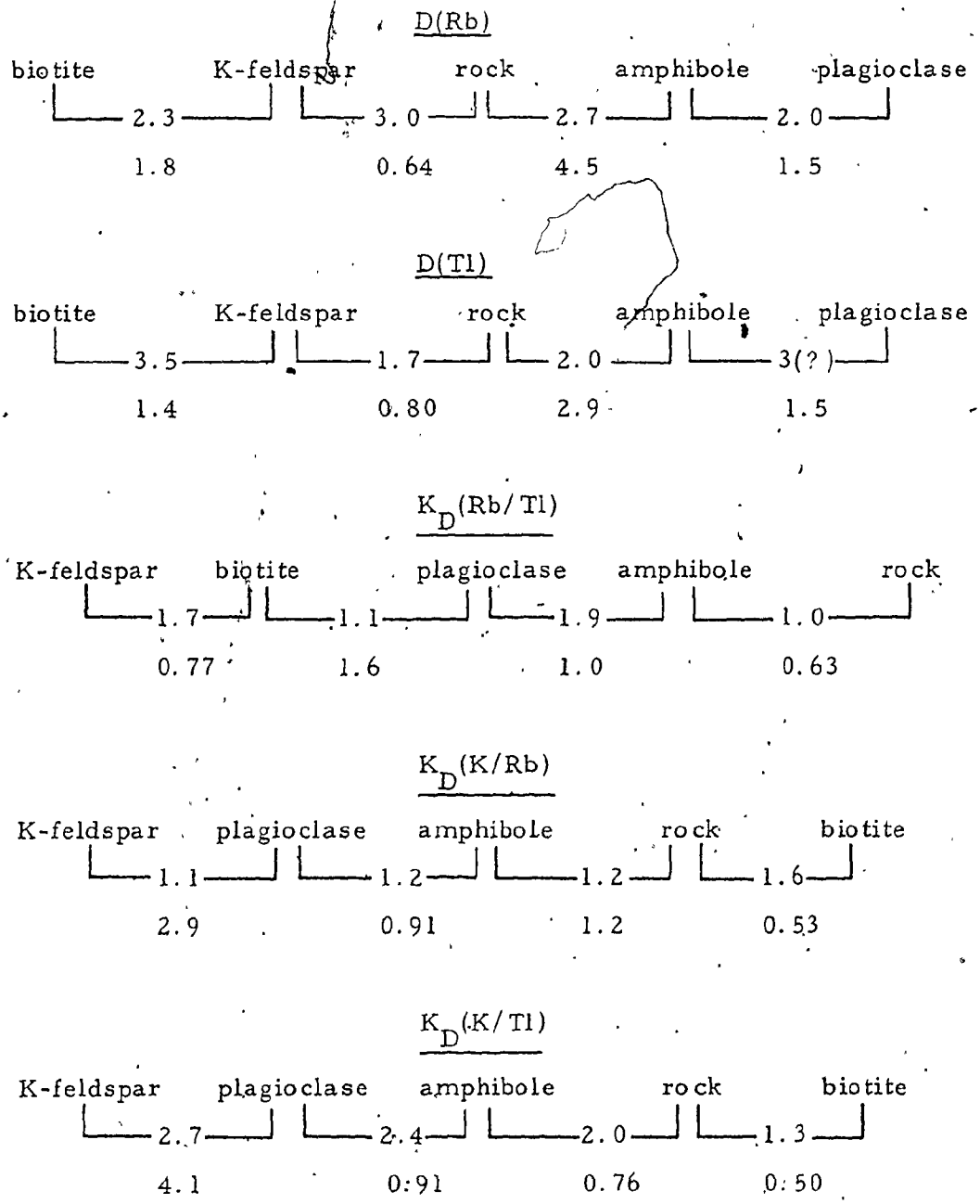

Table 5-11. Series of concentrations or ratios for the natural phases. Average D and K_D values are shown for adjacent pairs (first row). Included are also averages for the experimental pairs (second row) for comparison.

Ideally, comparison should be made between each pair of phases of similar composition (Chapter 3, e.g.). However, this is extremely tedious and will not be attempted in the following discussion, in which only gross features will be examined.

Thus, both sets of data (experimental and natural) show that Rb and Tl are concentrated in the two K-minerals, biotite and alkali feldspar, much more than the coexisting amphibole and plagioclase (Table 5-10, 5-11). There is also reasonable agreement for D(Rb) and D(Tl) for the pairs of biotite-alkali feldspar (see also Chapter 4), and amphibole plagioclase. However, D(Rb) and D(Tl) for the pairs of alkali feldspar-amphibole, alkali feldspar-plagioclase, biotite-amphibole and biotite-plagioclase are usually up to an order of magnitude higher for the natural materials than for experimental data. The behaviour of the rock also shows little resemblance between the two sets of data.

Turning to the K_D data, general consistency is observed for most of the Rb/Tl results and the position of the various phases in the preference series, except for the pair biotite-alkali feldspar. K_D(Rb/Tl) averages 1.3 for the two P3-Sl runs and 1.7 for all the experimental runs (Fig. 4-5), but is generally less than units for the natural pairs. Similarly, the natural biotite is relatively the lowest in K/Rb and K/Tl ratios, but is second only to the sanidine Sl in the experimental runs. Moreover, it will be recalled (section 5-2-4) that

phlogopite-melt K_D(K/Rb) for these runs is also about two times higher than as reported in the literature. At least part of the reason for this difference is the presence of Fe as a major element in natural biotites, since, as was demonstrated by Volfinger (1976), Fe substituted for Mg in phlogopite lowers the K_D(K/Rb) for the pair phlogopite/vapour by a factor of approximately 1.4. There is also little consistency in K_D(K/Rb) and for the other minerals between the two sets of data. However, the discrepancies may not be very serious since the K_D values are generally very close to one and there is a lack of data for some pairs of natural phases.

Due to the paucity of the experimental data, particularly for the test of equilibrium, further discussion on these data will not be too profitable. Hence the following will be limited to the data for natural materials only.

5-3-3. K, Rb and Tl correlations in natural materials

In this section, K, Rb and Tl relationships in natural biotite, alkali feldspar, amphibole, plagioclase and their host rocks will be examined, using the data reported in A-6 and A-7 (see also Table 5-4, for sample listing). In this respect, pairs of elements, Rb-Tl, K-Rb and K-Tl were plotted (Fig. 5-1 to 5-3) for all the phases of interest, and the fields of each phase are outlined using most of the available data. Some data points were rejected by comparison with the trends defined by the main body of the data.

Thus, Rb-Tl pairs (Fig. 5-1) show a more or less linear trend for all the phases, with most of the data lying within the range of Rb/Tl ratio between 65 to 400, the limit defined by Shaw et al. (1974) for most continental plutonic rocks. Noticeable exceptions are some alkali feldspars, which show a higher ratio at lower Rb and Tl concentrations, and some amphiboles, which show a lower ratio at higher concentrations.

Turning to the K-Rb pairs as shown in Fig. 5-2, amphibole and plagioclase show broader (probably due to larger amount of data available) but nevertheless linear trends, with possibly a slight K enrichment at lower K and Rb concentrations. Most biotites and alkali feldspars, however, show strong Rb enrichment with K concentration more or less confined to a narrow range of 8% and 10% respectively.

K/Rb ratios for most of the minerals lie between the range of 150 to 1000 with two exceptions: a) some hornblendes and a few plagioclases? which are higher than 1000, b) some alkali feldspars and about half of the biotite field, which are lower than 150. Most of the rocks fall into the region of K/Rb between 190 and 600. The higher limit is twice as high as the 'normal' upper limit defined by Heier and Adams (1964) and Taylor (1965). There is a trend of Rb enrichment in the region of high Rb and K concentration for the rocks, not unlike the pegmatitic-hydrothermal trend (Shaw, 1968), and appears to reflect those for the biotite and alkali feldspar.

Fig. 5-1. Rb-Tl relationships in natural minerals and their host rocks.

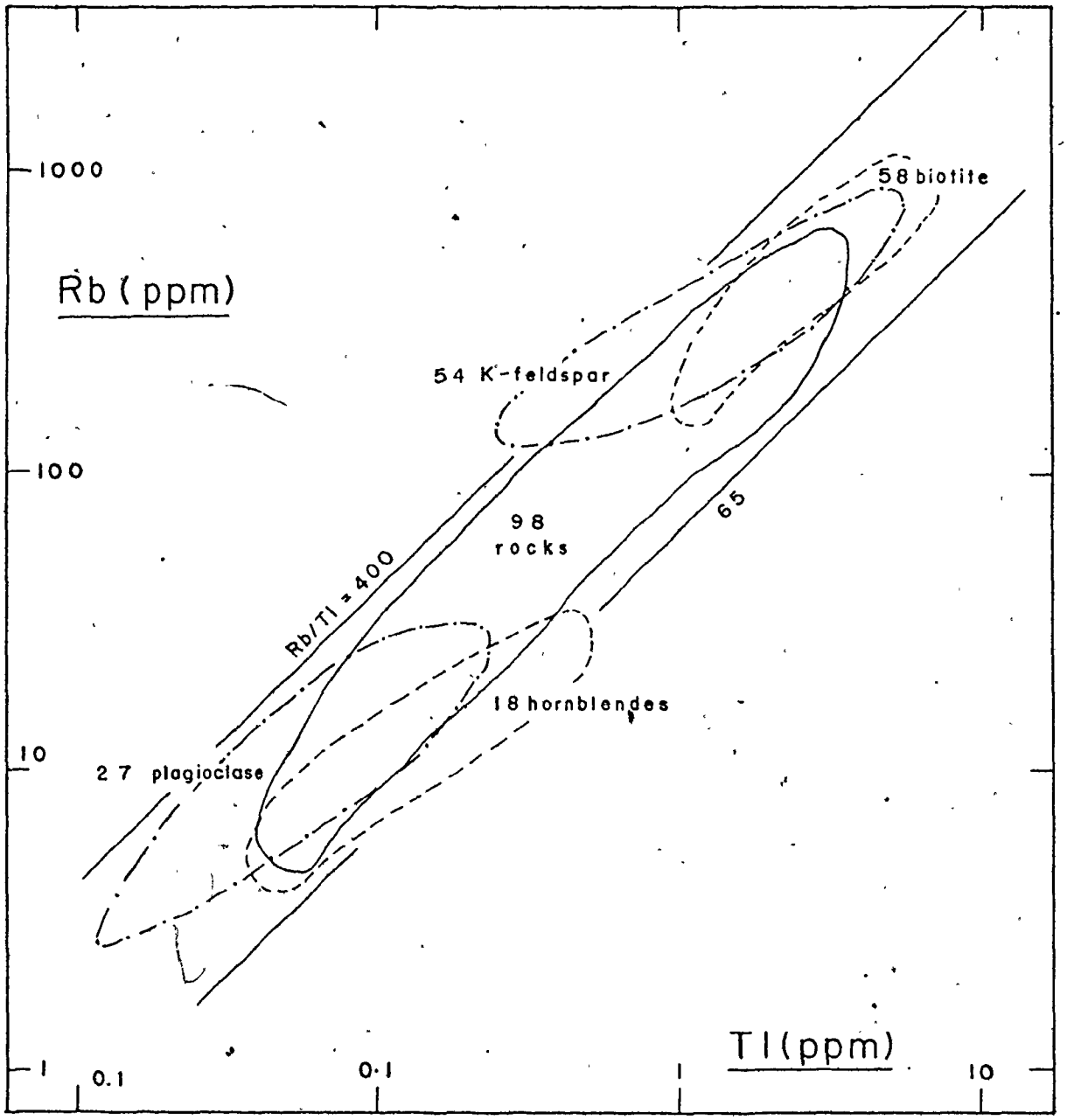
1000
100
10
1
Rb (ppm)
58 biotite
54 K-feldspar
98
rocks
65
Rb/Tl = 400
18 hornblendes
27 plagioclase
0.1
0·1
1
10
Tl(ppm)

Fig. 5-2. K-Rb relationships in natural minerals and their host rocks.

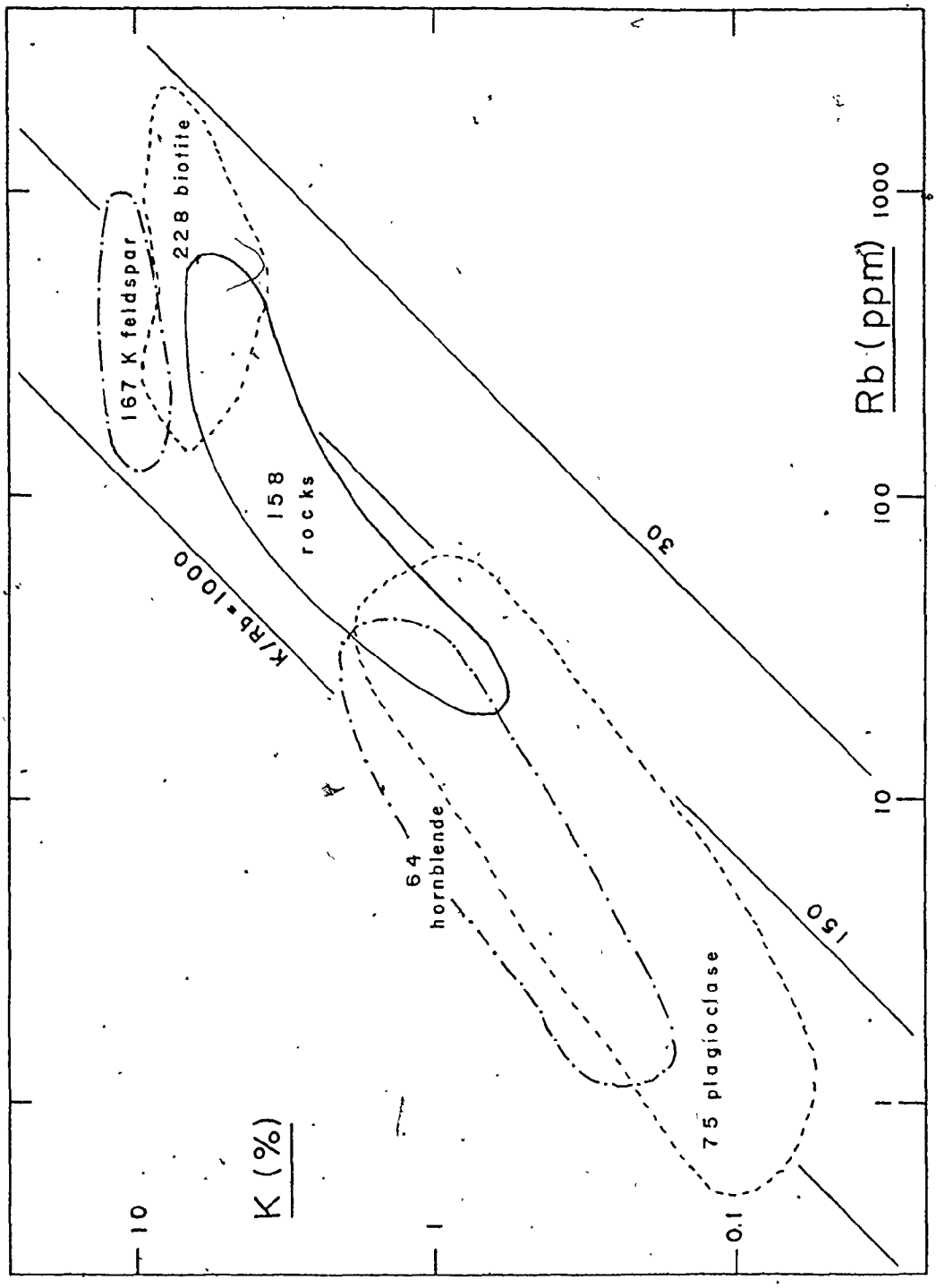
167 K feldspar
228 biotite
158 rocks
64 hornblende
75 plagioclase
K/Rb=1000
30
150
10
1
0.1
100
1000
Rb (ppm)
10
1
K (%)

Fig. 5-3. K-Tl relationships in natural minerals and their host rocks.

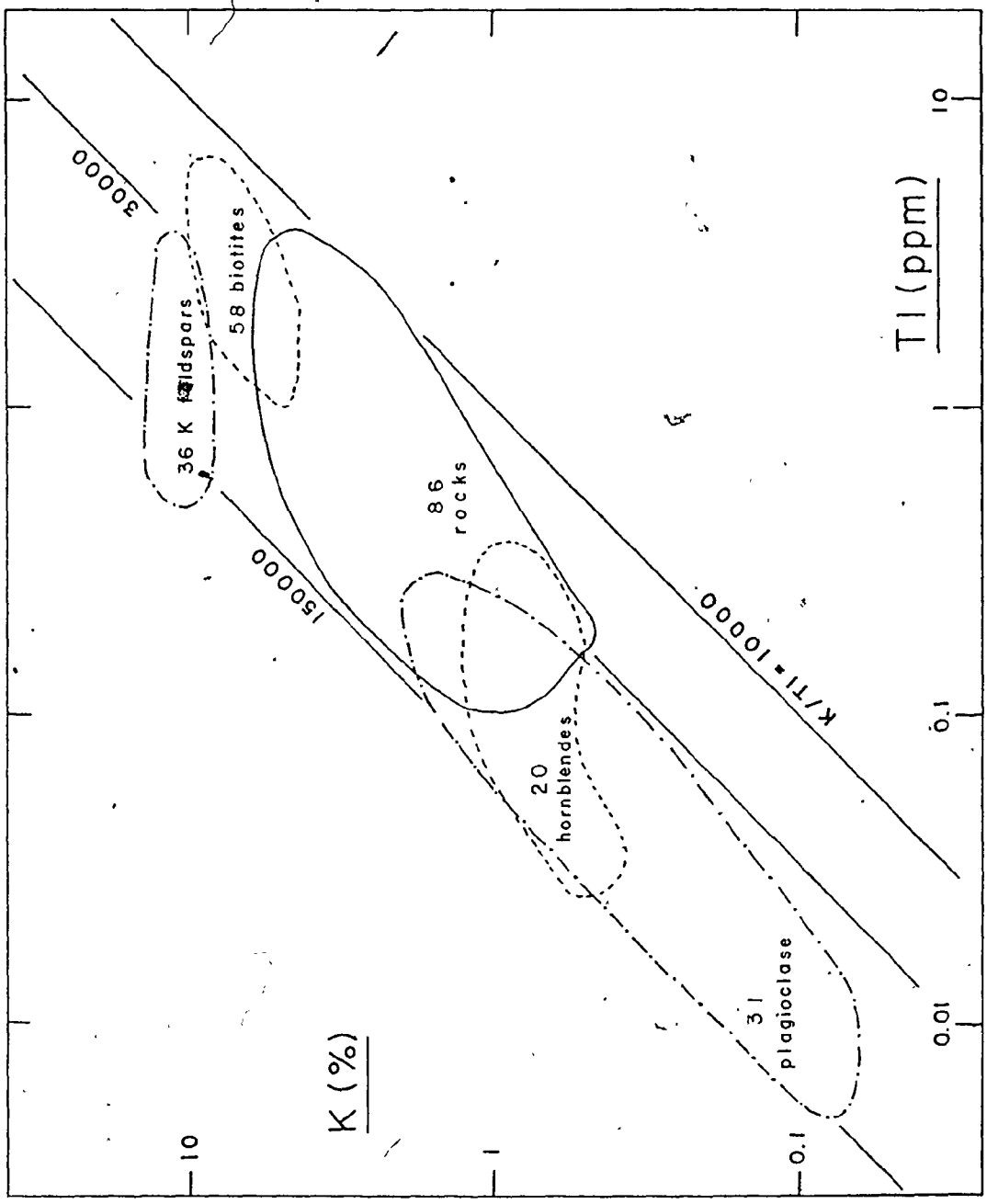
K (%)
Tl (ppm)
10
1
0.1
0.01
300000
150000
K/Tl = 10000
36 K feldspars
58 biotites
86 rocks
20 hornblendes
31 plagioclase

Behaviour of K-Tl pairs is very similar to that of K-Rb, except that the trends are not as well defined. K/Tl ratios for most of the phases lie within the limits of 30,000 and 130,000 as defined by Shaw et al. (1974), except for some biotites and rocks with K/Tl ratios as low as 10,000. Some of the rocks examined have lower K/Tl ratios than all the minerals, as was also the case with the Rb-Tl pair. The explanation for these Tl enrichment trends will be discussed shortly.

Thus it appears as if the alkali feldspar and biotite (and probably all K-minerals, see later discussion) were saturated in K and that the concentrations of Rb and Tl increased independently, in response to increased bulk concentrations. This is due to the fact that K is a major element in these minerals, subject to stoichiometric restrictions, whereas Rb and Tl are less so. (See also discussions in Chapter 6.)

5-3-4. Rb and Tl enrichment in potassic-minerals

The feasibility of K saturation and Rb enrichment in K-minerals for the explanation of the Rb-enrichment trend has been briefly discussed by Shaw (1968). The following is a more detailed discussion which includes Tl.

Maximum (stoichiometric) concentration of K in K-feldspar ($KAlSi_3O_8$) is 14% and in K-mica [phlogopite, $K_2(Si_6Al_2O_{20})(OH)_4$] is 9.37%. In natural species, K concentrations seldom exceed 12% and 9% respectively in alkali feldspar and mica. For K/Rb to be higher than 195, the "lower limit" of the main trend, the concentrations of Rb in feldspar and mica cannot exceed 720 and 481 ppm respectively. Similarly, the concentrations of Tl cannot exceed 4.67 and 3.1 respectively for K/Tl to be less than 30,000, the "lower limit" of continental plutonic rocks.

Many feldspars and micas have been reported to have Rb and Tl concentrations much higher than these limits. Thus Rb in the microcline, Ml used in this experimental study was initially over 2%. The maximum Rb (2.81%) so far reported was found in a microcline from a pegmatite in the Kola Peninsula (Borovik-Romanova and Sosedko, 1958). (See also summaries by Heier and Adams, 1964 and Taylor, 1965.) Rb in micas is even more enriched since they always contain more Rb and less K than the coexisting feldspars (see summaries ibid).

Ivanov et al. (1960) reported Tl concentrations of up to 1000 ppm for lepidolites from large pegmatites, though the normal range was 10-180 ppm. Similarly, Tl concentrations ranged from 1-70 ppm for phlogopite; 1-60 for biotite and 2-500 for muscovite. As for the feldspars, the ranges were: 10-20 ppm for microcline, 50-80 for amazonite and 4-50 for orthoclase (see also Albuquerque and Shaw, 1972).

Hence very low K/Rb and K/Tl ratios are commonplace in many potassic-minerals, particularly those from pegmatites. Although the ratios for the rock as a whole depend upon the ratios in all the phases, in the more silicic rocks, containing abundant K-minerals, contributions from the other phases will be very minor.

Moreover, it will be recalled that Rb in the microcline Ml always behaved as a major element, with very little substitution by K or Tl in all the experimental studies, even though the vapour phase was always highly enriched in K. Beswick (1973) claimed to have synthesized almost pure Rb-phlogopite and up to $(K_{0.5}Rb_{0.5})$sanidine. Presumably, such Rb-rich phases can also crystallize in nature if the composition of the melt permits. A similar argument probably also applies to Tl, although no such data is available at present.

5-4. Other minerals

In this section, other common rock-forming minerals, including muscovite pyroxene and olivine, which had not been studied experimentally, will be briefly discussed in comparison with the other minerals examined previously. Data for these minerals were treated in the same way as before and are reported in Table 5-12 and Figs. 5-4 to 5-6.

	D(Rb)			K_D(Rb/Tl)		
	muscovite	pyroxene	olivine	muscovite	pyroxene	olivine
biotite						
	c. 0.56±0.02(2)	f. 0.02±0.01(4)		c. 1.6±0.35(2)	f. 1.1±0.38(3)	
	d. 0.59±0.07(3)	k. 0.05±0.02(2)		d. 2.6±1.3 (2)	h. 2.3 (1)	
	i. 1.4 ±0.13(3)	h. 0.067 (1)		i. 1.6±0.07(3)	k. 1.7 (1)	
	k. 0.56 (1)			k. 2.2 (1)		
K-feldspar						
	c. 1.5 ±0.43(2)	f. 0.33 (1)		c. 1.7±0.22(2)	f. 0.23 (4)	
	k. 1.1 (1)	k. 0.50 (1)		k. 0.48 (1)	k. 0.83 (1)	
amphibole						
		h. 0.71 (1)			h. 0.71 (1)	
plagioclase						
		t. 0.77 (2)	h. 0.30		f. 0.56±0.04(2)	
		f. 1.4 ±0.32(2)	t. 0.47±0.32(3)		h. 0.54 (2)	
		k. 0.45±0.01(2)			k. 1.5 (2)	
		h. 0.92±0.02(2)				
rock						
	d. 1.6 ±0.5 (2)	t. 0.024±0.01(2)	h. 0.042 (1)	c. 1.3±0.07(3)	f. 1.5 ±0.15(3)	h. 0.25 (1)
	c. 3.5 ±0.42(2)	f. 0.28±0.11 (4)		d. 2.7±0.73(2)	h. 0.60±0.24(3)	
	k. 3.4 (1)	h. 0.072 (2)		k. 1.4 (1)	k. 0.79±0.57(3)	
		k. 0.050 (1)				

Table 5-12a, b and c. Matrices of reduced D and K_D values ($\bar{x} \pm 1s$) for pairs of natural phases not included in Table 5-4. See footnotes for Table 5-4 for samples and explanations.

	K_D(K/Rb)			K_D(K/Tl)		
muscovite	pyroxene		olivine	muscovite	pyroxene	olivine
biotite						
c. 1.6 ±0.21(3)	f. 0.38±0.01 (3)			c. 2.8 ±0.15 (2)	f. 0.83±0.24(4)	
d. 1.7 ±0.36(3)	h. 1.2 (1)			d. 5.3 ±0.32 (2)	h. 2.8 (1)	
i. 2.9 ±1.6 (3)	k. 1.0 ±0.1 (2)			i. 2.9 ±1.6 (3)	k. 1.6 (1)	
z. 2.1 (1)				h. 0.21 (1)		
K-feldspar						
c. 0.43±0.10(2)	t. 0.83 (1)			c. 0.56±0.05 (2)	t. 0.20 (1)	
h. 0.63 (1)	j. 0.50 (1)			k. 0.30 (1)	k. 0.34 (1)	
	f. 0.83 (1)					
	k. 0.40 (1)					
hornblende						
	h. 0.63 (1)				h. 0.43 (1)	
plagioclase						
z. 0.45 (1)	t. 0.23 (1)		r. 0.34 (1)	z. 1.2 (1)	f. 0.14±0.04(2)	
	f. 0.78±0.21 (2)				k. 2.3 ±1.7 (2)	
	h. 1.0 ±0.26 (3)					
	k. 0.63 (1)					
rock						
c. 0.98±0.13(2)	t. 0.75 (1)		t. 0.63±0.33(2)	c. 1.3 ±0.23 (2)	f. 0.60±0.12(4)	h. 0.026±0.01(3)
d. 0.73 (1)	j. 0.50 (1)		h. 2.0 (1)	d. 2.5 ±0.57 (2)	h. 0.28±0.16(5)	
k. 0.56 (1)	f. 0.38±0.08 (3)			k. 0.79 (1)	k. 0.70±0.13(3)	
	h. 0.72±0.28 (3)					
	k. 0.73±0.18 (2)					

Table 5-12b.

D(Tl)

	muscovite	pyroxene	olivine	pyrrhotite	pyrite	magnetite
biotite	c. 0.42±0.24(2) d. 0.28±0.15(4) i. 0.77±0.26(3) k. 0.25 (1)	f. 0.029±0.005(2) h. 0.029 (1) k. 0.043 (1)		j. 0.083±0.009(2) f. 0.059±0.008(2)	j. 0.014 (1) k. 0.13 (1)	a. 0.04 (1) b. 0.005±0.002(3) k. 0.04, 0.003(2)
K-feldspar	c. 1.6 ±0.71(2) k. 2.2 (1)	f. 0.14 (1) h. 0.42 (1)		j. 1.7 (1) f. 0.38 (1)	j. 0.11 (1)	a. 0.048 (1) b. 0.020±0.009(2) j. 0.10 (1) k. 0.027 (1)
amphibole		h. 1.0 (1)		j. 4.3 (1) f. 7.1 (1)		a. 0.18 (1) h. 3.7 (1)
pyroxene			h. 0.77±0.25(2)	f. 3.0 ±0.32 (3)	k. 0.31, 4.3 2.3 (3)	h. 3.2 ±1.3 (4) k. 1.5 ±0.22. (3)
plagioclase	z. 1.5 (1)	i. 1.5 ±0.48 (3) h. 0.43 ±0.32 (6) k. 1.5 ±0.14 (2)		f. 4.3 ±1.1 (2)	h. 1.6 (1) k. 0.45 (1)	a. 0.52 ±0.29 (2) b. 0.36 ±0.09 (3) f. 4.6 (1) h. 1.3 ±0.50 (4)
pyrite	s. 97 (1)			j. 13 ±3.6 (3)		h. 0.3 (1)
magnetite	k. 91 (2)		h. 0.15±0.03(2)	j. 17 (1)	j. 1.1 (1) h. 3.3 (1)	

Table 5-12c.

D(Tl)

muscovite	pyroxene	olivine	pyrrhotite	pyrite	magnetite
pyrrhotite					
j. 1.9 (1)	f. 0.34±0.04 (3)				
rock					
c. 2.6 ±0.22(2)	f. 0.25±0.023(3)	h. 1.4 ±0.62(3)	j. 0.47±0.33(5)	j. 0.31±0.17(3)	a. 0.28 (2)
d. 0.69±0.29(3)	h. 0.38±0.024(7)		f. 0.62±0.14(3)	2.4 ±0.61(4)	b. 0.05±0 002(2)
k. 2.4 (1)	k. 0.43±0.13 (3)			h. 3.2 (1)	f. 2.1 ±0.18 (2)
					h. 1.2 ±0.17 (6)

Table 5-12c (cont'd.)

5-4-1. Muscovite

The behaviour of K, Rb and Tl is muscovite is very similar to that observed for biotite. Thus, the concentrations of all three elements are similar for both minerals and are considerably higher than the other non-micaceous coexisting phases, including alkali feldspar and othe host rock. As was the case with biotite, Rb and Tl in muscovite (Fig. 5-5) show a rather linear relationship with 'normal' Rb/Tl ratios, and strong trends of Rb and Tl enrichment relative to K.

K saturation and hence Rb and Tl enrichment have also been reported by several workers for lepidolite, zinwaldite and pegmatitic orthoclase (e.g. see summaries by Heier and Adams, 1964 and Taylor, 1965). By analogy, such behaviour can probably be extended to all late stage potassic-minerals, provided that the bulk Rb and Tl concentrations were sufficiently high.

5-4-2. Pyroxene

In many ways, the behaviour of pyroxenes from basic igneous rocks (mostly basalts) is rather similar to that of plagioclase. Thus both minerals have similar Rb and Tl concentrations that cover rather large ranges and which are generally lower than the coexisting host rock and amphibole. Moreover, both minerals have rather linear K-Rb and K-Tl relationships. However, unlike plagioclase the Rb-Tl plot

Fig. 5-4. K-Rb relationships in sediments and some minerals not included in Figs. 5-1 to 5-3.

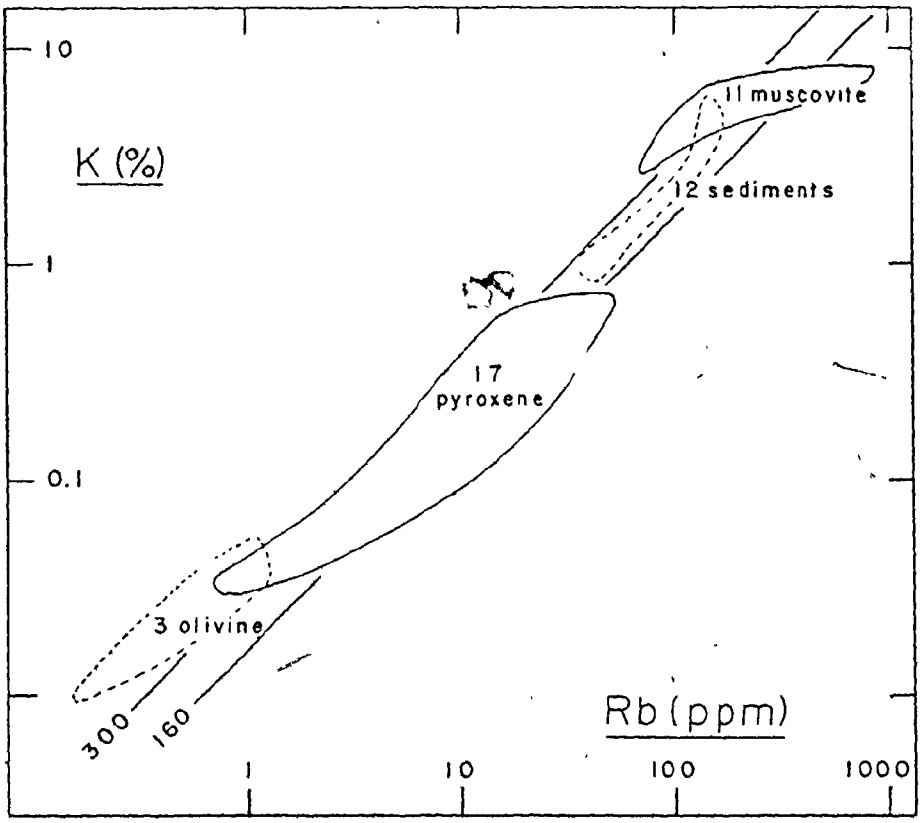
10
1
0.1
K (%)
11 muscovite
12 sediments
17
pyroxene
3 olivine
300
160
Rb (ppm)
1
10
100
1000

Fig. 5-5. Rb-T: relationships in sediments and some minerals.

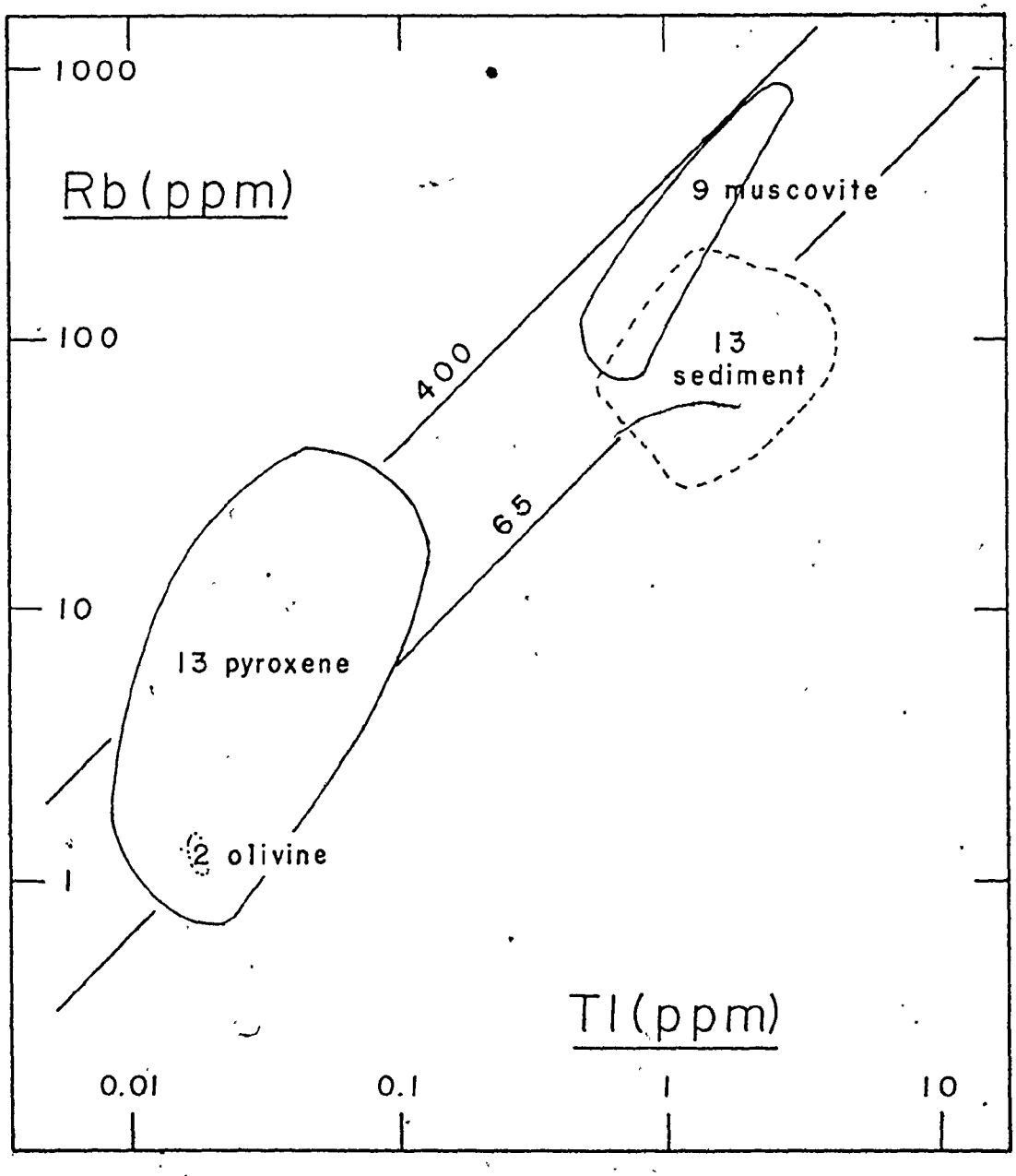
1000
Rb(ppm)
100
10
1
9 muscovite
13
sediment
400
65
13 pyroxene
2 olivine
Tl(ppm)
0.01
0.1
1
10

Fig. 5-6. K-Tl relationships in sediments and some minerals.

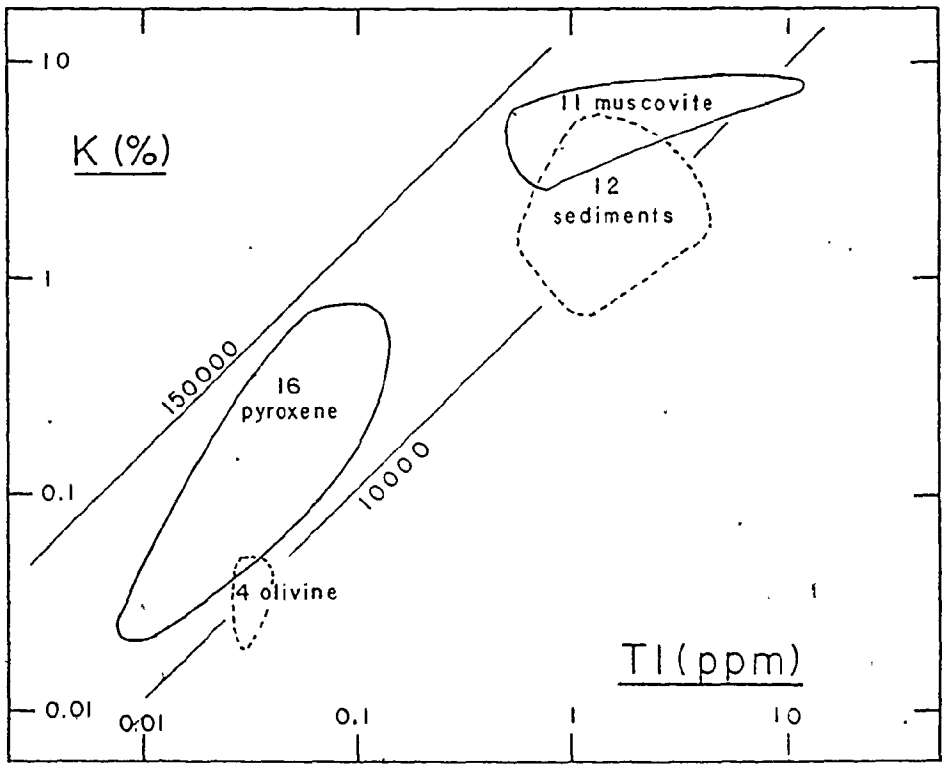
10
1
0.1
0.01
K (%)
0.01
0.1
1
10
Tl (ppm)
11 muscovite
12
sediments
16
pyroxene
4 olivine
150000
10000

(Fig. 5-5) for pyroxene shows a very wide field with no apparent trend. This behaviour also contrasts with the rather linear trends for both K-Rb and K-Tl plots and hence cannot be due entirely to analytical error or contamination.

5-4-3. Olivine

The few olivines analysed are uniformly very low in K, Rb and Tl concentrations, and slightly enriched in Tl relative to both Rb and K, as compared to other phases. Apart from possible analytical error, due to the very low concentrations, Tl enrichment can also be due to the presence of oxides, such as magnetite and chromite (see later discussions) as inclusions, which are very commonly found in olivine.

5-5. Tl in non-silicate minerals

Due to its dual properties, both as lithophile and sulfophile, Tl enrichment in some rocks has been attributed to its occurrence in sulphides (e.g. see Albuquerque et al., 1972 and section 5-3-3). Hence some pyrite and pyrrhotite were examined. Magnetite, the other non-silicate mineral, has also been reported to be sometimes enriched in Tl (e.g. see Shaw, 1952 and Wager and Brown, 1967) and hence was also included in this study.

The commonest and most difficult problem in trace element distribution studies is the possibility of disequilibrium, as discussed on several previous occasions. This is even more acute in the case of non-silicate minerals, due to the additonal possibility of different paths of formation such as liquid immiscibility and sulfide-rich hydrothermal fluid activities in igneous rocks. In sediments, the silicates of interest may be clastic whereas the sulphides are most likely syngenetic precipitates, organic or inorganic. Hence partition coefficients measured for silicate and non-silicate pairs may be irrelevant and serve only as a means for assessing the feasibility of Tl enrichment in non-silicate minerals.

5-5-1. Pyrrhotite

Tl in pyrrhotite is much less than the 'coexisting' biotite in all (4) of the cases studied, including both igneous and sedimentary varieties, as is also the one case of igneous alkali feldspar. However, Tl in pyrrhotite is higher than the alkali feldspar in a sedimentary rock and all the other phases - amphibole, plagioclase, pyroxene, pyrite, magnetite and the host rock. This places pyrrhotite between the potassic and non-potassic phases in the Tl preference series.

5-5-2. Pyrite

Tl in pyrite is much lower than all of the coexisting biotite, muscovite and alkali feldspar. The evidence is inconclusive for the pairs of pyrite-amphibole and pyrite-plagioclase for the two sulphide-bearing basic rocks used. Some (4 out of a total of 7) sedimentary sulphides are highly enriched in Tl, up to 6.6 ppm, about four times higher than the host-rock; whereas the rest are relatively lower, as are also all those from the Sudbury irruptives.

5-5-3. Magnetite

Magnetite behaves very similarly to pyrite: much lower in Tl than biotite and alkali feldspar, but inconclusive relative to plagioclase, amphibole and the host-rock. In silicic rocks, magnetite is higher in Tl than the coexisting amphibole, plagioclase and host-rock and vice versa for the basic rocks. It is also higher than the pyroxene in all of the basic rocks studied. It appears that in basic rocks with no potassic minerals, magnetite has the highest Tl concentration.

5-5-4. Summary

Tl concentration among the common non-silicate minerals decreases in the order of pyrrhotite-pyrite-magnetite. In all of the 4 igneous varieites studied, all three minerals are lower in Tl than the coexisting biotite, muscovite and alkali feldspar and higher than the pyroxene. Relative to the coexisting amphibole and plagioclase pyrrhotite

has higher Tl concentration, but the evidence is inconclusive for pyrite and magnetite: being higher for those from basic and lower for those from silicic igneous rocks. Some sedimentary pyrite (about half of the cases studied) is highly enriched in Tl, more so than the host rocks which are themselves rather Tl-rich. All the pyrrhotite studied is slightly lower in Tl relative to the host-rock.

Like some of the igneous rocks examined, some sedimentary rocks are highly enriched (Figs. 5-5 and 5-6) in Tl relative to both K and Rb. Such trends are apparently due to the contributions from the non-silicates which are known to contain negligible amounts of Rb and K, although Tl concentration due to other processes, such as chemical precipitation (e.g. see Shaw, 1952 and McGoldrick et al., 1978) are also possible.

5-6. Conclusion

In an assemblage of biotite-alkali feldspar-amphibole-plagioclase, both natural or experimental (hydrothermal), Rb and Tl concentrations decrease in the order as listed. D(Rb), D(Tl) and K_D(Rb/Tl) values measured for natural coexisting biotite-alkali feldspar and amphibole-plagioclase pairs show reasonable agreement with experimental results. However, natural D values for the pairs of biotite-amphibole, alkali feldspar-amphibole, biotite-plagioclase and alkali feldspar-plagioclase agree poorly with experimental values, being much higher for the natural pairs. Generally rather poor agree-

ment is also observed for most of the K_D(K/Rb) and K_D(K/Tl) values, although they are much closer to unity than the D values. Differences in bulk composition and lack of equilibration are the most likely reason for such discrepancies.

Some natural K-minerals, including muscovite, have very low K/Rb and K/Tl ratios, possibly as a consequence of the behaviour of these elements during fractional process. The non-potassic minerals, including amphibole, plagioclase, pyroxene and olivine, on the other hand, show much more constant K/Rb and K/Tl ratios, with only slight decrease at higher concentrations. Relatively more constant Rb/Tl ratios are also observed for all the silicate minerals studied, including the potassic ones and most of the rocks, with the exception of pyroxene.

In igneous rocks, Tl concentration in pyrrhotite, pyrite and magnetite decrease in the order as listed, and as a group, is generally intermediate in Tl concentrations between the potassic and non-potassic silicates, although the position of magnetite and pyrite are less certain and appears to depend on the bulk composition. Some sedimentary sulfides, especially pyrites are highly enriched in Tl.

In silicate rocks, the bulk of the Rb and Tl is contained in the K-minerals. The trends of Rb and Tl enrichment relative to K, observed for some rocks appear to reflect the behaviour of these minerals. In basic rocks, in which no K-minerals are present, the

highest Tl concentration is found in magnetite and possibly sulphides, although their genetic relationships to the silicates are uncertain. However, due to volumetric considerations, the bulk of the Tl will be contained in the silicate phases, including glass. Some igneous rocks are slightly and some sedimentary rocks are highly enriched in Tl relative to both K and Rb, reflecting the contributions from the non-silicate minerals.

CHAPTER 6

APPLICATION OF DATA: K, Rb AND Tl TRENDS IN MAJOR ROCK UNITS

6-1. Introductory Statement

In this chapter, an attempt will be made to apply the data obtained to explain fractionation trends observed in several types of crustal rocks.

6-2. K-Rb Trends

6-2-1. Introduction

The constancy of K/Rb ratios in rocks has been the subject of long and heated debates (e.g. see reviews by Heier and Adams, 1964; Taylor, 1965 and Shaw, 1968). Shaw (1968), after examining a number of suites of rocks by covariant analysis, defined three principal trends (Fig. 6-1):

1. main trend, comprising most continental and oceanic igneous suites, with K/Rb in the range of 195-433, differing somewhat from one suite to another; for each suite, there is a slight decrease in K/Rb with higher concentrations;

Fig. 6-1. Summary of possible and probable K-Rb fractionation trends in igneous and associated rocks. OT, oceanic tholeiitic basalts; MT, main trend; PH, pegmatitic-hydrothermal (from Shaw, 1968).

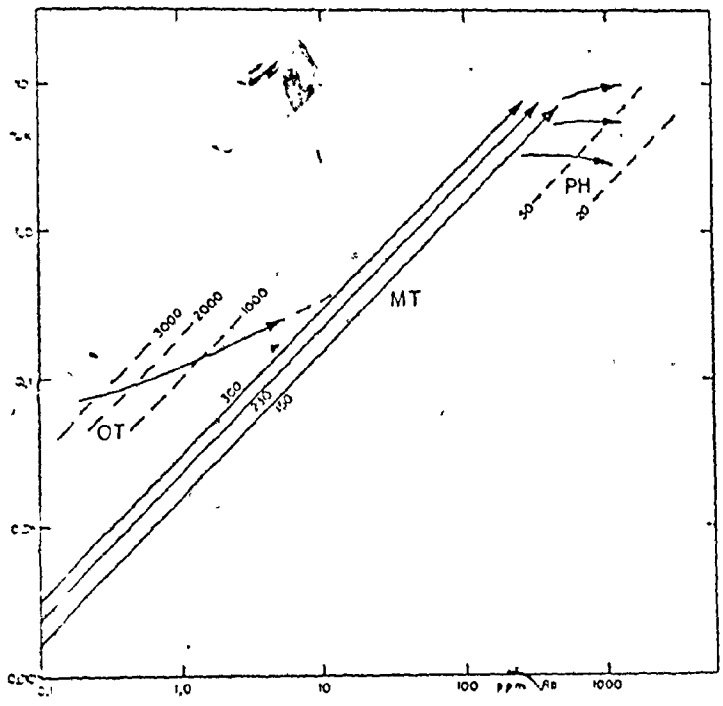
3000
2000
1000
OT
MT
PH
0.1
1.0
10
100
1000
ppm

2. oceanic tholeiitic trend, comprising all the oceanic tholeiites he reviewed, with K/Rb as high as 3500, decreasing as K and Rb concentrations increase, then merging with the main trend;

3. pegmatitic-hydrothermal trend, comprising many alkali-rich granites, syenites, pegmatites, greisens and related rocks, with very high K and Rb contents and very low K/Rb ratios.

With respect to 2, several trace element models have been proposed (e.g. Gast, 1968, Philpotts and Schnetzler, 1970 and Gill and Murthy, 1970). The following discussion will be concerned with 1 and 3, to which most of the data from this study are relevant.

6-2-2. Discussion of the main trend

The main trend was defined by a variety of rocks ranging from ultra-mafic to silicic in composition.

In the more mafic varieties, the main phases are olivine, pyroxenes and calcic plagioclase. Of these, plagioclase usually has the highest Rb and K concentrations as demonstrated previously, and hence will be the principal carrier for both elements. The field for plagioclase in the K-Rb scattergram (Fig. 5-2) spans K/Rb ratios from about 3000 to just over 100, but ratios are mostly over 300, especially for the more calcic plagioclase with low K and Rb. High K/Rb ratios have also been reported for some calcic plagioclases (e.g. Murthy and Griffin, 1970 and Heier, 1966).

K/Rb in pyroxenes from this study ranged from approximately 400 to 100, similar to and lower than the main trend. K/Rb for olivine is probably not too different from the main trend, although the scarcity of the data and the low concentrations render the data rather uncertain (see also Griffin and Murray, 1969).

Hence the main trend as defined by the mafic rocks represent a balance between plagioclase, with relatively higher K/Rb ratios and pyroxene, with relatively lower ratios. Since none of these major minerals concentrate K and Rb (Fig. 5-2), their host rocks would have low abundances, as observed.

In more silicic rocks, the dominant minerals are alkali feldspar, plagioclase, quartz and small amounts of biotite and amphibole, somewhat similar to the experimental system discussed in Chapter 5. In these rocks, the main carrier of K and Rb is alkali feldspar, due to its abundance and relatively high concentrations, although biotite usually has the highest concentration of Rb. K/Rb for alkali feldspar spans from just below 1000 to 100 and is the highest in most non-pegmatitic rocks relative to the other coexisting minerals (Section 5-3-3). Although calcic plagioclase may have very high K/Rb ratios, the more sodic ones in silicic rocks usually have lower values. Hence both feldspars have K/Rb ratios similar to or slightly higher than the main trend. Similarly,

K/Rb ratios for amphiboles are generally higher than the main trend, but due to its low abundance and low concentrations of K and Rb, its effect would be minor compared to alkali feldspar and mica. Although quantitatively also insignificant, the contribution from biotite far outweighs its abundance. K/Rb in biotite is generally the lowest of all the minerals in most rocks (Section 5-3-3). Three examples were chosen to illustrate this (Table 6-1). K/Rb of the granite G 145 (311) is almost the same as that of the alkali feldspar (316) which contains 88% and 75% of the total K and Rb of the rock, and which makes up 30 mode%. The 5 mode% of biotite, with K/Rb=85, contributes 20% and 6.4% of the total Rb and K respectively. The other phases, mainly plagioclase and quartz, make up 65% of the rock but only contain 5% and 6% of its Rb and K respectively.

For the monzodiorite (F135), 12.5 mode% of biotite contribute 64% and 30% of the total Rb and K. K/Rb for the biotite is 121, and ranges from 322 to 670 in the amphibole and plagioclase. K/Rb for the host rock is 261, reflecting the influence of the biotite, which out-weighs its low abundance. Similarly, for the gneiss F151, 8.4 mode% of biotite contributes 83% Rb and 60% K of the host rock. K/Rb for the rock is proportionately closer to that of the biotite (168) than the coexisting plagioclase (513) or alkali feldspar (612) which make up 67% and 1.4% respectively of the host rock.

		Kf	Pl	Bi	Am	Rock	Sum
G 145 granite							
	mode%	30	34.2	5.0			69.2
K	% in mineral	11.8	0.68	5.2		4.32	
	% in rock*	88	5.7	6.4			100
Rb	ppm in mineral	374	18.4	610		139	
	% in rock	75	4	20			99
	K/Rb	316	370	85		311	
F 135 monzodiorite							
	mode	7.8	32.3	12.5	41.6		92.4
K	% in mineral	11.2	1.10	5.53	0.91	2.07	
	% in rock	38	15	30	17		100
Rb	ppm in mineral	188	16.4	456	28.3	79.1	
	% in rock	17	6	64	13		100
	K/Rb	595	670	121	322	261	
F 151 gneiss							
	mode	1.4	66.5	8.4			76.3
K	% in mineral	9.73	0.41	7.23		1.07	
	% in rock	13	26	60			99
Rb	ppm in mineral	159	8.0	430		10	38
	% in rock	5	12	83			99
	K/Rb	612	513	168		268	

Table 6-1. Contributions of K and Rb from the constituent minerals in 1g of each of three rocks. Modal compositions from Gower, 1978 (G 145) and Longstaffe, 1978 (F 151 and F 135); concentrations from Table A-7.
* % contribution which the K in this mineral makes to all the K in the rock, Kf alkali feldspar, Pl plagioclase, Bi biotite, Am amphibole. Quartz is present in these samples but contains virtually no K, Rb and Tl.

Hence, the main trend as defined by the silicic rocks represents a balance of biotite with high Rb and K contents and low K/Rb ratios and the other phases which have higher ratios and, except for alkali feldspar, low contents (Fig. 6-2).

6-2-3. K/Rb fractionation trends; hypothetical models

Fractionation of K/Rb ratio in crustal materials can be studied by following the concentration paths in a number of hypothetical models of crystallization of a melt, each assumed to be a closed system. The theory and equations for trace element behaviour during anatexis have been developed by Gast (1968) and Shaw (1970) and different aspects have been subsequently discussed by many others. The following discussion is based on that of Shaw (1970), slightly modified for crystallization, using the partition coefficients for the mineral/rock pair for natural materials from this study (Table 6-2, from Table 5-5 and 5-7). D(K), not included in previous discussions is calculated from the relation

$$D(K) = D(Rb) \times K_D(K/Rb) \qquad (1)$$

Partition coefficients for quartz/rock are assumed to be 0.01 for both Rb and K. All partition coefficients are assumed to be constant during the whole process, which takes part in the absence of a vapour phase. The effect of temperature on partition coefficients, and of the presence of a vapour phase, will be discussed later.

Minerals	D(mineral/liquid) Rb	D(mineral/liquid) K	Modal % of crystallizing solids: BASALT MAGMA (M) A	BASALT MAGMA (M) B	GRANITE MAGMA (N) C	GRANITE MAGMA (N) D	GRANITE MAGMA (N) E
quartz	0.01	0.01			0.35	0.30	0.30
biotite	3.7	2.3			0.05	0.05	
K-feldspar	2.9	4.4			0.20	0.30	0.20
amphibole	0.37	0.44		0.10		0.05	
plagioclase	0.16	0.18	0.33	0.30	0.40	0.30	0.30
pyroxene	0.05	0.035	0.33	0.30			0.20
olivine	0.04	0.026	0.33	0.30			
$D_{Rb(bulk)}$			0.083	0.112	0.832	1.12	0.641
D_K (bulk)			0.081	0.116	1.07	1.88	0.944
c^o			Rb=30 ppm, K=0.83%		Rb=170 ppm, K=4.2%		

Table 6-2. Data for crystallization model calculations. Mineral/liquid partition coefficients from Table 5-5 and 5-7; bulk partition coefficients from equation 2; c^o concentration of the initial liquid; Assemblages A, B, C, D, E are explained in the text.

Fig. 6-2. K and Rb correlations in rocks (●) and their constituent minerals

△ alkali feldspar, □ biotite, ○ plagioclase

● amphibole. Tie-lines join the minerals and host rock.

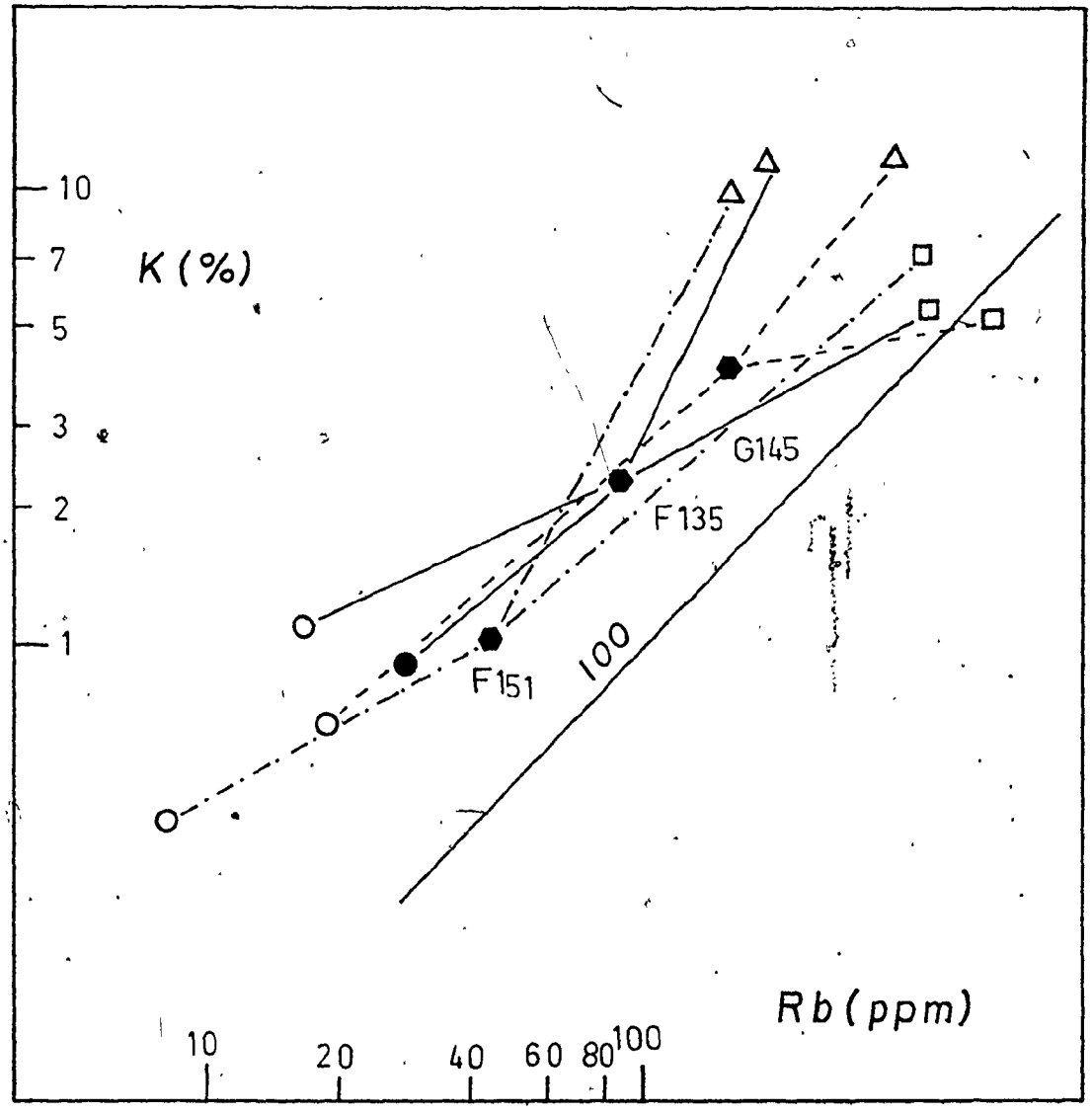
10
7
5
3
2
1
K (%)
G145
F135
F151
100
10
20
40
60
80
100
Rb (ppm)

Assuming a melt is formed in the lower continental crust and undergoes crystallization as it cools, if the phases α, β etc. are formed in constant proportions $P\alpha$, $P\beta$ etc., the bulk partition coefficient D for an element i is

$$D = P_\alpha D^{\alpha/l} + P_\beta D^{\beta/l} + \text{etc.} \qquad (2)$$

where $D^{\alpha/l}$ etc. is the partition coefficient for the pair c/liquid etc. Two mechanisms will be discussed:

a. continuous equilibrium, in which the crystals formed constantly remain in equilibrium with the liquid. The concentration of i in the residual liquid is

$$c_i^L = c_o \; / \; [F + D(1-F)], \qquad (3)$$

where F is the fraction of the residual liquid,

c_o is the initial concentration of i.

b. fractional crystallization, whereby the crystals are isolated from the liquid once they are formed. The concentration of i in the residual liquid is

$$c_i^l = c_o \times F^{D-1} \qquad (4)$$

The concentration of i in the corresponding solid c^S or c^s at any instant during the process is given by

$$c_i^S = c_i^L \times D \qquad (5)$$

or

$$c_i^s = c_i^l \times D \qquad (6)$$

K and Rb concentrations of the residual liquid during the crystallization of two initial liquids into solids of various modal compositions (Table 6-2) will be followed. Calculations are carried out for the crystallization fraction of 0.75, 0.90 and 0.975 (F=0.25, 0.10 and 0.025 respectively) of the original amount of the liquid, using both equations (3) and (4). The results are reported in Table 6-3 and some plotted in Fig. 6-3.

Composition of the first liquid to be considered is that of the average basalt (Turekian and Wedepohl, 1961) with 0.83% K and 30 ppm Rb (liquid M). Crystallization of an olivine-gabbro containing equal amounts of plagioclase, pyroxene and olivine alone (M - A) or with 10% amphibole (M - B) enriches the residual liquid linearly in both K and Rb. The amount of enrichment is higher with higher degree of crystallization (smaller F) and for each value of F, higher for the fractional model (c^l) than the equilibrium model (c^L), although the trends produced are similar in all the cases in which only mafic minerals are involved.

Composition of the second initial liquid to be considered is that of the average low-Ca granite (N, Turekian and Wedepohl, 1961).

	BASALT MAGMA (M)				GRANITE MAGMA (N)					
	A		B		E		F		G	
	Rb	K	Rb	K	Rb	K	Rb	K	Rb	K
F=0.25										
c^L	96	2.67	90	2.46	194	3.99	156	2.53	233	4.38
K/Rb	278		273		201		162		188	
c^l	107	2.97	103	2.83	214	3.85	143	1.24	279	4.54
K/Rb	278		275		180		87		163	
F=0.10										
c^L	172	4.81	149	4.06	200	3.95	153	2.34	251	4.42
K/Rb	280		272		198		153		176	
c^l	248	6.89	232	6.35	250	3.65	129	0.55	389	4.77
	278		274		146		43		123	
F=0.025										
c^L	283	7.98	224	6.02	203	3.93	152	2.27	261	4.44
K/Rb	281		269		195		149		170	
c^l	883	24.7	795	21.7	319	3.37	108	0.16	638	5.17
K/Rb	280		273		106		15		81	

Table 6-3. K and Rb concentrations and K/Rb ratios of the residual liquid for the crystallization of the mineral assemblages shown in Table 6-2.

Fig. 6-3. Composition of the residual liquids after crystallization of some of the hypothetical solids as shown in Table 6-3 from a basalt (M) and granite (N) magma, for crystallization of up to 97.5% of the original amount of liquid; open symbols and small letters fractional model, solid symbols and capital letters equilibrium model.

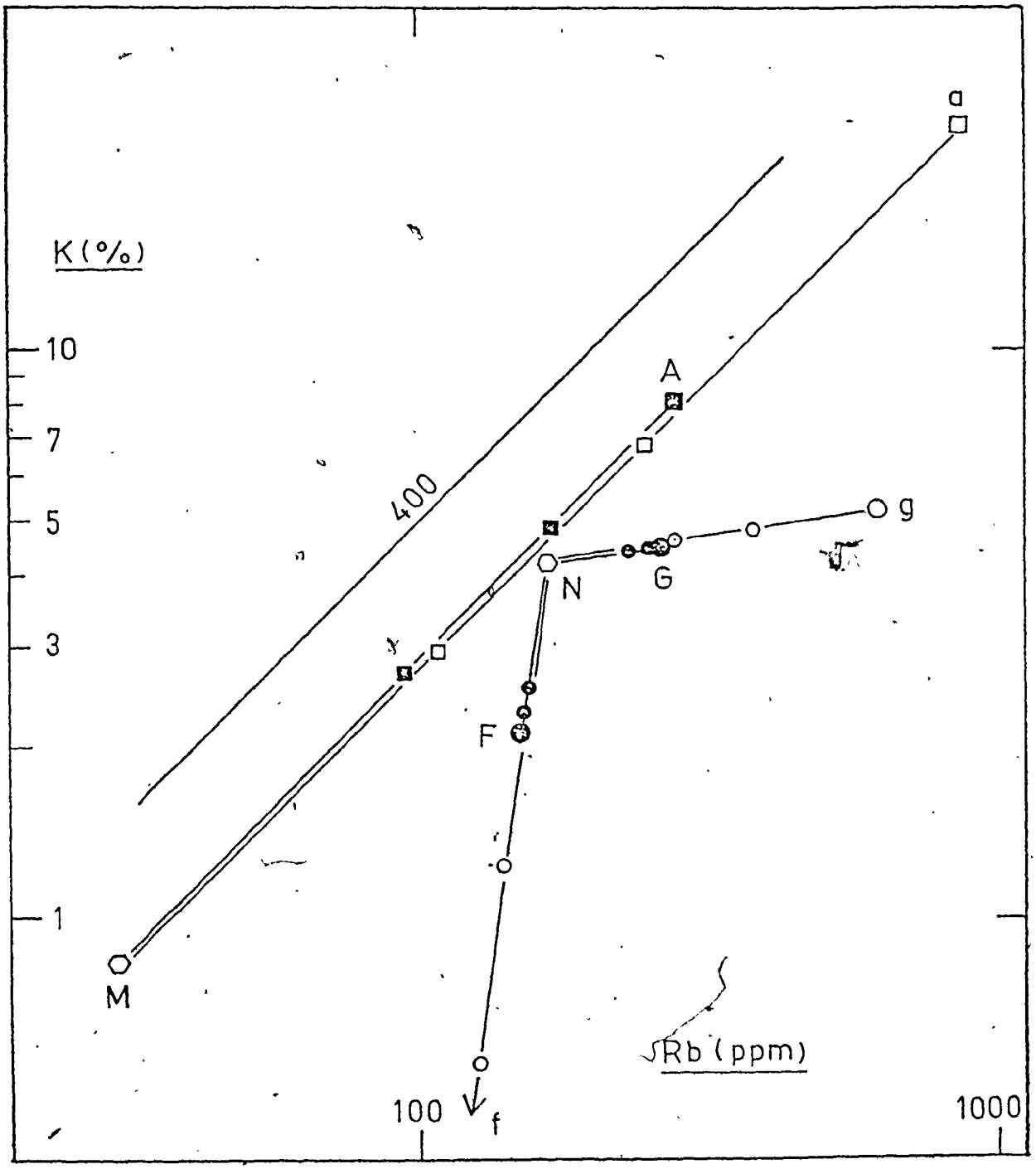
K(%)
10
7
5
3
1
400
a
A
g
N
G
F
M
f
100
Rb (ppm)
1000

Crystallization of solid with 20% each of alkali feldspar and pyroxene and 30% each of quartz and plagioclase (E) enriches both K and Rb in the liquid and lowers its K/Rb ratio. Crystallization of a solid with 20% alkali feldspar, 5% biotite, 35% quartz and 40% plagioclase (C) lowers K and raises Rb in the liquid. Finally, crystallization of equal amounts of plagioclase, quartz and alkali feldspar with 5% each of biotite and amphibole, a rock (D) similar to a minimum-melting granite (water saturated), impoverishes the melt in both K and Rb and lowers its K/Rb ratio rapidly.

According to equations (5) and (6), compositions of the solid will follow similar trends as the liquid as crystallization progresses. This is illustrated in the lower part of Fig. 6-4 using the same example (Table 6-2). Thus, fractional crystallization of 5% and 10% alkali feldspar from a melt W produces liquids H_1 and H_2 respectively, while the compositions of the corresponding solids are h_1 and h_2 respectively; both solids and liquids are progressively impoverished in Rb and K and increased in K/Rb ratio. Similar behaviour is obtained for the fractional crystallization of 5% and 10% biotite alone, which produces liquids J_1 and J_2 and solids j_1 and j_2. This part of the same diagram also illustrates the effect of the crystallization of biotite and alkali feldspar, which are responsible for the variation of K/Rb ratios in the melt and the solids as dis-

Fig. 6-4. K and Rb concentrations of initial liquid W and after fractional crystallization of 10% alkali feldspar (⬡) or biotite (▽), using partition data for natural materials (Table 6-3). Also shown are the initial concentrations of liquid Y and after fractional crystallization of 10% alkali feldspar, using experimental data for 500°C (△) and 700°C (□). Solid symbols denote compositions of the corresponding solids.

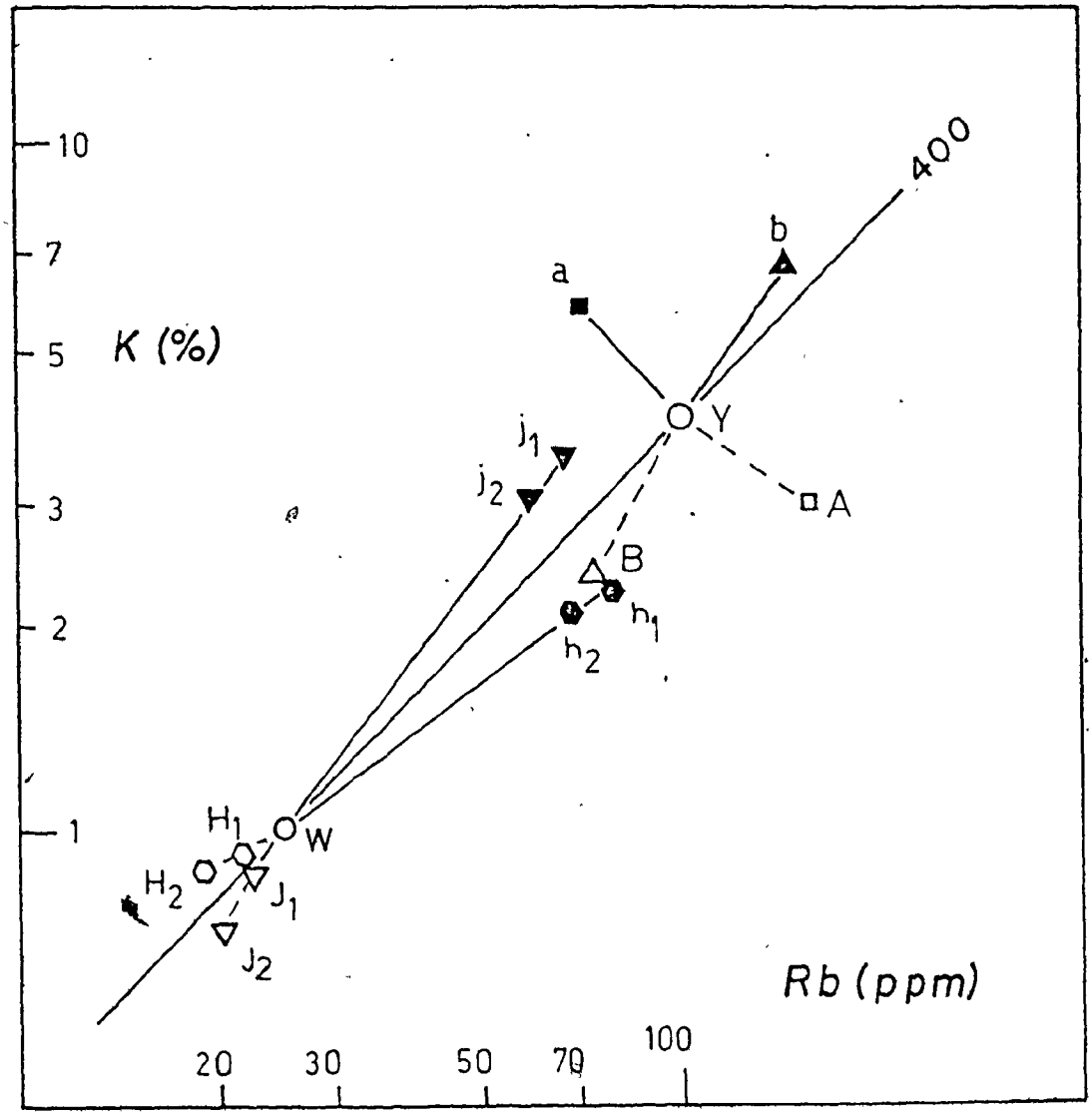
10
7
5
3
2
1
K (%)
400
a
b
Y
A
j_1
j_2
B
h_1
h_2
H_1
W
H_2
J_1
J_2
Rb (ppm)
20
30
50
70
100

cussed previously. Thus fractional crystallization of biotite increases the K/Rb ratio in the residual liquid and vice versa for the crystallization of alkali feldspar. The examples used in both cases are calculated for the fractional model (equation 4), but similar results would be obtained for the equilibrium model, as mentioned previously.

The effect of temperature on partition coefficients can be illustrated with the scanty data for the alkali feldspar/rhyolite pair from this study (Chapter 3). D(Rb) increases from 0.63 at 700°C to 1.8 at 500°C while K_D(K/Rb) decreases from 2.8 to 1.3 for the same temperature range (or D(K) decrease from 1.76 to 2.34, equation 1). The effect of temperature on the concentrations of the liquid and solid for the fractional crystallization of 30% feldspar alone from a liquid is shown in the upper part of Fig. 6-4. Thus, at higher temperature, crystallization of feldspar reduces the K/Rb ratio of the residual liquid more than at lower temperature. Conversely, a feldspar formed at higher temperatures would have relatively higher K/Rb ratio.

Although the temperature effect on partition coefficients for biotite/melt was not studied, Heier and Adams (1964) noted that the Rb concentration increases and K/Rb decreases in the series of biotite-muscovite-lepidolite (Fig. 6-5), i.e. from high to low temperature forms, similar to the alkali feldspars (section 3-4-1).

Fig. 6-5. Plots of Rb vs. K in micas and some coexisting feldspars. Tielines connect coexisting minerals.

△ Feldspar ○ Muscovite

● Biotite ⌀ Lepidolite

(from Heier and Adams, 1964).

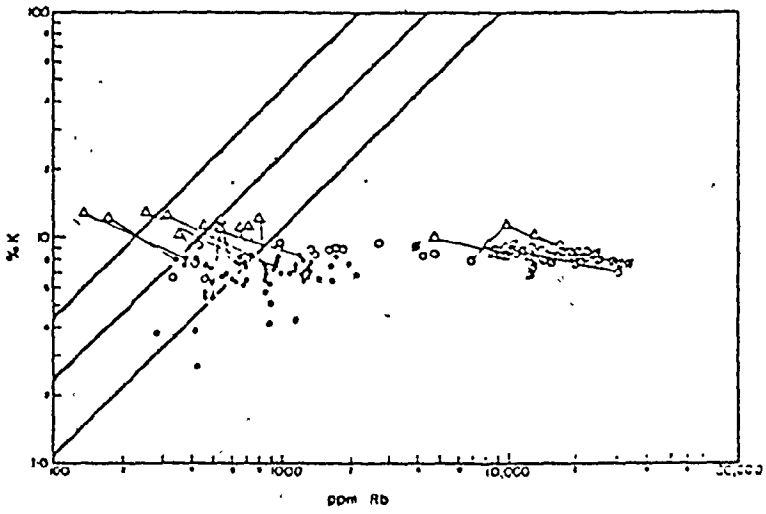
100
10
1.0
% K
100
1000
10,000
ppm Rb

Similarly, since plagioclase becomes more alkali-rich with lower temperature (Bowen, 1913), the trend of decreasing K/Rb with higher K (and Rb) concentrations observed for plagioclase (section 5-3-3) can also be attributed to temperature. Hence at least for feldspars and micas, the main carriers of K and Rb in most igneous and metamorphic rocks, crystallization at lower temperatures will form crystals with lower K/Rb ratios.

The effect of a vapour phase on the K/Rb ratio during the crystallization of a magma will be appraised using the experimental data for rhyolite/vapour (Chapter 3). Thus D(Rb) decreases from 1.1 to 0.80 while K_D(K/Rb) increases from 2.3 to 4.7 for the temperature range of 700°C to 500°C. Hence, compared to the coexisting rhyolite, the vapour has lower K/Rb ratio and approximately the same Rb concentration. Thus circulation and removal of a vapour phase from a melt raises its K/Rb ratio while a crystallizing solid which incorporates vapour will have lower K/Rb ratio. The former case can be envisaged in the early stage of crystallization of a melt formed at depth, such as from a granulite (N, Fig. 6-2) in which the early crystallate will be depleted in hydrous phases. Conversely, most pegmatites and many late-stage granites are usually water-rich.

Thus early stage of crystallization of a melt at high temperature will produce a mafic or ultra-mafic rock with low K and Rb concentrations, and with approximately the same K/Rb ratio as the liquid. Incorporation of alkali feldspar will raise, and of biotite will lower the K/Rb ratio in the solid. Formation of rocks of very low K/Rb ratios, such as those of the hydrothermal-pegmatitic trends is favoured by low temperature crystallization, low alkali feldspar/biotite ratio and incorporation of the vapour phase.

6-3. Crustal fractionation of Tl

6-3-1. Introductory statement

Most continental plutonic rocks have K/Tl in the range of 30,000 to 150,000 and Rb/Tl in the range of 65 to 400 (Shaw et al., 1974). On the K-Tl scattergram (Fig. 6-6), there is a region of very high concentrations and very low K/Tl ratios not unlike the pegmatitic-hydrothermal trend for K/Rb. However, no such trend of Tl enrichment is present in the Rb-Tl plot (Fig. 6-7). Both ratios are higher in most alkalic volcanic rocks and lower in most deep ocean tholeiites (subsequent study by Shaw and Fratta, pers. comm. shows that some, but not all of the tholeiites included in Figs. 6-6 and 6-7 were either altered or contaminated).

Fig. 6-6. Summary of K-Tl relationships in some major crustal rock units (from Shaw et al. 1974).

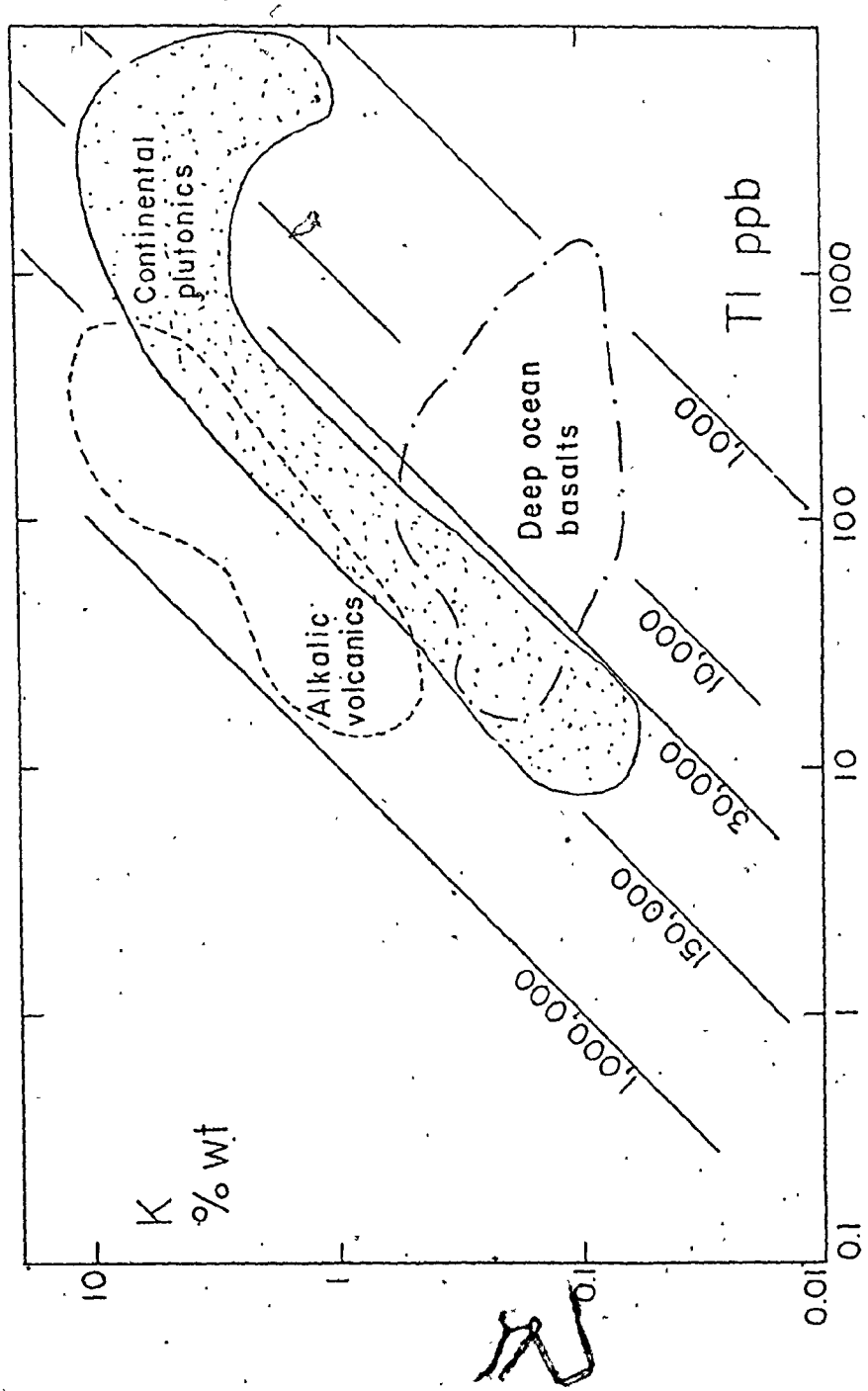
Continental plutonics
Deep ocean basalts
Alkalic volcanics
1000
10,000
30,000
150,000
1,000,000
Tl ppb
1000
100
10
1
0.1
K % wt
10
1
0.1
0.01

Fig. 6-7. Summary of Rb-Tl relationships in some major rock units (from Shaw et al., 1974)

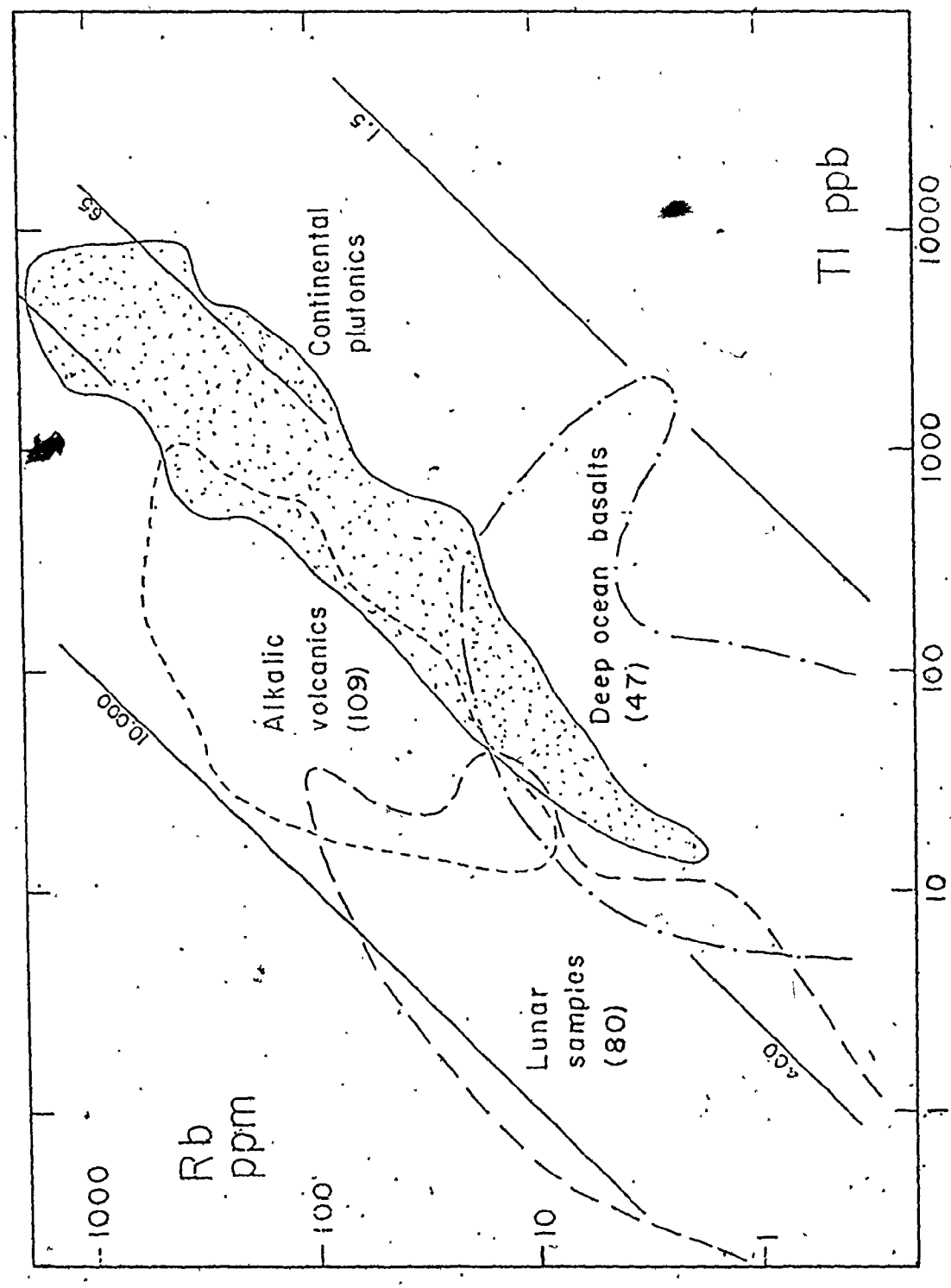
Rb
ppm
1000
100
10
1
Tl ppb
1
10
100
1000
10000
Continental
plutonics
Alkalic
volcanics
(109)
Deep ocean basalts
(47)
Lunar
samples
(80)
1.5
6.5
10,000
4.00

6-3-2. Continental plutonic rocks

The behaviour of K and Tl in continental plutonic rocks can be explained by the same principle as for the K and Rb pairs because of the similarities of Rb and Tl in most minerals and rocks. Such similarities are manifested in the near parallelism of Rb-Tl relationships (Fig. 6-7) in all the continental plutonic rocks accompanying strong enrichment in each element. This is possible also because of the relatively small contribution of Tl by the non-silicate minerals because of their generally low abundances.

6-3-3. Basalts

Three possible explanations for the behaviour of Tl in basalts, namely sulphide and silicate fractionation and sea-water alteration, will be examined.

Sulphide fractionation has been proposed to explain the enrichment of Tl in the tholeiites (e.g. Albuquerque et al., 1972 and McGoldrick et al., 1978). Such an explanation is very tempting in light of the data from this study (bearing in mind the uncertainty of the genetic relationship between coexisting sulphides and silicates):

a. Among the constituent minerals of a mafic rock, the sulphides usually have the highest Tl content.

b. That sulfide fractionation of Tl is not observed for most plutonic rocks is probably due to their generally low abundances and lower Tl contents relative to the potassic phases. Hence the effect of the sulphides would be negligible in most plutonic rocks, thus providing an explanation for the differences in Tl behaviour between plutonic and volcanic rocks.

Moreover, several recent studies indicate that many oceanic basalts contain magmatic sulphides, pyrite, chalcopyrite and pyrrhotite (Moore, 1976 and MacLean, 1977), and globules of a quenched sample of sulphide (Czamansky and Moore, 1977). It is the general consensus of these authors that oceanic basalts were saturated in sulphide prior to eruption although most of it might have been lost during crystallization and subsequent leaching. This provides a means of preferential concentration of Tl relative to K and Rb: since most people agree that alkalic basalts were formed by partial melting of the upper mantle at relatively high pressure and temperature and would have probably lost most of the sulphide prior to their formation. Conversely, deep ocean tholeiites are now believed to have been formed at lower temperature and pressure and hence would probably have retained some of the sulphide (for the models of basalt genesis, see summary by Wyllie, 1971, e.g.).

However, Moore and Fabbi (1971) found no difference in the S concentrations between tholeiitic and alkalic basalts and that Shimizaki and Clark (1973) showed experimentally that partial melting of mantle material would melt all FeS before any silicate would begin to melt. Hence, unless the sulphides behave differently in alkalic and tholeiitic basalts either during or subsequent to their genesis (and there is no reason to believe they do), it is difficult to envisage that sulphide fractionation can produce the different patterns observed. Moreover, Fratta and Shaw (pers. comm.) found no correlation of Tl and S in some dredge basalts.

Another non-silicate mineral, magnetite, has relatively high Tl content (Section 5-3-3). However, it is only present in small quantities and only in some basalts (e.g. see Mathez, 1976).

Sea water alteration of deep ocean basalts has been demonstrated (Hart, 1969) to produce differential enrichment of many alkali elements and subsequently lower K/Rb, K/Cs and Rb/Cs ratios (Fig. 6-8). Since Tl is intermediate between Rb and Cs in many crystallo-chemical properties, such a process will probably lead to lowering of K/Tl and Rb/Tl ratios as well. This provides another means for explaining the different behaviour of Tl between oceanic alkalic and tholeiitic basalts, since the former normally occurs in islands and sea-mounts and hence less subject to sea water alteration, while

Fig. 6-8. K/Rb (a) and K/Cs (b) vs. K content of submarine tholeiites. Tie-lines connect interior and marginal portions of corresponding samples. From Hart (1969).

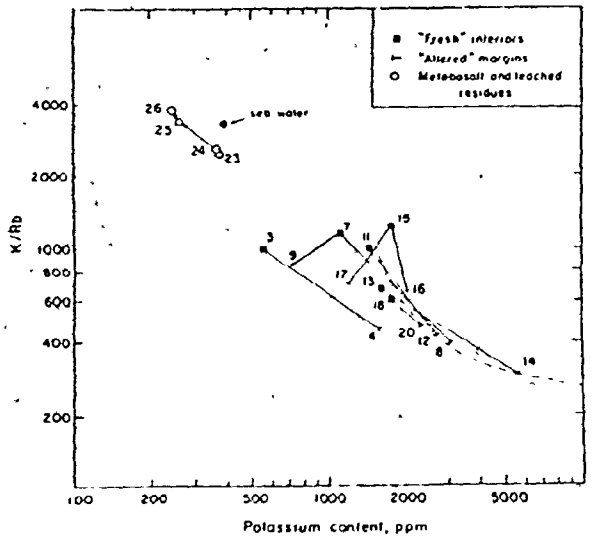
"Fresh" interiors
"Altered" margins
Metabasalt and leached residues
sea water
K/Rb
Potassium content, ppm

a.

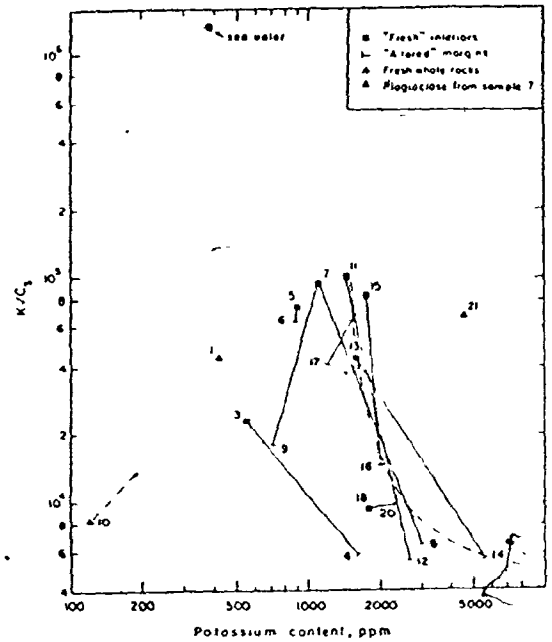
sea water
"Fresh" interiors
"Altered" margins
Fresh whole rocks
Plagioclase from sample 7
K/Cs
Potassium content, ppm

b.

the latter generally occur in deep ocean floors, as their name implies.

However, Hart (1969) also found that high K/Rb ratios are characteristic of fresh unaltered deep ocean tholeiites and, by analogy, it is also possible that low K/Tl and Rb/Tl ratios observed for these rocks are also primary features. Moreover, many of the basalts reviewed by Shaw et al. (1974) are fresh and unaltered.

Several mineral fractionation models have been proposed for the high K/Rb ratios observed for oceanic tholeiites: amphiboles (Hart and Aldricht, 1967 and Griffin et al. 1968); plagioclase (Murthy and Griffin, 1970 and Gill and Murthy, 1970). Although some of the amphiboles examined in this study have relatively low Rb/Tl ratios, none of them is sufficiently low to account for those of the tholeiitic basalts (Fig. 5-1). Furthermore, their 'normal' K/Tl ratios exclude them from being likely candidates for the fractionation of Tl from both K and Rb. Similarly, plagioclase can be excluded because of its 'normal' K/Tl and Rb/Tl ratios.

According to the experimental results discussed previously, K_D(Rb/Tl) = 2.5 and K_D(K/Tl) = 9.0 at 700°C for the pair sanidine/melt (Chapter 3). Crystallization of a sanidine-rich rock such as trachyte-basalt or phonolite at high temperatures, can have high K/Tl

and Rb/Tl ratios. However, the other major alkali-minerals (leucite, nepheline, alkali amphibole and pyroxene) as well as the most abundant phase, glass, of these alkalic basalts need to be similarly studied before any meaningful conclusion can be drawn.

6-4. Conclusion

The behaviour of K, Rb and Tl in most continental plutonic rocks, as reviewed by Shaw (1968) and Shaw et al. (1974) can be explained in terms of their behaviour in the constituent minerals, as evidenced in this study. The most important controlling phases are the K-minerals, feldspars and micas. Fractionation of a magma normally leads to an increase in the abundances of the incompatible elements, and early (high temperature) crystallization of K-minerals will probably lead to an enrichment of Rb and Tl relative to K, resulting in lowering of K/Rb and K/Tl ratios in the later crystallates. Presence of a vapour phase in such a scheme will enhance such trends and occurrence of many non-silicates, sulphides and oxides, will preferentially concentrate Tl relative to both Rb and Tl.

Complication arises when application of the present data to the behaviour of Tl in basalts is attempted. Lower Rb/Tl and K/Tl ratios observed for the oceanic tholeiites can be attributed to sulphide enrichment and/or sea-water alteration. However, there is no evidence to indicate that the alkalic basalts, with high K/Tl and Rb/Tl ratios,

have different S abundances or that all the oceanic tholeiites were altered by sea-water.

CHAPTER 7

CONCLUSION

The partition coefficients of Rb and Tl between the experimental pair alkali feldspar-vapour vary somewhat with the composition, structure and thermal history of the feldspar used. For a K-rich sanidine synthesized directly from a gel, the results at 800°C are: D(Rb) = 2.8, D(Tl) = 0.42, K_D(Rb/Tl) = 7.6, K_D(K/Rb) = 1.7 and K_D(K/Tl) = 11. When a Na-rich natural sanidine was used, lower D(Rb) and D(Tl) and higher K_D(K/Rb) and K_D(K/Tl) were obtained; whereas if a Rb-rich microcline was used, higher D(Rb) and K_D(Rb/Tl) and lower K_D(K/Rb) were obtained. The discrepancies in these as well as in all the other experiments studied, which involved alkali feldspars, can be explained most satisfactorily by the effect of composition. However, there are other complications, since the feldspar more or less retained its initial structure and composition in the regular runs. The effect of this structural (and possibly also major element composition) disequilibrium on trace element distribution is not known due to the

interaction of other factors (see next paragraph). However, more consistent results for all the feldspar studied were obtained for the fusion runs, in which structural equilibrium was achieved. Nevertheless, experiments with both of these natural feldspars indicate that for the alkali feldspar-vapour pair, D(Rb) and D(Tl) increase while K_D(Rb/Tl), K_D(K/Tl) and possibly also K_D(K/Rb) decrease from high to low temperatures.

The role of kinetics is also difficult to assess in these experiments. Thus previous heating of the capsules at 900°C (fusion runs) recudes the differences in the results for different starting alkali feldspars, but at the same time, converts them to the same final structural state (high sanidine). Moreover, test-runs with the natural sanidine showed that equilibrium was probably reached within 14 days.

Partition coefficients measured for the rhyolite-vapour pair show a slight preference of both Rb and Tl for the vapour phase, and very little dependence on temperature. Partition coefficients for the alkali feldspar-rhyolite pair were obtained by multiplying the D and K_D values for the pairs feldspar-vapour and rhyolite-vapour. Very similar results were also obtained by the direct equilibration of alkali feldspar and rhyolite. Such results can be used semi-quanti-

tatively as geothermometers for volcanic rocks and in some cases, also for some plutonic rocks, or as indicators of secondary reactions such as alteration and contamination. Results for the Na-rich alkali feldspar-rhyolite pair show that both D(Rb) and D(Tl) increase from less than 1 (0.63 and 0.20 respectively) at 700°C to greater than 1 (1.8 and 1.5 respectively) at 500°C. Thus the effect of alkali feldspar fractionation depends upon the temperature; at high temperatures, both Rb and Tl favour the melt and at lower temperatures, the feldspar.

Fusion runs with phlogopite-alkali feldspar pairs show that the limit of ideal behaviour for Rb lies between 0.52% to 1.7% in phlogopite and between 0.25% to 1.45% in alkali feldspar. Tl appears to have behaved ideally for concentrations of up to 650 ppm in either mineral, irrespective of their Rb concentration and previous thermal history. The following average partition coefficients at 700°C for phlogopite-sanidine were obtained for the runs in which Rb appeared to have behaved ideally: D(Rb) = 2.3, D(Tl) = 1.3, K_D(Rb/Tl) = 1.9, K_D(K/Rb) = 0.31 and K_D(K/Tl) = 0.56.

In a multiple-phase system of biotite, alkali feldspar, amphibole, and plagioclase, average Rb and Tl concentrations decrease in the order as shown, for both experimental and natural materials. This reflects the combined effect of the structure of the minerals and the size of the substituting trace element. In these minerals, only K

is favourable to substitution by the large Rb and Tl and hence the K-minerals usually contain much more (up to over an order of magnitude) Rb and Tl than the coexisting non-K minerals. Within each of these two groups of minerals, the amount of substitution permitted depends upon the tightness with which the atoms are packed, being relatively the least for the tectosilicates because of the three-dimensional arrangement of the atoms.

However, the difference in Rb and Tl concentration between the K-phases and the non-K ones are relatively much more pronounced in the natural than in the experimental materials. This is probably because under hydrothermal conditions the crystals behave differently, as most of the natural mafic minerals and plagioclase were formed in the absence of a vapour phase. In this case, the effect of the vapour phase appears to be a loosening of the structure of the minerals and hence making substitution by the larger Rb and Tl easier. The K-minerals are relatively less affected since the favourable sites (K) are already present. Other explanations such as surface adsorption and disequilibrium are considered unlikely because they will affect all the minerals to more or less the same extent and also because of the similarities of some of the experimental results to those for natural materials.

For natural K-minerals, variations in Rb and Tl concentrations are much greater than that in K. Hence K/Rb and K/Tl ratios vary greatly, generally decreasing with higher concentrations of K, Rb and Tl. On the other hand, the non-K minerals, including pyroxenes and olivine, generally have more constant K/Rb and K/Tl ratios which show a slight decrease with higher concentrations. Rb/Tl ratios are more constant for all the silicate minerals, possibly with the exception of the pyroxenes.

Concentrations of Tl for pyrrhotite, pyrite and magnetite decrease in the order as shown. As a group, Tl concentrations for these non-silicate minerals are intermediate between the K and non-K silicates. This provides a means for Tl-enrichment relative to both Rb and K since these non-silicate minerals generally do not contain appreciable amounts of K and Rb.

The trends of decreasing K/Rb and K/Tl ratios with higher concentrations of K, Rb and Tl, which have been observed for many suites of rocks can be explained by the behaviour of the constituent minerals. Thus at high temperature, crystallization of mafic minerals and plagioclase from a melt will lead to a more or less proportionate enrichment of K, Rb and Tl in the melt. High temperature crystallization of alkali feldspar will result in enrichment of Rb and Tl but will also result in lower K/Rb and K/Tl ratios in the melt. On the other hand, lower temperature crystallization of alkali feldspar, and also K-

micas will form rocks of low K/Rb and K/Tl ratios. Formation of rocks of very low ratios, such as found in some alkali rich granites and pegmatites, is favoured by relatively low temperature of crystallization of abundant micas and alkali feldspar and incorporation of vapour.

Although sea-water alteration and accumulation of sulfides and oxides can possibly lead to Tl enrichment and consequently low K/Tl and Rb/Tl ratios, as observed for some tholeiite basalts, at present there is no plausible explanation for the high ratios observed for some alkalic basalts. More studies on the behaviour of sulfides in basalts and partitioning of K, Rb and Tl between the minerals of alkalic basalts are needed in order to shed light on this problem.

Appendix 1. Experimental techniques

A-1-1. Preparation of capsules

Two different methods are employed in the preparation of the capsules, the choice of which depends on whether they contain a single solid and a vapour (SSV) or more than one solids and a vapour (MSV).

A-1-1-1. SSV runs

The method for the preparation of the capsules for the SSV runs is similar to that described by Orville (1963) and many others. The sample container is a gold capsule of the dimensions of either A or B in Table A-1. These capsules are cut from gold tubes to lengths of about 1" and boiled in dilute HCl to clean and saturate them with chloride. One end of the capsule is crimped with a pair of flat-jawed plyers and welded in a D.C. graphite arc-welder. The starting solid is first introduced into the capsule through the open end with the aid of a small funnel. The liquid is then introduced by means of a disposable micro-syringe. The weights of both starting materials are obtained by weighing by difference. Usually the solid and liquid each weigh in the range of 20-100 mg, depending on whether A or B type is used and the length of the capsule. The open end of the filled capsule is then crimped and welded. In order

	Material	Inner diameter	Outer diameter	Length
a. Capsule*				
A	gold	0.16	0.18	1-1.25
B	gold	0.10	0.12	1-1.25
C	gold/silver	0.052	0.072	0.75-1
D	gold/silver	0.052	0.072	0.50
b. Pressure Vessel				
large		0.50	2.25	9.5
small		0.25	1.0	8.0

Table A-1. Dimensions of capsules and pressure vessels (in inches).

*manufactured by Johnson Matthew & Mallory Limited.

to prevent vaporization of the liquid during welding, the other (welded) end of the capsule is wrapped in a piece of wet paper tissue which is soaked in a beaker of water.

A-1-1-2. MSV runs

In the MSV runs, up to five solids can be placed inside a single type-A or three in a type-B capsule together with a liquid. Each, except one, of the powdered solids is placed in a type-C or type-D capsule. The type-C capsules are placed alongside each other while the type-D ones are placed lengthwise inside the outer capsule. The ends of the inner capsules are crimped at both ends but are not welded, so that the solid inside do not mix with each other, but the liquids can diffuse in and out to act as a transporting agent. The last solid and the vapour can then be introduced, as described for the SSV runs, into the outer capsule, which is sealed by welding.

A-1-2. Experimental procedure

The welded capsules are placed inside a cold-seal pressure vessel (Table A-1 and Tuttle, 1949), heated by an upright split resistance furnace. The small vessels can accommodate up to three type-B capsules alongside each other while the large vessel can accommodate up to five type-B or three type-A capsules. Temperature is regulated by

both a rheostat in the power supply and an external Cr-Al thermocouple and circuit breaker. Temperature of the experiment is measured by another external Cr-Al thermocouple, the sensing end of which is placed inside a well, which closely adjoins the sample chamber. Temperature from this thermocouple is recorded continuously in a Speedomax W, 12-channel recorder, calibrated against the melting point of pure NaCl (800.4°C).

Pressure inside the vessels is maintained by an automatic hydraulic pump using distilled water as the pressure medium and recorded by a Bourdon-type gauge.

During the duration of the successful runs of approximately one month, temperature fluctuation is less than a maximum of 10°C, usually 5°C, and pressure fluctuation is less than 5%.

At the end of each run, the vessel is quenched by quickly removing the furnace and applying a spiral air blast, made from a copper tube, wrapped around its length. When the temperature drops to below 300°C, usually within 5-10 min., the vessel is further cooled by a beaker of water until it is cold enough to handle.

Appendix 1-3. Treatment of run products

The vessel is opened and the capsules removed and cleaned with de-ionized water. Individual capsules are weighed to check for

leakage. The successful capsule is then cut open under de-ionized water and the capsule and contents are boiled to reduce adsorption of elements. The solid is later separated from the liquid by filtration using a Millipore filtering system.

In the case of the MSV runs, the procedure is similar except that after the outer capsule is cut open, the solid and liquid inside (as well as each small inner capsule) are treated separately and the liquids are combined together after filtering.

Part of the solid of some of the runs is examined with X-ray diffraction and a small portion of some is examined under a petrographic microscope. The bulk of the solids as well as all the liquid are analyzed with atomic absorption spectroscopy (Appendix 5).

Appendix 2. X-ray diffraction technique

All X-ray diffraction (XRD) studies were conducted with a Phillips wide angle goniometer, using Cu radiation. Each sample was scanned from $2\theta = 5^{o}$ or 10° to 60° at a speed of $2\theta = 2^{o}$/min. and a chart speed of 2 cm/min.

Each diffractogram was compared to published ASTM patterns or to patterns obtained with the starting material for identification.

Structural state of the alkali feldspars is studied with the 3-peak method (Wright, 1968). The results are listed in Table A-2. The $\bar{2}01$ peak from the final sanidine Sl of most regular runs (SSV or MSV) is usually very broad and poorly defined. In such case, the 2θ value is not given. In a few, there is a relatively well-defined $\bar{2}01$ peak together with one or more additional weak ones. In such a case, the strongest one is given in parentheses. In a plot of $2\theta_{\bar{2}04}$ vs. $2\theta_{060}$ (Fig. 2-12), the structural state of the final feldspar is read from the graph, and also from the absence or presence of the $1\bar{3}1$ peaks (for sanidine and microcline respectively). Exsolution, if present, is indicated by the presence of two or more $\bar{2}01$ peaks or by a single broad peak at 2θ of about 21°.

Due to the small amount of material available and because the final powder was not ground, some of the XRD patterns obtained are very poor in quality, with most of the less intense peaks missing or very fuzzy. The structural state of these (not included in Table A-2) was determined only by the presence or absence of the more intense $1\bar{3}1$ peak.

Sample	Initial mineral	Temp. (°C)	$\bar{2}01$	2θ(°) 060	$\bar{2}04$	Final mineral*
Regular SSV runs						
32-Eh	S1	500	(21.35)	41.80	51.06	sanidine, exsolved
33-E1	S1	500	--	42.00	51.18	sanidine
6-1	S1	500	(21.44)	41.80	51.05	sanidine exsolved
8-8	S1	600	--	41.90	51.05	sanidine, exsolved.
9-Eh-1	S1	700	(21.75)	41.85	51.00	sanidine, exsolved
8-7	S1	700	--	41.90	51.10	sanidine; exsolved
9-3	M1	500	21.05	41.87	50.65	microcline, homogeneous
9-4	M1	700	20.90	41.95	50.77	microcline, homogeneous
Fusion SSV runs						
14-3	M1	700	21.05	41.62	51.05	sanidine, homogeneous
14-6	S1	800	21.64	41.58	50.83	sanidine, homogeneous
14-8	M1	800	21.05	41.62	50.90	sanidine, homogeneous
14-9	S2	800	21.15	41.75	51.00	sanidine, homogeneous
14-10	S2	800	21.10	41.70	50.95	sanidine, homogeneous
14-5	S1	800	--	41.75	51.20	sanidine, homogeneous
Regular MSV runs						
11-4	S1	500	--	41.75	50.95	sanidine, exsolved

Table A-2. Cont....2

11-5A	S1	500	(20.85)	41.67	50.74	sanidine, exsolved
11-5B	M1	500	21.28	42.18	51.00	microcline, homogeneous
11-7A	S1	600	21.07	41.67	50.85	sanidine, exsolved
11-7B	M1	600	20.95	41.70	50.45	microcline, homogeneous
13-1	M1	700	21.12	41.87	50.67	microcline, homogeneous
13-2	M1	700	21.10	41.68	50.63	microcline, homogeneous
13-3	M1	700	21.18	41.80	50.61	microcline, homogeneous
13-5	S1	600	(21.68)	41.74	50.93	sanidine, exsolved
14-13	M1	600	21.26	41.95	50.85	microcline, homogeneous
14-15	M1	600	21.10	41.85	50.60	microcline, homogeneous
14-16A	M1	600	21.10	41.80	50.62	microcline, homogeneous
Fusion MSV runs						
15-2	S2	700	21.05	41.80	51.05	sanidine, homogeneous
15-4	S2	700	21.15	41.75	51.00	sanidine, homogeneous
15-9	S2	700	21.12	41.75	50.97	sanidine, homogeneous
15-15	S2	700	21.09	41.65	50.95	sanidine, homogeneous
15-19	S2	700	21.10	41.67	50.94	sanidine, homogeneous
15-20	S2	700	21.07	41.65	50.93	sanidine, homogeneous

Table A-2. Cont....

15-21	S2	700	21.13	43.00	51.25	sanidine, homogeneous

Table A-2. XRD data for alkali feldspar identification, using the three-peak method of Wright (1968) ($CuK\alpha_1$ radiation).

*Final structural state is identified by both Fig. 2-12 and presence or absence of $1\bar{3}1$ reflection; ( ) the most intense of two or more peaks; -- very broad peaks.

Appendix 3. Preparation of natural samples

Each of the rock samples was crushed by a steel-jawed crusher and a pulverizer equipped with ceramic or tungsten-carbide plates, to less than about 5 mm. This coarse powder was quartered to obtain 30-50 g which was all crushed to pass through a -200 mesh sieve. The rest of the coarse powder was repeatedly sieved and crushed until sufficient amount of powder of size between -100 to -200 mesh was obtained for mineral separation.

Mineral separation was conducted with standard techniques using heavy liquids and a magnetic separator. Purity of most of the mineral separates were 99% or better except: (a) some sodic plagioclases and alkali feldspars contained up to 15% of mainly quartz and other alkali feldspars; (b) some amphiboles contained up to 2% biotite or chlorite; (c) some olivines contained small amounts of minute opaque inclusions; (d) most magnetites contained 5% or more of silicates. Corrections based on the nature and amount of the impurities, and their elemental concentrations were made whenever possible.

Appendix 4. Analytical technique

Up to 1.5 g of the silicate powder (rock or mineral) was decomposed with 25 ml of a mixture of hydrofluoric (HF) and perchloric ($HClO_4$) acids in the ratio of HF to $HClO_4$ of 1 to 3 by volume. After evaporation to near dryness, the residue was boiled in 2 ml of hydrobromic acid (Hbr) and 50 ml deionized water, with a few drops of bromine added to oxidize Tl to Tl^{3+}. After boiling the solution (with the cover on) to expel all the excess bromine, Tl was then quantitatively extracted into 10 ml of isopropyl ether. The aqueous residue was quantitatively recovered and diluted to 200 ml for the determination of Rb (solution E). This solution was further diluted 50 times for the analysis of K (solution A).

Sulphide and oxide samples were decomposed by nitric acid (HNO_3) or aqua regia mixture and then treated in the same way as for silicates.

For the solids resulting from the hydrothermal experiments, the volume of solution E was reduced to 50 ml which was diluted 20 times for solution A. The vapours did not require decomposition (i.e., the addition of HF and $HClO_4$ mixture); but were otherwise treated in the same way as the solids.

Standards for Rb and K were prepared from reagent-grade RbCl and KCl which contained approximately matching amounts of Al and

Fe as matrix. Some portion of the solution E, either after Rb determination or from previous batches were mixed and evaporated to reduce their volume by about one-fifth (40 ml per sample). This solution was then extracted twice with isopropyl ether to produce a Tl-free base solution to be used for the preparation of Tl standards as follows: Working Tl-standard solutions of different concentrations were prepared by introducing the appropriate amounts of a Tl-stock solution, (prepared from $TlNO_3$ or TlCl) and a few drops of bromine into 50 ml portions of the Tl-free base solution. This mixture was boiled and Tl extracted as for the samples.

All analysis was performed with a Perkin-Elmer 303 or 603 AAS unit. K and Rb were determined by the conventional flame-technique using an acetylene-air mixture as fuel. A Na-buffer, used to suppress ionization was introduced externally from a reservoir by means of a device shown in Fig. A-4-1.

Tl was determined by introducing and evaporating the ether solution into the Ta-boat attached to the AAS unit. When dry, the boat was pushed into the flame and the signal produced was recorded in a chart-recorder. Other details were described by Fratta (1974) and Korkisch (1970).

Fig. A-4-1. Device for introducing the external buffer into the aspiration chamber of the AAS unit. Dimension of the plastic block is approximately 2 x 1 x 0.6 cm^3.

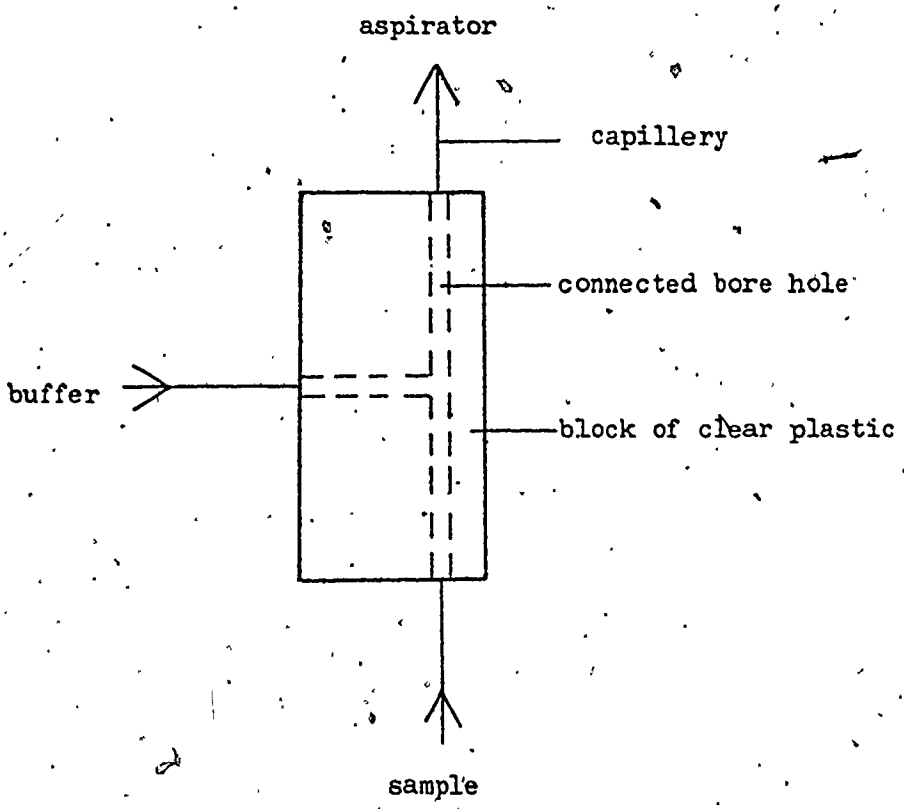
aspirator
capillery
connected bore hole
buffer
block of clear plastic
sample

Appendix 5. Evaluation of analytical uncertainties

The analytical accuracy and precision obtained in this study can be evaluated from the results of K, Rb and Tl determinations of some reference samples (Tables A-3 and A-4). Of these, ON-64 is a reference sample used only at McMaster University and S-118 is a sulfide-rich sample used in this study only. The others are international standards and the elemental values are quite well known, except for Tl.

Thus precision, expressed as coefficient of variation ($C=100\ s/\bar{x}$) for samples with three or more determinations, is about 10% for both K and Rb (Table A-3) and between 4% to 15% for Tl.

Generally speaking, the results obtained in this study agree reasonably well with the "usable values" of Abbey (1977) for K (Table A-4), but are biased towards higher values for Rb ranging from 12% for GSP-1 to 35% for G-2. Turning to Tl, reasonable agreement is observed for GSP-1, G-2 and also probably for AGV-1, if the high value of Flanagan (1973) is ignored. The Tl-value for W-1 from this study is more than two times higher than all the other reported results. However, only one determination was obtained for this study, and in light of the rather good agreement for the other samples, such a discrepancy may have little statistical significance.

One of the main problems encountered in the analysis of natural silicates is the compensation for the effect of the matrix (due

	K(%)	Rb(ppm)	Tl(ppm)
GSP-1	granodiorite		
			1.31
		306	1.42
			1.40
			1.31
	4.52	293	1.10
	4.13	280	0.91
	4.79	293	1.24
	4.18	300	1.50
	3.79	263	1.30
	3.86	244	1.10
	4.79	263	1.14
	3.97	267	1.24
$\bar{x}$	4 25	280	1.25
s	0.40	21	0.16
C%	9	7	13
G-2	granite		
		230	0.99
			0.96
W-1	diabase		
	0.51	22	0.25
GA			
			0.93

	K(%)	Rb(ppm)	Tl(ppm)
AGV-1	andersite		
	2.61	91	0.31
	2.45	92	0.30
	2.15	90	0.30
	2.19	77	0.31
$\bar{x}$	0.35	88	0.31
s	0.22	7.1	0.012
C%	9	8	4
ON-64	gabbro		
	1.00	44	0.15
	0.96	41	0.17
$\bar{x}$	1.98	43	0.16
BR	basalt		
	1.28	57	0.054
	1.24	55	0.046
S-118	sulphide-bearing schist		
	0.75	28	0.35
	0.79	25	0.42
	0.90	30	0.31
	0.93	33	0.30
	0.88	26	0.41
$\bar{x}$	0.85	28	0.36
s	0.076	3.2	0.055
C%	9	11	15

Table A-3. K, Rb and Tl abundances of some reference samples from this study.

	GSP-1	AGV-1	BR	G-2	W-1	ON-64	S-118
K(%)							
This work							
x	4.25	2.35	1.26		0.51	1.00	0.85
C%	9	9	--		--	--	9
n	8	4	2		1	2	5
Recommended*							
	4.59	2.43	1.17		0.53	1.00(M)	
Rb(ppm)							
This work							
x	280	88	56	230	22	42	28
C%	7	8	--	--	--	--	11
n	9	4	2	1	1	2	5
Recommended*							
	250	67	47	170	21	41(M)	
Tl(ppm)							
This work							
x	1.25	0.31	0.05	0.97	0.25	0.17	0.36
C%	13	4	--	--	--	--	15
n	12	4	2	1	1	1	5
Others #							
a.	1.3	1.0		1.0	0.11		
b.		0.28		1.05	0.11		
c.	1.5	0.56		1.10	0.11		
d.	0.7-1.6	0.3-1.6		0.9-1.3			
e.	1.15				0.13		

Table A-4. Summary of K, Rb and Tl for some reference rocks.

*M from Muysson (personal communication), all others from Abbey, 1977; # a. Flanagan (1973), b. Albuquerque et al. (1972), c. Sighinolfi (1973), d. Fleischer (1969), e. Fratta (1974); -- not determined.

chiefly to the major elements). Various matrix-correction techniques are used for different instruments and different operators. In this study, amounts of Al and Fe similar to those expected of the samples were added to the working standards for all three elements. In the case of K and Rb, the effect of the alkalis and alkali earths, which are not extracted by the ether under the specific conditions (Korkisch, 1970), were countered by saturating the flame in Na, by means of the Na-buffer.

However, the composition of the samples used in this study varied tremendously because both whole rock samples of different compositions and different minerals were analysed in the same batch. Also different amounts of the samples were used according to both the availability and the concentration (predicted) of Tl in the minerals. Hence it was very difficult to match the matrix of the standards, the samples and the reference materials.

Nevertheless, all the values obtained for GSP-1, for which the most data are available from this study, and whose composition (granodiorite) is similar to most of the samples used in this study, do not show serious conflict with the other reported values. Compositions of the experimental samples are much more uniform, and hence the accuracy would be better than that for the natural samples, probably better than ±5%.

The elemental detection limits depend on the amount of dilution. Thus for 1 g of a sample dissolved in 200 ml of water (solution E), the detection limit for Rb is 4 ppm. If solution A is 50 times diluted from E, the detection limit for K is 0.04%. Detection limit for Tl, extracted into 10 ml of ether is about 10 ppb.

Appendix 6 Analytical results on natural samples

Descriptions of the natural samples used for this study, are reported in Table A-6 and the analytical results for K, Rb and Tl are listed in Table A-7.

Suite	Catalogue number	Rock type	Locality	Reference/donor
a.	All(18)	various plutonics	Jackfish Lake area, N. Ontario	Longstaffe (1978)
b.	All(12)	" "	English River area, N. Ontario	Gower (1978)
c.	All(9)	various plutonic, pegmatite and metamorphic	Preissac-Lacorne area, Quebec	Siroonian (1957)
d.	All(5)	pelitic schist	Dell Twp. Sudbury, Ontario	Kwak (1968)
e.	All(8)	metamorphics	Loon Lake area, N. Ontario	Chiang (1965)
f.	All(6)	norites, breccia	drill cores at 2700' level, Strathcona Mine, Sudbury, Ontario	J. Crocket
g.	All(16)	granites, granodiorites	N. Portugal	Albuquerque (1971, 1974, 1975)
h.	HA-F1A	alkalic basalt	1801 Flow, off Hwy. 19, Kaupulehu, Hawaii	This author
	HA-F1B	" "	1801 Flow, off Hwy. 19, Puhia Pele, Hawaii Is.	" "
	HA-F2A	tholeiitic basalt	1950 Flow, off Hwy. 11, Hawaii Is.	" "
	HA-F2A	" "	1.5 mi. S. of HA-F2A	" "
	OAHU-F1A	nephelenite	Oahu Is., Hawaii	" "
	HA-10	alkalic basalt	Kahala Mt., Hawaii	J. Crocket
	720608-4	peridotite nodule	Montpezat Velay, France	D. M. Shaw
	700527-2N	herzolite nodule	Sauterrie Riom, France	" "
	PH-21, PH-10	holeiitic basalt	Pizon Is.	H. Beatis

Table A-5. Cont....2

	FH-41, FH-16 FH-47, FH-14	holeiitic basalt	Fernandina Is	H. Beatis
	AIY-1	basalt	Aiyansh, British Columbia	N. Church (Brown, 1969)
	Mar-A	andersite	Hwy. 3, 5 mi. west of Greenwood, B. C.	N. Church
	720606-3	basalt dyke	Freyssenet, Coiron, France	D. M. Shaw
	721104-4	gabbro	Hwy. 62, 9.6 S. of Bancroft	" "
i.	All(6)	meta-pelite	Littleton Formation, New Hamshire	" " (1954a, b; 1956)
j.	Ore	massive ore in schist	Thompson Mine, Manitoba	J. Crocket
	Bi Schist	biotite schist in ore	Thompson Mine, Manitoba	" "
	CC-A	sulphide ore	Copper Cliff Mine, Sudbury	" "
	CV-44	Precambrian schist	Homestake Mine, Lead, S. Dekota	J. D. Vine
	CV-455A	Schist	near Sheppard Hill, S. E. of Adelaide, Australia	" "
	CV-26C	pyrite concretion	Nugget, Lincoln County, Wyoming	" "
	V-368C	shale	8 mi. S. of Comfort, Kendall County, Texas	" "
	B-129-1	biotite schist in ore	Heath Steele Mine, New Brunswick	J. Crocket
	All BCA-series	Precambrian black shale	various parts of the Canadian Shield	Cameron and Jonasson (1972)
k.	MF 720707-9	diabase dyke	Metachewan, Ontario	M. Fratta
	721104-2	gabbro	near Bancroft, Ont.	D. M. Shaw
	70-147-2B	gabbro	Tudor Twp., Ontario	" "
	720608-5	sanidine trachyte	Ischia, Italy	" "

Table A-5. Cont. . . . 3

IM-10-64	gabbro	Iron Mountain	T. N. Irvine
IB-65-2A	pyroxenite	Polaris Complex, B. C.	" "
IB-65-127A	peridotite	" " "	" "
690422-1	granite	Glamorgan Twp., Ontario	Pacesova (1973)
690422-2	marble	Glamorgan Twp., Ontario	" "
690422-3	amphibolite	Glamorgan Twp., Ontario	" "

Table A-5. Description of samples used in this study.

Table A-6. K, Rb and Tl analyses of rocks and minerals from this study.

Abbreviations: BI biotite, MU muscovite, KF alkali feldspar, PL plagioclase, CPX clinopyroxene, OPX orthopyroxene, HB amphibole, WR rock, GM groundmass, PY pyrite, PO pyrrhotite, MT magnetite, GT garnet, SP spinel, SE sphene, AL aluminum silicate, AP apatite

---- not analysed, 0.0 not detected.

GKF groundmass alkali feldspar,

MKF megacryst alkali feldspar.

* K and Rb analyses by Albuquerque. Only GKF data were used in the discussions of Chapters 5 and 6.

a. Various plutonic rocks from Jackfish Lake

	K(%)	Rb(ppm)	Tl(ppm)
F-98 GNEISS			
BI	2.83	148.	1 22
KF	9.07	166.	.31
PL	1.47	20.	.18
WR	1.50	37.	.08
F-151 GNEISS			
BI	7.23	430.	2.97
KF	9.73	159.	.18
PL	.41	8.	.08
WR	1.07	38.	.60
F-110 GNEISS			
BI	7.78	680.	4.96
KF	10.81	339.	.84
PL	1.79	39.	.27
WR	3.08	114.	.34
F-73 GNEISS			
BI	6.87	505.	1.91
KF	8.73	198.	.82
WR	1.40	48.	.29
F-150 GNEISS			
BI	4.84	262.	1.59
KF	12.68	88.	.57
PL	.39	9.2	.12
WR	.75	34.	.25
F-149 GNEISS			
BI	6.78	368.	2.60
PL	.58	8.0	.13
MT	--	--	.10
WR	1.10	33.	.25
F-103 F.P. GNEISS			
BI	5.93	355.	1.43
WR	.95	34.	.32
F-10 F P. GNEISS			
BI	4.69	254.	1.38
WR	1.13	42.	.25
F-37 GRANODIORITE			
BI	9.54	258.	.22
KF	12.59	291.	.74
HB	.78	116.	.15
PL	.22	97.	.52
WR	2.86	99.	.30
F-118 GRANODIORITE			
BI	5.60	574.	3.52
KF	11.13	309.	.75
HB	.84	10.	.21
PL	1.18	24.	.24
WR	2.38	87.	.28

	K(%)	Rb(ppm)	Tl(ppm)
D-1 GRANODIORITE			
BI	5.76	434.	2.24
KF	11.82	187.	.42
HB	.76	12.	.21
WR	2.18	53.	.17
F-26 GRANODIORITE			
KF	11.69	318.	.85
HB	.82	27.	.36
WR	2.90	100.	.33
F-3 GRANODIORITE			
BI	4 95	396.	2.32
KF	9.93	222.	.51
HB	.65	0.0	.13
PL	1.70	26.	.20
WR	2.18	60.	.24
F-21 DIORITE			
BI	4.49	254.	2.02
HB	.60	16.	.19
PL	.53	6.9	.10
WR	.91	21.	.15
F-46 SYENITE			
KF	11.69	324.	.79
HB	.51	0.0	.21
PL	3.88	4.0	.14
MT	0.00	0.0	.04
WR	2.94	76	.27
F-135 MONZODIORITE			
BI	5.53	456.	3.22
KF	11.18	188.	.43
HB	.91	28.	.30
PL	1.10	16.	.14
WR	2.07	79.	.43
F-24 LEUCODIORITE			
HB	.59	0.	.09
PL	1.29	18.	.14
WR	1.10	15.	.11
F-146 DIORITE			
HB	.81	24.	.25
PL	.21	6.1	.09
WR	.79	29.	.20

b. Various plutonic rocks from English River Belt

	K(%)	Rb(ppm)	Tl(ppm)
145 GRANITE			
BI	4.78	575.	3.82
KF	11.84	374.	1.91
PL	.68	18.	.14
WR	4.34	139.	.89
350B GNEISS			
BI	6.78	516.	6.40
KF	10.15	244.	1.18
PL	1.39	21.	.10
WR	3.92	79.	.40
886 GNEISS			
BI	6.83	504.	3.99
KF	11.80	183.	.91
PL	1.07	15.	.12
WR	3.45	64.	.34
135 GRANODIORITE			
BI	7.37	666.	5.70
KF	12.98	263.	1.33
PL	.65	11.	.07
MT	.07	3.7	.02
WR	2.20	67.	.40
596A TONALITE			
BI	8.05	524.	3.35
KF	10.14	129.	.68
PL	.51	4.1	.07
MT	.01	5.3	.02
WR	1.33	50.	.38
835B LEUCO-TONALITE			
BI	7.61	706.	3.56
PL	.14	3.6	.01
WR	.58	46.	.26

	K(%)	Rb(ppm)	Tl(ppm)
715 TONALITE			
BI	6.97	415.	2.43
PL	.15	4.3	.04
MT	.03	1.0	.02
WR	.52	29.	.18
106B GNEISS			
BI	7.72	505.	3.97
PL	.15	0.0	.03
EP	.27	14.	.12
WR	.92	51.	.29
350A GNEISS			
BI	7.35	416.	2.28
HB	1.99	23.	1.75
PL	.12	3.4	.01
WR	.95	47.	.28
110A TONALITE			
BI	6.72	509.	4.30
KF	12.15	197.	.86
PL	.82	9.6	.11
GT	.10	0.0	.12
WR	4.09	69.	.34
835A AMPHIBOLITE			
HB	.15	4.0	.05
PL	.08	3.5	.01
WR	.12	4.6	.05
867A AMPHIBOLITE			
HB	.56	10.7	.061
PL	.11	2.7	.012
WR	.37	6.1	.044

c. Granite and pegmatite from Preissac-Lacorne Area Quebec

	K(%)	Rb(ppm)	Tl(ppm)
J-2 GRANITE			
MU	8.78	2458.	8.79
BI	6.82	2887.	19.9
WR	.76	634.	3.15
D228 BIO-MUS GRANITE			
BI	6.69	468.7	3.26
EP	.17	6.8	.50
D413 HB-MONZONITE			
HB	.78	22.5	.50
LA 3 AMPHIBOLITE			
HB	.49	34.	.45
BI	7.63	2157.	15.74
WR	.91	211.	1.56
J-281 GRANITE			
HB	.54	9.7.	.14
BI	6.19	629.	4.54
H-6 BIO-MUS GRANITE			
BI	10.20	2172.	14.300
KF	7.04	3932.	20.110
MU	8.32	1194.	46.590
L-11 PEGMATITE			
KF	12.05	5500.	41.2
MU	8.52	7121.	31.9
L-10 PEGMATITE			
KF	10.93	3682.	22.4
KF	11.39	2962.	17.3
MU	7.81	5747.	20.5
WR	.76	497.	2.2
N-8 GRANITE			
MU	9.43	1707.	6.24
BI	8.57	2965.	15.39
WR	2.67	519.	2.52

d. Pelitic schists from Grenville

	K(%)	Rb(ppm)	Tl(ppm)
T-290-1A SCHIST			
GT	0.00	1.2	.04
MU	--	75.	.78
BI	6.58	419.	3.15
WR	1.51	64.	1.35
T-156-1B SCHIST			
GT	0.00	8.0	.05
BI	--	475.	1.14
MU	--	255.	1.05
WR	--	168.	2.22
T-231-1A SCHIST			
GT	.51	18.	.02
MU	7.13	474.	.47
BI	6.37	692.	2.77
WR	--	--	.81
T-232-10 SCHIST			
MU	5.35	276.	1.42
BI	4.00	456.	4.44
GT	0.00	13.	.03
WR	2.65	124.	1.39
T-292-1 SCHIST			
BI	6.21	560.	3.53
GT	0.00	10.	.05
WR	3.43	200.	1.24

e. Amphibolites from Loon Lake

	K(%)	Rb(ppm)	Tl(ppm)
703 AMPHIBOLITE			
HB	1.64	0.0	.08
BI	7.94	236.	1.53
KF	12.05	142.	.32
WR	3.29	117.	.62
704 AMPHIBOLITE			
HB	1.37	0.0	.08
BI	7.60	189.	1.42
WR	1.96	60.	.46
724 AMPHIBOLITE			
HB	1.08	11.	.05
BI	7.64	207.	1.58
744 AMPHIBOLITE			
HB	1.10	15.	.26
BI	7.32	408.	3.92
753 AMPHIBOLITE			
HB	.91	9.3	.06
BI	7.39	224.	1.35
756 AMPHIBOLITE			
HB	1.17	11.	.09
BI	7.55	305.	2.66
761 AMPHIBOLITE			
HB	1.22	16.	.14
BI	9.11	314.	2.51
788 AMPHIBOLITE			
HB	--	12.	.13
BI	8.16	651.	6.35

f. Irruptives, Strathcona Mine

	K(%)	Rb(ppm)	Tl(ppm)
SUD 27-1	FELSIC NORITE		
KF	5.73	173.	.63
OPX	.16	5.8	.09
PO	--	--	.24
BI	5.93	426.	2.66
WR	.92	36.	.36
SUD 27-2	NORITE		
OPX	.15	17.	.09
BI	6.07	438.	3.03
PL	.98	14.	.04
WR	1.15	40.	.34
SUD 27-3	NORITE		
PL	.48	7.3	.03
OPX	.07	5.5	.04
BI	7.85	413.	2.25
PO	--	--	.11
WR	.61	22.	.24
SUD 27-5	NORITE		
BI	5.43	321.	2.41
OPX	.12	11.	.06
PL	.43	6.7	.04
PO	--	--	.19
WR	1.10	39.	.26
SUD 27-7	BRECCIA		
MT	--	--	.22
WR	1.02	32.6	.11
SUD 27-8	NORITE		
MT	--	--	.41
PL	1.02	24.	.09
WR	.50	35.	.19

g. Granites and granodiorites from N. Portugal*

	(K%)	Rb(ppm)	Tl(ppm)
A51 GRANODIORITE			
BI	7.94	345.	--
KF	11.96	145.	--
A55 GRANODIORITE			
BI	7.73	400.	--
KF	11.66	145.	--
A79 GRANODIORITE			
BI	7.98	550.	--
KF	11.30	210.	7.34
WR	3.17	185.	2.07
A46 MUS-B			
BI	7.59	800.	--
KF	12.25	320.	6.60
WR	3.29	220.	2.03
A156 GRANODIORITE			
BI	7.93	1160.	--
KF	9.99	430.	4.08
WR	3.84	315.	1.89
A17 GRANODIORITE			
BI	7.65	1225.	--
KF	11.43	580.	3.66
WR	3.71	290.	1.77
A81 GRANODIORITE			
BI	8.02	1320.	--
KF	12.62	700.	4.40
A328 GRANODIORITE			
BI	7.95	950.	--
KF	11.52	400.	3.71
WR	3.42	280.	2.31

	K(%)	Rb(ppm)	Tl(ppm)
A202 GRANODIORITE			
KF	9.13	290.	6.73
WR	3.55	240.	3.49
A190 GRANODIORITE			
GKF	9.98	525.	10.8
MKF	9.83	515.	4.42
WR	4.19	275.	2.30
A280 GRANITE			
GKF	10.19	585.	8.96
MKF	8.93	485.	5.05
WR	4.19	280.	3.11
A293 GRANITE			
GKF	9.30	600.	3.98
MKF	9.51	550.	3.26
WR	4.10	360.	2.55
A509 GRANITE			
GKF	10.50	735.	5.41
MKF	10.33	625.	4.23
WR	4.25	375.	2.73
A546 GRANITE			
KF	--	550.	11.51
WR	--	320.	2.66
A109 GRANITE			
KF	--	830.	4.36
WR	--	275.	2.39
A72 VEIN GRANITE			
KF	9.31	660.	11.51
WR	--	245.	1.78

h. Basalt and related rocks from various areas

	K(%)	Rb(ppm)	Tl(ppm)
HA-F1A ALKALIC BASALT			
OL	.04	0.0	.04
HA-F1B ALKALIC BASALT			
OL	.05	1.0	.03
MT	--	--	.23
WR	.61	24.	.18
HA-F2A BASALT			
OL	.02	0.0	.03
MT	--	--	.02
WR	.29	0.0	.01
HA-F2B BASALT			
OL	.02	0.0	.11
WR	.29	0.0	.06
OAHU-F1 ALKALIC BASALT			
OL	.03	0.0	.03
WR	1.02	0.0	.02
HA-10 ALKALIC BASALT			
PL	.12	0.0	.01
CPX	0.0	0.0	.01
GM	.56	7.3	.03
720678-4 BASALT			
CPX	0.0	0.0	0.003
OPX	0.0	0.0	0.004
WR	.05	2.3	.006
SP	--	--	.040
OL	0.0	0.0	0.004
700527-2N PERIDOTITE			
CPX	.23	7.4	.008
OPX	.67	36.4	.060
OL	0.0	0.0	0.004
SP	.22	2.5	0.000

	K(%)	Rb(ppm)	Tl(ppm)
PH-21 THOLEIITE			
PL	.41	0.0	.022
CPX	.10	0.0	.036
MT	--	--	.034
WR	.78	0.0	.029
FH-41 THOLEIITE			
PL	.07	0.0	.012
WR	.37	0.0	.032
PH-10 BASALT			
PL	.14	0.0	.035
MT	--	--	.052
CPX	.03	0.0	.014
WR	.81	0.0	.050
FH-16 BASALT			
PL	.12	0.0	.006
WR	.35	0.0	.17
FH-47 BASALT			
PL	.06	0.0	.077
CPX	.07	0.0	.014
MT	0.0	0.0	.058
WR	.26	0.0	.20
FH-14 BASALT			
CPX	.03	1.2	.007
PL	.09	4.0	.009
WR	.38	14.0	.027
AIY-1 BASALT			
MT	--	--	.09
PL	.67	0.0	.056
WR	1.39	0.0	.067
MAR-A ANDERSITE			
PL	.73	28.	.11
CPX	.06	3.0	.013
WR	2.98	103.	.313
720606-3 BASALT			
HB	.55	38.	.027
CPX	.24	27.	.027
MT	--	--	.099
WR	1.79	91.	.071
721104-4 GABBRO			
MT	--	--	.025
PY	--	--	.081
AP	.04	10.	.067
PL	.52	15.	.049
CPX	.54	19.	.034
PX	.56	17.	.018
BI	6.74	241.	.62
WR	.37	0.	.025

i. Meta-pelite, Littleton Formation

	K(%)	Rb(ppm)	Tl(ppm)
L-36 GNEISS			
BI	5.34	198.	1.15
MU	6.73	226.	.84
L-41 GNEISS			
MU	6.26	614.	5.63
CL	.49	33.	.37
L-62 SCHIST			
MU	6.36	146.	1.11
BI	2.98	269.	1.80
L-66 SCHIST			
BI	1.67	151.	.98
MU	5.55	287.	1.28
L-49 SCHIST			
MU	5.32	123.	.53
BI	4.24	471.	3.65
AL	0.00	.83	.03
L-54B SCHIST			
MU	3.92	118.	.56
AL	.29	28.5	.20

j. Sedimentary and low-grad metamorphic rocks from various areas

	K(%)	Rb(ppm)	Tl(ppm)
MASSIVE ORE			
PO	--	--	.11
PY	0.0	0.0	.26
BI SCHIST			
PO	--	--	.18
BI	5.35	267.	3.24
WR	.74	32.	1.18
CC-A SULPHIDE ORE			
BI	7.01	346.	2.41
PL	.51	12.	.04
HB	.37	5.5	.04
PO	0.0	0.	.16
WR	1.61	71.	.60
KL-BA SCHIST			
PY	--	--	.06
MT	--	--	.06
PO	--	--	.95
KF	4.64	157.	.57
OT	0.0	85.	.41
WR	.88	45.	.25
CV-44 SCHIST			
PO	--	--	.05
OT	.17	13.1	.08
WR	.08	0.0	.06
CV-455A SCHIST			
PY	--	--	.12
PO	--	--	1.01
MU	7.83	480.	11.14
WR	1.5	0.0	.24
CV-26C PYRITE CONCRETION			
PY	--	--	.34
WR	0.0	39.	.23
V-368C SHALE			
PY	--	--	1.25
WR	1.82	81.	4.14
B-129-1 SCHIST			
PY	--	--	6.59
OT	.05	0.0	1.01
WR	.05	12.	2.57

	K(%)	Rb(ppm)	Tl(ppm)
BCA 022001 SHALE			
WR	0.0	12.	.066
BCA-020001 SHALE			
WR	3.92	165.	.98
BCA-037002			
PO	--	--	.56
WR	1.12	55.	1.72
BCA 038001 SHALE			
PO	--	--	.19
WR	5.56	141.	1.17
BCA 0600001 SHALE			
PY	--	--	2.18
WR	5.03	135.	1.36
BCA 650001 SHALE			
PO	--	--	1.50
PY	--	--	.10
WR	1.3	66.	.70
BCA 069001 SHALE			
PO	0.0	0.0	.60
WR	2.14	109.	2.43
BCA 150001 SHALE			
PO	--	--	.63
WR	0.0	0.0	.68
BCA 169001-8 SHALE			
PY	--	--	2.31
WR	1.38	58.	.81
BCA 171008 SHALE			
PY	--	--	.08
WR	0.0	0.0	.33
BCA 176003 SHALE			
WR	3.69	157.	3.02
BCA 180006 SHALE			
PY	--	--	2.11
WR	1.00	37.	2.00

k. Miscellaneous

	K(%)	Rb(ppm)	Tl(ppm)
MF 720707-9 DIABASE DYKE			
CPX	.39	15.	.13
MT	--	--	.23
WR	1.06	25.	.32
DMS 721104-2 GABBRO			
PL	.44	7.6	.09
PY	--	--	.04
PX	.60	17	.13
BI	8.23	221.	2.82
70-147-2B GABBRO			
HB	1.04	15.	26
WR	1.53	20.	.87
PO	--	--	1.81
	5.87	101.	.35
720608-5 SANIDINE TRACHYTE			
KF	4.66	144.	.59
CPX	.70	52.	.10
WR	3.59	227.	.34
IM-10-64 GABBRO			
PL	.08	3.0	.01
CPX	.04	.7	.02
MT	--	--	.03
WR	.10	5.2	.04
IB-65-2A			
PX	0.00	0.00	.01
MT	--	--	.02
IB-65-127A			
HB	--	--	.07
BI	--	--	.75
690422-1 GRANITE			
KF	11.07	772.	1.07
PL	.42	21.	.16
MT	0.00	1.3	.03
MU	7.35	811.	2.37
BI	6.17	1439.	9.37
WR	3.84	235.	.98
690422-2 MARBLE			
CT	.01	1.0	.01
SE	--	--	.01
PX.	.01	1.8	.01
690422-3 AMPHIBOLITE			
HB	1.09	18.	.21
KF	8.96	223.	.56
PL	.33	5.4	.03
SP	.02	2.5	.01
WR	.93	33.	.58
BI	6.76	1047.	4.85
AP	.02	2.1	.16

REFERENCES

Abbey, S. (1977), Studies in "Standard Samples" of Silicate rocks and minerals. Part 5, 1977 Edition of "Usable" values . Geol. Surv. Can. Paper 77-34.

Ahrens, L.H (1952), The use of Ionic Potential. Part I. Ionic Radii of Elements. Geochim. Cosmochim. Acta, 2:155-169.

_____ (1945), The Geochemical Relationship between Tl and Rb in Minerals of Igneous Origin. Trans. Geol. Soc. S. Africa, 48:207-231.

_____ (1948), The Unique Association of Tl and Rb in Minerals. J. Geol., 56:578-590.

De Albuquerque, C.A.R. (1973), The Origin of Enclaves in Granitic Rocks from Northern Portugal. Geol. Soc. S. Afr. Spec. Publ. 3P:479-493.

_____ (1974), Geochemistry of Biotites from Granitic Rocks, Northern Portugal. Geochim. Cosmochim. Acta, 37:1779-1802.

_____ (1975), Partition of Trace Elements in Coexisting Biotite Muscovite and Potassium Feldspar of Granitic Rocks, Northern Portugal. Chem. Geol., 16:89-108.

De Albuquerque, C.A.R., Muysson, J.R. and Shaw, D.M. (1971), Tl in Basalts and Related Rocks. Chem. Geol., 10:41-58.

_____ and Shaw, D.M. (1972), Thallium in Handbook of Geochemistry, Vol. II/3 81. Ed. K.H. Wedepohl.

Arth, J.G. (1976), Behaviour of Trace Elements during Magmatic Process: A summary of theoretical models and their application. J. Res. U.S.Geol. Surv., 4:41-48.

_____ and Hanson, G.N. (1972), Quartz Diorite Derived by Partial Melting of Eclogite or Amphibolites at Mantle Depths. Contr. Mineral. Petrol., 37:161-174.

_____ and _____ (1975), Geochemistry and Origin of the Precambrian Crust of the Crust of Northeastern Minnesota. Geochim. Cosmochim. Acta, 39:325-362.

Banno, S. and Matsui, Y. (1973), On the Formulation of Partition Coefficient for Trace Element Distribution between Minerals and Magma. Chem. Geol., 11:1-16.

Barbieri, M., Formaseri, M. and Penta, A. (1968), Rubidium and Potassium Relationship in Some Volcanoes of Central Italy. Chem. Geol., 3:189-197.

Berlin, R. and Henderson, C.B.M. (1968), A Reinterpretation of Sr and Ca fractionation trends in Plagioclase from Basic Rocks. Earth Planet. Sci. Lett. 36:79-83.

Bernotat, W.H., Carron, J.P., Lagache, M. (1976), K-Rb and Rb-Cs Partition between K-Feldspars and Biotites of Precambrian Granites from Sinai, with a Discussion of K/Rb Partition Coefficients. Tscher. Min. Petr., 23:23-28.

Beswick, A.E. (1973), An Experimental Study of Alkali Metal Distribution in Feldspars and Micas. Geochim. Cosmochim. Acta, 37:183-208.

Blattner, P. and Bird, G.W. (1974), Oxygen Isotope Fractionation between Quartz and K-Feldspar at 600° C. Earth Planet. Sci. Lett. 23:21-27.

Borovik-Romanova, T.F. and Sosedko, A.F. (1960), Tl-Rb Ratio in Minerals from the Kola Peninsula Pegmatites according to the data of Spectrographic Analysis. Geochem. Internat. 1:34-42.

Bowen, N.L. (1913), The Melting Phenomena of Plagioclase Feldspars. Am. J. Sci., Ser. 4, 35:577-599.

Brown, A.S. (1969), Aiyansh Lava Flow, British Columbia. Can. J. Earth Sci., 6:1460-68.

Butler, J.R., Bowden, P. and Smith, A.Z. (1962), K/Rb ratios in the Evolution of the Younger Granites of Northern Nigeria. Geochim. Cosmochim. Acta, 26:89-100.

Cameron, E. M. and Jonasson, I. R. (1972), Mercury in Precambrian Shales of the Canadian Shield. Geochim. Cosmochim. Acta, 36:985-1005.

Carron, J. and Lagache, M. (1969), Géochemie du Potassium et du Rubidium dan les Granodiorites à Biotite et Amphibole du Sud-est de la Corse. C.R. Acad. Sc. Paris, Série D, t. 269, 2076-2079.

_____ and _____ (1971), La Distribution des Elements Alcalins Li, Na, K, Rb dans les Minéraux Essentiels des Granites et Granodiorites du Sud de la Corse. Bull. Soc. Fr. Minéral. Cristallogr., 94:70-80.

Chelishchev, N. F. (1967), Laboratory Studies in the Distribution of Rare Alkalies between Potassium Minerals and Aqueous Solutions at High Temperatures and Pressures. Doklady Acad. Sci. U.S.S.R. Earth Sci. Sect. 175:205-207.

Chiang, M. C. (1965), Element Partition between Hornblende and Biotite in the Rocks from Loon Lake Aureole, Chandos Township, Ont. Unpub. M.Sc. Thesis, McMaster University.

Condie, K. C. (1976), Trace Element Models for the Origin of Archean Volcanic Rocks in The Early History of the Earth, Ed. B. F. Windley, Wiley and Sons Ltd., 419-424.

Czmansky, G.K. and Moore, J.G. (1977), Composition and Phase Chemistry of Sulfide Globules in Basalts from the Mid-Atlantic Ridge Rift Valley near 37° N. Lat. Geol. Soc. Amer. Bull. 88, 587-599.

Demin, A.M. and Khitarov, D.N. (1958), Geochemistry of Potassium, Rubidium and Thallium in Application to Problems in Petrology. Geochemistry, 6:721-734.

Drake, M.J. and Weill, D.F. (1975), Partition of Sr, Ba, Ca, Y, Eu^{2-}, Eu^{3+} and Other Rare Earth Elements between Plagioclase Feldspar and Magmatic Liquid: An Experimental Study. Geochim. Cosmochim. Acta, 39:689-712.

Dudas, M.J., Schmitt, R.A. and Harward, M.E. (1971), Trace Element Partitioning between Volcanic Plagioclase and Dacitic Pyroclatic Matrix. Earth Planet. Sci. Lett. 11:440-446.

Dupuy, C. and Allegre, C.J. (1972), Fractionnement K/Rb dans les Suites Ignimbritique dis Toscane une example de Rejuvenation Crustale. Geochim. Cosmochim. Acta., 36:437-458.

_____, Fratta, M. and Shaw, D.M. (1973), Partition Coefficient of Tl compared with Rb. Earth Planet. Sci. Lett. 19:209-212.

Eugster, H. (1955), The Cesium-Potassium Equilibrium in the System Sanidine-Water. Ann. Rpt. Geophys. Lab. Carnegie Inst., Washington, 54:112-113.

Ewers, G.R. and Keays, R.R. (1977), Volatile and Precious Metals Zoning in Broadlands Geothermal Field, New Zealand. Econ. Geol. 72:1337-

Flanagan, F.J. (1973), 1972 Values for International Geochemical Reference Samples. Geochim. Cosmochim. Acta, 37: 1189-1200.

Foland, K.A. (1973), Alkali Diffusion in Orthoclase. Proc. Symp. Geoch Transport Kinetics, Washington.

Fratta, M. (1974), AAS Determination of PPB amounts of Thallium in Silicate Rocks. Can. J. Spect. 19:33-37.

Fung, P.C. and Shaw, D.M. (1978), Na, Rb and Tl Distributions between Phlogopite and Sanidine by Direct Synthesis in a Common Vapour Phase. Geochim. Cosmochim. Acta, 42: 703-708.

Gast, P.W. (1968) Trace Element Fractionation and the Origin of Tholeiitic and Alkaline Magma Type. Geochim. Cosmochim. Acta, 32:1057-1086.

Gill, J.B. and Murthy, R.V. (1970), Distribution of K, Rb, Sr and Ba in Nain Anorthosite Plagioclase. Geochim. Cosmochim. Acta, 34:401-408.

Gower, C.F. (in prep. 1978), The Tectonic and Petrogenetic History of the Kenora Area, English River Subprovince. Unpubl. Ph.D. Thesis, McMaster Univ.

Greenland, L.P. and Campbell, E.Y. (1977) Variation of Se, Te, In, Tl and Zn with Differentiation of Tholeiitic Magma. Neus. Jahr. Min. Mit. H. 3, 112-118.

Griffin, W.L., Murthy, V.R. and Phinney, W.C. (1968), K/Rb in Amphiboles and Amphibolites from Northeast Minnesota. Earth Planet. Sci. Lett., 3:367-370.

_____ and Murthy, V.R. (1969), Distribution of K, Rb, Sr and Ba in Some Minerals Relevant to Basalt Genesis. Geochim. Cosmochim. Acta, 33:1389-1414.

Grossman, L. and Larimer, J.W. (1974), Early Chemical History of the Solar System. Rev. Geophys. 12:71-101.

Hakli, T.A. and Wright, T.L. (1967), The Fractionation of Nickel between Olivine and Augite as a Geothermometer. Geochim. Cosmochim. Acta, 31:877-884.

Hart, S.R. (1969), K, Rb, Cs, and K/Rb, K/Cs Ratios of Fresh and Altered Submarine Basalts. Earth Planet. Sci. Lett. 6: 295-303.

_____ and Aldrich, L.T. (1967), Fractionation of K/Rb by Amphiboles: Implications regarding Mantle Composition. Science 155:325-327.

_____ and Nalwalk, A.J. (1970), K, Rb, Cs and Sr Relationships in Sub-Marine Basalts from the Puerto Rico Trench. Geochim. Cosmochim. Acta, 34:145-155.

Hart, S.R. and Brooks, C. (1974), Clinopyroxene-Matrix Partitioning of K, Rb, Cs and Ba. Geochim. Cosmochim. Acta, 38: 1797-1806.

Heier, K.S. and Taylor, S.R. (1959), Distribution of Li, Na, K, Rb, Cs, Pb and Tl in Southern Norwegian Precambrian Alkali Feldspars. Geochim. Cosmochim. Acta, 15: 284-3-4.

_____ and Adam, S. (1964), Geochemistry of Alkali Metals. Phys. Chem. Earth (2), L.H. Ahren, Ed.

Hofmann, A.W. and Giletti, B. (1970), Diffusion of Geochronologically Important Nuclides in Minerals under Hydrothermal Conditions. Eclogae Geol. Hel., 63:141-150.

Hopson, C.A. and Eugster, H. (1955), The Tl-K Equilibrium in the System Sanidine-Water. Ann. Rpt. Geophys. Lab. Carnegie Inst. Washington, 54:113-114.

Iiyama, J.T. (1968), Experimental Study of the Distribution of Trace Elements between Two Feldspars. 1. Distribution of Rb, Cs, Sr and Ba at 600°C. Geochem. Int., 5:433-452.

_____ (1972), Behaviour of Trace Elements in Feldspar under Hydro-Thermal Conditions, in Feldspars, Ed. MacKenzie, W.S. and Zussman, J. Manchester Univ. Press, 717 p.

Iiyama, J. T. (1974), Substitution, Deformation Locale de la Maille et Equilibre de Distribution des Elements en Traces entre Silicates et Solution Hydrothermale. Bull. Soc. Fr. Mineral. Cristallogr., 97:143-151.

_____ and Volfinger, M. (1976), A Model for Trace Element Distribution in Silicate Structures. Mineral. Magazine, 40:555-564.

Ivanov, V. V., Volgin, V. Yu., Krasnov, A. A. and Lizunov, N. V. (1968), Thallium. Translated from Talliy, in Internat. Geol. Review (1969), 11:97.

Kajiwara, Y., Krouse, H. R. and Sakai, A. (1969), Experimental Study of Sulfur Isotope Fractionation between Co-existing Sulfide Minerals. Earth Planet. Sci. Lett. M, 271-277.

Kogarko, L. N. (1959), Distribution of Alkali Metals and Tl in the Granitoids of the Turgoyak Pluton. Geochem. Internat. 5:557.

Korkisch, J. (1969), Modern Methods for the Separation of Rare Metal Ions. Pergamon Press, 311-350.

Korringa, M. K. and Noble, D. C. (1971), Distribution of Sr and Ba between Natural Feldspar and Igneous Melt. Earth Planet. Sci. Lett. 11:147-151.

Kwak, T. A. P. (1968), Metamorphic Petrology and Geochemistry of the Grenville Province-Southern Province Boundary, Dell Township, Sudbury, Ontario. Unpublished Ph. D. Thesis, McMaster University.

Lagache, M. (1968), Etude Experimentale de la Repartition des Elements - Trace Entre la Leucite L'Orthose et des Solutions Hydrothermales. Le Rb a 600°C. Compt. Rendus, 267:141-144.

_____ (1971), Etude Experimentale de la Repartition du Césium entre Les Feldspaths Sodi Potassiques et des Solutions Hydrothermales a 700°C 1000 Bars. C.R. Acad. Sci. Paris, 272:1328-1330.

_____ and Sabatier, G. (1973), Distribution des Elements Na, K, Rb, Cs a L'Etat de Trace et Entre Feldspaths Alcalins et Solutions Hydrothermales a 650°C 1 Kbar - Donnees Experimentale et Interpretation Thermodynamics. Geochim. Cosmochim. Acta, 37:2617-2640.

Lange, I.M., Reynolds, R.C. and Lyons, J.B. (1966), K/Rb Ratios in Coexisting K-Feldspar and Biotites from Some New England Granites and Metasediments. Chem. Geol. 2:89-104.

Larimer, J.W. (1967), Chemical Fractionation in Meteorites. I. Condensation of the Elements. Geochim. Cosmochim. Acta, 31:1215-1238.

Laughlin, A.W. (1973), K, Rb and Sr Abundances in Minerals of the Rutherford and Morefield Pegmatites, Amelia, Virginia. Earth Planet. Sci. Lett. 17:375-379.

Lin, T.H. and Yund, R.A. (1972), Potassium and Sodium Self Diffusion in Alkali Feldspar. Contrib. Mineral. Petrol. 34:177-184.

Lobach-Zhuchenko, S.B. and Vasilyeva, S.N. (1970), Two Trends in the Behaviour of Rubidium in the Formation of Leucocratic Granites. Geochem. Int. 12:1477-1482.

Longstaffe, F.J. (1977), The Oxygen Isotope and Elemental Geochemistry of Archean Rocks from Northern Ontario. Unpubl. Ph.D. Thesis, McMaster Univ.

MacLean, W.H. (1977), Sulfides in Leg 37 Drill Core from the Mid-Atlantic Ridge, Can. J. Earth Sci. 14:674-683.

Mathez, E.A. (1976), Sulfur Solubility and Magmatic Sulfides in Submarine Basalt Glass. J. Geophys. Res. 81:4269-4275.

_____ and Yeats, R.S. (1976), Magnetic Sulfides in Basalt Glass from DSDD Hole 319A and Site 320, Nazca Plate in Yeats, R.S. et al. Initial Report of the Deep Sea Drilling Project 34:363-373.

McGoldrick, P.J., Heays, R.R. and Scott, R.B. (in print 1978), Thallium, a Sensitivity Indicator of Rock/Sea Water Interaction and of Sulfur Saturation of Silicate Melts.

McIntire, W.L. (1963), Trace Element Partition Co-Efficients, A Review of Theory and Application to Geology. Geochim. Cosmochim. Acta, 27:1209-1264.

Meituv, G.M. (1962) Geochemistry of Rare Elements in the Lead-Zinc Deposits of the Klichkinskii Region (Eastern Transbaikaliya). Geochemistry, 7:694-706.

Moore, J.G. and Fabbi, B.P. (1971), An Estimate of the Juvenile Sulfur Content of Basalts. Contrib. Mineral. Petrol. 33:118-127.

Morey, G.W. and Hesselgesser, J.M. (1951), The Solubility of Some Minerals in Superheated Steam at High Pressures. Econ. Geol. 46:821-835.

_____ and Chen, W.T. (1955), The Action of Hot Water on Some Feldspars. Amer. Mineralogists, 40:996-1000.

Murthy, V.R. and Griffin, W.L. (1970), K/Rb Fractionation by Plagioclase Feldspars. Chem. Geol. 6:265-271.

Mysen, B. and Seitz, M.G. (1974), Trace Element Partitioning Determined by Beta Track Mapping - An Experimental Study using Carbon and Samarium as Examples. J. Geophys. Res. 80:2627-2635.

Nickel, E.H. (1961), The Mineralogy of the Bernic Lake Pegmatite Southeastern Manitoba. Dept. of Mines and Techn. Surv. Ottawa Mines Branch Tech. Bull. TB 20, 1-38.

Nockolds, S.R. (1965), The Behaviour of Some Elements during Fractional Crystallization of Magma. Geochim. Cosmochim. Acta, 30:267-278.

Orville, P.M (1963), Alkali Ion Exchange Between Vapor and Feldspar Phases. Am. J. Sci., 261:201-237.

Pacesova, M. (1973), K-Rb-Tl Relationship in Some Gneissic Rocks. Unpub. M.Sc. Thesis, McMaster Univ.

Philpotts, J.A., Schnetzler, C.C. and Hart, S.R. (1969), Submarine Basalts: Some K, Rb, Sr, Ba, Rare-Earth, H_2O and Carbon Dioxide Data Bearing on Their Alteration. Modification by Plagioclase and Possible Source Materials. Earth Planet. Sci. Lett., 7:293-299.

_____ and Schnetzler, C.C. (1970), Speculations on the Genesis of Alkaline and Subalkaline Basalts following Exodus of the Continental Crust. The Canadian Mineralogist, 10:375-380.

Rhodes, J.M. (1969), On the Chemistry of Potassium Feldspars in Granitic Rocks. Chem. Geol. 4:373-392.

Ringwood, A.E. (1955), The Principles governing Trace Element Distribution during Magmatic Crystallization. Part I. The Influence of Electronegativity. Geochim. Cosmochim. Acta, 7:189-202.

Roux, J. (1971), Etude Experimentale sur la Distribution des Elements Alcalins Cs, Rb et K Entre L'Albite, la Nephelene et les Solutions Hydrothermale. These de 3eme Cycle, Univ. Paris-Sud.

Roux, J., Volfinger, M., Lagache, M., Iiyama, J.T., Sabatier, G. and Wyart, J. (1971), Ideal Solid Sojution Formation by Substitution of Alkali and Alkali Earth Elements in Silicates. Miner. Soc. Jap. Spec. Pap. 1:214-221. Proc. IMA-IAGOD Meetings, 70, IMA Vol.

Sen, N., Nockolds, S.R. and Allen, R. (1959), Trace Elements in Minerals from Rocks of the Southern California Batholith. Geochim. Cosmochim. Acta, 16:58-78.

Shaw, D.M. (1952), Geochemistry of Thallium. Geochim. Cosmochim. Acta, 2:118-154.

_____ (1957), The Geochemistry of Gallium, Indium and Thallium: A Review. Phys. Chem. Earth, 2:164-205.

_____ (1968), A Review of K-Rb Fractionation Trends by Covariance Analysis. Geochim. Cosmochim. Acta, 32:573-601.

_____ (1954a), Trace Elements in Pelitic Rocks. Part 1. Variation during Metamorphism Bull. Geol. Soc. Amer. 65:1151-1166.

_____ (1954b), Trace Elements in Pelitic Rocks. Part 2. Geochemical Relations. Bull. Geol. Soc. Amer. 65:1167-1182.

_____ (1956), Trace Elements in Pelitic Rocks. Part 3. Major Elements and General Geochemistry. Bull. Geol. Soc. Amer. 67: 919-934.

_____ (1970), Trace Element Fractionation during Anatexis. Geochim. Cosmochim. Acta, 34:237-242.

Shaw, D.M. (1972), Development of the Early Continental Crust. Part 1. Use of Trace Element Distribution Co-Efficient Models for the ProtoArchean Crust. Can. J. Earth Sci. 9:1577-1595.

_____ (1977), Trace Element Behaviour during Anatexis. Proc. Chapman Conf., Partial Melting in the Earth's Upper Mantle, Oregon (1976).

_____ (1978), Trace Element Behaviour during Anatexis in the Presence of a Fluid Phase. Geochim. Cosmochim. Acta, 42:933-943.

_____, Schwarcz, H.P. and Sheppard, S.M.F. (1965), The Petrology of Two Zoned Scapolite Skarns. Can. J. Earth Sci. 2:577-595.

_____, Dupuy, C., Fratta, M. and Helsen, J. (1974), An Application of Factor Analysis to Basic Volcanic Rock Geochemistry. Bull. Volc. Tome XXXVIII-4, 1070-1089.

Shimazaki, H. and Clark, L.A. (1973), Liquidus Relations in the FeS-FeO-SiO_2-Na_2O System and Geologic Interpretations. Econ. Geol. 68:79-96.

Shimizu, N. (1974), An Experimental Study of the Partitioning of K, Rb, Cs, Sr, and Ba between Clinopyroxene and Liquid at High Pressures. Geochim. Cosmochim. Acta, 38:1789-1796.

Sighinolfi, G.P. (1973), Determination of Thallium in Geochemical Reference Samples by Flameless Atomic Absorption Spectroscopy. Atomic Absorption Newsletter, 12:136-138.

_____ and Santos, A.M. (1974), Tl in Deep-Seated Crustal Rocks. Geochim. Cosmochim. Acta, 38:641-646.

Sippel, R.F. (1963), Sodium Self Diffusion in Natural Minerals. Geochim. Cosmochim. Acta, 27:107-120.

Siroonian, H.A. (1957), A Geochemical Study of Lithium Distribution in the Granitic Rocks of the Preissac-Lacorne Area, Quebec. M.Sc. Thesis (Unpubl.), McMaster Univ.

Smith, R.N., Ewers, G. and Keays, R.R. (1974), Volatile Metal Haloes as a Guide to Base Metal Deposits. Abs. Geol. Soc: Australia Joint Specialist GP. Mtg., 64-67.

Solodov, N.A. (1959), Certain Regularities of Distribution of Rare Elements in Sharply-Zoned Granite Pegamtites. Geokhimiya 4:388-405.

Sretenskaya, N.G. (1967), Eksperimental, Noye Issledovaniye Oblasti Mineralogii i Geokhimii Redkikh Elementov (Experimental Studies in Rarer Element, Mineralogy and Geochemistry), Nauka, Moscow.

Tauson, L.V. and Buzaev, N.N. (1957), Tl in Minerals of the Central Susamyr Batholith. Geochem. Internat., 7:703.

Taylor, S.R. (1965), The Application of Trace Element Data to Problems in Petrology, Phys. Chem. Earth, 6:133-214.

_____ and Heier, K.S. (1960), The Petrological Significance of Trace Element Variations in Alkali Feldspars. Proc. XXI, Int. Geol. Congr. (Norden), XIV, 47-61.

_____, _____ and Sverdrup, T. (1960), Trace Element Variations in Three Generations of Feldspars from the Landsverki Pegmatite, Evje, Southern Norway. Norsk. Geol. Tidsskr. 40:133-156.

Turekian, K.K. and Wedepohl, K.H. (1961), Distribution of the Elements in some Major Units of the Earth's Crust. Bull. Geol. Soc. Amer., 72:175.

Tuttle, O.F. (1949), Two Pressure Vessels for Silicate-Water Studies. Geol. Soc. Amer. Bull. 60:1727-1729.

_____ and Bowen, N.L. (1950), High Temperature Albite and Contiguous Feldspar. J. Geol. 58:572.

_____ and _____ (1958), Origin of Granite in Light of Experimental Studies in the System $NaAlSi_3O_8$-$KAlSi_3O_8$-SiO_2-H_2O. Geol. Soc. Am. Mem. 74.

Volfinger, M. (1975), Effect de la Composition de Micas Dioctaedriques sur les Distributions des Elements Alcalins en Traces. Bull. Soc. Fr. Mineral. Cristallogr. 98:49-52.

Volfinger, M. (1976), Effect de la Temperature sur les Distributions de Na, Rb et Cs Entre la Sanidine, Les Muscovite sous une pression de 1 Kbar. Geochim. Cosmochim. Acta, 40: 267-282.

Voskresenskaya, N. T. (1959), Geochemistry of Tl and Rb in Igneous Rocks. Geochemistry, 5:599-605.

_____ (1961), Thallium in Some Hydrothermal Deposits of the Greater Caucasus. Geochem. 8:731-739.

_____ (1969), Tl in Sedimentary Sulphides. Geochem. Internat. 6: 225-236.

Wager, G. M. and Mitchell, R. L. (1951), The Distribution of Trace Elements during Strong Fractionation of Basic Magma. A Further Study of the Skaergaard Intrusion, East Greenland. Geochim. Cosmochim. Acta, 1:129-208.

White, A. J. R. (1966), Genesis of Migmatites from the Palmer Region of South Australia. Chem. Geol. 1:165-200.

Whitney, P. R. (1969), Variation of the K/Rb Ratio in Migmatitic Paragneisses of the Northwest Adirondacks. Geochim. Cosmochim. Acta, 33:1203-1211.

Whittaker, E. J. W. and Muntus, R. D. (1970), Ionic Radii for use in Geochemistry. Geochim. Cosmochim. Acta, 34:945-956.

Wright, T. L. (1968), X-Ray and Optical Study of Alkali Feldspars. II. An X-Ray Method for Determining the Composition and Structural State from Measurement of 2 Theta Values for Three Reflections. Am. Mineral. 53:88-104.

Wyllie, P.J. (1971), The Dynamic Earth, Textbook in Geoscience. John Wiley and Sons, Inc., 416 p.

Yoder, H.S., Stewart, D.B. and Smith, J.R. (1957), Ternary Feldspars. Carnegie Inst. Wash. Yr. Bk, 56, 206-214.

Zartmann, R.E. (1964), A Geochronologic Study of the Lone Grove Pluton from Llano Uplift, Texas. J. Petrol. 5:359-408.

Zielinsky, R.A. and Frey, F.A. (1974), An Experimental Study of the Partitioning of a Rare Earth Element (Gd) in the System Diopside-Aqueous Vapour. Geochim. Cosmochim. Acta, 38:545-566.

Zlobin, B.I. (1958), Geochemistry of Tl in Alkalic Rocks. Geochem. Internat., 5:560.